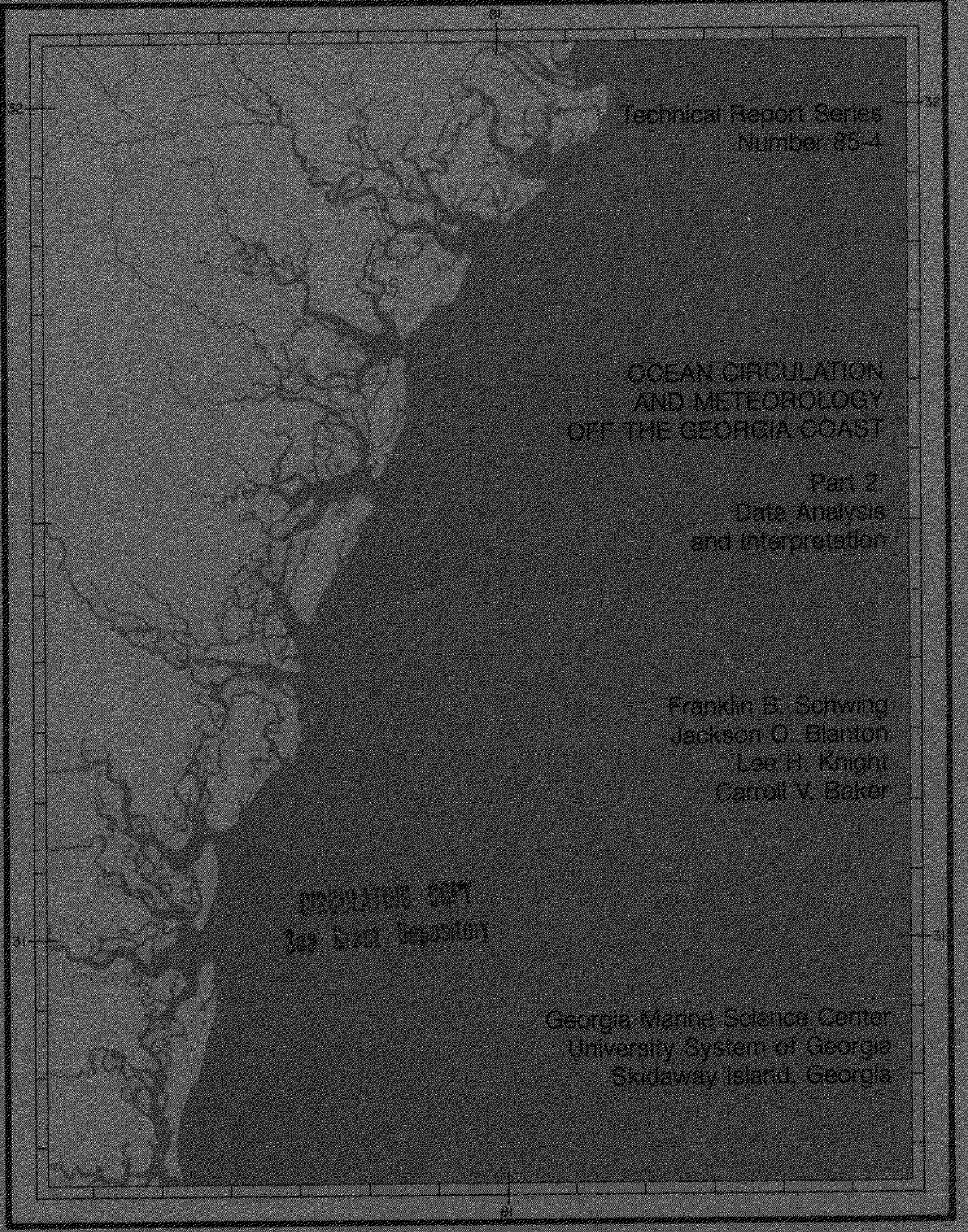

Technical Report Series
Number 85-4

OCEAN CIRCULATION AND METEOROLOGY OFF THE GEORGIA COAST

Part 2
Data Analysis and Interpretation

Franklin E. Schwing
Jackson O. Blanton
Lee H. Knight
Carroll V. Baker

Georgia Marine Science Center
University System of Georgia
Skidaway Island, Georgia

OCEAN CIRCULATION AND METEOROLOGY OFF THE GEORGIA COAST - PART 2.

DATA ANALYSIS AND INTERPRETATION

Technical Report 85-4

by

Franklin B. Schwing, Jackson O. Blanton, Lee H. Knight,

and Carroll V. Baker

Skidaway Institute of Oceanography
Post Office Box 13687
Savannah, Georgia 31416

TABLE OF CONTENTS

ABSTRACT

Real-time meteorological and oceanographic data are now being routinely collected at Savannah Navigational Light Tower (SNLT), a fixed platform located 17 km offshore from Savannah, Ga. Several years (1977-1984) of these data, supplemented with other regional observations, are analyzed and interpreted to characterize the ocean climatology of the South Atlantic Bight (SAB) inner shelf. Interannual, seasonal, synoptic and tidal periods are emphasized.

More frequent and intense current fluctuations occur in the spring and fall, which are transition periods between typical summer (minimum variance) and winter regimes. Other seasonal characteristics include a warming of the water column with an appropriate steric sea level response, and a deepening of the thermocline during late spring and summer. These changes are primarily due to seasonal shifts in the pattern of atmospheric pressure systems and their associated winds, although changes in freshwater runoff, Gulf Stream position and seasonal heating cycles are probably important as well. Year-to-year variations in the timing of these events are quite apparent in the observations.

All hydrographic parameters are highly responsive to wind changes due to frontal passages at 3- to 14-day periods, increasing from winter to summer. Alongshore wind is the predominant forcing mechanism. Although the direction of wind varies greatly during the year, the current is primarily alongshelf at all times, with evidence of surface and bottom Ekman layers noted. The current is also much more stable and rectilinear than the wind. The sea level field in the SAB is highly coherent and approximately in phase at all frequencies, and well correlated with the current.

Tidal currents and sea level are predominantly semi diurnal. With depth, tidal ellipses weaken, become more rectilinear, and rotate clockwise. Wind often presents a distinct summer diurnal period. Oceanographic parameters are dominated by tidal oscillations, but synoptic scale motions are an important contributor to the mean circulation pattern of the inner shelf region of the SAB.

KEYWORDS

Atlantic	Hydrography
Climate	Ocean
Coast	Shoreline
Current	Tide
Data	Weather
Georgia	Wind

ACKNOWLEDGMENTS

Many of the analyses displayed in this report were conducted with the help of George Marmorino when he was at Florida State University. We express our appreciation to him for his help and diligence.

This study was sponsored by the Department of Energy, Contract No. DE-AS09-80EV10331. We are grateful to David Hayes at the Savannah River Laboratory and Gary Howell at the University of Florida for valuable advice and support in the early stages of this project. We thank Suzanne McIntosh and Anna Boyette for drafting the figures, and Susan Salyer for organizing and typing the manuscript. We also wish to thank Berry Beckham, Lester Lamhut and a host of other personnel at Skidaway Institute who collectively made this project a reality. We express our gratitude to the U.S. Coast Guard for permission to use the Savannah Navigational Light Tower, and to the crew of the U.S. Coast Guard Cutter Papaw, especially Lt. Commander Guy T. Goodwin and Mr. Sherman Colley for their assistance during recent deployments. This report is published as a part of the Georgia Marine Science Center's Technical Report Series issued by the Georgia Sea Grant Program under NOAA Office of Sea Grant #NA 80 AA-D00091.

I. INTRODUCTION

The coastal ocean of the South Atlantic Bight (SAB) is an area heavily used by man for recreation, industry, transportation and fishing. Energy-related activities along the coast may conflict with these uses if such activities are not carefully managed. It is necessary to assess the natural biological, chemical and geological properties of this area to evaluate the impact of man's varied activities on the system.

To understand the dynamic processes affecting this system, an understanding of the circulation of nearshore waters is needed. One of the important goals of research being conducted by Skidaway Institute of Oceanography (SKIO) under the sponsorship of the U. S. Department of Energy (DOE) is to characterize the climatology of the nearshore region of the SAB. It is within this context that the Savannah Navigational Light Tower (SNLT, Figs. 1, 2) is used as a permanent research site (Schwing et al., 1983a, 1984).

The nearshore environment is complex and highly variable. Circulation in this region is a result of interactions between a number of meteorological and hydrodynamic variables such as direction and intensity of wind stress, tidal action, river discharge, density gradients, sea level slope, and bottom friction. This is especially true off the coast of Georgia, where the irregular bathymetry and coastal boundary further complicate the hydrography. The shoreline is not smooth, but perforated by tidal inlets every 10 to 20 km. Some inlets are connected to major rivers (Pee Dee, Savannah, and Altamaha) which discharge a significant volume of freshwater into the coastal ocean. Others are relatively brackish pocket estuaries emptying large areas of salt marsh. Output from these inlets, modulated by large

amplitude tidal currents, forms a 10- to 20-km-wide band of turbid, relatively low salinity water, along the coast. A frontal zone is imbedded between this band of water and the coastal ocean and greatly influences both tidal and subtidal circulation in this region (Blanton, 1980a, 1981; Blanton and Atkinson, 1983). The SNLT is located within this regime and may be situated in either region of water, depending upon local conditions and season.

Several other technical reports have been published in which data from SNLT and the nearshore region were presented and discussed. Data collected at SNLT during 1977 were presented in unfiltered and filtered form in Blanton et al. (1978, 1980), but discussion of these data was minimal. So, a description of their analysis is included in this report. Blanton (1980b) and Blanton and Maddox (1980) dealt more with nearshore transport and coastal sea level fluctuations, respectively. Data from those reports are discussed here. Part I of this report (Schwing et al., 1984) described the design, operation, and use in oceanographic research of SNLT. A detailed description of the analyses performed on SNLT and associated data, along with a presentation of SNLT data obtained in 1980 through 1984, was also included in Part I. A detailed summary of these data and the results of their analysis are found in this report. Data collected during 1984 subsequently to Part I are also presented here (see appendix). The major portion of this report deals with the analysis and interpretation of low-frequency fluctuations in the data, although a section on tidal and other periodic analyses is included. The primary focus here is the description of seasonal characteristics of SAB hydrography and meteorology relative to the nearshore environment and SNLT, with particular emphasis on the

circulation and associated controlling factors. Discussion of daily weather and tidal scales is included, as these events greatly contribute to the total circulation regime of the region.

II. DATA AVAILABLE

The majority of data analyzed and described in this report were obtained from SNLT, although data were obtained from external sources as well. Instrumentation at SNLT (Fig. 3) does not operate continuously due to eventual sensor failure as well as occasional damage by severe weather or vandalism. Typical deployment at SNLT is made in association with other scientific work being conducted in the SAB, and data are taken during the course of those operations. Instruments are usually left in place after each field study and continue to provide information until the data quality deteriorates or data acquisition stops entirely. At that point, an attempt is made to retrieve instruments that are not working and to repair or replace them as soon as possible. Due to economic and personnel constraints, as well as problems due to foul weather, it is not always possible to do this immediately. Therefore, data collection at SNLT is not a continuous process, but consists of a series of discrete time spans over which an optimal amount of data has been obtained for as many parameters as possible. As we gain more experience, SNLT will operate on a more continuous basis, providing real-time information on meteorological and oceanographic conditions.

In addition to the limitations inherent in attempting to collect continuous data series, there is also a need to describe and analyze data in discrete time series. Data may be divided on several time scales. In our analysis, the largest of these scales is a seasonal one,

consisting of time series of several weeks to months in length. These series generally extend as long as a reasonable number of sensors remain operating on SNLT. Data described in this report are divided into ten time periods of seasonal scale. Start and end times of seasonal series are presented in Table 1. A majority of the analyses have been devoted to the first six periods, from 1977 through 1981.

A second way of interpreting data is by determining monthly statistics for each parameter. Monthly summaries are an effective way to describe the climatology of each parameter, as well as to compare interannual variability.

Another division of data is on a synoptic time scale. This is particularly useful when analyzing data in the frequency domain. Many event scales are elucidated by filtering the data set as described in Part I; that is, by removing energy at certain frequencies that may mask events at other frequency scales. The response characteristics of the filters used in these analyses are presented in Table 2. All parameters measured at SNLT respond to frontal passages on event scales of 3 to 14 days.

Other scales analyzed have a more regular period but do not appear in all records. Semidiurnal and diurnal tides show up in sea level, current, and pressure time series. Overtides can also be seen in unfiltered data. Data are also analyzed for a fortnightly signal. Winds are checked for evidence of the daily sea breeze. The analysis performed at these time scales depends on the parameter involved.

To elaborate on data obtained at SNLT, or to substitute for missing data, time series are also created and analyzed from other data sources in addition to SNLT. sea level records from the National Ocean Survey

(NOS) tide gauge at Ft. Pulaski have been used at times when data from SNLT were not available. Additional sea level series from coastal tide gauges and nearshore subsurface pressure stations have been used to calculate sea level gradients. Wind data from the National Weather Service (NWS) office at Travis Field, west of Savannah (Fig. 1), have been compared to those from SNLT and used as a substitute during times of missing data. Additional current meter records from various locations in the SAB have been compared to SNLT data as well. All external data records are trimmed to a length identical to that of existing SNLT series, and simultaneous series are resampled to a common data interval and similarly analyzed. Results from these externally obtained data are found throughout this report.

III. SNLT DATA SUMMARY

Data collected at SNLT from 1977 through January 1983 have been presented in weekly and monthly plot summaries in previous reports (Blanton et al., 1978, 1980; Schwing et al., 1984). A detailed description and analysis of these data are presented here. Analysis emphasizes subtidal, weather-associated events, as well as tidally related phenomena. Much of the analysis was done on an entire time period (Table 1), thus allowing us to compare seasonal variations in these events. Unless otherwise noted, x-components of vectors designate the east direction; y-components designate the north direction. Furthermore, in describing wind directions, we adhere to the oceanographic convention in which the stated direction specifies the direction <u>toward</u> which the wind blows.

III.1. Time Series

Time series of each parameter were plotted by seasonal time period (Figs. 4-11). These series were 40 hr low-pass filtered to remove tidal signals and elucidate low-frequency meteorological events. The series can be compared visually to identify individual events common to all series as well as the relative importance of these events by parameter. Results of spectral analysis on these series are described beginning with Section III.3. Tidal fluctuations are discussed in Section IV.

III.1.1. Wind stress

Wind component stick vectors (Fig. 4) and time series (Fig. 5) are presented as wind stress. Wind stress (dynes/cm^2) was calculated using the quadratic speed law with a drag coefficient of 2×10^{-3}. Variations in low-frequency wind stress occur at periods of 3 to 14 days and are associated with meteorological frontal passages through the SAB region (Chao and Pietrafesa, 1980; Klinck, Pietrafesa and Janowitz, 1981). Wind at SNLT rotated generally in a clockwise manner as fronts progressed eastward. Such wind events occurred more frequently and with greater intensity in winter and early spring (Fig. 5a,b,d,e) in response to seasonal differences in the regularity and strength of weather frontal events (Schwing, Kjerve and Sneed, 1983c).

Strongest wind stress during spring was generally to the east and north (Figs. 4a,b,d, 5a,b,d). The exception was spring 1981 (Period 5) when three strong southwesterly events occurred during the second half of the record (Figs. 4e, 5e). During the fall, the strongest stress was usually to the southwest (Figs. 4c; 5c,f). Summer wind was generally to the northeast in association with the strong Bermuda High, and events

were weaker and occurred less frequently than during other seasons (Figs. 4b,c; 5b,c,d, f). These results are consistent with the wind climatology of the SAB described by Weber and Blanton (1980). At all times wind stress over water at SNLT was approximately four times that over land, a response to increased thermal gradients and reduced surface roughness (Schwing and Blanton, 1984).

III.1.2. Ocean current

Ocean current stick vectors (Fig. 4) and time series (Fig. 6) are presented for the bottom current (1 m off the bottom) during Periods 1-3 and for the mid-depth current (8 m off the bottom) during Periods 4-5. Time series in Figure 6 are for velocity components rotated to coordinates of major and minor axes for each period. Major axis was defined as the direction in which variance of flow was maximized. Bottom major axis was generally east-west (Period 1 = 61°, Period 3 = 90°), while mid-depth major axis was nearly north-south (Period 4 = 34°, Period 5 = 27°).

Current also varies in response to weather changes on a 3 to 14 day time scale (Lee and Atkinson, 1983; Schwing, Kjerfve and Sneed, 1983b; Schwing, Blanton and Oey, 1985). Like wind stress events, current fluctuations were more frequent and intense during early spring and fall. Current was highly responsive but lagged to changes in wind stress. Predominantly northeasterly wind stress during Periods 2-4 produced current alongshelf to northeast (Fig. 4b-d). Period 5 wind stress alternating between northeast and southwest generated a similar pattern in current direction (Fig. 4e). As the wind vector rotated clockwise, current direction also rotated in a clockwise direction. Current,

however, was more likely to rotate in a counterclockwise manner following passage of a front (cf. Fig. 4e, Period 5). Local bottom bathymetry off the southeastern U.S. tends to rectify current in an alongshelf orientation and produce highly polarized flow (Schwing et al., 1985). In general, the current vector was oriented clockwise from the wind vector by several degrees.

III.1.3. Sea level

The limited amount of data at SNLT as well as additional data from Ft. Pulaski (Fig. 7) show the influence of wind stress and current on subtidal sea level. Changes in subtidal sea level are controlled by rotating wind patterns during frontal passages on scales of 3 to 14 days and seasonally by fluctuations in steric height (Schwing et al., 1983c) and the Gulf Stream (Blaha, 1984). Wind stress to thesouthwest or west produced onshore current, causing a rise in coastal sea level. Northeastward or eastward wind and current generated a lowering of sea level (Schwing et al., 1985). Each frontal passage produced low-frequency sea level fluctuations of 20 to 50 cm. Again, the amplitude and frequency vary seasonally.

III.1.4. Temperature

Temperature time series (Figs. 8-10) showed seasonal effects. Superimposed on seasonal warming and cooling trends of the lower atmosphere were fluctuations on the order of 4-8C. These variations were a reflection of frontal movements bringing synoptic-scale warm and cool air masses into the SAB region.

Water temperature presented in this report varies between a minimum of about 10C in January (Fig. 9a) and a maximum of over 30C in late July (Fig. 9b,c,f). In general, temperature at all three underwater levels changed at the same rate. Surface temperature fluctuated more than lower level temperature (Fig. 9), reflecting a dampened response to warmer and cooler air masses moving through the SAB region (Fig. 8). Seasonal warming and cooling of the atmosphere was transferred through the entire water column, as evidenced by long-term trends in the time series in Figures 9 and 10. Also defined in these time series is the deepening of the thermocline during late spring and summer. Mid-level temperature was similar to that near the bottom in late winter and throughout much of the spring (Fig. 10a,b, Periods 1, 2) but nearly identical to surface temperature in summer and fall (Fig. 10b-f, Periods 2-6).

In addition to seasonal fluctuations in the thermocline at SNLT, the water column underwent periodic episodes of thorough mixing in response to very energetic springtime weather events (cf. Fig. 10a). During periods of relatively low wind stress, thermal stratification was established as the surface layer warmed more rapidly in response to seasonal atmospheric warming. During frontal passages, high wind stress on the surface effectively mixed the entire water column, thereby warming the bottom layer. The surface layer became slightly cooler during this time as well; this resulted from heat loss to an atmosphere that cooled following the frontal passage and the mixing of the surface layer with cooler bottom water. The long-term effect of this is an increase in the overall water temperature.

III.1.5. Salinity

Over long time periods, salinity measurements became increasingly inaccurate due to instrument drift and sensor deterioration. Although the quality of the low-passed salinity time series (Fig. 11) is marginal, certain aspects of the data seemed quite valid. Major fluctuations in low-frequency salinity occurred on a cycle of about seven days, within the synoptic weather period. Salinity measurements were visually correlated with wind and current data. Water temperature also visually correlated with salinity, particularly during spring. Direct onshore flow or alongshore flow to the southwest forced cooler, more saline oceanic water into the nearshore zone and increased the salinity at SNLT by as much as 5 ppt. Flow offshore or to the northeast removed highly saline water, allowing warmer fresh riverine input to occupy a wider band of inner shelf extending beyond SNLT.

III.1.6. Barometric pressure

Barometric pressure time series (Fig. 8) were dominated by synoptic-scale weather events. Low-pass filtering of these series removed very little of the overall energy, especially in comparison to current and sea level. At this latitude (31°57'N) there is some daily variability in pressure due to atmospheric heating (Pietrafesa and Janowitz, 1980) but this was removed by the filtering process. Dominant fluctuations in barometric pressure resulted from the movement of high and low pressure systems through the coastal zone (Oort and Taylor, 1969). Variation through the year in the amplitude and frequency of weather-related pressure was on a scale similar to that for wind and current.

Although sea level records are often adjusted to account for the "inverse barometer effect" of atmospheric pressure on sea level (Hamon, 1962; Pietrafesa and Janowitz, 1980), such adjustments of SNLT data were unnecessary since sea level was determined from the measurement of subsurface pressure. Note that coastal sea level records from Ft. Pulaski, Charleston, and Daytona Beach were adjusted for local barometric pressure.

The low-frequency time series described above demonstrate the intimate coupling between circulation, hydrography, and meteorological frontal passages at SNLT. Frontal movements, defined by variations in barometric pressure and air temperature, produce fluctuating wind, which in turn, causes changes in nearshore current, sea level, water temperature, and salinity. This is particularly evident from examination of weekly and monthly summaries of SNLT data in the appendix. A more complete description of the response of the coastal ocean to atmospheric changes is contained in Part I (Fig. 12 in Schwing et al., 1984; Schwing et al., 1983).

III.2. Monthly Statistical Summary

Monthly means and standard deviations of 40 hr low-passed data are summarized in Tables 3-7 and Figures 12-15, and monthly vector statistics are included in Tables 8-9 and Figure 16. Changes during the year as well as interannual variability can be identified from these summaries.

III.2.1. Wind stress

Wind regime at SNLT showed a definite seasonal pattern. Wind blew generally northeast and north in spring and summer with the exception of May, a transition month between highly variable wind in February-April and the summer regime dominated by the Bermuda High (Fig. 12, Table 3,8) (Weber and Blanton, 1980; Blanton et al., 1985). Interannual variability was lowest in July, also the month of lowest wind variance. August was another transition month between summer and autumn regimes (Weber and Blanton, 1980). The August 1980 wind followed the summer pattern of flow to the northeast, while 1977 and 1981 winds were northwesterly, similar to the September wind. The October wind shifted southwest and was strong and highly variable. The winter wind exhibited a definite change from the spring and fall pattern. Wind in November reversed to an easterly direction and rotated south-southeast in December and south in January. Wind variance was also greatest in winter.

The major axis of the wind was northwest-southeast in January and February. It rotated counterclockwise through spring and summer to a northeast-southwest orientation in October and returned northwest-southeast in November and December (Fig. 16). With the exception of August 1980, all monthly mean vectors were smaller than monthly standard deviations of components.

Wind intensity also varied significantly from month to month (Fig. 17). The strongest wind generally occurred during late fall and early winter. This is particularly true for the occurrence of wind greater than 12.5 m/s (25 knots), speed typically associated with small craft advisories given by the National Weather Service (NWS). Two other peaks

April and August. Speed was greatly reduced during June and September, when wind greater than 10 m/s blew less than 10% of the time, as opposed to about 25% during October and December.

III.2.2. Ocean current

Mean current (Fig. 12, Tables 4, 9) rotated clockwise during spring and summer, flowing north in February and nearly east by July and August. The current returned to a northerly flow in September, probably in response to the autumn wind regime. Unlike the wind orientation, the current major axis changed little from February to August (Fig. 16). During these months the axis was oriented generally northeast-southwest, although interannual differences existed. The axis shifted in September in a counterclockwise direction with major and minor axes becoming almost equal in length. In summer the axes were nearly rectilinear.

Subtidal current at SNLT is balanced between frictional and pressure forces. Wind stress and bottom friction combine to produce a rather complicated nearshore current regime in water less than 20 m deep (Schwing et al., 1983b, 1985). Coupling between wind stress and current produces a clockwise flow relative to the wind, while bottom stress forces current in a counterclockwise direction. Wind and current direction are similar at SNLT; both flow predominantly alongshore to the northeast (Fig. 12). Mean current at 8 m was typically clockwise of wind during the summer; this was possibly a response in the Ekman sense to consistent wind to the northeast.

III.2.3. Sea level

Wind-forced sea level variability usually cannot be seen in mean monthly statistics (Fig. 13, Table 5). An exception to this was the August 1980 sea level at nearby Ft. Pulaski (Savannah). sea level at this time was lower than during July, possibly in response to the continuing northeasterly wind pattern. sea level in August 1981 at SNLT, however, increased from the previous month. The higher 1981 level may have been due to a piling up of water on the coast caused by onshore-directed wind. Other increases in sea level occurred in response to freshwater runoff in March (Atkinson, Blanton and Hayes, 1978) and steric increases due to ocean warming in May and June (Pattullo et al., 1955). The depression in July may have been due to a change in Gulf Stream position and/or strength (Blaha, 1984). The relationship of coastal sea level to Gulf Stream fluctuations is speculative, but earlier works by Green (1944) and Taylor and Stewart (1959) contain indirect evidence of this coupling. Lowest magnitude in monthly mean sea level occurred during winter when fresh water runoff was small, water temperature and steric effects were at a minimum, and wind to the north was likely to induce a depressed coastal sea level.

III.2.4. Temperature

Air and water temperatures at SNLT showed an expected trend of minimum values in January and maximum values in July and August (Fig. 14, Table 6). Within this trend was some year-to-year variability, especially evident in spring (Fig. 15). Temperature in April and May 1977 (Fig. 15a) averaged about 4 and 6C higher than during the same months of 1980 (Fig. 15b). This trend of warmer temperature is evident

than water temperature during spring and summer, this was not always the case at SNLT. Depressed temperature in April and May 1980 was due to cooler-than-usual air temperature as indicated by warm water relative to that of the air. Water temperature during late summer was also warmer than air, as the air underwent more rapid seasonal cooling. Variance in temperature was greatest during winter and spring, at a minimum in summer, and increasing again in September and October. Variance was also much greater for air temperature relative to that of the water.

Periods of thermal stratification existed at SNLT. Temperature at mid-depth (8 m from the bottom) was almost identical to that 1 m from the bottom during late winter and spring; this indicated a relatively shallow thermocline (Fig. 14). Mid-depth temperature increased throughout summer, becoming equal to surface temperature (13 m from bottom) by late summer. Thus, the water column gradually warmed from surface to bottom as the thermocline became deeper through summer.

III.2.5 Salinity

Since the amount of salinity data collected at SNLT was small and its quality was questionable, discussion of such data is limited (Table 7). Monthly means were lower than typical oceanic values due to a significant freshwater input from several southeastern rivers and estuaries (Atkinson et al., 1978).

III.3. Time Series and Autospectral Variance

Utilizing the period breakdown described in Table 1, time series and auto- and cross-spectral relationships between various parameters, as well as their variation during different periods are described.

Unless otherwise noted, x and y refer to east and north wind components (m/s), and u and v refer to east and north current components (cm/s), respectively. Tau (wind stress) units are dynes/cm^2.

III.3.1. Wind forcing

Low-passed wind time series (Figs. 4-5) show seasonal and weather related effects. Variability due to seasonal changes previously described in monthly statistics was greatest in spring, when wind stress was high and direction highly variable. By mid-May, stress was reduced and stabilized in a predominantly east to northeast direction.

Highest variance in wind spectra occurred along the x (east) axis, which contained two to six times more variance than the y (north) component (Fig. 18, Table 10). Seasonally, the highest total variance occurred in spring. The most energetic periods of oscillation ranged from around six days to the total length of the time series. However bands of maximum variance showed seasonal variability. Maximum variance during spring (Periods 1, 5, Figs. 18a,e) was in the five- to eight-day band, consistent with the typical weather frequency at this time. The summer peak (Periods 2, 4, Figs. 18b,d) was closer to 8-10 days, representative of longer, less energetic weather cycles during summer (Brooks and Mooers, 1977; Schwing et al., 1983b,c). Variance in summer periods was also considerably diminished. In fall (Periods 3, 6, Figs. 18c,f), the low-frequency spectra was almost completely red, owing to high seasonal variability of fall as a transition period. More than 30% of total wind variance in Period 6 was in the band greater than 10 days (Table 10).

Rotary spectral analysis for low-frequency events in the weather band produced ellipses in which the major axes were oriented typically east-west (Table 11). Variation from this orientation seldom varied by more than 25° in a counterclockwise direction. Ellipse stability was highly variable and lowest in spring. Weather-associated wind ellipses were elongated, almost to the point of being rectilinear in fall. Ellipses for lower subtidal periods (three to six days) were more circular than those at periods greater than six days.

III.3.1a. Comparison of SNLT and land-based wind

Blanton et al. (1985) and Schwing and Blanton (1984) compared SNLT wind with data from a land-based site at Travis Airfield in Savannah (Fig. 1). Ocean wind magnitude was twice that of land-wind, a function of reduced surface roughness and stronger vertical thermal gradients over water (Fig. 19). The two wind regimes occasionally vary in direction as well. Statistics from wind time series taken during summer (Period 2) show this to be true (Fig. 20, Table 12). Spectrally, low-passed SNLT wind was more energetic than land-wind at all frequencies (Fig. 21).

III.3.2. Ocean current

Bottom current spectra (Periods 1-3, Fig. 22a,b, Table 13a) were dominated by the u(east) component, with two to three times more variance than v(north). The v component at mid-depth (Periods 4, 5, Fig. 22c, Table 13b), however, contained three times the variance of u. Like low-frequency wind, total spectral variance was greatest in spring but only slightly more than for summer (Period 2). The most energetic band

(in rotary spectra) was that greater than 6 days, with a secondary peak at 3-5 days (Fig. 23c, Table 14). Maximum variance during spring (Period 1) occurred in a 6- to 8-day band, with a secondary peak at 2.5 days. Mid-depth current was most energetic at 6 days in both u and v components, although v had three times as much variance (Table 13). Summer variance was greatest in an 8- to 10-day band, with a lesser variance maximum at 3.5 days. In the case of Period 3, the fall data set, maximum variance for the u component was in a 7- to 10-day band and no significant variance occurred at higher subtidal frequencies. In all cases, u and v were in phase.

Rotary spectral analysis of current showed that subtidal ellipses were fairly consistent for each depth. Major axes were approximately aligned with northeast-southwest shoreline orientation. Bottom major axes were oriented on a 60-240° axis with the mid-depth major axis lying on a 30-210° plane (Table 15). Stability was higher than that for low-frequency wind but lower than that for tidal current. Current stability was also greater at 2- to 5-day periods than at longer periods. Current ellipses were nearly rectilinear, much more so than for wind. This is apparent in low-frequency stick vector plots (Fig. 4). Wind events gradually rotated, while rectilinear current shifted more rapidly.

III.3.3. Cross-spectral comparisons

East (x) and north (y) wind components were cross-correlated with the major axis vector of SNLT current for each data period. Just as current was visually correlated with wind variation, as discussed in Sections I and II, cross-spectral correlations (Fig. 23, Table 16) were

significant at most autospectral peaks (Tables 11, 15). In almost every case, only one or two significant peaks existed at periods greater than two days. Significant peaks discussed in this section were coherent at the 95% confidence level (α=.05) and had a notably large cross-spectral value between the two correlated series. Coherence calculations tell whether or not a relationship is statistically significant, while the magnitude of the cross-spectrum tells if the relationship is of physical importance and interest. Although both wind components were about equally correlated with current, the east component seemed to have a greater effect, as cross-spectral values between the x vector and current were larger.

Periods of high correlation between wind stress and current included 2-3 and 6 days in spring (Fig. 23a,b,g,h); 8-12 days in summer (Fig. 23c,d); and 5-7 days in the predominantly red spectral signature of fall (Fig. 23e,f). Based on cross-spectral values, current at mid-depth (Fig. 23g,h) was more closely coupled to wind than was bottom current (Fig. 23a-f). Current and wind during spring were more closely coupled than during summer or fall. Most wind variance was in the east component for all data periods (Table 10). Cross-spectra were greater between east wind and the primary axis of current. Both wind components, however, were about equally correlated with current, and rotary spectral analysis showed current was consistently correlated with wind stress parallel to shoreline.

Most coherent wind was oriented clockwise of V at mid-depth whereas coherent wind was mostly counterclockwise of bottom current principal axis. This disparity might be interpreted as an Ekman effect, where the middle sensor is predominately in some portion of the surface

Ekman layer and the bottom sensor is in a frictionally retarded bottom layer. Vertical shear induced by vertical density gradients cannot be ruled out (Blanton and Atkinson, 1983). However, the extremely complex interaction between meteorological forcing and bottom topography in such a shallow environment makes it difficult to define precisely the effect wind stress has on rotation of current with depth.

The water column at SNLT is shallow enough to expect the effect of wind stress on the surface to be felt at the bottom (Csanady, 1973; Blanton, 1981,; Schwing et al., 1983b, 1985). Despite this, the increased effect of bottom friction would be expected to dampen wind effects near the bottom. Therefore, spring (Period 5) mid-depth current data should reflect a stronger wind influence than bottom current data. Since the principal axis of mid-depth current (V) at this time was 27°, one would expect the north (y) wind component to dominate. However,wind in the x direction had a higher total variance (Fig. 23g). Larger cross-spectral values were found between the x component of the wind and V , the principal axis of the current vector at periods of maximum auto-variance. The x wind component was highly coherent with the principal current component at six days but actually lagged the current by 3 hr (Fig. 23g). A similar phase relationship was noted in the nearshore region off South Carolina (Schwing et al., 1983b). A simple linear barotropic model (Schwing et al., 1985) explains this seemingly unlikely relationship to be a consequence of the combined effect of wind-induced transport due to the Coriolis force and transport induced by the cross-shelf pressure gradient. Current and y wind were correlated at 6 and 14 days with no significant phase lag (Fig. 23h).

An independent rotary spectral analysis showed no significant coherence between wind stress and mid-depth current for spring (Period 5) at periods less than 4 days (Fig. 24). For periods greater than 4 days, however, current (V = 27°) was significantly coherent with wind blowing in an orientation approximately parallel to the shoreline. Phase between stress and mid-depth current was insignificant from zero at all significantly coherent periods.

The bottom current in spring (Period 1) was oriented more to the east (V = 61°). The north wind component was coherent with the bottom current at 5.5 and 20 days, similar to significant frequencies for mid-depth (Table 16). However, bottom current lagged north wind by 20 hr at 5.5 days indicating that wind stress takes considerably more time to affect the bottom. The highest cross-spectral value between east wind stress and current was at 11.5 days with no significant phase lag. A secondary peak occurred at 2 days, when current lagged by about 3 hrs.

The current during the summer (Period 2, V = 79°) was coherent and in phase with x and y winds in the 8- to 10-day band (Figs. 23c,d, Table 16). Additionally x wind and current were coherent at 3.5 days. The east wind was much more energetic (Fig. 23c), and resultant cross-spectral comparisons with current were greater.

Fall data (Period 3) produced primarily red spectra. The principal current was rotated even more clockwise (V = 90°) and was expected to be more coherent with the east wind component, provided that no rotation of internal stress occurs with depth. Again, variance was higher for the x wind component (Fig. 23e), and cross-spectral values between x and V were larger than for y wind. The east wind component was coherent at 5-7 days, leading current by 18 hr. The y component was significant and

in phase with the current at 9.5 days (Fig. 23f). Rotary spectra indicate that wind and current were not as closely coupled in fall as during other seasons.

III.4. Sea level

Although sea levels from both SNLT and Ft. Pulaski are described in this report, the difference in total variance between the two sites was not significant (Figs. 25-26). Variance in spring was greatest, up to three times as great as during summer. Most low-frequency sea level variance was concentrated in the 6- to 10-day band (Table 17). The spectral peak in summer (Period 2, Fig. 26c) was 8 days with secondary peaks at 2 and 3.5 days. Variance in spring (Fig. 26e) and fall (Fig. 26g) was highest in the 10- to 12-day band with spectra primarily red for Periods 4 and 5.

III.4.1. Sea level cross-correlations with wind and current

Wind and current were cross-spectrally analyzed with sea level. Current from two data periods were cross-correlated with local sea level records: Period 2 with Ft. Pulaski (Savannah) sea level (Fig. 25a,b) and Period 5 with SNLT sea level (Fig. 25c,d). Wind was correlated with Ft. Pulaski, Periods 2 and 4 (Fig. 26a-d), and SNLT, Periods 5 and 6 (Fig. 26e-h).

As coastal sea level set-up and set-down is affected to a great degree by low-frequency wind and current, it may be expected that cross-correlations with sea level were expected to match up well with those described in the previous section (Lee and Brooks, 1979; Schwing et al., 1983b,1985) (Fig. 23). Unfortunately, correlations between sea

level data from SNLT and wind and current (Periods 5 and 6) were poor. Therefore, the following discussion concentrates on cross-correlations with Ft. Pulaski sea level (Periods 2 and 4).

Period 2 sea level at Ft. Pulaski had cross-spectral amplitudes with the u (east) current component (Fig. 25a) that were 2-2.5 times those with v (north) current (Fig. 25b). Correlations were significant between the u component and sea level at all frequencies greater than 2 days. Maximum cross-spectral values occurred at 8 days when both components and the two parameters were significantly coherent ($r^2 = .9$). Current and sea level always were approximately 180° out of phase. Maximum drop in sea level corresponded to maximum easterly (u) or northerly (v) current, while maximum high sea level correlated with westerly (-u) and southerly (-v) current. However, maximum v current led minimum sea level by 5 hr and maximum u led by 8 hr, approximately the resampled data interval of 6 hr. A secondary cross-spectral peak was coherent at 3.5 days with sea level lagging v by 1 hr and u by 2.5 hr.

The relationship of sea level with wind stress in Period 2 (Figs. 26a,b) was very similar to that with current, with coherent cross-spectral amplitudes occurring at 8 days. A secondary peak (Figs. 26a,b) was very similar to that with current, with coherent cross-spectral amplitudes occurring at 8 days and a secondary peak occurring at 3.5 days. Sea level was also approximately 180° out of phase with wind in the x direction. However maximum northward (+y) wind led the sea level minimum by 12 hr at 8-10 days and 17 hr at 3 days. Thus, while wind and current in the period were in phase (Fig. 23), it

took several hours for sea level to respond to low-frequency meteorological forcing.

Rotary correlations between wind stress and sea level during Period 2 were significantly coherent in the 2.5-4.5 day band at all wind directions. At the 6-10 day period, sea level was significantly coherent with northeast and southwest stress.

Cross-spectral amplitudes of Ft. Pulaski sea level in Period 4 were also about twice as large with the x (east) wind stress component (Fig. 26c) than y (north) component (Fig. 26d). The two series were coherent in the 3- to 12-day band, with a maximum cross-spectral value with the x-component at 7 days, the period of maximum autospectral amplitude for sea level and east stress. Wind led sea level at this frequency by 12 hr, identical to that for Period 2. A secondary cross-spectral peak occurred at 12 days where wind led by 8 hr. Maximum cross-spectral amplitude between sea level and y wind component was at 9 days, also the period of maximum autospectral amplitude for that wind component. Sea level lagged wind by 27 hr. Although sea level was coherent with both components throughout the 3- to 12-day band, sea level phase lags were consistently higher (about 1 day) to the y component. sea level responded most rapidly to the x component.

Rotary spectra showed Period 4 wind stress and sea level coherent throughout 3- to 12-day periods for northeast and southwest stress, matching well with the relationship of wind stress to V .

Both rotary and component cross-spectral analyses between current and sea level at SNLT during Period 5 showed poor coherence at significant autospectral frequencies (Figs. 25c,d, 26e,f). The only coherent period was 2 days, when spectral variance was very low.

Likewise, wind and sea level in Period 5 (Fig. 26e,f) were coherent only at periods greater than 17 days, well within the red part of the spectra. Wind and sea level in Period 6 (Fig. 26g,h), also predominantly red spectrally, were coherent in the y direction at 4 days, a secondary autospectral peak. Wind led by about one day, although the cross-spectral amplitude at this period was much lower than for lower frequencies.

III.4.2. Sea level relationships in the SAB

Ft. Pulaski sea level data from Period 4 (Fig. 7b) were analyzed along with barometrically adjusted coastal sea level from Charleston, S.C. and Daytona Beach, Fla., and subsurface pressure at two locations along the 15-m isobath off Georgia and Florida (Fig. 27) to describe interactions of sea level in the SAB. Coastal sea level variance was greatest at Ft. Pulaski and smallest at Daytona Beach (Table 18). Subsurface pressure variance at 15 m also decreased from north to south and was smaller than associated coastal stations. The distribution of variance by frequency was similar at each site, although variance at periods greater than 10 days increased to the south and increased the total percentage of variance for periods longer than 2 days in that direction as well.

All five sea level stations were highly correlated and nearly all were in phase at periods greater than 3 days (Fig. 28, Table 19). Even along the most extreme length scale between Charleston and Daytona Beach, the lag was only about 12 hr at 6.6 days, from north to south (Fig. 28a). All other phase relationships at 6.6 days are within the statistical confidence interval or approximate the resampled data

interval of 6 hr. The five sites were also in phase (+/- 1 hr) at semidiurnal and diurnal frequencies, in agreement with NOAA tidal prediction tables.

The x (east) component of Savannah wind was highly coherent with Ft. Pulaski sea level over the 3- to 12-day band with sea level lagging by 4-13 hr (Fig. 26c). The y (north) wind component was also coherent with sea level, although correlations were lower than for the x component, and led sea level at Ft. Pulaski by 20-30 hr in the 4.5- to 10-day band (Fig. 26d).

The x component during Period 4 also was correlated with alongshore sea level slope (Fig. 29, 30a,c, Table 19), measured between Charleston and Daytona Beach (Fig. 29a), as well as offshore at the 15-m isobath (Fig. 29b). However, east wind stress was more highly correlated and more nearly in phase with slope at 15 m (Fig. 30d, Table 19). The y wind was correlated and in phase with coastal sea level slope at 6.6 days (Fig. 30b), but the relationship between north stress and slope at 15 m was not significant (Fig. 30d). A comparison of the two slope-series showed spectra that were partitioned differently by band (Table 18). The spectrum of slope at 15 m has a single peak at 6.6 days and closely matches the x wind spectrum (Fig. 30c). However, the coastal slope spectrum shows variance distributed more evenly across a broad frequency band (Fig. 30a). The difference in the two spectra is particularly evident in the 2- to 3-day band. This high frequency subtidal variance is unrelated to wind stress but is possibly due to local irregularities in topography near the coast that induce more local variance in coastal sea level and in slope.

In addition to the cross-correlation described above for Period 4, significant correlations of SAB sea level with wind stress and other sea level series during other periods are given in Table 19. Coastal sea level records were highly coherent at periods of about one week during all seasons. The correlation of sea level with wind stress was high, but the period varied with season. Coastal alongshore slope was also coherent with east wind stress usually in periods of a week, but not correlated with north stress during other periods.

IV. TIDAL PROCESSES

Although the majority of this report concerns subtidal-frequency events at SNLT, there are important tidally related phenomena in some of the data. Unfiltered sea level, current, salinity, temperature, and, to a lesser extent, time series for wind all contain significant variability at semidiurnal and diurnal scales. Harmonic analysis was performed on the 29-day series of unfiltered data to obtain spectra for tidal frequencies.

IV.1. Tidal Sea level at SNLT

Water level (Figs. 31, 32, Table 20) at SNLT was dominated by the semidiurnal tidal component containing two orders of magnitude more variance than the diurnal component. The diurnal inequality was evident in time series superimposed upon the 1.5-2.5 m semidiurnal tidal range. A fortnightly (14-day) signal was also present in time series producing as much or more variance as the diurnal tides. Fortnightly variance was similar to weather events discussed previously. This is especially evident in Figure 32b (Period 6). The quarter-diurnal overtide was

present in the spectra for Period 6 (Fig. 32b) as well, but not for Period 5 (Fig. 32a).

IV.1.1. Tidal sea level in the SAB

As with low-frequency sea level events (Section III.4.2.) tidal sea level near SNLT (Ft. Pulaski) was closely coupled to tidal fluctuations throughout the SAB (Figs. 33, 34). Relative tidal variance at each station was similar to subtidal events as well. Due to funneling effects in the bight, Ft. Pulaski showed the greatest tidal range (Fig. 33a,b). Tidal amplitudes decreased south (Fig. 33b,c) and offshore (Fig. 33c) from Savannah. This is also seen in the autospectra of the unfiltered series (Fig. 34). The signals at all stations were approximately in phase at the semidiurnal and diurnal periods.

IV.2. Tidal Current

Tidal current (Figs. 35-36, Tables 21, 22) was even more dominated by the semidiurnal component than sea level. Rotary spectral statistics for this parameter are summarized in Table 21. For bottom current (Figs. 35a-c, 36a-c, Periods 1-3) most energy was in the v direction. The semidiurnal for v was highly regular and higher in variance than that for u, with some fortnightly variability also apparent in the spectra. The diurnal component, however, was practically nonexistent. The u vector, on the other hand, had more variability due to subtidal events and less tidal energy relative to v. The tidal ellipse was more stable than for low-frequency events and fairly elongated, with the major axis oriented approximately perpendicular to the shoreline at a

150-330° angle (Table 22). Tidal variance constituted more than 70% of the total variance in the total current spectra.

A comparison between Periods 1-3 and 4-5 indicates that tidal current may differ at various depths. At 8 m from the bottom (Figs. 35d and e, 36d and e, Table 21), the u component was more energetic and had a larger variance at semidiurnal periods. The diurnal component was not as important but the quarter-diurnal overtide was significant. The v component was more affected by subtidal events, and semidiurnal variance was an order of magnitude lower than that for u. This disparity in semidiurnal energy was not as great at 1 m above the bottom (Table 21). Although tidal ellipse stabilities at 1 and 8 m were all extremely high,the ellipse at 8 m was less rectilinear than near bottom, and the major axis was situated only 10-20° clockwise of east compared to a bottom direction of south-southeast (Table 22). Percent of total energy due to semidiurnal components was similar at both depths.

Irregularities in bottom topography may force bottom tidal current along isobaths or around obstacles that do not line up with the shoreline. Increased bottom friction at 1 m may also force bottom current in a counterclockwise direction. Kundu, Blanton and Janopaul (1981) discuss differences in current with depth on the Georgia inner shelf.

For both depths u and v, semidiurnal components were highly coherent (r^2 >.9) with each other, while diurnal constituents were not significant. At semidiurnal periods, v leads u by 25-60° (1-2 hr) indicating the tidal ellipse rotates in a clockwise direction.

Semidiurnal current and sea level were highly coherent (r^2 >.97) at both depths (Fig. 37). The u current component lagged sea level by

about 90° (3 hr) at the semidiurnal period, while v led by 1-2 hr. Only Period 5 diurnal current and sea level (Fig. 37e,f) were significantly coherent. The v current was approximately in phase with water level and u lagged by 5 hr.

IV.3. Diurnal Wind

Stability of the diurnal wind ellipse was not nearly as great as that of current, owing to the large influence of weather events on wind (Table 22). Ellipse shapes also varied greatly from period to period, although they were more circular than current tidal ellipses. The sea breeze effect is much more distinct during summer when thermal gradients across the land-ocean boundary are greatest (Table 22).

Harmonic analysis was performed on the major axis (57°) component of unfiltered wind from Period 3 (Figs. 38, 39). Period 3 wind was chosen to maximize the daily sea breeze, which we found to be strongest during summer. Highest wind variance occurred at 24 hr (Fig. 39) at almost four times more variance than for weather events. A smaller peak in wind spectrum is seen at 12 hr. Major axis wind was not significantly coherent with u current (Fig. 39a) but significant with v (Fig. 39b) at the .05 level where current led by slightly more than 6 hr (90°). Rotary spectral analysis verified maximum coherence between diurnal wind and current and occurred with north-south current.

To highlight details of the daily sea breeze and its possible effect on nearshore current, wind and current time series were band-pass filtered centered about 24 hr. A close correlation between these band-passed series (Fig. 40) over a fortnightly cycle would indicate that residual current after filtering out tidal and weather

effects would be primarily wind driven. However, a visual correlation between these series shows them to be completely out of phase. Although both wind and current band-passed series have obvious 14-day signals, residual tidal current over this period is not due to the sea breeze. Instead, the fortnightly current appeared to be astronomically driven.

IV.4. Tidal Salinity

Salinity variations were predominantly semidiurnal (Fig. 41, 42, Table 23) with a significant diurnal peak in the spectrum, although tidal events accounted for very little of the total variance in the series, particularly when compared to other components. Period 5 data (Fig. 41b, 42b) showed a particularly strong diurnal signal, but it is unlikely that this is typical for this location.

V. SUMMARY

Savannah Navigational Light Tower (SNLT) has been used as an instrument platform to periodically collect coastal meteorological and hydrographic data since 1977. Sufficient data have been obtained to characterize the atmospheric and marine climatology of the South Atlantic Bight inner shelf on monthly and annual scales. Monthly mean statistics show seasonal patterns in all parameters measured at SNLT. Seasonal shifts in the pattern of atmospheric pressure systems produce changes in monthly mean wind and current direction and intensity as well as relative sea level. Changes in freshwater runoff, Gulf Stream position, and seasonal heating and cooling of air and water columns possibly contribute to the annual pattern. Interannual variations related to year-to-year fluctuations also exist.

Inner shelf circulation is highly responsive to wind changes due to meteorological frontal passages on scales of 3 to 14 days. These variations are also evident in other hydrographic parameters, including sea level, temperature, and salinity. The length and intensity of these weather-associated events varies seasonally. Due to the shallow depth and proximity to riverine input, current at SNLT is steered in an alongshore orientation relative to wind direction and the local isobath orientation. Different combinations of forces, particularly the interaction between wind and bottom stress, produce different current regimes at different depths.

Although the low-frequency fluctuations described above contribute a great deal of variability into the hydrography at SNLT, they tend to be masked by oscillations generated by the dominant tidal regime. Tidal current generally flows perpendicular to the coast, although variation with depth again exists. Tidal events account for a majority of the variance in unfiltered current, sea level, and salinity.

The dynamics of the SAB inner continental shelf are a complicated balance of many forces. Wind and bottom stress, tidal flow, freshwater runoff, pressure and density gradients, and irregular bathymetry all contribute to this balance. Although the complex interactions between these forces is still not completely understood, it is hoped that results contained in this report will contribute to our knowledge of nearshore circulation. While new information has been obtained, new questions have also developed. These problems will be addressed in future efforts aimed at describing and understanding the hydrography of the nearshore region of the South Atlantic Bight.

LITERATURE CITED

Atkinson, L. P., J. O. Blanton, and E. Haines. 1978. Shelf flushing rates based on distribution of salinity and freshwater in the Georgia Bight. Estuar. Coastal Mar. Sci. 7: 465-472.

Blaha, J. P. 1984. Fluctuations of monthly mean sea-level as related to intensity of the Gulf Stream from Key West to Norfolk. J. Geophys. Res. 89: 8033-8042.

Blanton, J. O. 1980a. The transport of freshwater off a multi-inlet coastline, p. 49-64. In P. Hamilton and K. B. McDonald, eds., Estuarine and wetland processes. Plenum Publishing Corp., New York.

Blanton, J. O. 1980b. Transport of water and salt off the Georgia coast 9-11 May 1978. Georgia Marine Science Center Technical Report Series, no. 80-3, Savannah, Ga.

Blanton, J. O. 1981. Ocean currents along a nearshore frontal zone on the continental shelf of the southeastern United States. J. Phys. Oceanogr. 11: 1627-1637.

Blanton, J. O., L. L. Bailey, D. W. Hayes, and A. S. Dicks. 1978. Data Report no. 1: Oceanographic and meteorological data 15 km off the coast of Georgia. Georgia Marine Science Center Technical Report Series, no. 78-6. Savannah, Ga.

Blanton, J. O., L. L. Bailey, D. W. Hayes, and A. S. Dicks. 1980. Data Report no. 2: Oceanographic and meteorological data 15 km off the coast of Georgia. Georgia Marine Science Center Technical Report Series, no. 80-5. Savannah, Ga.

Blanton, J. O. and W. C. Maddox, Jr. 1980. Data report on sea-level fluctuations in the South Atlantic Bight, 1977. Georgia Marine Science Center Technical Report Series, no. 80-6. Savannah, Ga.

Blanton, J. O. and L. P. Atkinson. 1983. Transport and fate of river discharge on the continental shelf of the southeastern United States. J. Geophys. Res. 88: 4730-4738.

Blanton, J. O., F. B. Schwing, A. H. Weber, L. J. Pietrafesa, and D. W. Hayes. 1985. Wind stress climatology in the South Atlantic Bight In: L. P. Atkinson and D. W. Menzel and K. A. Bush, eds., Oceanography of the Southeastern United States Continental Shelf, Coastal Estuarine Sci., Vol. 2. American Geophysical Union, Washington, D.C. pp. 10-22.

Brooks, D. A. and C. N. K. Mooers. 1977. Wind-forced continental shelf waves in the Florida current. J. Geophys. Res. 82: 2569-2576.

Chao, S.-Y. and L. J. Pietrafesa. 1980. The subtidal response of sea level to atmospheric forcing in the Carolina capes. J. Phys. Oceanogr. 10: 1246-1255.

Csanady, G. T. 1973. Wind-induced barotropic motions in long lakes. J. Phys. Oceanogr. 3: 429-438.

Green, C. K. 1944. Summer upwelling- northeast coast of Florida. Science 100: 546-547.

Hamon, B. V. 1962. The spectrums of mean sea-level at Sydney, Coff's Harbour, and Lord Howe Island. J. Geophys. Res. 67: 5147-5155.

Klinck, J. M., L. J. Pietrafesa, and G. S. Janowitz. 1981. Continental shelf circulation induced by a moving, localized wind stress. J. Phys. Oceanogr. 11: 836-848.

Kundu, P. K., J. O. Blanton, and M. M. Janopaul. 1981. Analysis of current observations on the Georgia shelf. J. Phys. Oceanogr. 11: 1139-1149.

Lee, T. N. and D. A. Brooks. 1979. Initial observations of current, temperature and coastal sea-level response to atmospheric and Gulf Stream forcing on the Georgia Shelf. Geophys. Res. Lett. 6: 321-324.

Lee, T. N. and L. P. Atkinson. 1983. Low-frequency current and temperature variability from Gulf Stream frontal eddies and atmospheric forcing along the southeast U.S. continental shelf. J. Geophys. Res. 88: 4541-4567.

Oort, A. H. and A. Taylor. 1969. On the kinetic energy spectrum near the ground. Mon. Weather Rev. 97: 623-636.

Pattullo, J., W. Munk, R. Revelle, and E. Strong. 1955. The seasonal oscillation in sea-level. J. Mar. Res. 14: 88-156.

Pietrafesa, L. J. and G. S. Janowitz. 1980. Lack of evidence of southerly propagating continental shelf waves in Onslow Bay, N.C. Geophys. Res. Lett. 7: 113-116.

Schwing, F. B., J. O. Blanton, L. Lamhut, L. H. Knight, and C. V. Baker. 1983a. A real-time telemetry system for hydrographic and meteorological data collection in the South Atlantic Bight In: C. D. Tollios, M. K. McElroy, and J. Syck, eds., 1983 Working Symposium on Oceanographic Data. Proc. IEEE Computer Society Press, Silver Springs, Md. pp. 44-50.

Schwing, F. B., B. Kjerfve, and J. E. Sneed. 1983b. Nearshore coastal currents on the South Carolina continental shelf. J. Geophys. Res. 88: 4719-4729.

Schwing, F. B., B. Kjerfve, and J. E. Sneed. 1983c. Sea-level oscillations in a salt marsh lagoon system. Anales Instituto Ciencias del Mar y Limnologia UNAM 10(1): 231-236.

Schwing, F. B. and J. O. Blanton. 1984. The use of land- and sea-based wind data in a simple circulation model. J. Phys. Oceanogr. 14: 193-197.

Schwing, F. B., J. O. Blanton, L. Lamhut, L. H. Knight, and C. V. Baker. 1984. Ocean circulation and meteorology off the Georgia coast - Part I. Real-time telemetry system for data collection. Georgia Marine Science Center Technical Report Series, no. 84-1. Savannah, Ga.

Schwing, F. B., J. O. Blanton, and L.-Y. Oey. 1985. Frictional response of continental shelf water to local wind forcing. J. Phys. Oceanogr. 15: 1733-1746.

Taylor, C. B. and H. B. Stewart, Jr. 1959. Summer upwelling along the east coast of Florida. J. Geophys. Res. 64: 33-40.

Weber, A. H. and J. O. Blanton. 1980. Monthly mean wind fields for the South Atlantic Bight. J. Phys. Oceanogr. 10: 1256-1263.

LIST OF TABLES

Table 10. Variance (dynes^2/cm^4) and percentage of total variance in low-frequency bands for 40 hr low-passed a) east (x) and b) north (y) wind stress components, by period.

Table 11. Low-frequency (subtidal) rotary vector statistics for 40 hr low-passed wind. Total kinetic energy (m^2/s^2) is shown for low-frequency bands, by period, which account for a significant amount of the total energy. ROTC refers to the ratio of minor axis to major axis, a measure of rectilinearity. STAB represents ellipse stability, and IANG represents the orientation of the major axis relative to north.

Table 12. Statistical summary of land (Travis) and SNLT wind data dervied from 40 hr low-passed time series (30 May-4 July 1977); n = 859 hourly values. SE and NE refer to components offshore and alongshore, respectively. Spectral statistics represent averages for bands greater than 40 hr.

Table 13. Variance (cm^2/s^2) and percentage of total variance in low-frequency bands for 40 hr low-passed a) east (u) and b) north (v) current components, by period.

Table 14. Variance (cm^2/s^2) and percentage of total variance in low-frequency bands for V , principal axis of 40 hr low-passed current vector, by period.

Table 15. As Table 11 for 40 hr low-passed current. Total kinetic energy in cm^2/s^2.

Table 16. Cross-correlation statistics, by period, for significant frequencies, comparing x and y wind components and V , principal axis of current. Positive phase indicates wind

leads. NS indicates phase not statistically different from zero.

Table 17. Variance (cm^2) and percentage of total variance in low-frequency bands for 40 hr low-passed sea-level from Ft. Pulaski and SNLT, by period.

Table 18. Variance (cm^2) and percentage of total variance in low-frequency bands for sea-level and subsurface pressure stations during Period 4. Variance data for coastal (CHS-DB) and 15 m isobath alongshelf sea-level gradients are included.

Table 19. Cross-correlation statistics, by period, for significant frequencies, comparing wind stress, sea-level stations, and alongshelf sea-level gradients. Positive phase indicates first series leads. NS indicates a phase not statistically different from zero.

Table 20. Tidal harmonics, by period, for 29-day records of SNLT and Ft. . Pulaski 3 hr low-passed sea-level. Important tidal components and overtides are shown, along with tidal and total variance in series. The abbreviation %V represents the percentage of total variance contained in tidal constituents.

Table 21. Tidal harmonics, by period, for 29-day records of 3 hr low-passed a) u and b) v current components at SNLT. Important tidal components and overtides are shown, along with tidal and total variance in series. The symbol %V is represents percentage of total variance contained in tidal constituents.

Table 22. Summary of primary tidal components, by period, from rotary spectral analysis for 3 hr low-passed wind and current at SNLT. Total kinetic energy in m^2/s^2 for wind and cm^2/s^2 for current. ROTC is the ratio of minor axis to major axis; STAB is ellipse stability; and DIR is the orientation of major axis relative to the north. The symbol %E represents the percentage of the total variance contained in that frequency.

Table 23. Tidal harmonics, by period, for 29-day records of 3 hr low-passed salinity at SNLT. Important tidal components and overtides are shown, along with tidal and total variance in series. The symbol %V represents the percentage of total variance contained in tidal constituents.

LIST OF FIGURES

period. a) Period 2, b) Period 4, c) Period 5, and d) Period 6.

Figure 8. Time series of 40 hr low-passed barometric pressure (upper) and air temperature (lower) at SNLT, for Periods 1-5 (a-e). See individual figures for time period.

Figure 9. Time series of 40 hr low-passed surface (upper) and bottom (lower) water temperature at SNLT (Figure 3), for Periods 1-6 (a-f). See individual figures for that time period.

Figure 10. Time series of 40 hr low-passed water temperature at SNLT, comparing temperature at three levels (Figure 3) for Periods 1-6 (a-f). See individual figures for time periods. Generally, surface temperatures follow upper curve and bottom temperatures follow lowest curve.

Figure 11. Times series of 40 hr low-passed salinity at SNLT. a) Period 4, b) Period 5, and c) Period 6. See individual figures for time period.

Figure 12. Monthly mean vectors of SNLT winds and currents. Vector A denotes the mean for that month for all values from all years of data. Vectors b, c, d, and e define monthly means from 1977, 1980, 1981, and 1983-84, respectively. North is toward top of figure.

Figure 13. Monthly means and standard deviations of sea-level from SNLT, with data from Ft. Pulaski (Savannah), Charleston, and Daytona Beach included as reference. Monthly means from 1977, 1980, 1981, and 1983-84 are represented by open symbols. Means are relative to an arbitrary datum plane

unique to each location. Vertical lines represent one standard deviation from mean. Means for all years combined are represented by closed symbols connected by an oscillating line.

Figure 14. Means for each month for all air and water temperature data collected for SNLT. Vertical lines define ranges of monthly mean temperatures for each month. Temperature was recorded during only one year for January, February, June, October, November, and December.

Figure 15a. Monthly means and standard deviations of SNLT air and water temperature during 1977. The legend is the same as that for Figure 14.

Figure 15b. Monthly means and standard deviations of SNLT air and water temperature for 1980 (defined by broken standard deviation lines) 1981 (defined by solid standard deviation lines), and 1983-84 (defined by dotted standard deviation lines). The legend is same as that for Figure 14.

Figure 16. Monthly mean vectors and principal axes of SNLT wind stress and currents. Arrows represent monthly mean vectors. Crosses denote major and minor axes of standard deviation about the mean. North is toward top of figure. Currents from 1977 were obtained 1 m from bottom; 1980 and 1981 currents were obtained 8 m from bottom.

Figure 17. Monthly variations in intensity of wind speed at SNLT. Shaded areas represent percentage of monthly wind speeds greater than 5, 7.5, 10, and 12.5 m/s, respectively. For example, winds during January blew greater than 5 m/s 75%

of the time, greater than 7.5 m/s 58% of the time, greater than 10 m/s 33% of the time, and greater than 12.5 m/s 18% of the time. Unshaded area represents percentage of wind speeds less than 5 m/s. All wind data at SNLT during 1977 - January 1984 (Periods 1-8) were used in the analysis.

Figure 18. Auto- and cross-spectral plots of east (TAUX) and north (TAUY) 40 hr low-passed wind stress components at SNLT for a) Period 1, b) Period 2, c) Period 3, d) Period 4, e) Period 5, and f) Period 6. Order of plots is as follows. First column of plots includes autospectrum of series 1 (TAUX), and series 2 (TAUY), and cross-spectrum of the two series. Confidence intervals of 95% are shown. Second column includes auto- and cross-spectra from column one, divided by frequency. This represents variance preserved. Third column includes plots of coherence squared, phase, and gain between the two series. Confidence levels 50, 80, 90, 95, and 99% are shown for coherencere shown for coherence squared. A confidence interval of 95% for phase is also given.

Figure 19. Regression of land-based (Travis Field, Savannah Airport) wind speed on SNLT wind speed, showing approximate 2:1 ratio between ocean and land winds. Data from Period 1 (21 February-16 March 1977).

Figure 20. Stick vector diagrams of 40 hr low-passed time series, Period 2, 30 May-4 July 1977. SAV represents land wind from Travis Field, and SNLT represents ocean wind from SNLT. Currents obtained 1 m above bottom at SNLT. All data are

in oceanographic convention; i.e., wind vectors point downwind. Vectors are plotted for every six hours.

Figure 21. Autospectra of 10 hr low-passed land (SAV) and ocean (SNLT) wind time series, Period 2, 27 May-7 July 1977. The total energy in vectors is expressed in variance units.

Figure 22. Auto- and cross-spectral plots of east (u) and north (v) 40 hr low-passed current components at SNLT; for a) Period 1, b) Period 2, and c) Period 5. Refer to Figure 17 for details.

Figure 23. Auto- and cross-spectral plots of 40 hr low-passed east (TAUX) and north (TAUY) wind stress versus major axis current component (VTHETA) at SNLT; a,b) Period 1; c,d) Period 2; e,f) Period 3; and g,h) Period 5. Refer to Figure 17 for details.

Figure 24. Rotary spectral correlation between 40 hr low-passed wind stress and principal current component (V = 62.8° from east) at SNLT, for Period 5. Solid lines enclose wind directions and frequencies at which current was coherent with wind at 90% (.48) and 95% (.64) confidence levels. Broken lines represent phase, in degrees, between wind and current. Positive phase indicates wind lags current. Concentric circles represent frequency in cycles per day. Compass directions and current-and-shoreline orientation are included.

Figure 25. Auto- and cross-spectral plots of 40 hr low-passed east (u) and north (v) current at SNLT versus sea level at Ft.

Pulaski (a,b) (Period 2; at SNLT (c,d) Period 5. Refer to Figure 17 for details.

Figure 26. Auto- and cross-spectral plots of 40 hr low-passed east (TAUX) and north (TAUY) wind stress at SNLT versus sea level at Ft. Pulaski (a,b) Period 2 and c,d) Period 4; and at SNLT (e,f) Period 5 and (g,h) Period 6. Refer to Figure 17 for details.

Figure 27. Time series of 40 hr low-passed a) sea level from Charleston (upper) and Daytona Beach (lower), and b) subsurface pressure at 15 m isobath off Georgia (upper) and Florida (lower), during Period 4.

Figure 28. Auto- and cross-spectral plots of 40 hr low-passed a) Charleston versus Daytona Beach sea level; b) Georgia versus Florida subsurface pressure; c) Ft. Pulaski sea level versus Georgia subsurface pressure; and d) Daytona Beach sea level versus Florida subsurface pressure, during Period 4. Refer to Figure 17 for details.

Figure 29. Time series of 40 hr low-passed alongshore sea level slope (lower) calculated between a) Daytona Beach and Charleston, and b) Florida and Georgia sea level differences during Period 4. Positive values indicate northward slope. East wind stress at SNLT is presented in upper plot for comparison.

Figure 30. Auto- and cross-spectral plots of 40 hr low-passed a) east (TAUX) and b) north (TAUY) stress at SNLT versus alongshore sea level slope at coast, c) east (TAUX) and d) north

Figure 37. Auto- and cross-spectral plots of 3 hr low-passed east (x) and north (y) current at SNLT versus sea-level; at Ft. Pulaski, a,b) Period 2 and c,d) Period 4; and at SNLT, e,f) Period 5 - first 29 days and g,h) Period 5 - last 29 days. Refer to Figure 17 for details.

Figure 38. Time series of 3 hr low-passed wind stress at SNLT during Period 3 (lower), showing daily variance along major axis of wind (57°N). North (y) tidal current at SNLT presented in upper plot for comparison.

Figure 39. Auto- and cross-spectral plots of 3 hr low-passed a) east (u) and b) north (v) current versus major axis wind stress (57°N) at SNLT during Period 3. Refer to Figure 17 for details.

Figure 40. Time series of wind stress and current at SNLT during Period 3, band-passed with a filter centered about 24 hr to define daily events. Fortnightly (14-day) tidal cycle is seen in series. From top to bottom, time series are wind stress major axis, wind stress minor axis, east current, and north current.

Figure 41. Time series of 3 hr low-passed salinity at SNLT showing tidal variations during first 29 days of a) Period 4, b) Period 5, and c) Period 6.

Figure 42. Autospectral plots of 3 hr low-passed salinity at SNLT showing variance and variance preserved during a) Period 4, b) Period 5, and c) Period 6.

Table 1.

Period		No. Hourly Values
1	17 Feb 1977 - 17 May 1977	2122
2	26 May 1977 - 21 July 1977	1345
3	27 July 1977 - 20 Sept 1977	1321
4	3 Apr 1980 - 20 Aug 1980	3332
5	7 Mar 1981 - 22 May 1981	1844
6	20 July 1981 - 23 Oct 1981	2291
7	12 Nov 1982 - 23 Dec 1982	984
8	5 Nov 1983 - 21 Jan 1984	1848
9	2 Mar 1984 - 12 July 1984	3192
10	13 July 1984 - 31 Dec 1984	4128

Table 2.

Filter Characteristics for Filters Used in Processing SNLT Data

	3 hour low-pass	40 hour low-pass
0.25 amplitude period (frequency)	3 hr (8.0 cpd)	40 hr (0.6 cpd)
0.1 amplitude period (frequency)	2.6 hr (9.2 cpd)	34 hr (0.7 cpd)
Number of weights	5	193
Data loss, each end	2 hr	4 days

Table 3.

Sensor: Wind Units: m/s

	1977			1980			1981			1983-84		
	n	$\bar{x}$ ± sd		n	$\bar{x}$ ± sd		n	$\bar{x}$ ± sd		n	$\bar{x}$ ± sd	
		East	North		East	North		East	North		East	North
Jan.										63	-0.15±3.73	-2.81±5.18
Feb.	29	2.95±3.71	3.17±4.32									
Mar.	124	0.65 5.40	1.06 4.21				85	2.41±3.83	0.18±3.59			
Apr.	120	0.94 4.50	1.68 2.94	93	2.78±5.23	2.19±3.90	120	0.12 4.99	1.96 2.98			
May	57	-1.65 2.97	0.36 2.60	124	0.22 3.99	2.21 3.99	71	0.02 3.49	-0.76 4.00			
June	120	2.85 3.95	0.78 1.95	120	0.88 4.40	2.47 2.90						
July	69	1.11 3.32	2.14 1.44	124	1.05 3.59	3.01 2.53	33	2.80 2.71	3.74 3.22			
Aug.	124	-1.72 3.09	1.43 2.25	63	3.06 2.26	4.86 1.29	124	-1.04 4.33	0.31 3.97			
Sept.	61	-0.30 4.20	0.32 2.58				120	-1.54 3.72	0.12 2.33			
Oct.							74	-1.87 4.71	-2.25 4.31			
Nov.										92	2.13 5.11	0.04 4.56
Dec.										124	1.38 5.04	-2.18 6.14

	Average		
	n	$\bar{x}$	
		East	North
Jan.	63	-0.15	-2.81
Feb.	29	2.95	3.17
Mar.	209	1.37	0.70
Apr.	333	1.16	1.92
May	252	-0.26	0.95
June	240	1.87	1.63
July	226	1.32	2.85
Aug.	311	-0.48	1.68
Sept.	181	-1.12	0.19
Oct.	74	-1.87	-2.25
Nov.	92	2.13	0.04
Dec.	124	1.38	-2.18

Table 4.

Sensor: Current Units: cm/s

	1977			1980			1981			Average		
	n	x ± sd		n	x ± sd		n	x ± sd		n	x	
		East	North		East	North		East	North		East	North
Feb.	29	0.99±1.98	5.13±2.05							29	0.99	5.13
Mar.	124	0.12 3.79	3.24 2.68				85	1.46±2.06	0.60±5.23	209	0.66	2.17
Apr.	120	2.21 4.29	5.12 2.63	93	4.28±4.05	2.93±5.41	120	1.44 4.11	0.54 6.25	333	2.51	2.86
May	57	1.74 4.62	2.63 1.68				71	1.65 2.96	-0.15 5.03	128	1.69	1.09
June	120	4.06 4.85	2.67 2.69							120	4.06	2.67
July	69	7.16 3.14	2.08 1.26							69	7.16	2.08
Aug.	124	5.36 3.92	1.62 1.63							124	5.36	1.62
Sept.	61	0.47 0.45	3.38 4.14							61	0.47	3.38

Table 5.

Sensor: Sea Level Units: cm

	1977		1980		1981		1983-84	
	n	$\bar{x}$ ± sd	n	$\bar{x}$ ± sd	n	$\bar{x}$ ± sd	n	$\bar{x}$ ± sd
	Ft. Pulaski						SNLT	
Jan.								
Feb.							63	25.0±9.59
Mar.					85	33.0±11.60		
Apr.			93	14.8± 9.87	120	23.0 13.45		
May	8	34.9± 2.55	124	23.1 11.97	71	42.0 7.30		
June	120	23.4 10.23	120	22.1 15.37				
July	65	5.4 5.83	124	12.6 9.86	33	28.0 10.08		
Aug.			63	1.4 5.84	124	43.0 7.33		
Sept.					120	44.0 12.21		
Oct.					74	38.0 9.90		
Nov.							92	29.0 10.83
Dec.							124	17.0 9.10

	1977					1980					1981					1983-84		
	n	Air	Surf	Mid	Bot	n	Air	Surf	Mid	Bot	n	Air	Surf	Mid	Bot	n	Air	Surf
Jan																63	7.73 ±3.05	9.50 ±0.41
Feb	29	13.24 ±2.19	11.34 ±0.86	10.45 ±0.41	10.43 ±0.39													
Mar	124	16.18 ±2.85	14.68 ±2.06	13.82 ±1.55	13.76 ±1.53						85	14.01 ±2.35	13.95 ±0.49	13.55 ±0.41	13.20 ±0.40			
Apr	120	20.00 ±2.10	19.86 ±1.91	18.29 ±1.26	18.20 ±1.33	73	14.22 ±1.57	15.48 ±0.65	14.96 ±0.44	14.63 ±0.37	120	20.05 ±1.73	18.63 ±1.71	18.14 ±1.73	17.56 ±1.57			
May	57	22.69 ±1.69	23.27 ±1.11	22.66 ±0.95	23.04 ±0.69	71	16.24 ±1.69	17.86 ±1.42	17.40 ±1.56	17.11 ±1.25	71	21.18 ±1.73	21.47 ±0.62	21.26 ±0.60	20.66 ±0.62			
June	120	27.74 ±1.57	28.56 ±0.87	27.82 ±0.62	27.54 ±0.60													
July	69	29.28 ±0.84	30.58 ±0.63	30.17 ±0.41	30.43 ±0.79						33	30.47 ±1.13	30.51 ±0.17	30.48 ±0.14	29.69 ±0.10			
Aug	124	28.84 ±0.95	30.71 ±0.47	30.45 ±0.41	30.29 ±0.39						124	29.04 ±1.93	28.90 ±1.31	28.84 ±1.18	27.80 ±1.17			
Sept	61	28.83 ±0.85	29.95 ±0.20	29.70 ±0.20	29.56 ±0.20						120	27.33 ±3.49	27.10 ±0.56	27.18 ±0.48	26.20 ±0.47			
Oct											74	22.93 ±2.59	24.32 ±1.49	24.30 ±1.53	23.26 ±1.64			
Nov																92	15.40 ±3.40	17.97 ±0.89
Dec																124	10.47 ±6.44	14.96 ±2.31

	Average				
	n	Air	Surf	Mid	Bot
Jan	63	7.73	9.50		
Feb	29	13.24	11.34	10.45	10.43
Mar	209	15.30	14.38	13.71	13.53
Apr	313	18.67	18.37	17.46	17.12
May	199	19.89	20.70	20.28	20.08
June	120	27.74	28.56	27.82	27.54
July	102	29.67	30.56	30.27	30.19
Aug	248	28.94	29.81	29.56	29.05
Sept	181	27.63	28.06	28.03	27.33
Oct	74	22.93	24.32	24.30	23.26
Nov	92	15.40	17.97		
Dec	124	10.47	14.96		

Table 6.
Temperature - Means + Standard Deviations (C°)

Table 7.

Sensor: Salinity Units: ppt

	1977		1980		1981		Average	
	n	$\bar{x}$ ± sd	n	$\bar{x}$ ± sd	n	$\bar{x}$ ± sd	n	$\bar{x}$
Feb.								
Mar.								
Apr.		L3	73	31.69±1.30	97	33.62±0.66	170	32.79
May		L3	39	33.63 0.61	71	31.05 0.69	110	31.96
		L1	24	33.52 0.92			24	33.52
June								
July				L1	33	29.31 0.86	33	29.31
Aug.				L1	91	28.27 0.92	91	28.27
Sept.								
Oct.								

Table 8.

Vector Statistics - Wind Stress (dynes/cm^2)

		Component E	Component N	Vector Speed	Vector Dir.	Standard Deviation of Axes Major	Standard Deviation of Axes Minor	Angle of Major Axis (deg. from N)
1977	Feb	0.40	0.35	0.53	49	1.01	0.58	140
	Mar	0.14	0.16	0.21	41	1.21	0.84	104
	Apr	0.17	0.16	0.23	47	0.84	0.55	89
	May	-0.12	0.01	0.12	275	0.45	0.19	54
	June	0.34	0.08	0.35	77	0.64	0.25	83
	July	0.12	0.17	0.21	35	0.45	0.12	68
	Aug	-0.17	0.08	0.19	295	0.50	0.19	67
	Sept	-0.05	0.01	0.05	281	0.64	0.26	66
1980	Apr	0.38	0.31	0.49	51	1.11	0.71	72
	May	0.00	0.21	0.21	0	0.83	0.34	63
	June	0.14	0.28	0.31	27	0.98	0.32	56
	July	0.13	0.32	0.35	22	0.69	0.33	54
	Aug	0.36	0.53	0.64	34	0.51	0.16	46
1981	Mar	0.32	-0.02	0.32	94	0.80	0.57	124
	Apr	-0.03	0.18	0.18	351	1.10	0.32	63
	May	-0.08	-0.19	0.21	203	1.10	0.25	35
	June							
	July	0.34	0.45	0.54	37	0.71	0.05	40
	Aug	-0.10	0.01	0.10	276	0.97	0.24	50
	Sept	-0.04	-0.01	0.14	266	0.58	0.25	67
	Oct	-0.38	-0.41	0.56	223	1.52	0.24	47
1983	Nov	0.36	0.04	0.36	84	1.17	0.89	130
1984	Dec	0.22	-0.49	0.54	156	1.47	0.96	140
1984	Jan	-0.12	-0.50	0.72	193	1.07	0.49	141

Weighted Monthly Means

Jan	-0.12	-0.50	1.07	0.49	141
Feb	0.40	0.35	1.01	0.58	140
Mar	0.21	0.09	1.04	0.73	112
Apr	0.16	0.21	1.01	0.51	75
May	-0.05	0.05	0.81	0.28	53
June	0.24	0.18	0.81	0.29	69
July	0.16	0.29	0.62	0.22	55
Aug	-0.06	0.24	0.69	0.21	56
Sept	-0.11	0.00	0.60	0.25	67
Oct	-0.38	-0.41	1.52	0.24	47
Nov	0.36	0.04	1.17	0.89	130
Dec	0.22	-0.49	1.47	0.96	141

Table 9.

Vector Statistics - Currents (cm/s)

		Component E	Component N	Vector Speed	Vector Dir.	Standard Deviation of Axes Major	Standard Deviation of Axes Minor	Angle of Major Axis (deg. from N)
1977	Feb	0.99	5.13	5.22	11	3.37	2.22	138
	Mar	0.12	3.24	3.24	1	6.03	2.58	59
	Apr	2.21	5.12	5.58	23	6.84	1.98	61
	May	2.04	2.99	3.62	34	6.86	1.14	72
	June	4.06	2.67	4.86	57	7.54	2.18	64
	July	7.18	2.08	7.48	74	4.46	1.17	72
	Aug	5.36	1.62	5.60	73	5.74	1.76	74
	Sept	0.47	3.38	3.41	8	6.54	5.60	120
1980	Apr	4.28	2.93	5.19	56	9.11	2.85	35
1981	Mar	1.46	0.60	1.58	68	7.49	2.65	10
	Apr	1.44	0.54	1.54	69	10.40	2.12	32
	May	1.65	-0.15	1.66	95	8.09	1.64	29
				Weighted Monthly Means				
	Mar	0.66	2.17	2.27	17	6.62	2.61	39
	Apr	2.44	2.86	3.76	27	8.74	2.25	44
	May	1.69	1.09	2.01	57	7.38	1.36	50

Table 10a.

East Wind Component (x)

Period	1		2		3		4		5		6	
	Var.	%	Var.	%	Var.	%	Var.	%	Var.	%	Var.	%
>10d	.091	20.1	.016	9.0	.030	22.0	.097	30.1	.036	9.8	.091	32.2
6-10	.061	13.5	.027	15.2	.026	19.1	.073	22.7	.101	27.5	.030	10.7
3-6	.102	22.6	.044	24.8	.020	14.7	.087	27.0	.114	31.3	.045	15.7
2-3	.098	21.5	.029	16.3	.012	8.8	.005	1.6	.007	1.9	.003	0.9
>2d	.3524	77.7	.1160	65.3	.0880	64.6	.2620	81.4	.2575	70.5	.1688	59.5
total	.4536		.1775		.1364		.3220		.3657		.2832	

Table 10b.

North Wind Component (y)

>10d	.048	19.8	.003	10.3	.007	17.0	.043	26.2	.064	24.1	.069	31.5
6-10	.049	20.3	.006	20.6	.010	24.3	.035	21.3	.061	23.1	.037	17.1
3-6	.058	23.9	.009	30.9	.010	24.3	.046	28.0	.090	34.1	.020	9.2
2-3	.042	17.4	.004	13.7	.004	9.7	.002	1.2	.007	2.6	.001	0.4
>2d	.1975	81.4	.0220	75.5	.0310	75.3	.1260	76.7	.2222	83.9	.1268	58.2
total	.2425		.0291		.0411		.1644		.2648		.2177	

Table 11.

Wind Low-frequency rotary statistics

Period	Band (days)	Total KE	ROTC	STAB	IANG (N)
1	6.4-32	15810	.39	.17	90°
2	>6.3	5857	-.07	.60	81
2	2.7-4.75	3310	.37	.46	84
3	>6	7720	.04	.48	65
4	3.7-26	30036	.34	.44	63
5	>13.5	10030	.21	.21	84
5	4.5-9	11150	.31	.50	55
6	>5.8	28822	.14	.75	47

Table 12.

	Land Wind	Ocean Wind
SE Comp $\bar{x}$ ± sd (m/s)	0.57 ± 1.46	0.01 ± 2.47
NE Comp $\bar{x}$ ± sd (m/s)	1.22 ± 1.76	3.17 ± 3.83
Mean Speed (m/s)	1.35	3.17
Mean Dir.	70°	45°
Band (> 40 hr) Variance (m^2/s^2)	2.63	13.28

Table 13a.

East Current Component (u)

Period	1		2		3		4		5		6	
	Var.	%	Var.	%	Var.	%	Var.	%	Var.	%	Var.	%
>10d	2.90	17.6	1.83	10.8					2.51	23.0		
6-10	3.44	20.9	4.27	25.2					2.92	26.8		
3-6	3.23	20.0	6.38	37.7					3.43	31.5		
2-3	3.92	23.8	1.41	8.3					.071	0.7		
>2d	13.548	82.3	13.886	82.0					8.923	82.0		
total	16.465		16.915						10.876			

Table 13b.

North Current Component (v)

>10d	1.40	19.8	0.73	13.8					9.32	29.1		
6-10	1.38	19.5	1.38	26.2					9.72	30.4		
3-6	1.21	17.1	1.40	26.6					8.68	27.1		
2-3	1.43	20.3	0.60	11.3					0.17	0.6		
>2d	5.407	76.7	4.103	77.9					27.89	87.2		
total	7.043		5.268						31.998			

Table 14.

Current Component V_θ (°N)

Period	1		2		3		4		5		6	
V_θ =	61°		79°		90°				27°			
	Var.	%	Var.	%	Var.	%	Var.	%	Var.	%	Var.	%
>10d	3.54	17.2	2.20	10.9	2.33	16.5			10.85	27.4		
6-10	4.33	21.0	5.15	25.5	4.08	28.9			11.98	30.3		
3-6	3.99	19.4	7.48	37.1	3.66	25.9			11.43	28.9		
2-3	4.92	23.9	1.75	8.7	0.70	4.9			0.21	0.5		
>2d	16.782	81.5	16.59	82.0	10.768	76.2			34.468	87.1		
total	20.588		20.184		14.116				39.606			

Table 15.

Current Low-frequency rotary statistics

	Band (days)	Total KE	ROTC	STAB	IANG(N)
1	5.3-32	10170	.02	.59	61°
1	2-3	4617	.07	.74	62
2	>6.3	9080	.05	.57	73
2	2.7-4.75	4393	-.12	.85	68
3	>9	10120	.15	.58	100
3	3.6-6	3335	.04	.48	58
4	>3	9260	-.10	.72	34
5	>4.5	28043	-.12	.78	27

Table 16.

Low-frequency wind-current cross-correlations

Data Period	V_θ	Period(days)	cross-spectrum	r^2	Phase(hr)
		Wind x vs V_θ			
1	61°	10	6.53	.62	-5.4 NS
		2.2	4.06	.79	3.7
2	79	8	4.42	.74	-8.1 NS
		3.4	4.36	.78	-1.3 NS
3	90	6	2.61	.58	18.5
5	27	17	16.5	.84	-22.8
		6	20.6	.96	-2.7 NS
		Wind y vs V_θ			
1	61	20	4.54	.65	96
		5.75	4.58	.54	20.4
2	79	8	2.18	.81	4.6 NS
3	90	11.8	2.30	.51	-3.1 NS
5	27	6	12.8	.69	6 NS

Table 17.

Component Sea Level

Period	1		2		3		4		5		6	
			Ft. Pulaski								SNLT	
	Var.	%	Var.	%	Var.	%	Var.	%	Var.	%	Var.	%
>10d			7.01	13.7					43.	23.4	42.	37.5
6-10			19.45	38.1					50.	27.2	25.	22.4
3-6			13.06	25.6					25.	13.6	14.	12.5
2-3			2.86	5.6					1.	0.54	0.2	0.2
>2d			42.38	83.0					119.	64.7	81.	72.6
total			51.031						184.		119.	

Table 18.

Period 4 SAB Sea Level

	Charleston		Ft. Pulaski		Daytona Beach		Ga 15 m		Fla 15 m		Coastal slope		15 m slope	
	Var.	%	Var.	%	Var.	%	Var.	%	Var.	%	Var.	%	Var.	%
>10d	31.21	21.8	43.69	27.0	29.37	29.1	19.62	21.5	15.18	32.1	0.42	25.4	.202	14.0
6-10	30.15	21.0	33.68	20.9	27.71	21.5	31.59	34.7	15.05	31.8	0.27	16.2	.532	36.8
3-6	32.48	22.7	40.18	24.9	19.31	19.1	19.91	21.8	8.59	18.2	0.43	25.6	.372	25.8
2-3	5.03	3.5	6.17	3.8	3.06	3.0	0.20	0.2	0.19	0.4	0.21	12.3	.009	0.6
>2d	98.883	69.0	123.710	72.7	73.451	72.7	71.314	78.2	39.004	82.5	1.325	79.5	1.115	77.2
total	143.281		161.075		100.982		91.156		47.290		1.667		1.445	

Table 19.

Significant Sea Level Cross-Correlations

	Period(days)	Cross-Spectrum	r^2	Phase(hr)
Period 1				
CHS - DB	7	257.0	.63	8.2 NS
τ_x - CHS	2-3	7.29	.77	8.6
τ_y - CHS	NS			
Period 2				
τ_x - FP	8	8.34	.70	-2.9 NS
	3.4	4.90	.82	1.3 NS
τ_y - FP	8	3.97	.73	10.6 NS
	2.8	0.95	.57	14.2
u -FP	8	120.0	.90	6.5 NS
	3.4	63.7	.93	9.6 NS
v - FP	8	58.3	.69	4.8 NS
	3.2	27.2	.83	0.8 NS
CHS - DB	8	243.0	.98	3.1 NS
τ_x - slope	8-10	.623	.53	40
τ_y - slope	NS			
Period 3				
CHS- DB	9.4	245.0	.76	13.8 NS
τ_x - CHS	9.4	11.0	.72	15.8 NS
τ_y - CHS	9.4	6.77	.79	19.4
τ_x - slope	6	0.66	.52	6.2 NS
τ_y - slope	NS			
Period 4				
CHS - DB	44	555.0	.89	10.7 NS
	6.5-8.7	445.0	.90	5.7 NS
GA - FLA	7.3-11	299.0	.84	1.8 NS
FP - GA	7.3-11	472.0	.92	1.6 NS
DB - FLA	9.4-11	313.0	.88	2.9 NS
τ_x - FP	11.9	19.0	.55	7.4 NS
	6.6	29.7	.89	12.0 NS
τ_y - FP	8.7-10	20.2	.84	27.0
	4.7-6	11.1	.71	21.9
τ_x - coastal slope	6.6	2.59	.62	8.9 NS
τ_y - coastal slope	6.6	1.29	.59	1.2 NS
τ_x - 15 m slope	6.6	3.57	.78	1.2 NS
τ_y - 15 m slope	NS			
Period 5				
CHS - DB	22	378.0	.92	1.6 NS
	9.3	167.0	.68	23.4
	3.6	79.5	.80	7.8
τ_x - slope	2.8	.304	.56	32.6 NS
τ_y - slope	NS			
τ_x - SNLT	NS			
τ_y - SNLT	NS			
Period 6				
CHS - DB	17	704.0	.88	8.3 NS
	6	412.0	.75	10.8
τ_x - slope	NS			
τ_y - slope	NS			

Table 20.

Parameter Sea Level — Tidal Harmonics

Units cm

Constituent	Period	1		2 Ft. Pul		3		4 Ft. Pul		5 SNLT		6 SNLT	
		A	E	A	E	A	E	A	E	A	E	A	E
M_2	12.42			105.85	-57°			106.79	-36°	86	36°	91	-13°
$S_2 + K_2$	12.00			13.58	112			21.73	29	14	18	14	18
N_2	12.66			26.40	21			24.94	93	23	73	20	66
L_2	12.19			9.43	82			5.29	75	7	-162	2	120
$K_1 + P_1$	23.93			13.84	60			8.64	-15	5	-92	10	40
O_1	25.82			6.12	-130			5.47	-6	8	93	5	-105
M_4	6.21			3.88	41			3.63	79	0.2	-119	2	-65
M_6	4.14			1.09	168			0.62	-122	0.3	-157	0.3	32
M_8	3.105			0.47	-70			0.14	-53	0.1	121	0.2	-132
$\sum V$ - tides				6209.44				6322.66		1764.		2025.	
Total V				6288.85				6476.79		1975.80		2083.01	
% V				99				98		89		97	

Table 21a.

Parameter East Current (u) Tidal Harmonics

Units cm/s

Constituent	Period	1		2		3		4 15 days		5		6	
		A	E	A	E	A	E	A	E	A	E	A	E
M_2	12.42	9.88	-101°	6.96	-147°	6.89	135°	22.42	-126°	20.44	-66°		
$S_2 + K_2$	12.00	2.73	-170	0.86	-19	1.44	-11	3.76	-81	3.25	-86		
N_2	12.66	2.47	177	1.70	-66	1.71	145			6.17	-34		
L_2	12.19	0.89	-24	0.85	-1	0.42	-69			2.51	95		
$K_1 + P_1$	23.93	0.57	147	1.13	-58	0.57	-150	0.76	-78	0.55	-143		
O_1	25.82	0.93	20	0.82	-130	0.51	159	1.75	-109	1.22	31		
M_4	6.21	0.35	88	0.73	58	1.33	-117	1.45	10	1.05	137		
M_6	4.14	0.20	-160	0.14	33	0.20	-166	0.24	-23	0.14	-12		
M_8	3.105	0.04	-126	0.08	-143	0.14	-43	0.06	-25	0.06	133		
$\sum V$ - tides		50.66		27.62		27.57		261.28		237.67			
Total V		70.07		54.72		52.10		305.35		260.76			
% V		81		50		53		86		91			

Table 21b.

Parameter North Current (v) Tidal Harmonics

Units cm/s

Constituent	Period	1		2		3		4 15 days		5		6	
		A	E	A	E	A	E	A	E	A	E	A	E
M_2	12.42	13.88	69°	13.90	9°	13.06	-65°	8.17	9°	4.96	55°		
$S_2 + K_2$	12.00	3.15	-2	1.66	171	1.62	156	2.25	146	0.32	61		
N_2	12.66	3.60	-33	4.11	79	2.49	-88			1.78	87		
L_2	12.19	1.33	63	2.29	160	1.17	139			1.08	-140		
$K_1 + P_1$	23.93	0.77	180	0.20	-76	1.34	-165	0.32	-158	1.20	-101		
O_1	25.82	1.25	146	0.53	-77	0.71	-154	2.76	21	0.58	69		
M_4	6.21	0.66	-125	0.62	137	0.79	-30	0.72	167	0.42	-36		
M_6	4.14	0.47	-2	0.66	166	0.63	-30	0.08	138	0.14	28		
M_8	3.105	0.28	-128	0.14	-85	0.24	48	0.01	75	0.01	29		
$\sum V$ - tides		110.12		109.64		92.04		40.02		15.50			
Total V		123.09		123.86		99.81		97.30		61.33			
% V		89		89		92		41		25			

Table 22.

SNLT Primary tidal components - rotary spectra summary

	Total KE	ROTC	STAB	DIR (N)	%E
		Winds 24 HR			
1	4245	.07	.31	127°	9
2	3061	.30	.42	132	14
3	3311	.20	.41	123	19
4	1759	.76	.52	162	8
5	1806	.55	.24	85	6
6	1286	.57	.64	153	5
		Currents 12.42 HR			
1	76660	.23	.94	150°	79
2	58230	.25	.96	151	74
3	47750	.31	.92	151	65
4	59200	.42	.92	108	78
5	139770	.41	.98	99	77
		Currents 6.21 HR			
3	3403	.70	.43	110°	5
4	380	.16	.81	117	0.5
5	687	.28	.73	120	0.4

Table 23.

Parameter Salinity

Units ppt

Tidal Harmonics

Constituent	Period	1		2		3		4		5		6	
		A	E	A	E	A	E	A	E	A	E	A	E
M_2	12.42							0.40	-133°	0.14	91°	0.16	-22°
$S_2 + K_2$	12.00							0.14	-118	0.01	-138	0.23	65
N_2	12.66							0.20	-72	0.06	134	0.06	-67
L_2	12.19							0.09	-75	0.06	-34	0.04	7
$K_1 + P_1$	23.93							0.20	125	0.06	65	1.06	128
O_1	25.82							0.08	168	0.11	-157	0.08	-79
M_4	6.21							0.04	-12	0.03	-173	0.01	91
M_6	4.14							0.01	-113	.000045	118	0.01	-21
M_8	3.105							0.01	-20	.001	-23	0.03	-84
$\sum V$ - tides								0.14		0.02		0.61	
Total V								0.99		0.57		1.24	
% V								14		4		49	

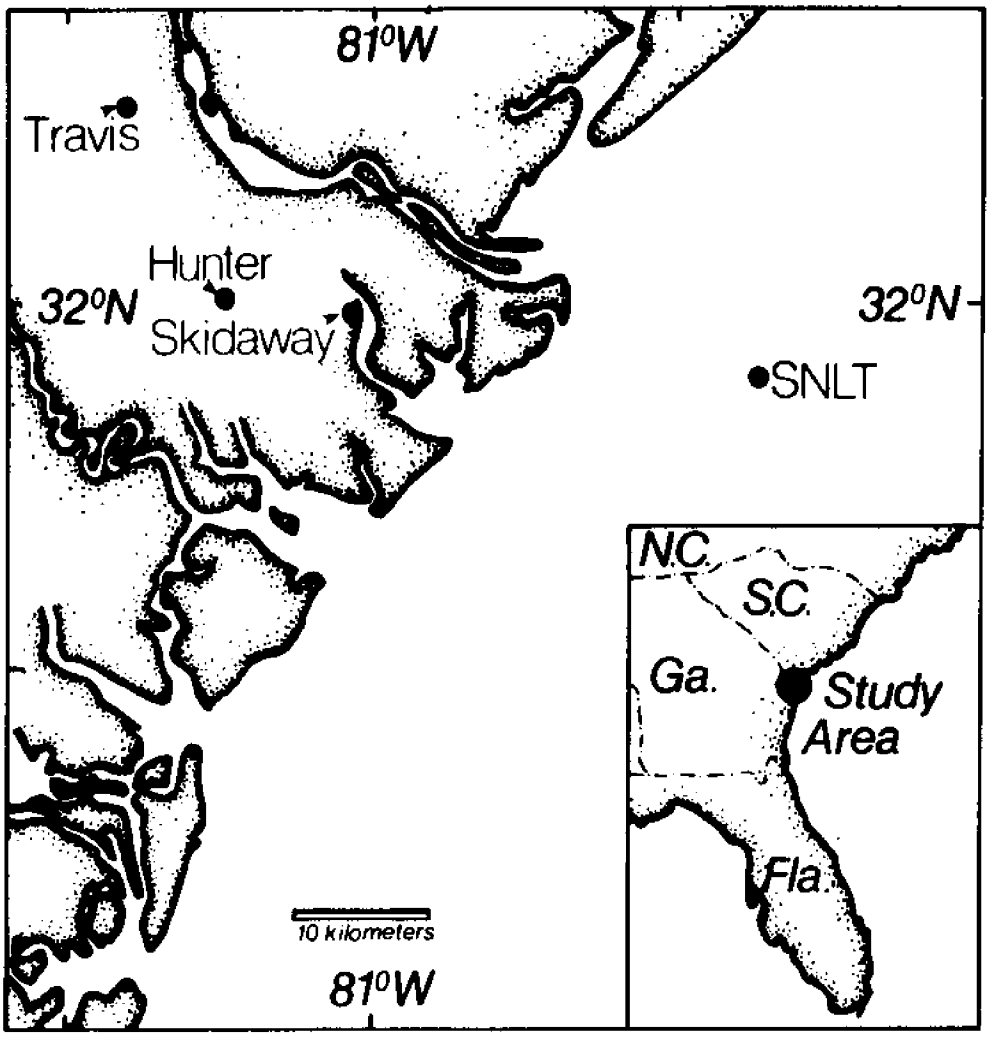

Figure 1. Map showing location of Savannah Navigational Light Tower (SNLT), Skidaway Institute of Oceanography, Hunter Army Air Field, and Travis Field (National Weather Service). Meteorological data from Hunter and Travis were used to calibrate SNLT instrumentation.

Figure 2. Savannah Navigational Light Tower (SNLT).

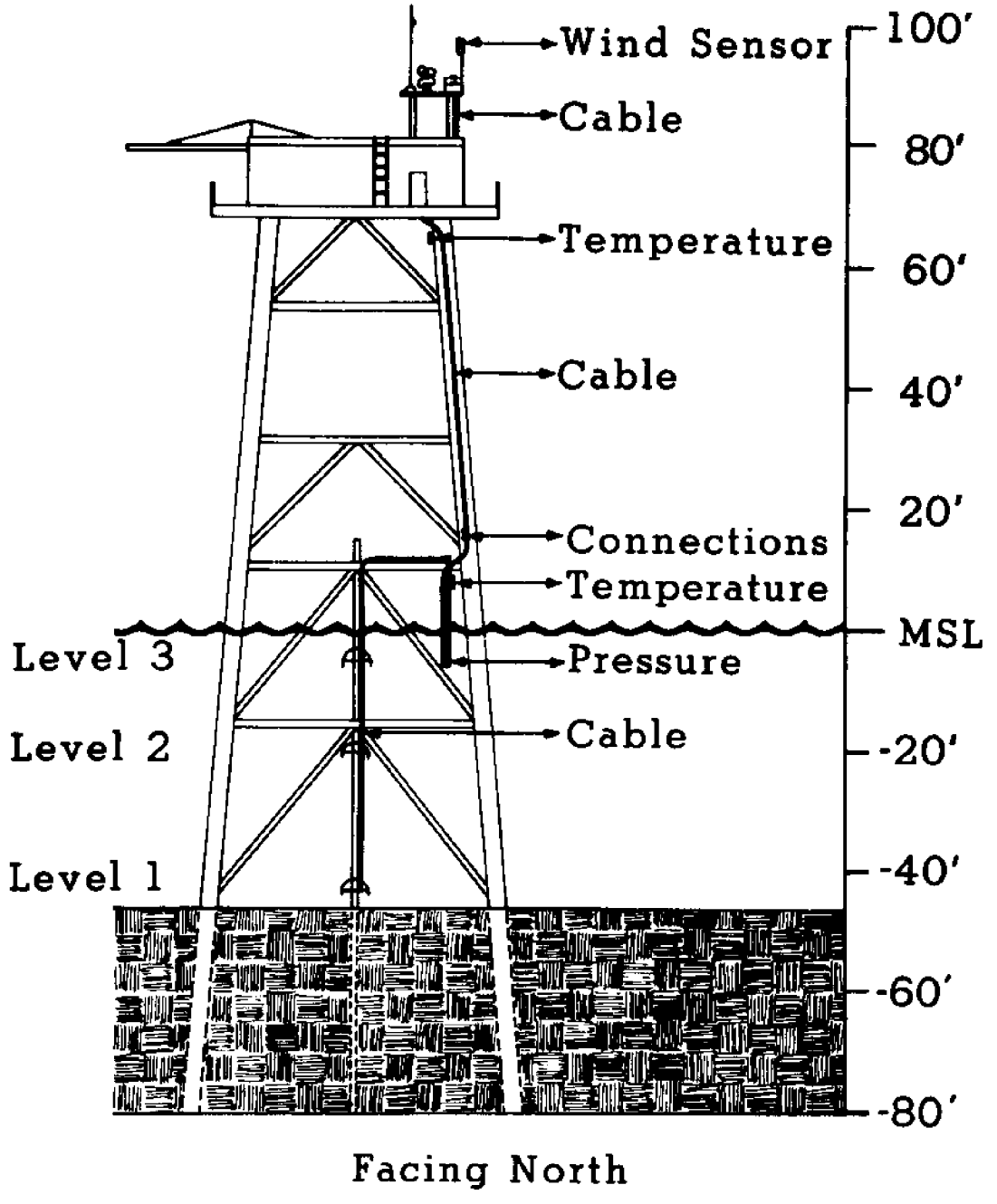

Figure 3. Schematic of SNLT showing location of oceanographic and meteorological instrumentation. Current, conductivity, and temperature are measured at each underwater level, located 1, 8 and 13 m from bottom, exemplified by Levels 1, 2, and 3, respectively.

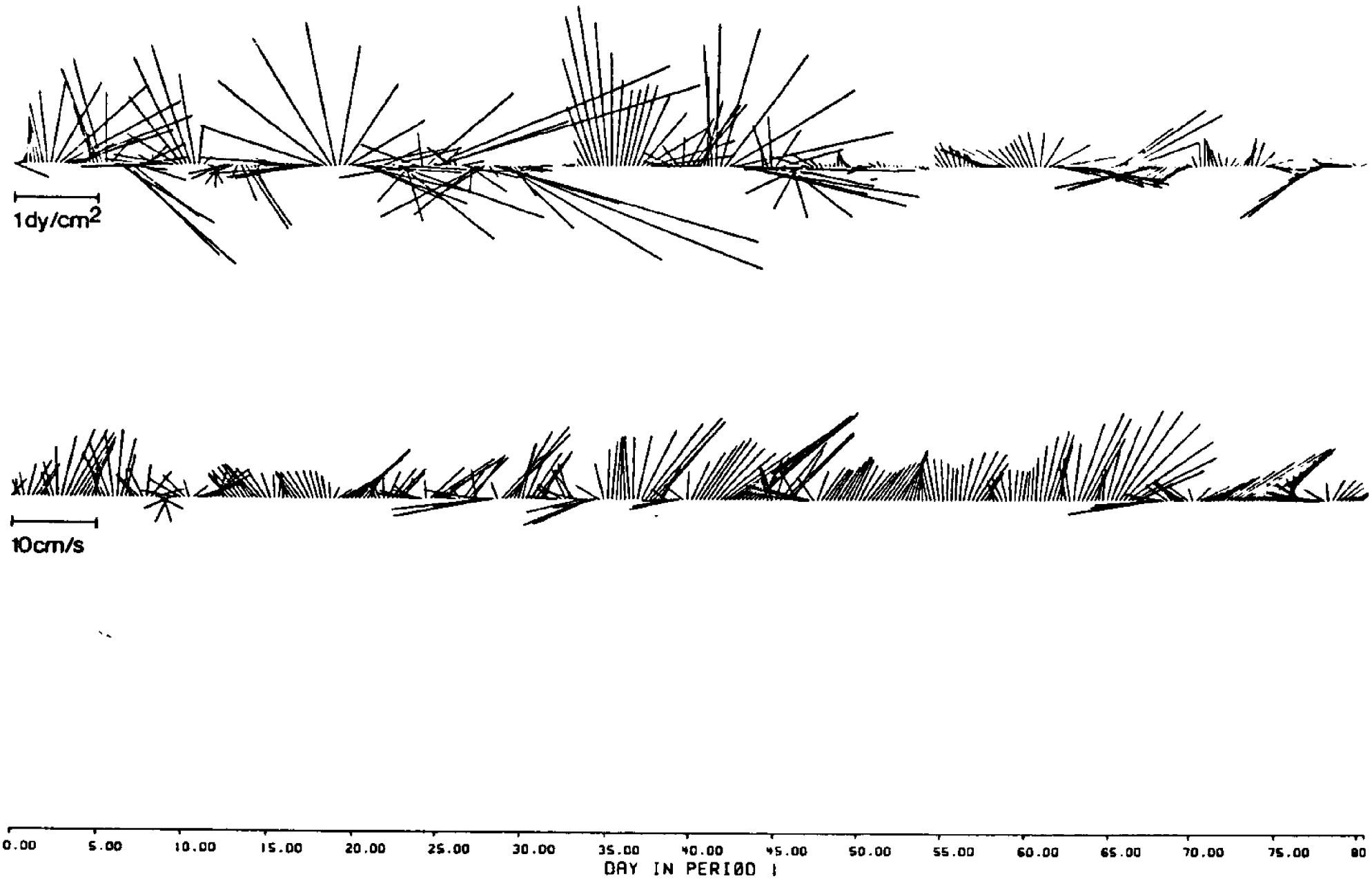

Figure 4a. Period 1, 21 February - 13 May 1977. Stick vector plot of 40 hr low-passed wind stress (dyne/cm^2) and current (cm/s) at SNLT. North is toward top of figure.

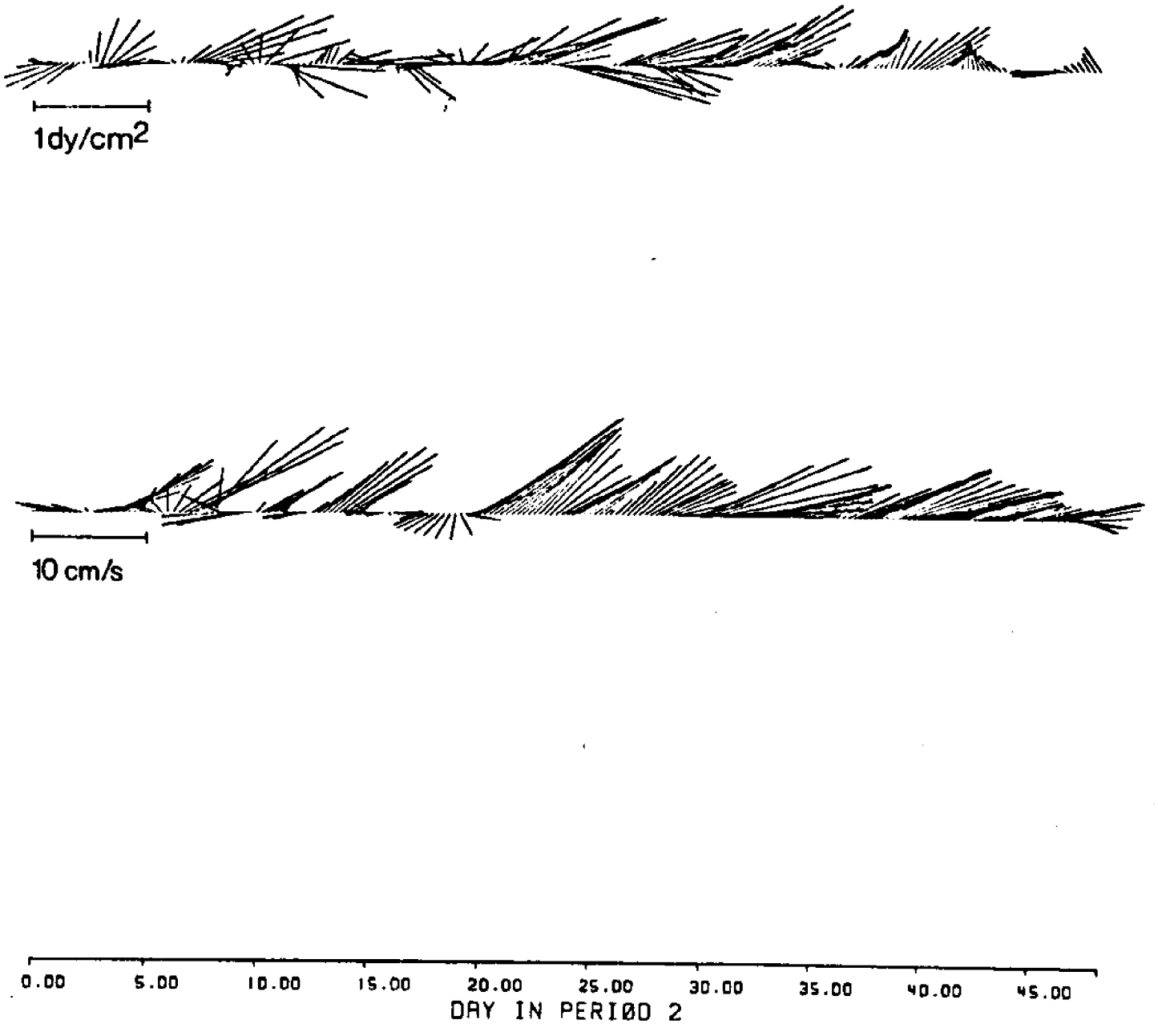

Figure 4b. Period 2, 30 May - 17 July 1977. Stick vector plot of 40 hr low-passed wind stress (dyne/cm^2) and current (cm/s) at SNLT. North is toward top of figure.

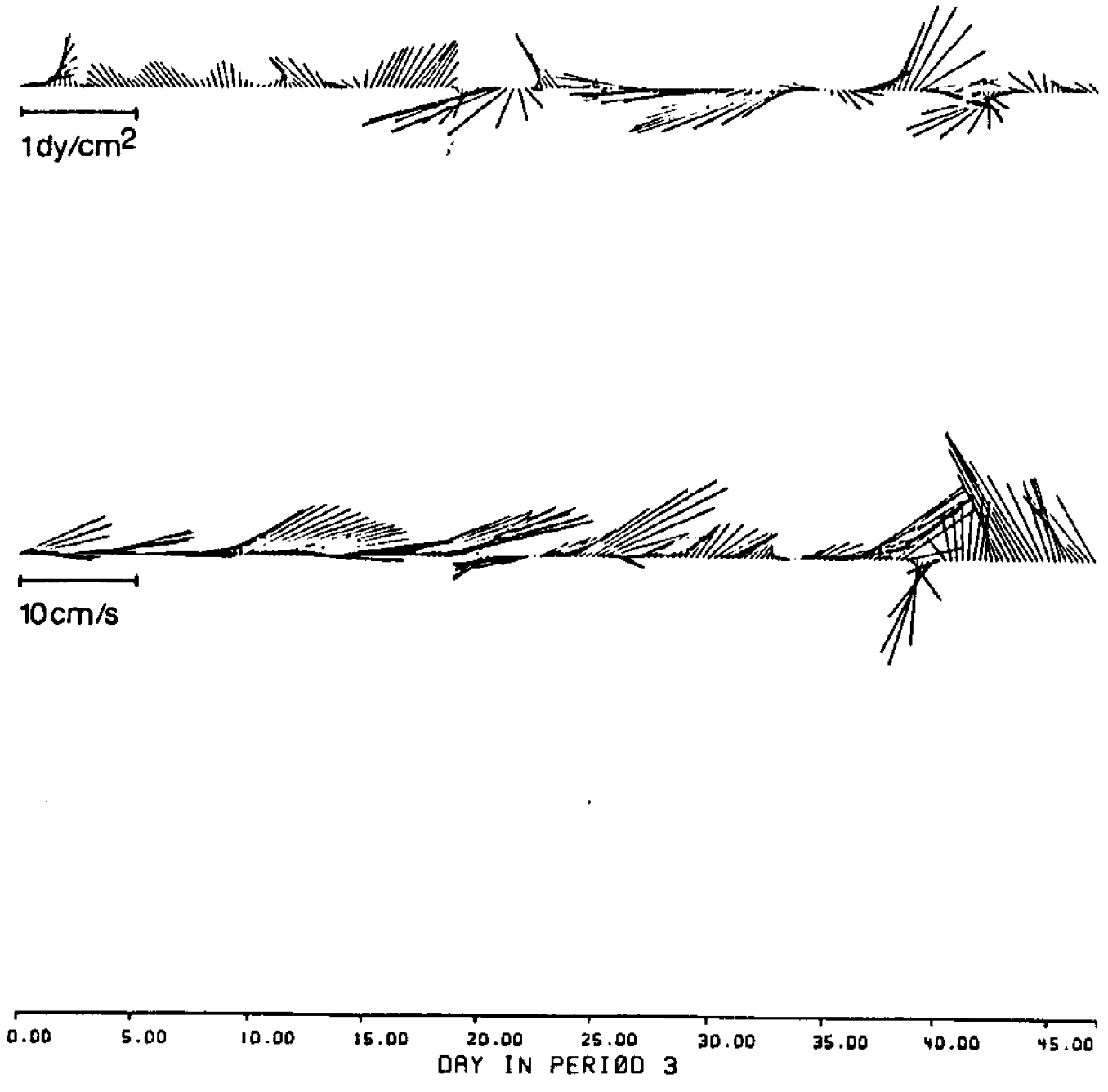

Figure 4c. Period 3, 31 July - 16 September 1977. Stick vector plot of 40 hr low-passed wind stress (dyne/cm^2) and current (cm/s) at SNLT. North is toward the top of figure.

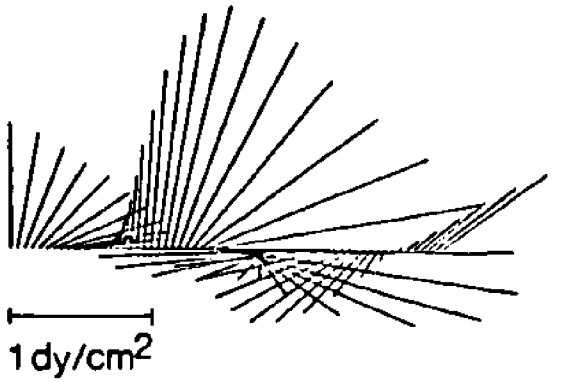

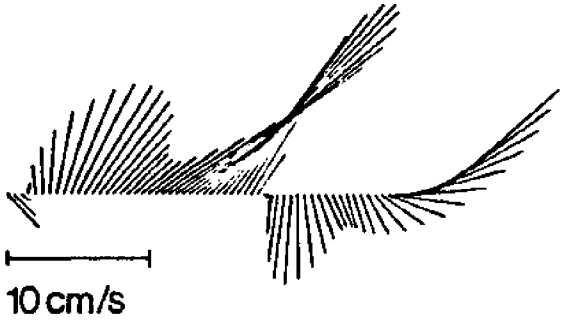

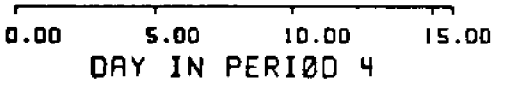

Figure 4d. Period 4, 7 - 22 April 1980. Stick vector plot of 40 hr low-passed wind stress (dyne/cm^2) and current (cm/s) at SNLT. North is toward top of figure.

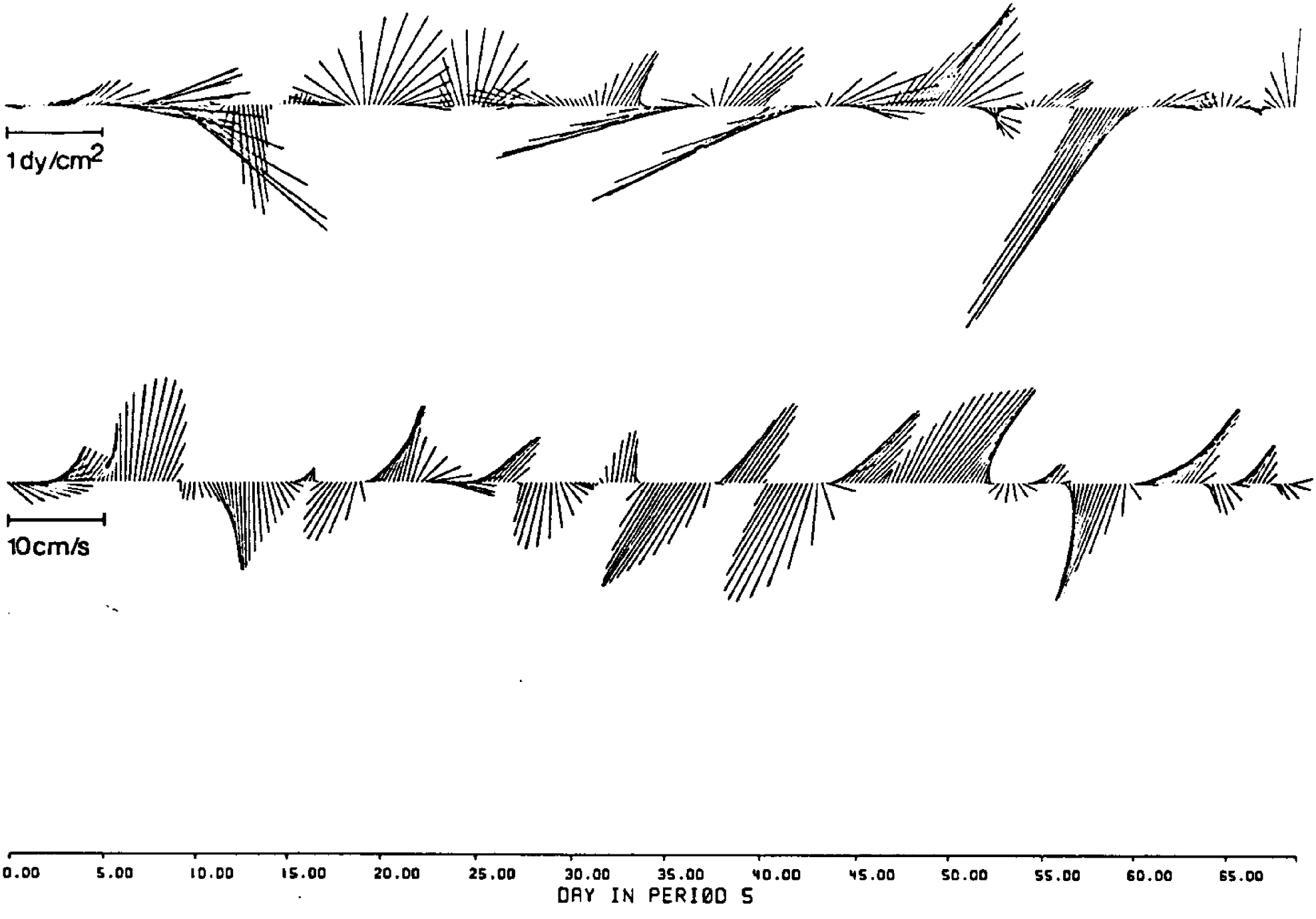

Figure 4e. Period 5, 10 March - 18 May 1981. Stick vector plot of 40 hr low-passed wind stress (dyne/cm^2) and current (cm/s) at SNLT. North is toward top of figure.

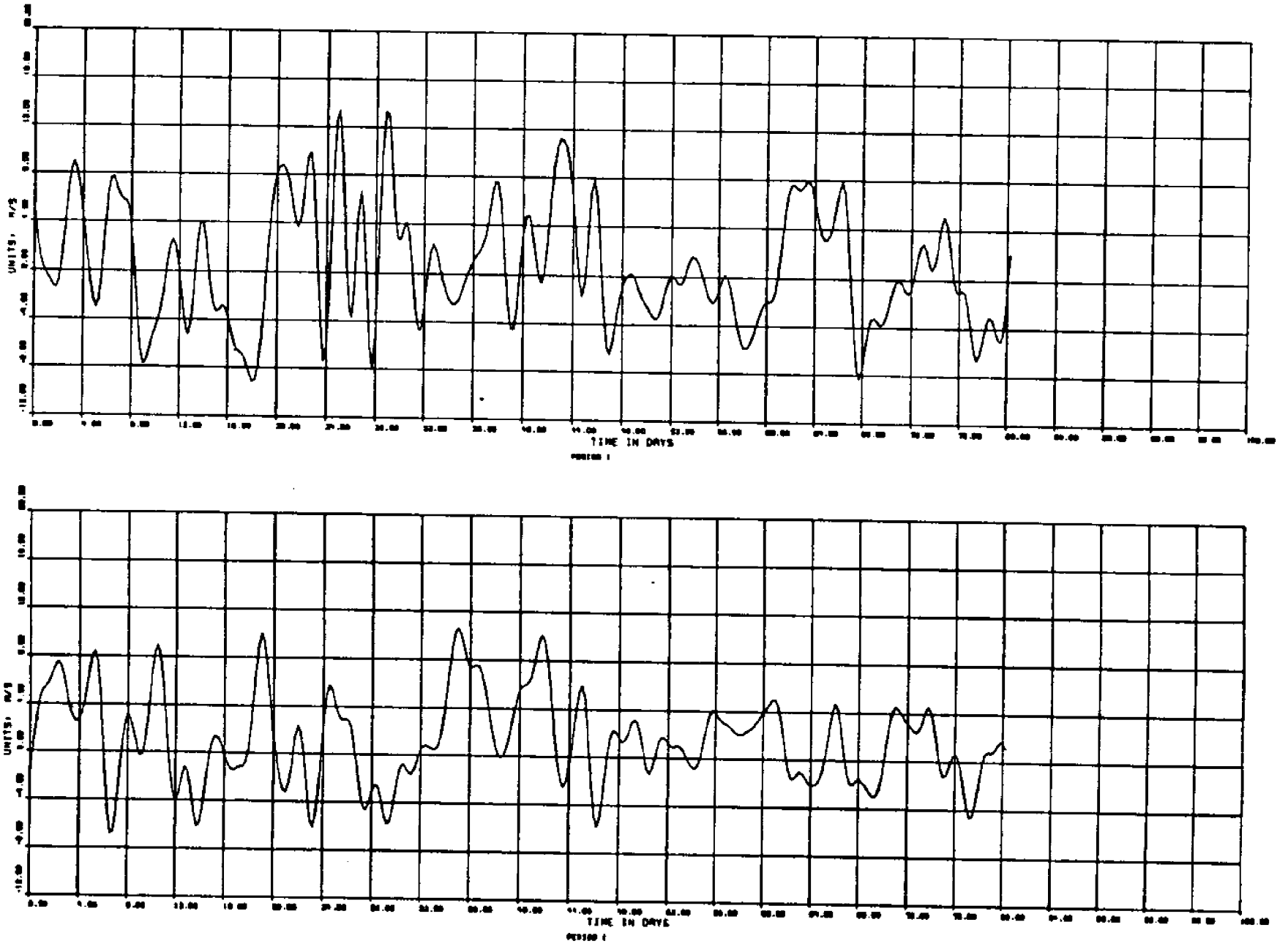

Figure 5a. Period 1, 21 February - 13 May 1977. Time series of east (TAUX) and north (TAUY) 40 hr low-passed wind speed components (oceanographic convention) at SNLT.

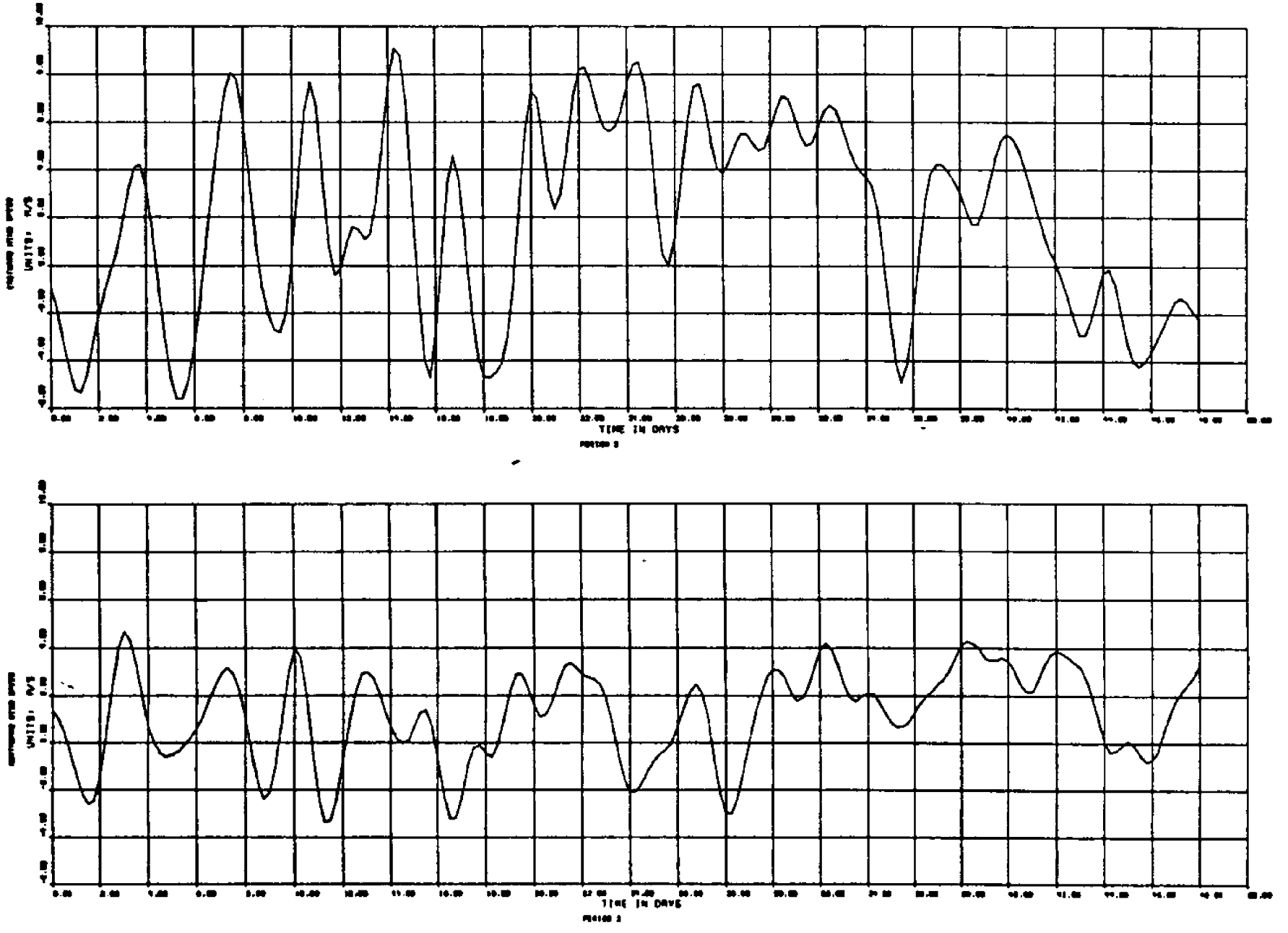

Figure 5b. Period 2, 30 May - 17 July 1977. Time series of east (TAUX) and north (TAUY) 40 hr low-passed wind speed components (oceanographic convention) at SNLT.

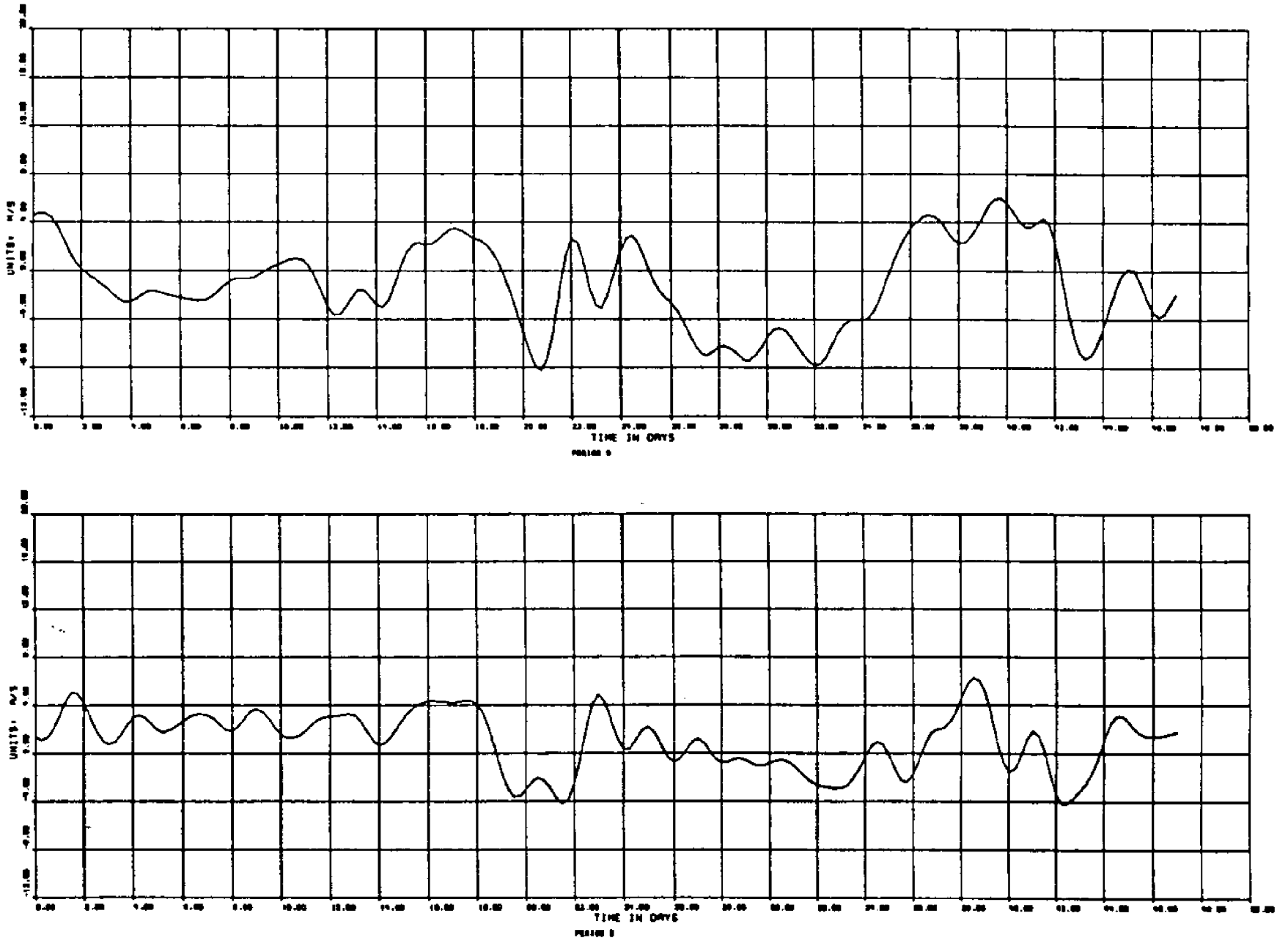

Figure 5c. Period 3, 31 July - 16 September 1977. Time series of east (TAUX) and north (TAUY) 40 hr low-passed wind speed components (oceanographic convention) at SNLT

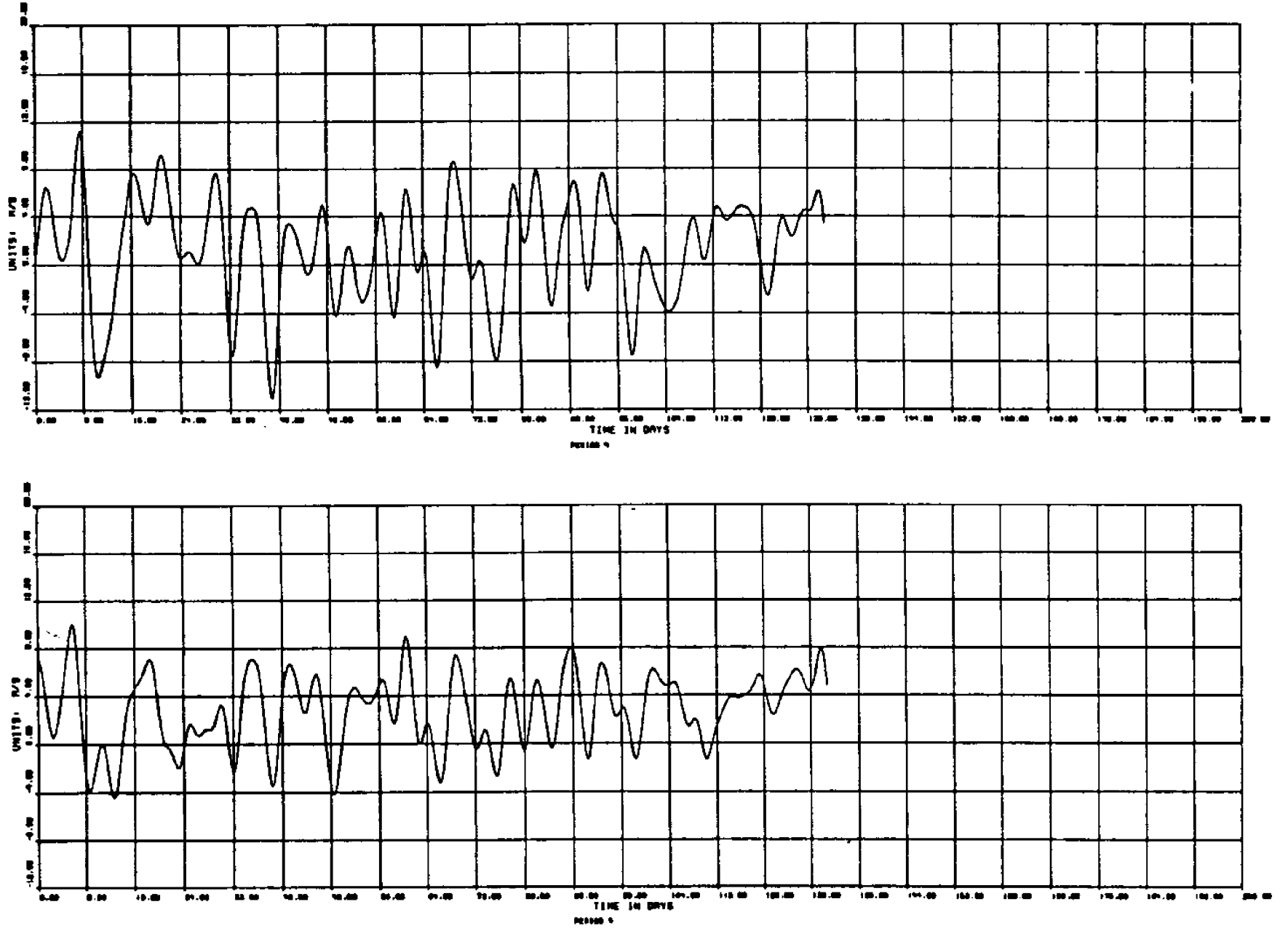

Figure 5d. Period 4, 7 April - 16 August 1980. Time series of east (TAUX) and north (TAUY) 40 hr low-passed wind speed components (Oceanographic convention) at SNLT.

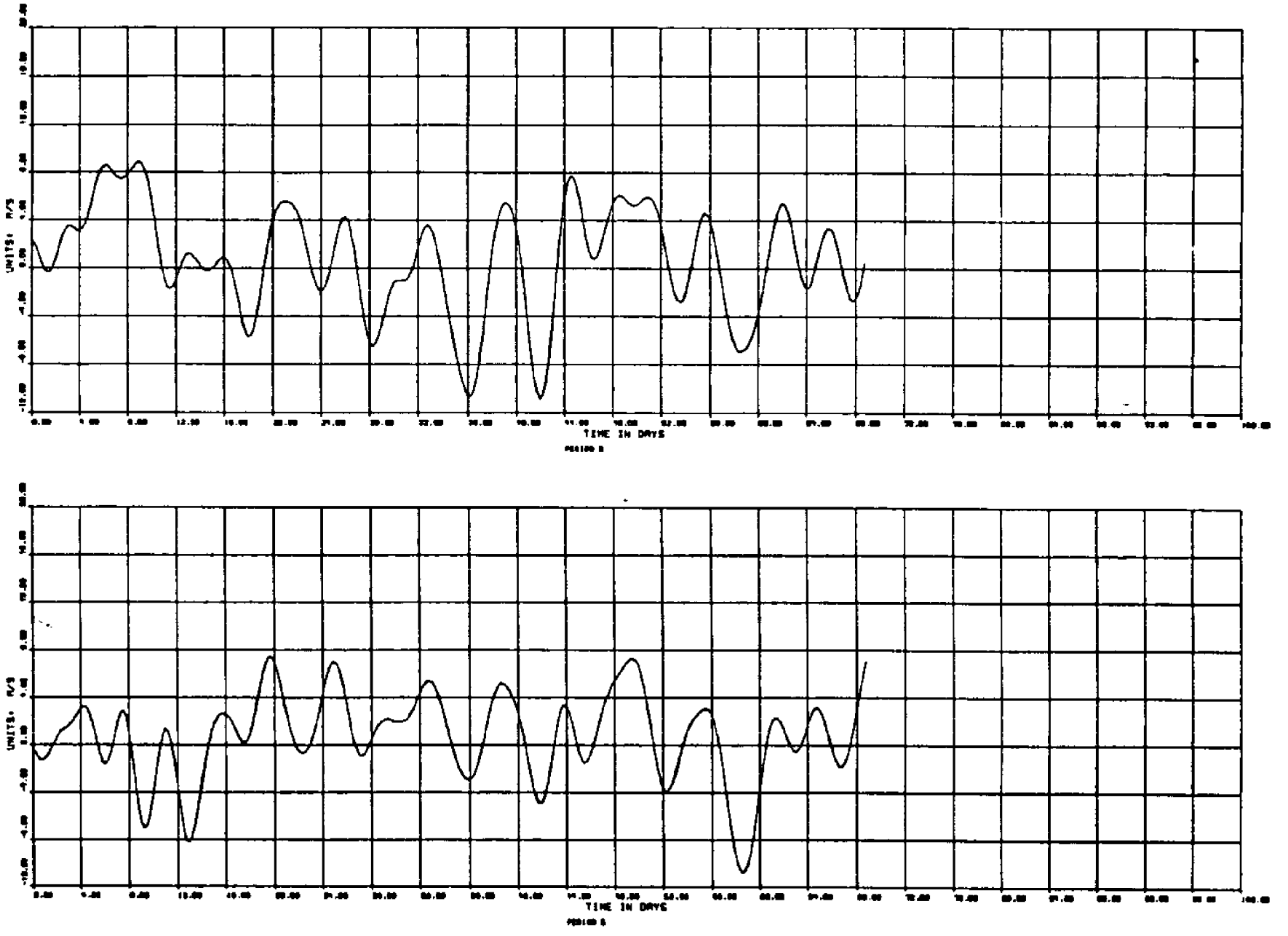

Figure 5e. Period 5, 10 March - 18 May 1981. Time series of east (TAUX) and north (TAUY) 40 hr low-passed wind speed components (oceanographic convention) at SNLT.

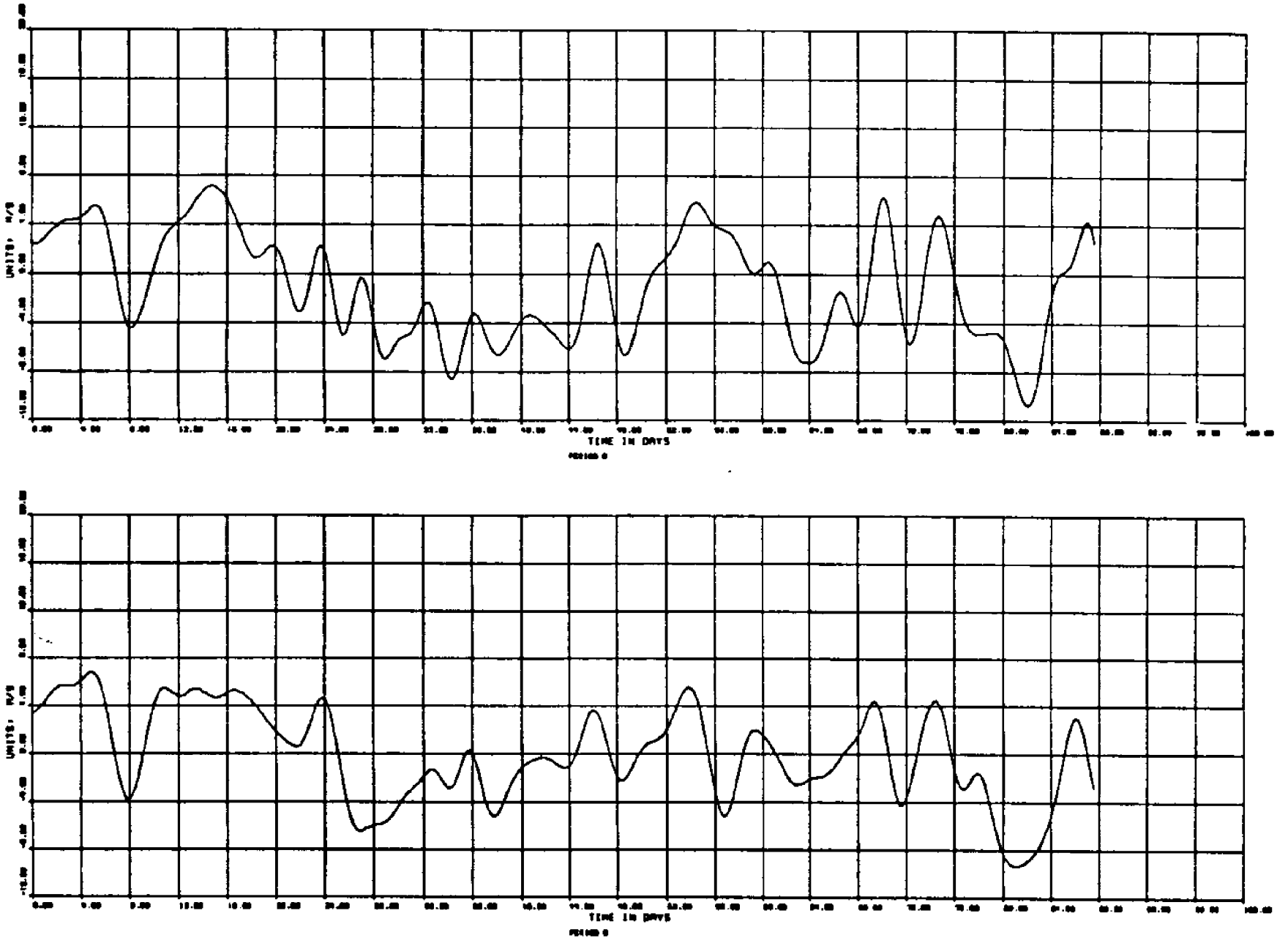

Figure 5f. Period 6, 23 July - 10 October 1981. Time series of east (TAUX) and north (TAUY) 40 hr low-passed wind speed components (oceanographic convention) at SNLT.

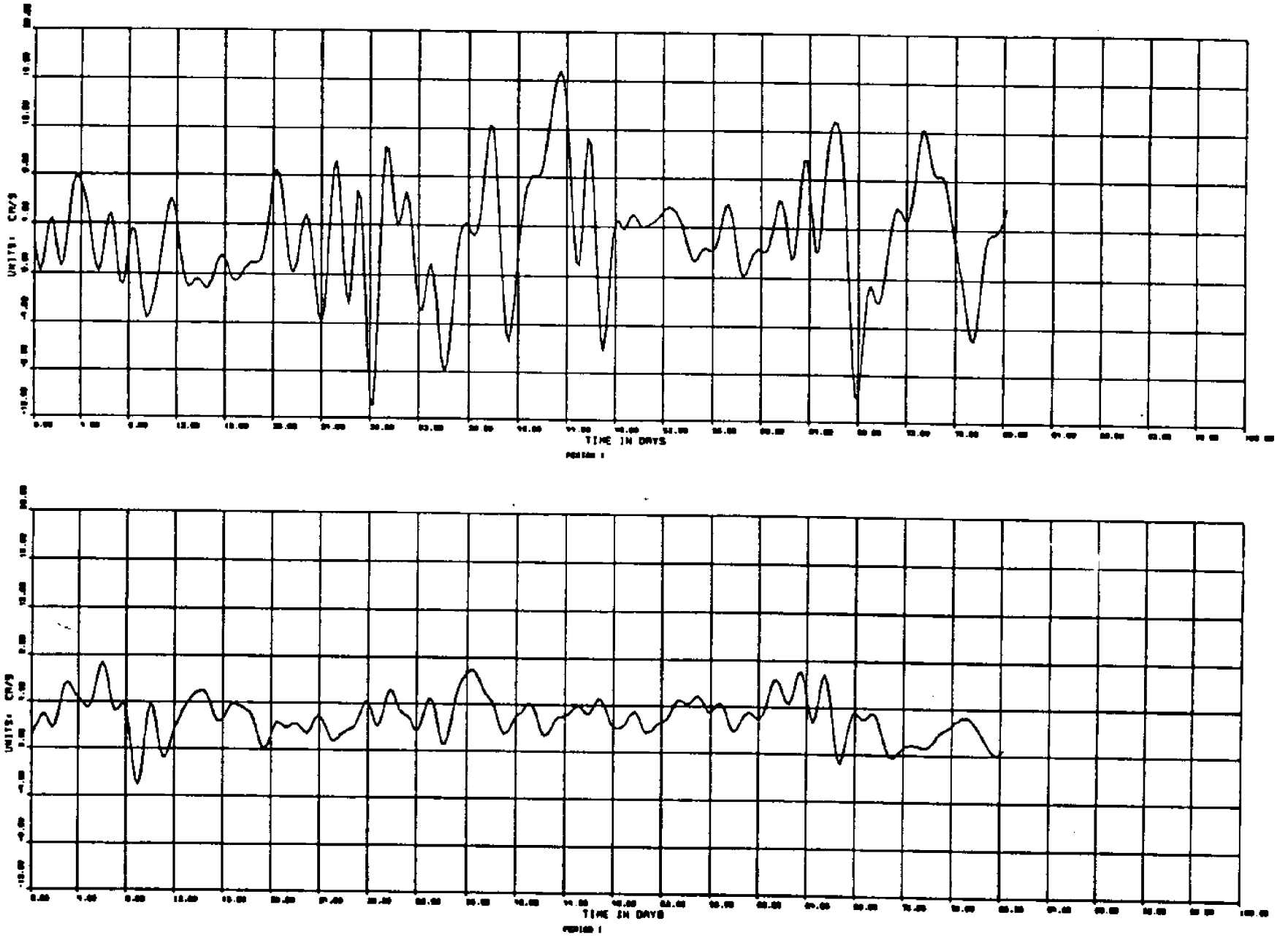

Figure 6a. Period 1, 21 February - 13 May 1977. Time series of major (upper) and minor (lower) 40 hr low-passed current components (cm/s) at SNLT. Angle of major axis relative to north is 61°. Records are from bottom.

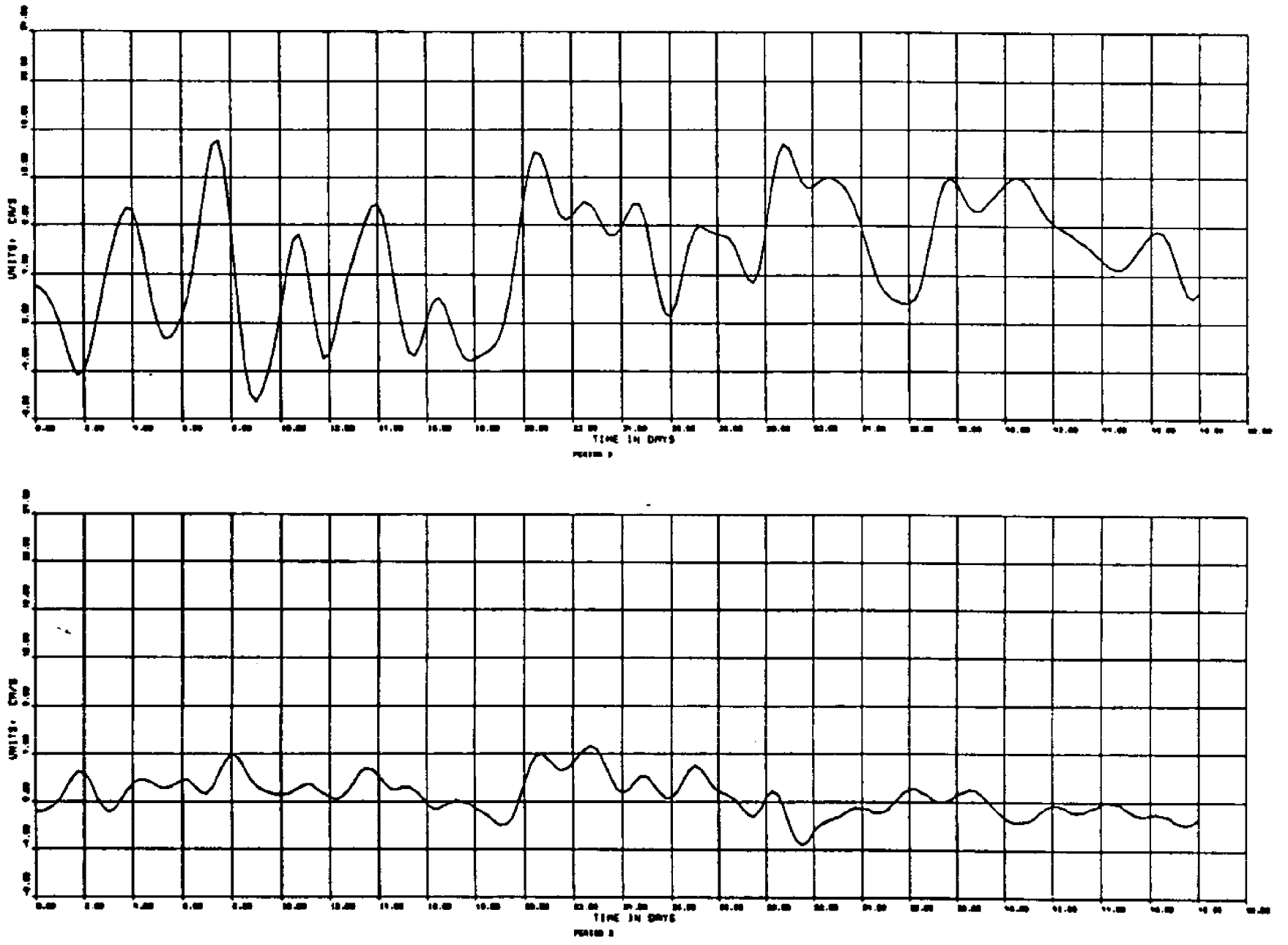

Figure 6b. Period 2, 30 May - 17 July 1977. Time series of major (upper) and minor (lower) 40 hr low-passed current components (cm/s) at SNLT. Angle of major axis relative to north is 79^{o}. Records are from bottom.

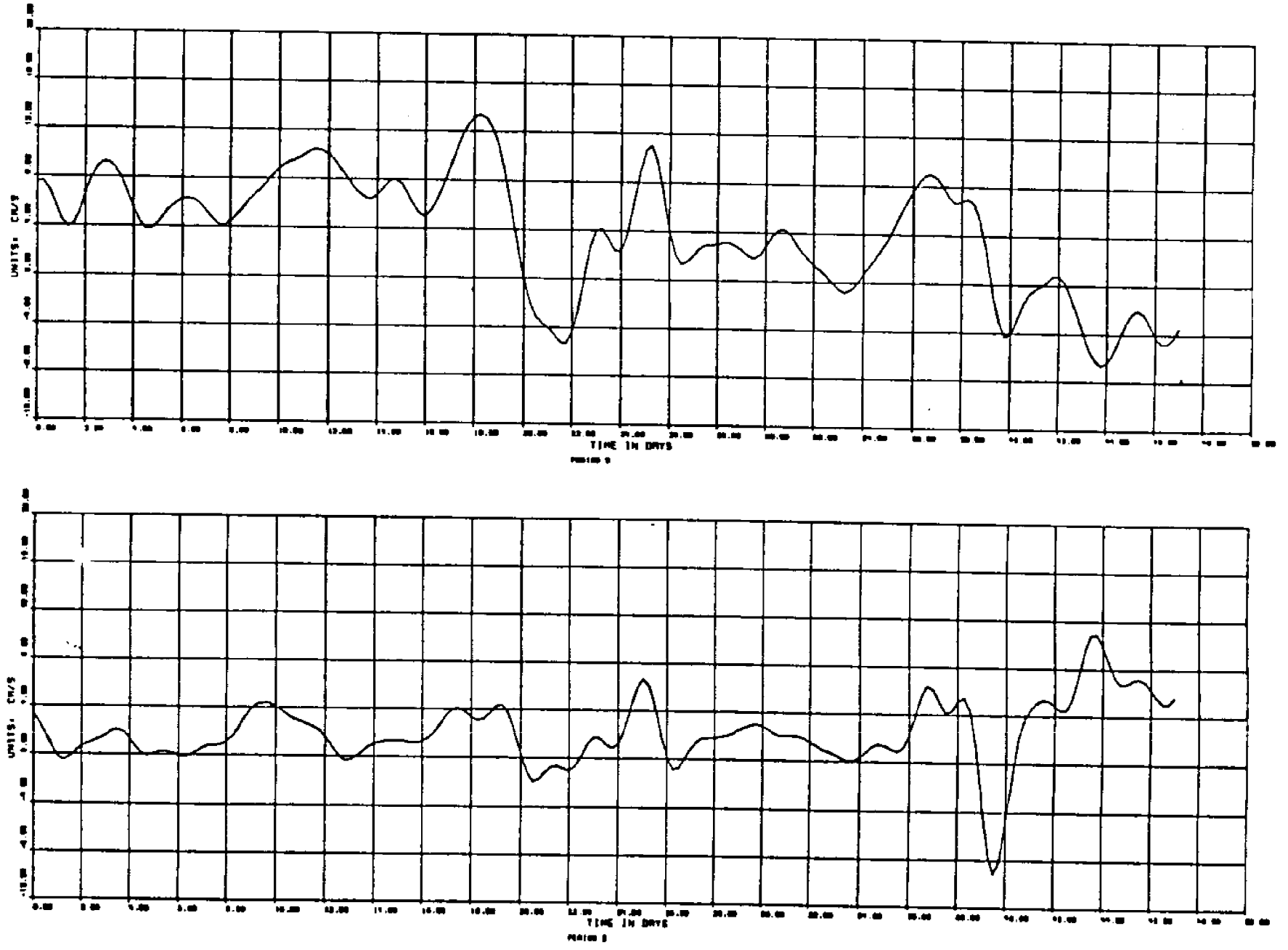

Figure 6c. Period 3, 31 July - 16 September 1977. Time series of major (upper) and minor (lower) 40 hr low-passed current components (cm/s) at SNLT. Angle of major axis relative to north is 90°. Records are from bottom.

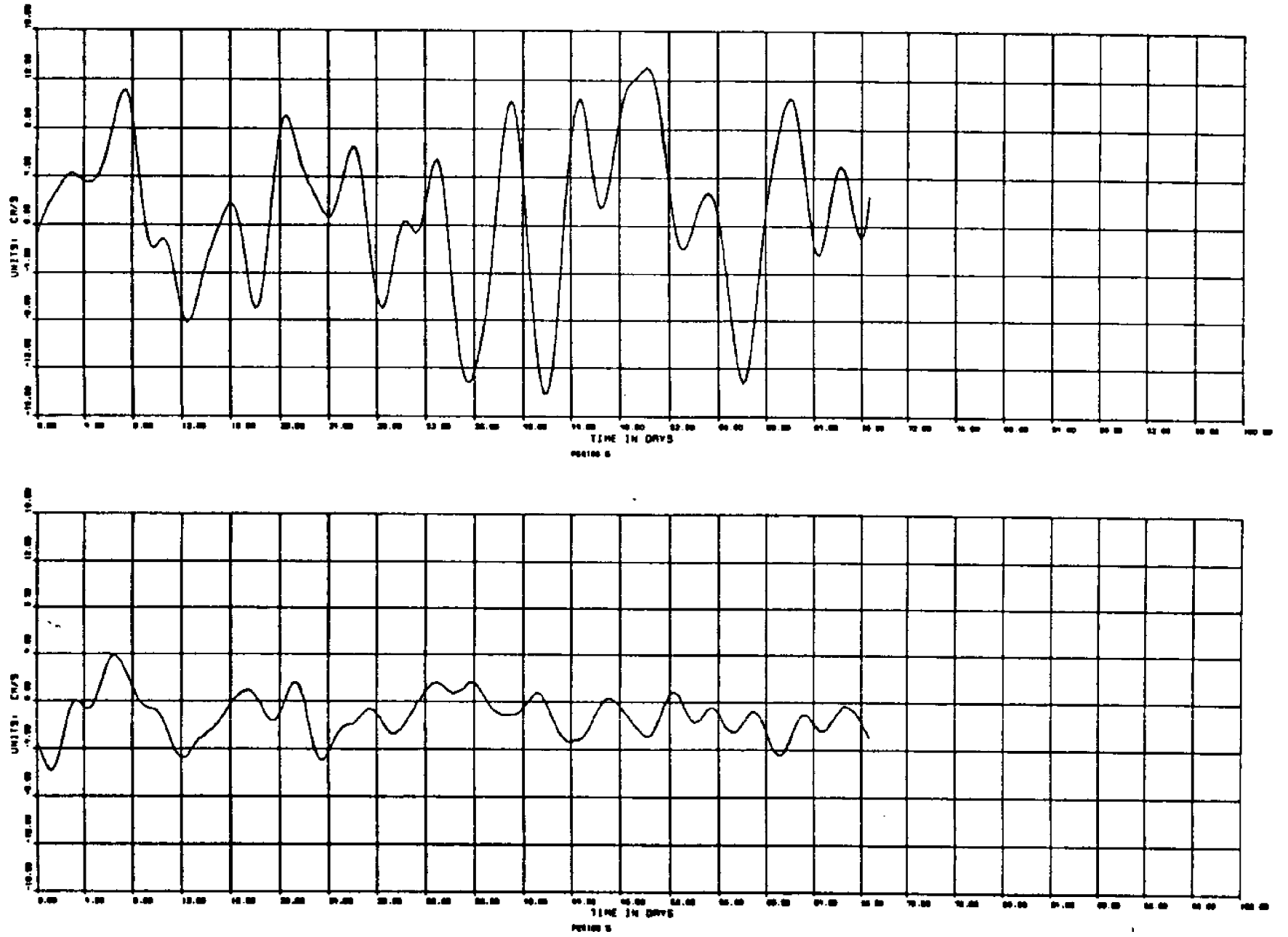

Figure 6d. Period 5, 10 March - 18 May 1981. Time series of major (upper) and minor (lower) 40 hr low-passed current components (cm/s) at SNLT. Angle of major axis relative to north is 27°. Records are from mid-depth.

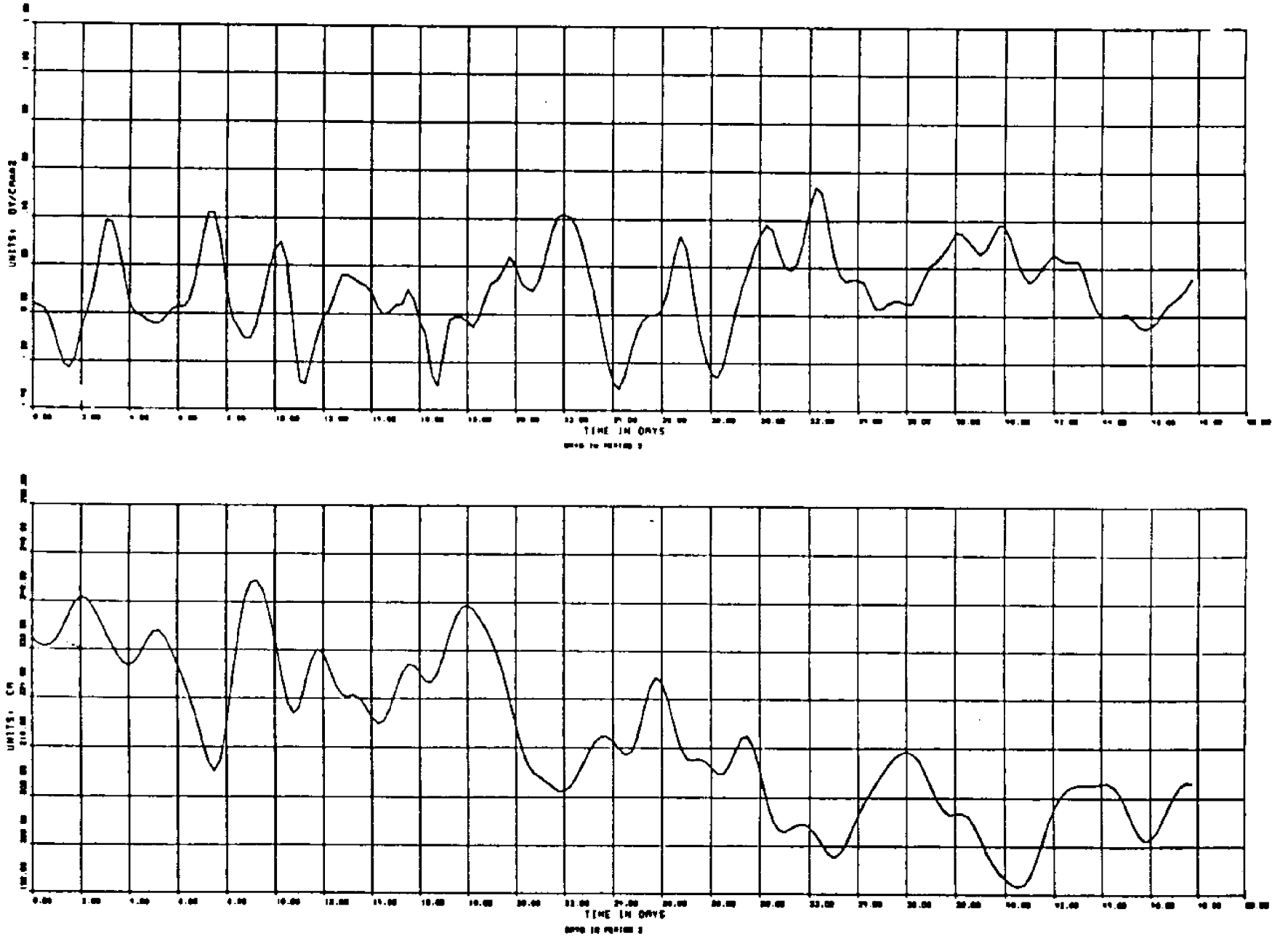

Figure 7a. Period 2, 30 May - 17 July 1977. Time series of 40 hr low-passed wind stress (north component) and sea level at Ft. Pulaski.

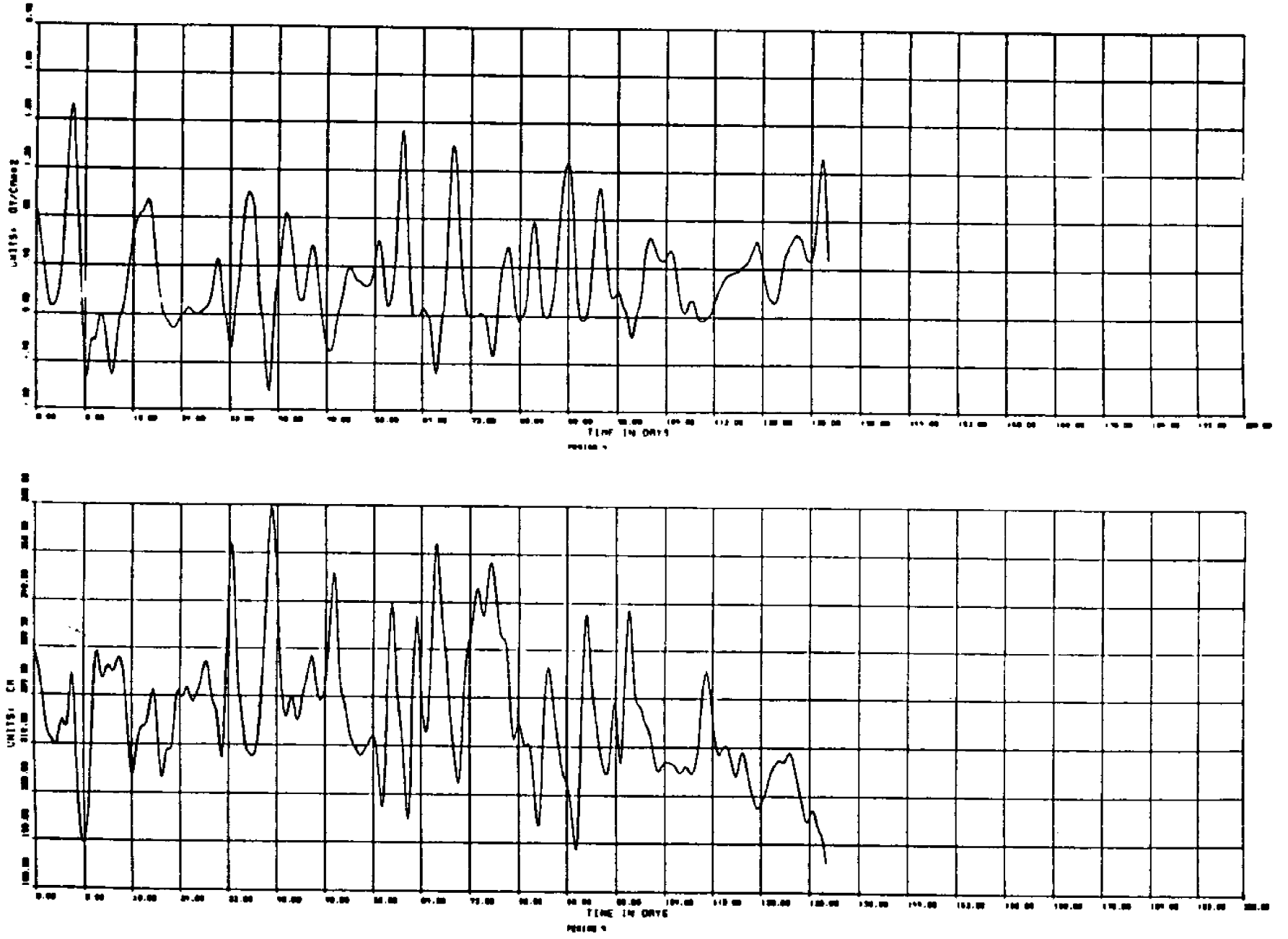

Figure 7b. Period 4, 7 April - 16 August 1980. Time series of 40 hr low-passed wind stress (north component) and sea level at Ft. Pulaski.

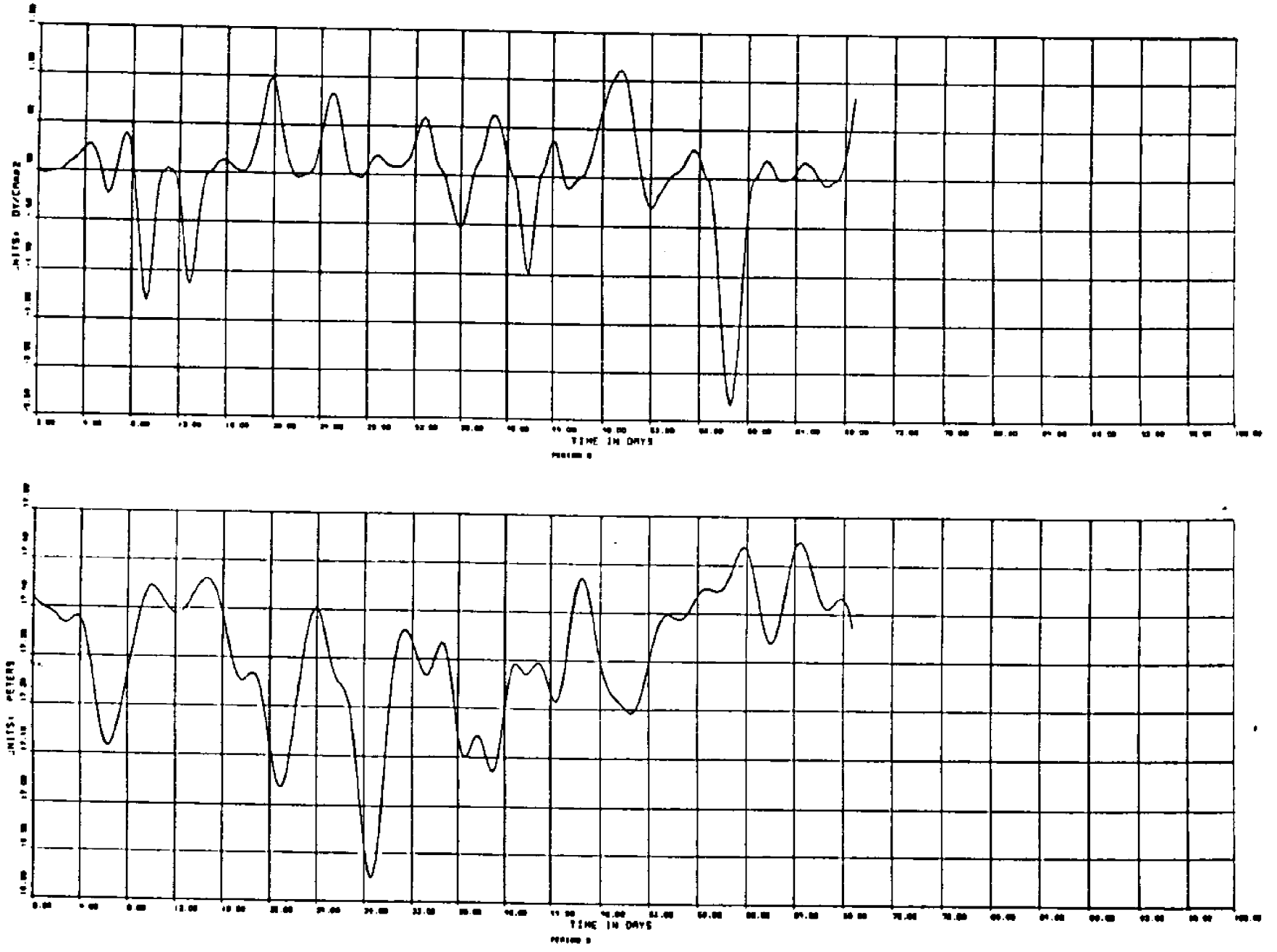

Figure 7c. Period 5, 10 March - 18 May 1981. Time series of 40 hr low-passed wind stress (north component) and sea level at SNLT.

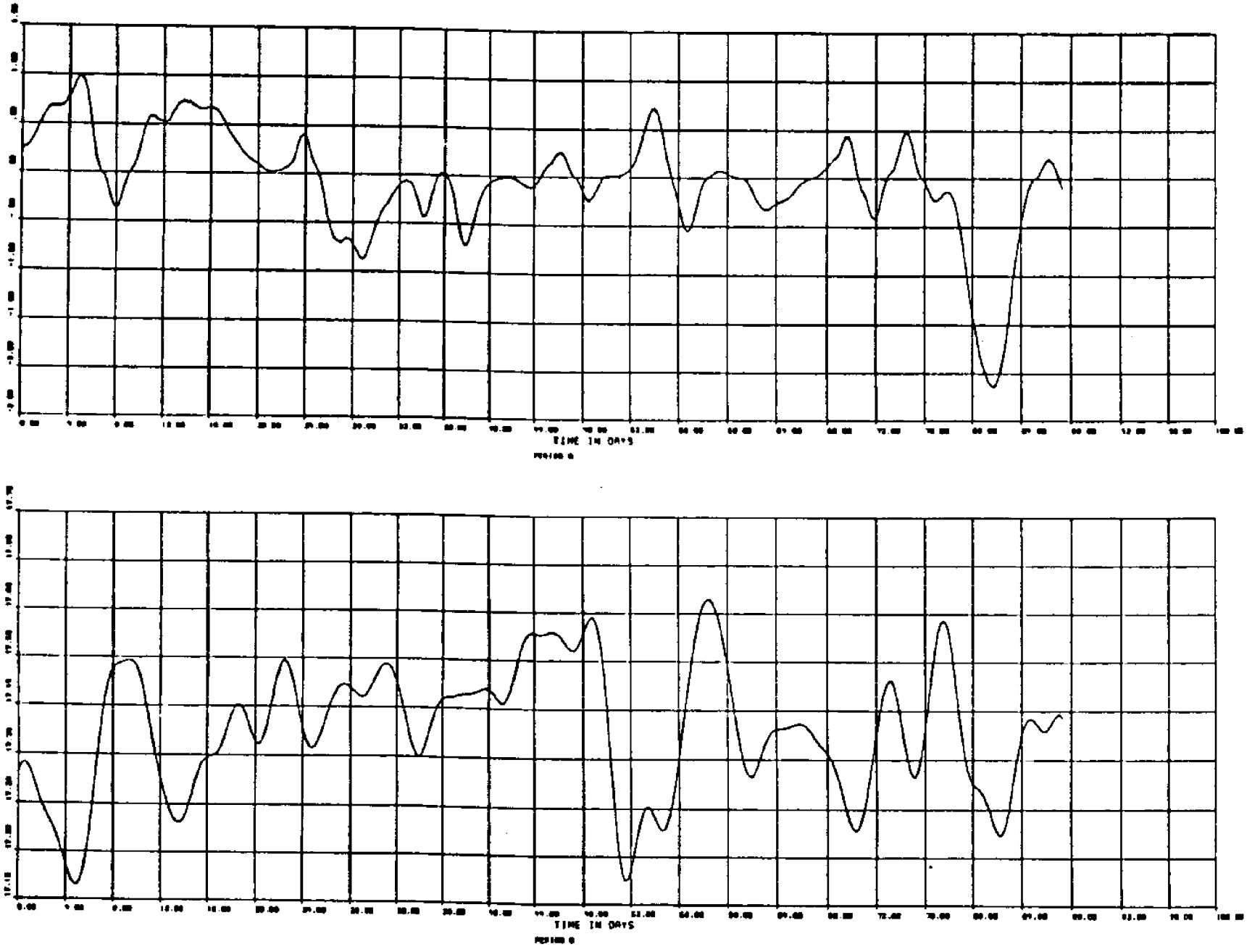

Figure 7d. Period 6, 23 July - 10 October 1981. Time series of 40 hr low-passed wind stress (north component) and sea level at SNLT.

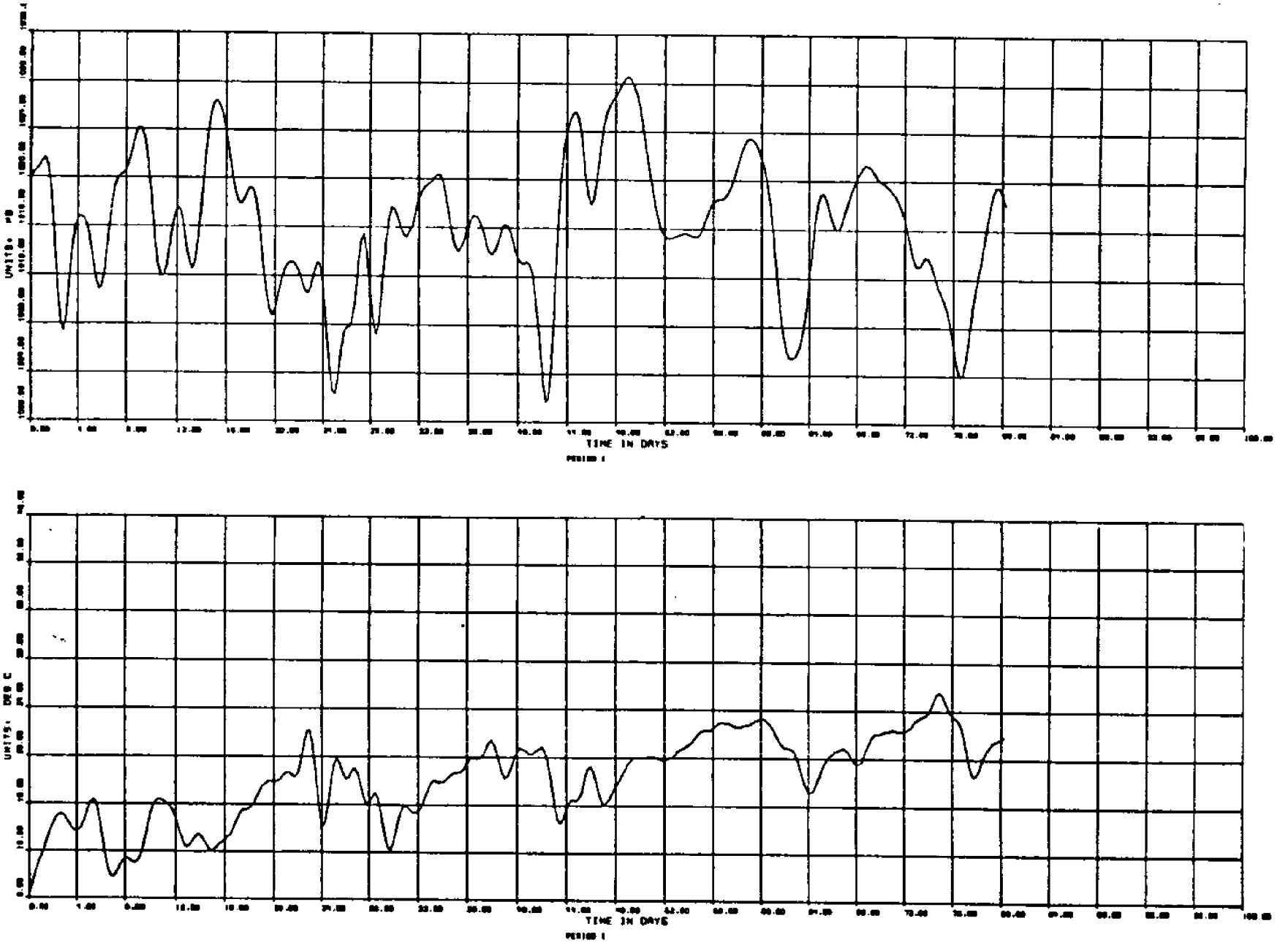

Figure 8a. Period 1, 21 February - 13 May 1977. Time series of 40 hr low-passed barometric pressure (upper) and air temperature (lower) at SNLT.

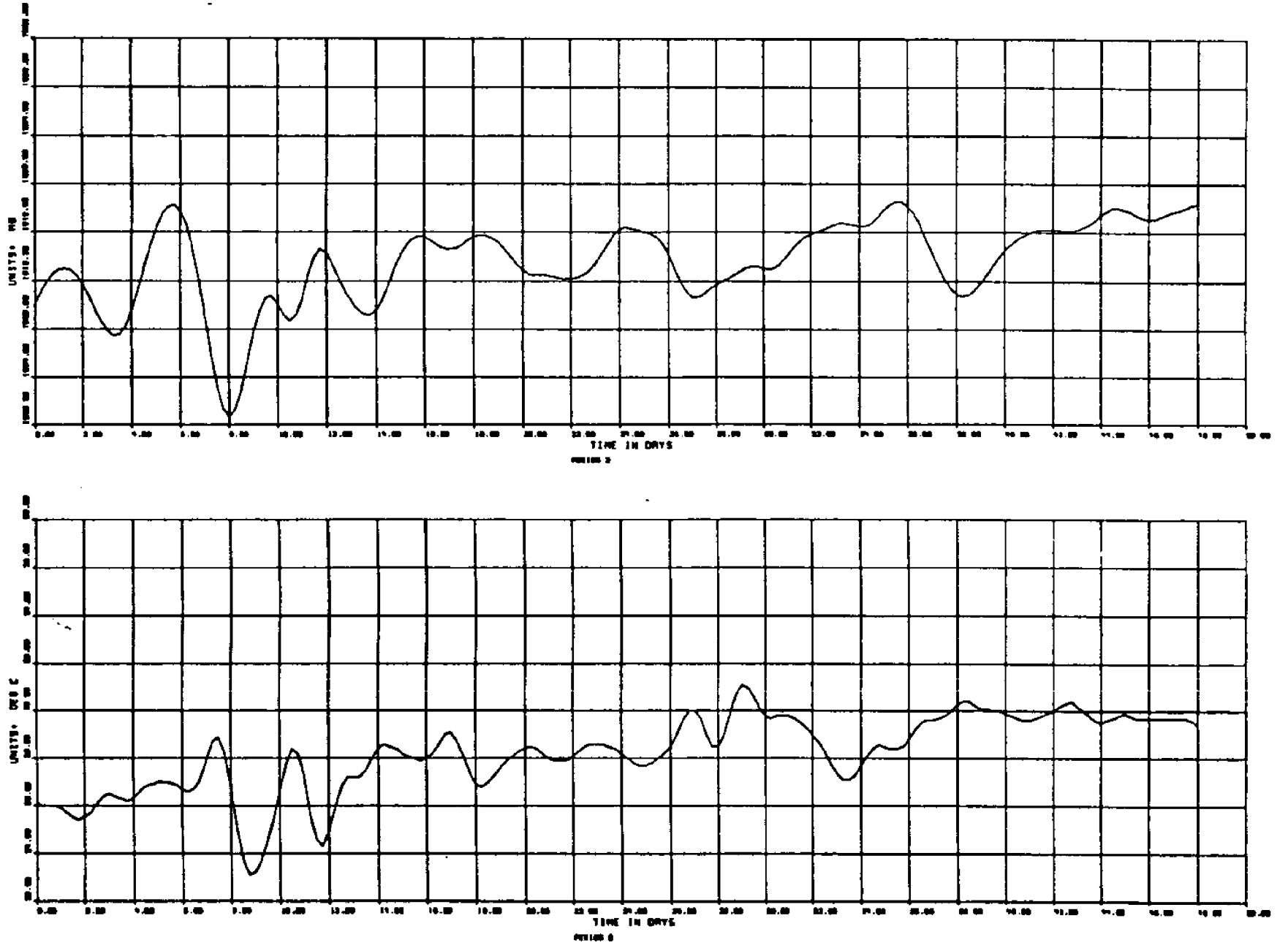

Figure 8b. Period 2, 30 May - 17 July 1977. Time series of 40 hr low-passed barometric pressure (upper) and air temperature (lower) at SNLT.

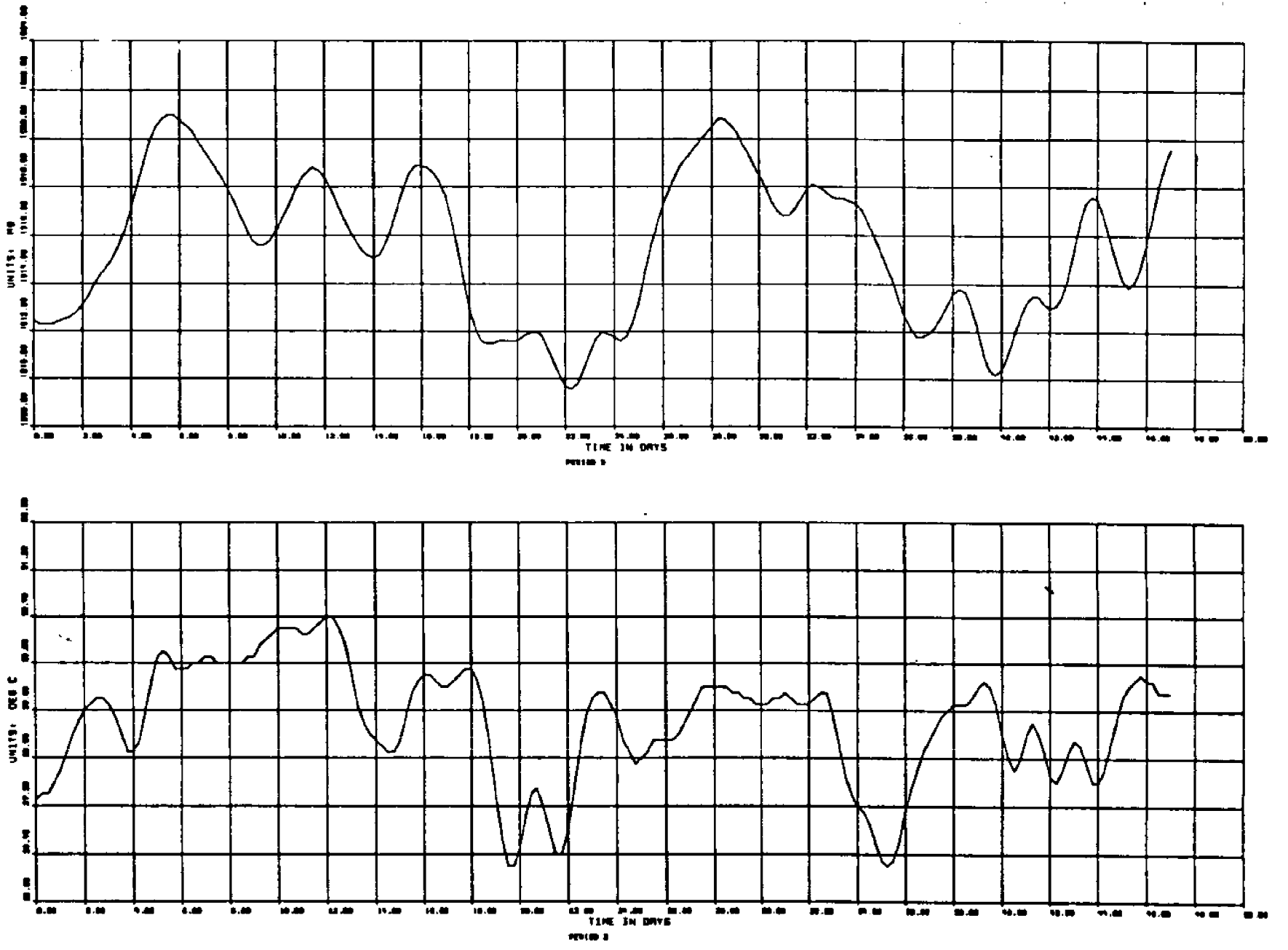

Figure 8c. Period 3, 31 July - 16 September 1977. Time series of 40 hr low-passed barometric pressure (upper) and air temperature (lower) at SNLT.

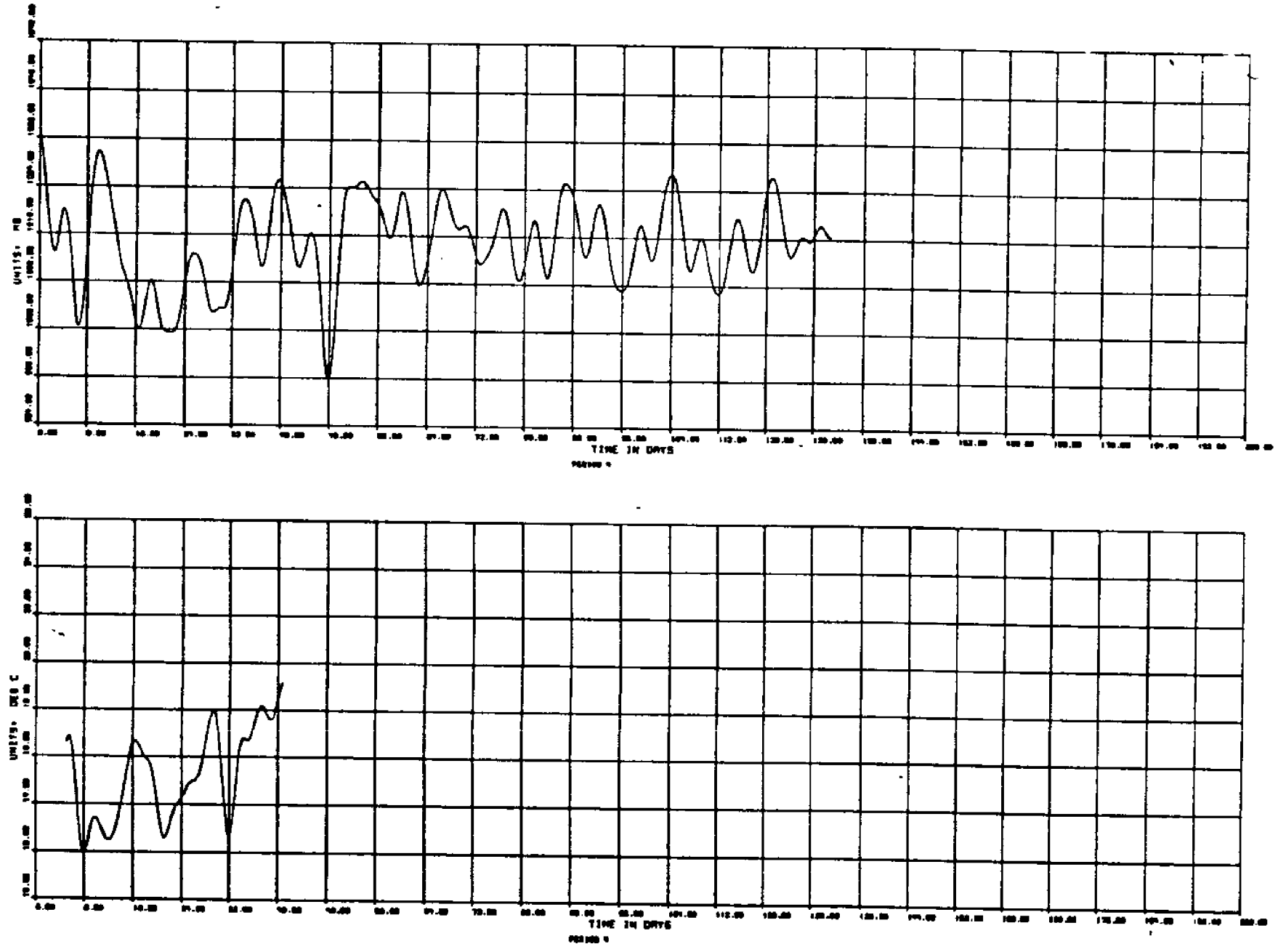

Figure 8d. Period 4, 7 April - 16 August 1980. Time series of 40 hr low-passed barometric pressure (upper) and air temperatures (lower) at SNLT. (Air temperature is from 9 April - 18 May 1980.)

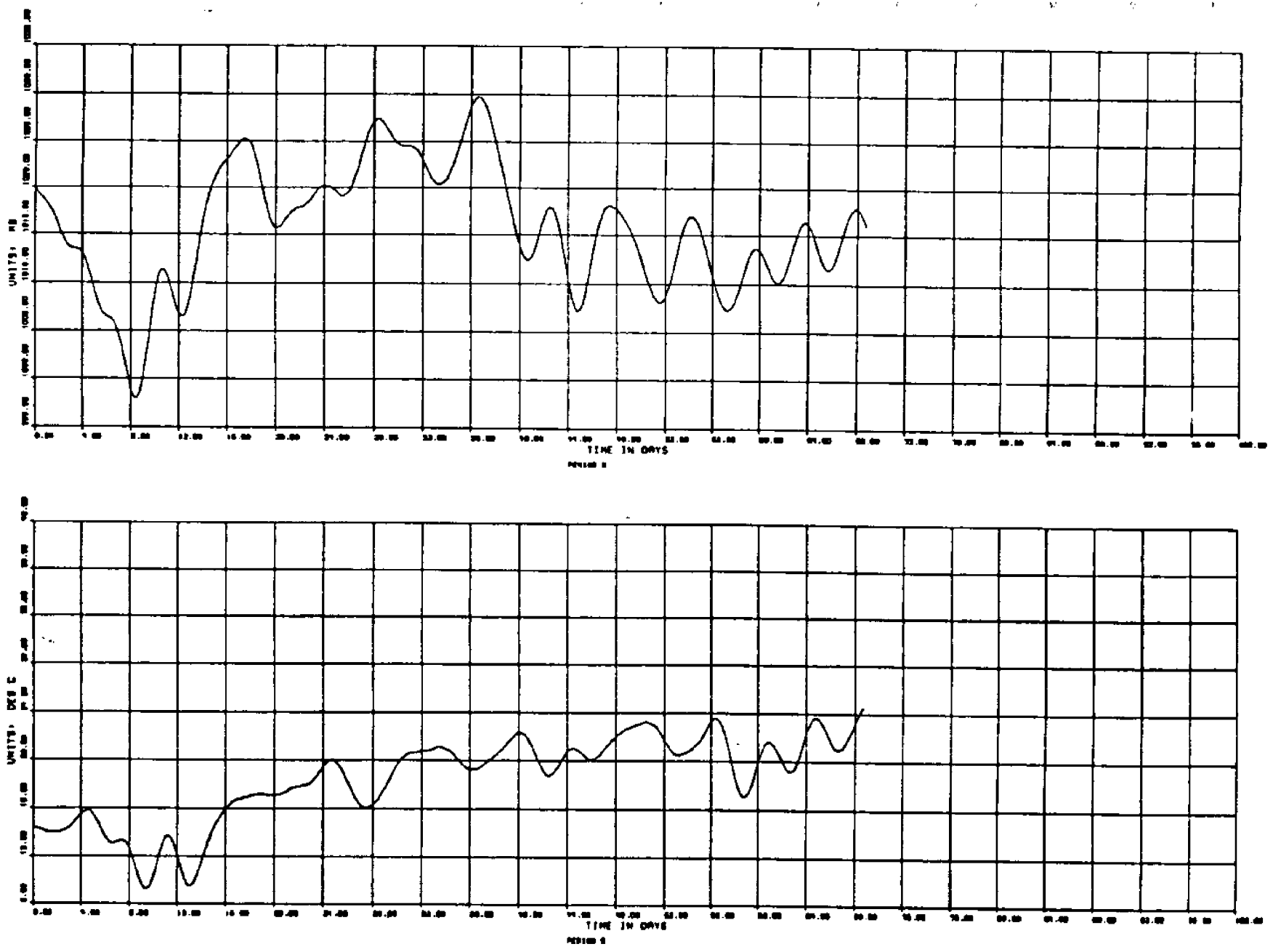

Figure 8e. Period 5, 10 March - 18 May 1981. Time series of 40 hr low-passed barometric pressure (upper) and air temperature (lower) at SNLT.

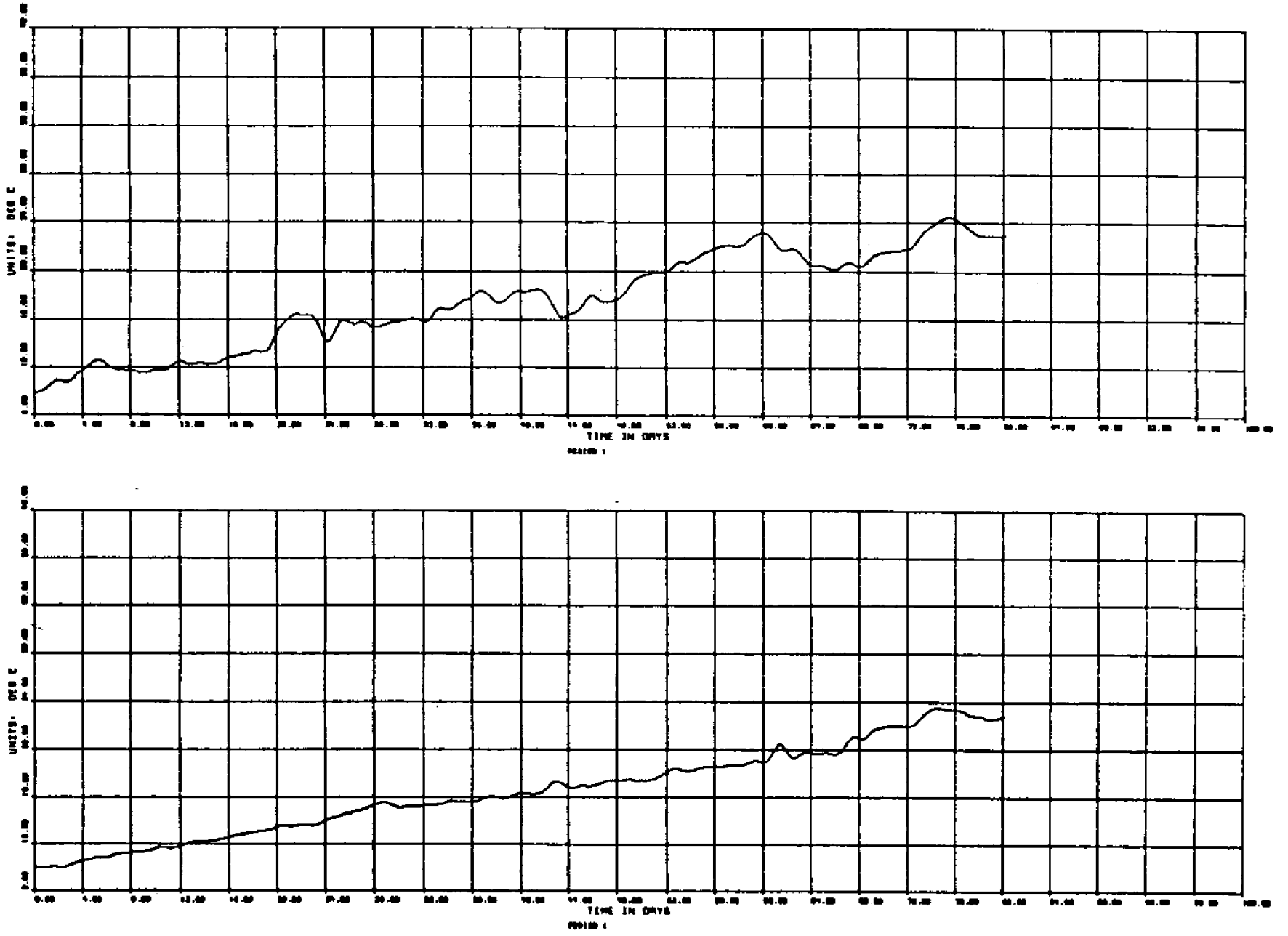

Figure 9a. Period 1, 21 Februrary - 13 May 1977. Time series of 40 hr low-passed surface (upper) and bottom (lower) water temperature at SNLT.

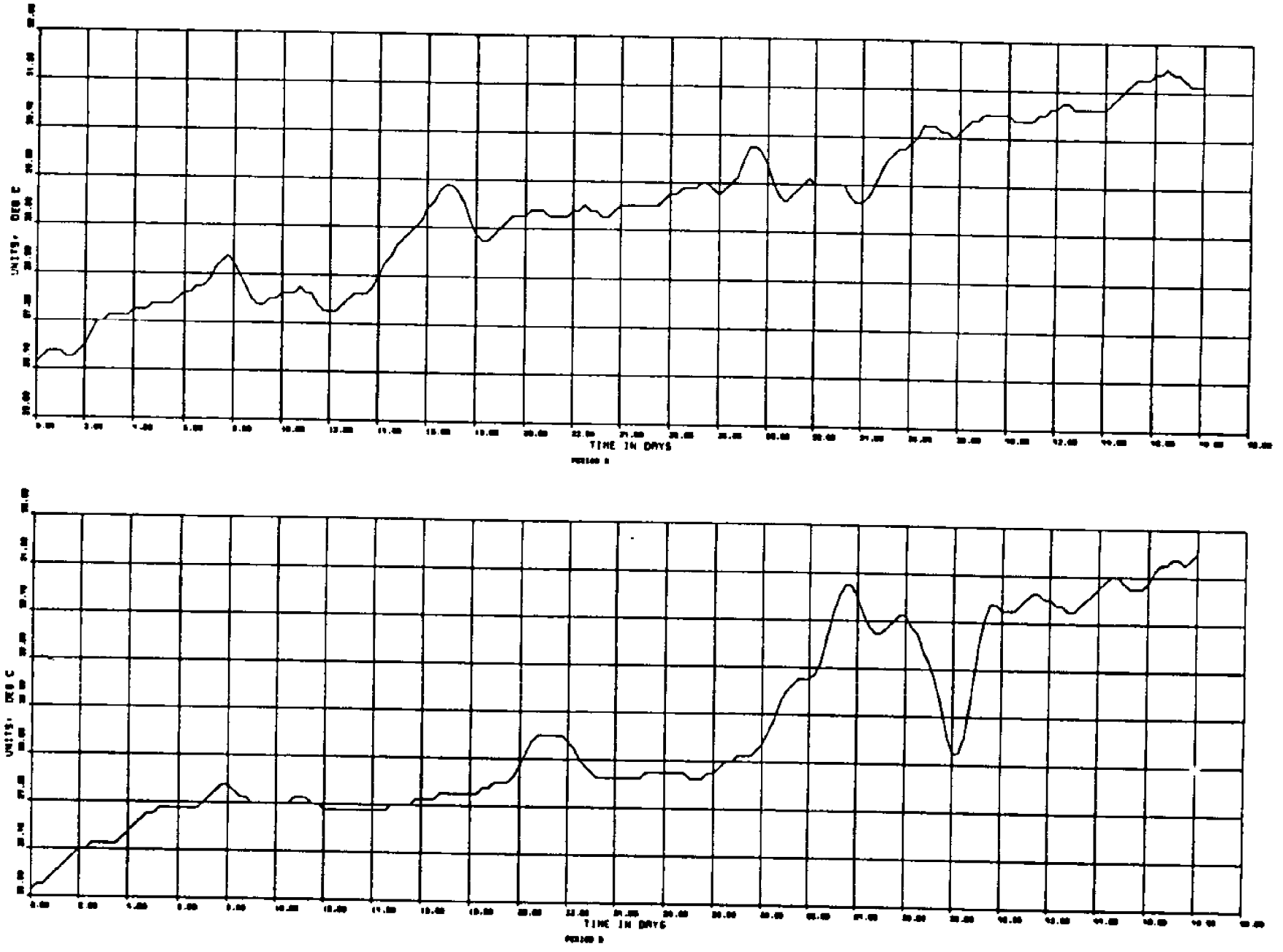

Figure 9b. Period 2, 30 May - 17 July 1977. Time series of 40 hr low-passed surface (upper) and bottom (lower) water temperature at SNLT.

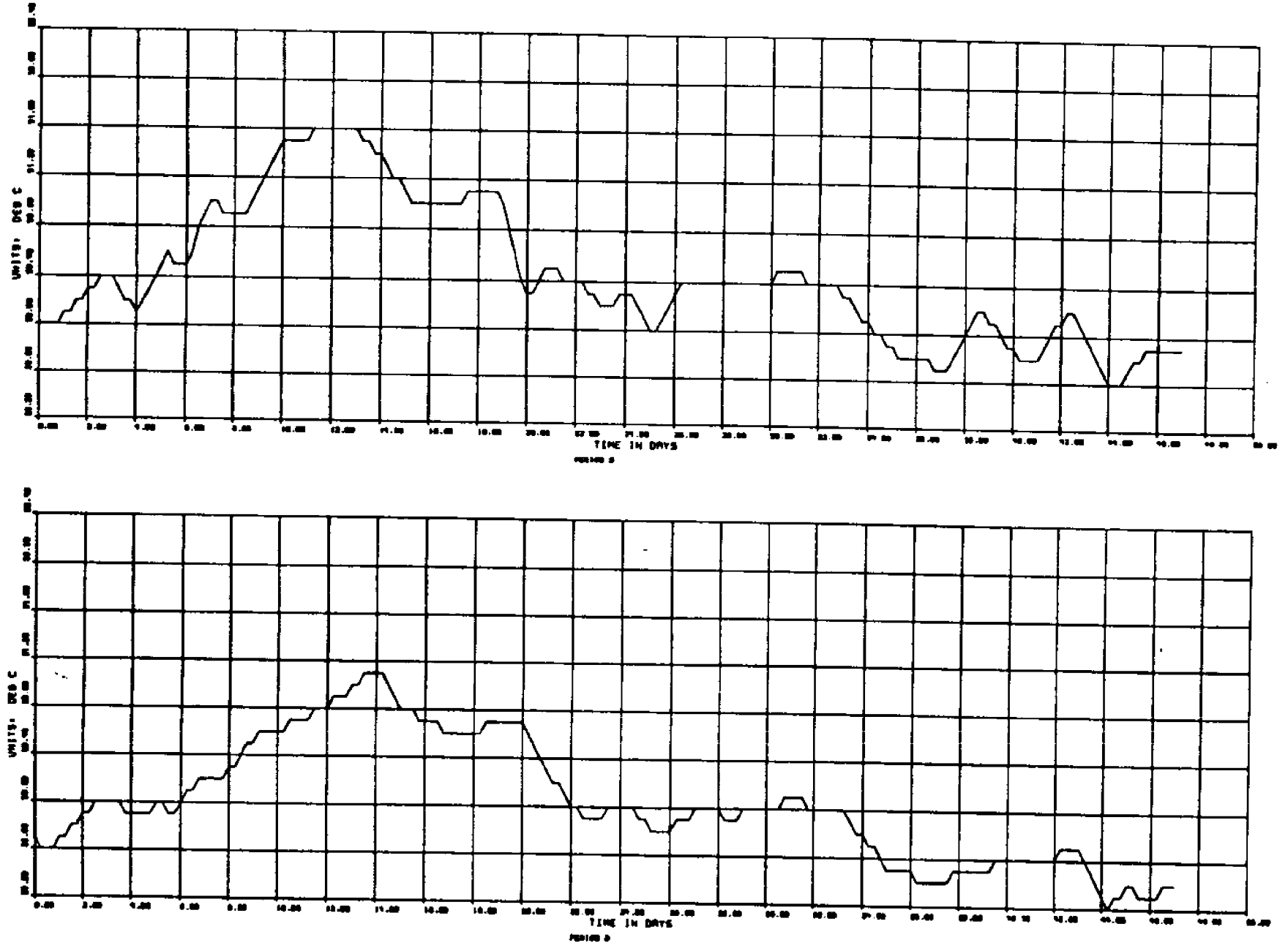

Figure 9c. Period 3, 31 July - 16 September 1977. Time series of 40 hr low-passed surface (upper) and bottom (lower) water temperature at SNLT.

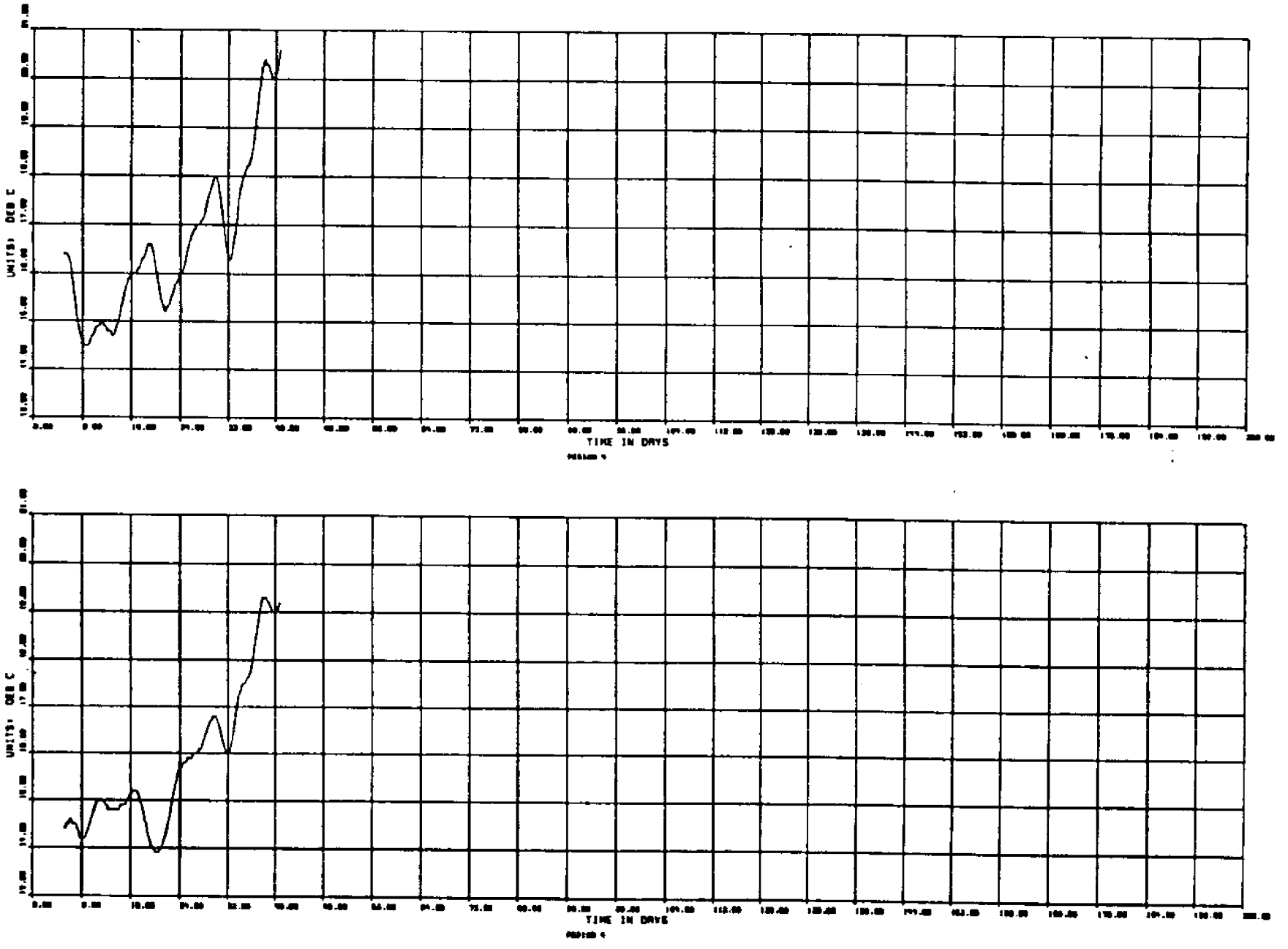

Figure 9d. Period 4, 9 April - 18 May 1980. Time series of 40 hr low-passed surface (upper) and bottom (lower) water temperature at SNLT.

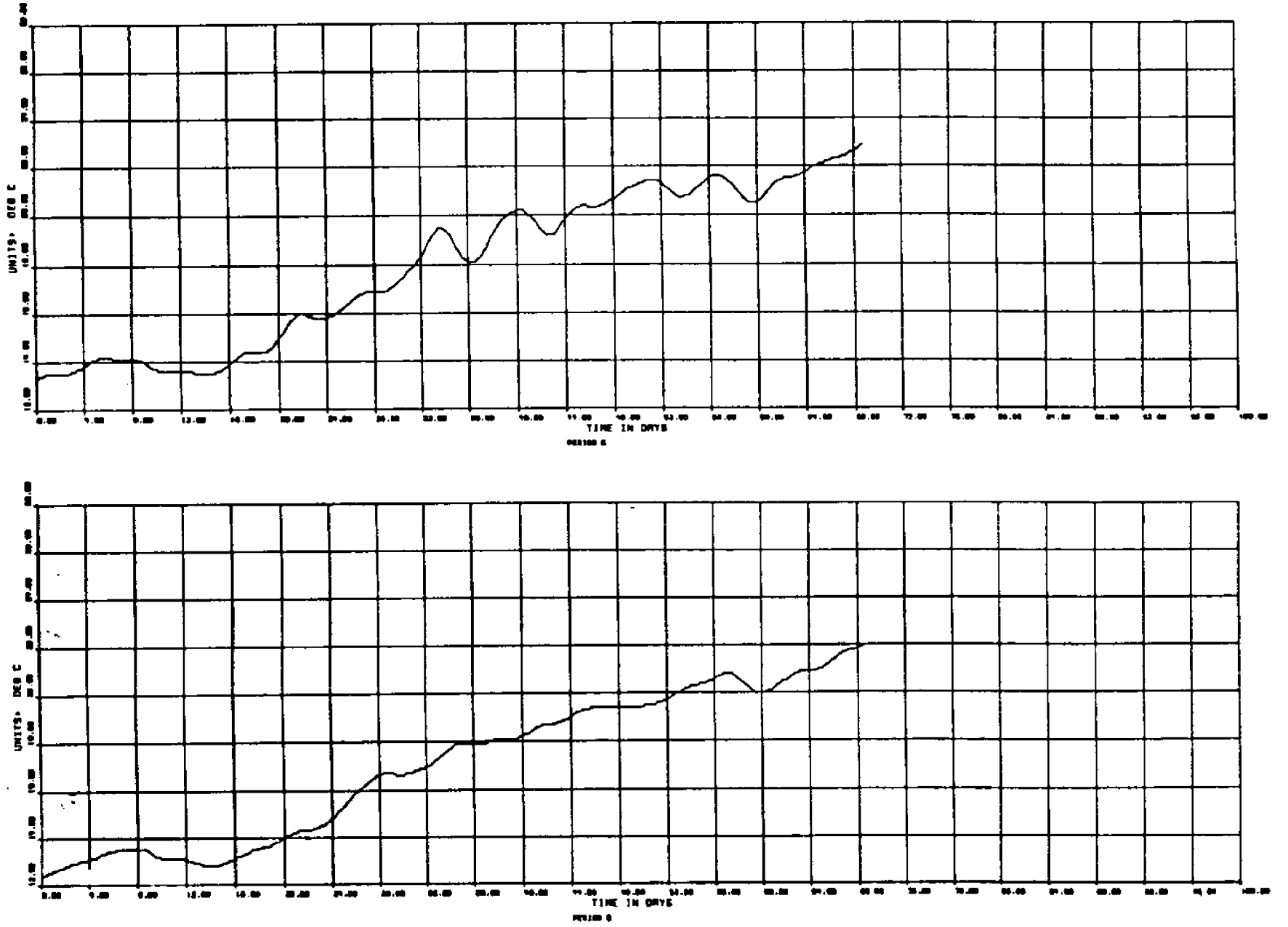

Figure 9e. Period 5, 10 March - 18 May 1981. Time series of 40 hr low-passed surface (upper) and bottom (lower) water temperature at SNLT.

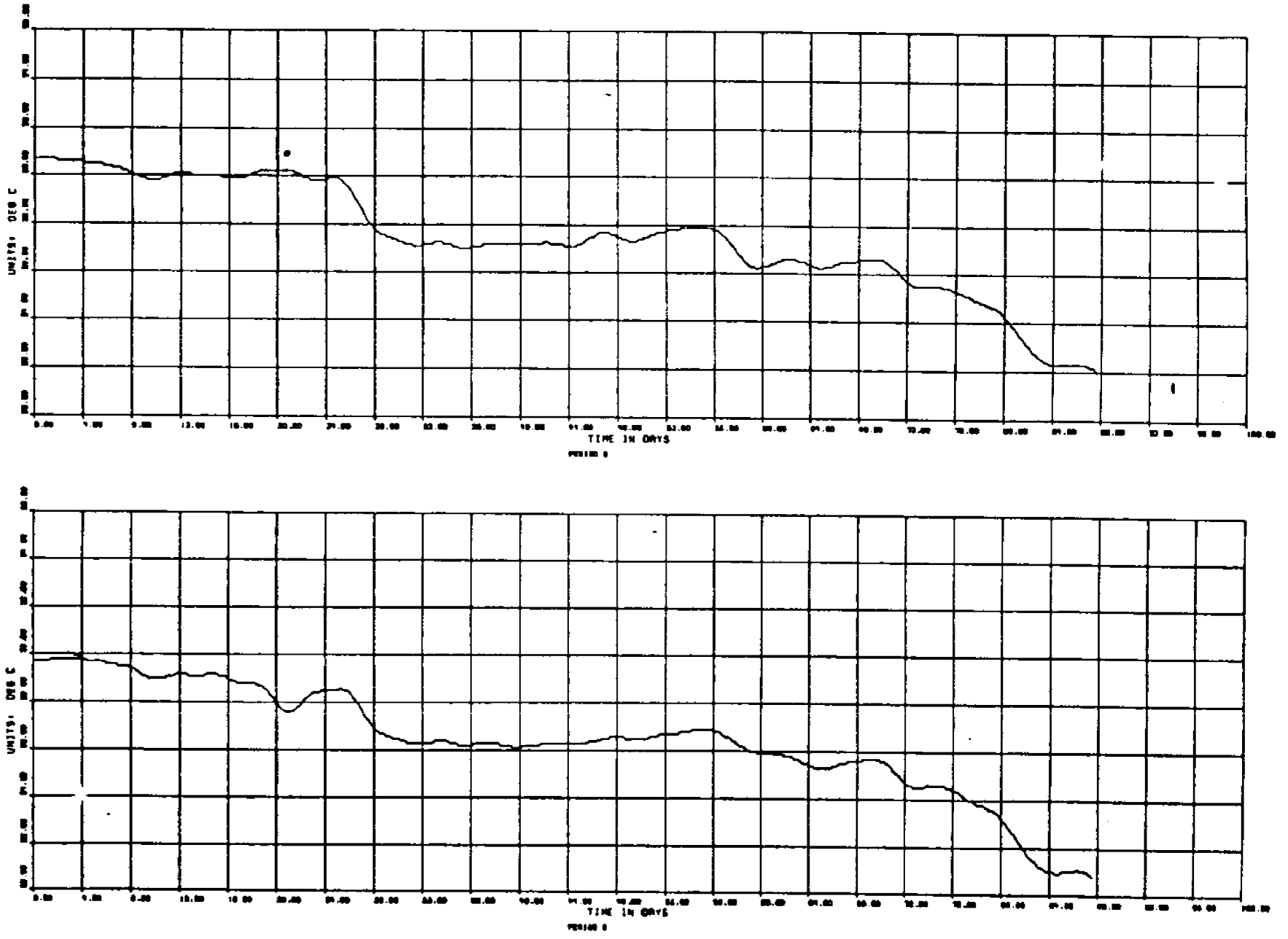

Figure 9f. Period 6, 23 July - 10 October 1981. Time series of 40 hr low-passed surface (upper) and bottom (lower) water temperature at SNLT.

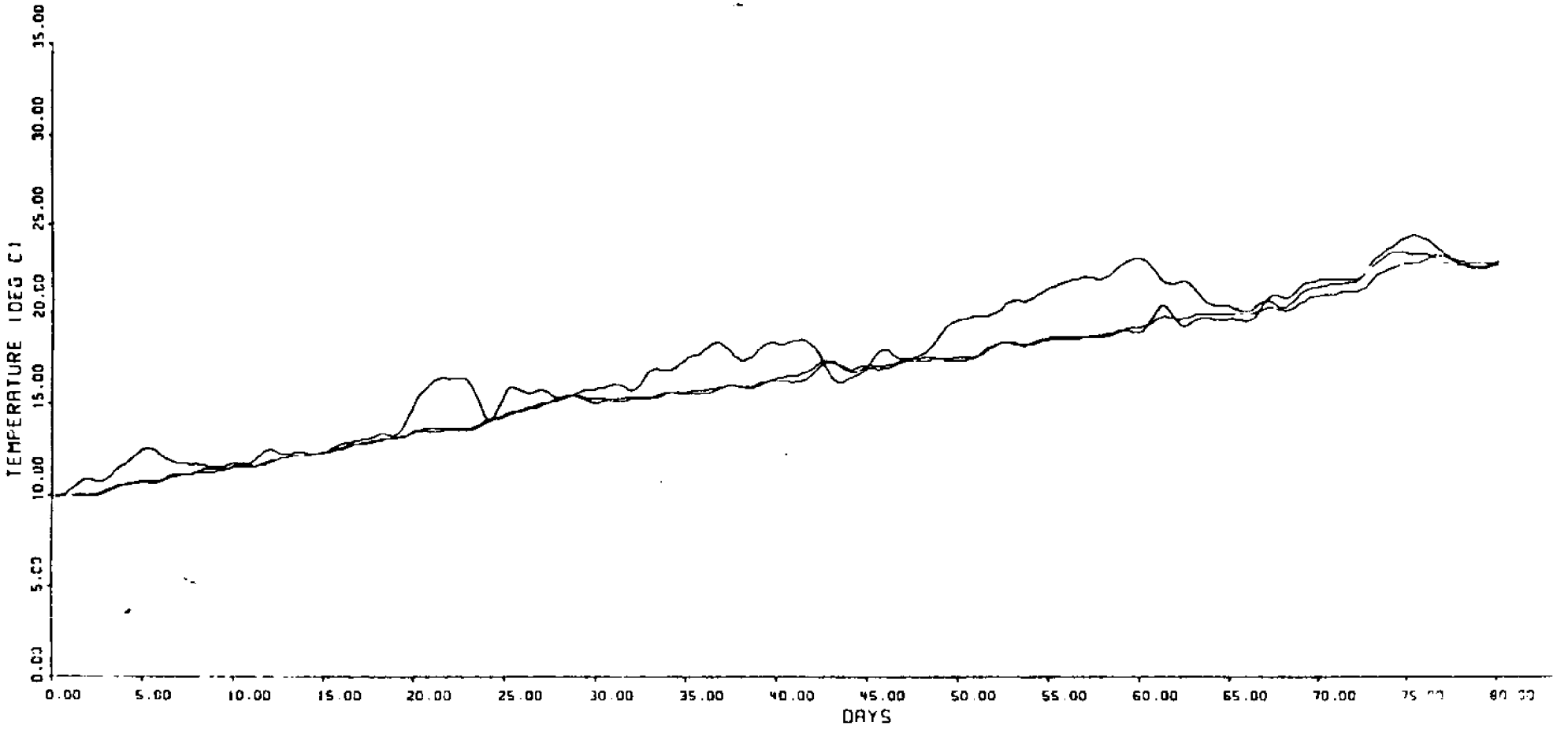

Figure 10a. Period 1, 21 February - 13 May 1977. Time series of 40 hr low-passed water temperature at SNLT comparing temperatures at three levels.

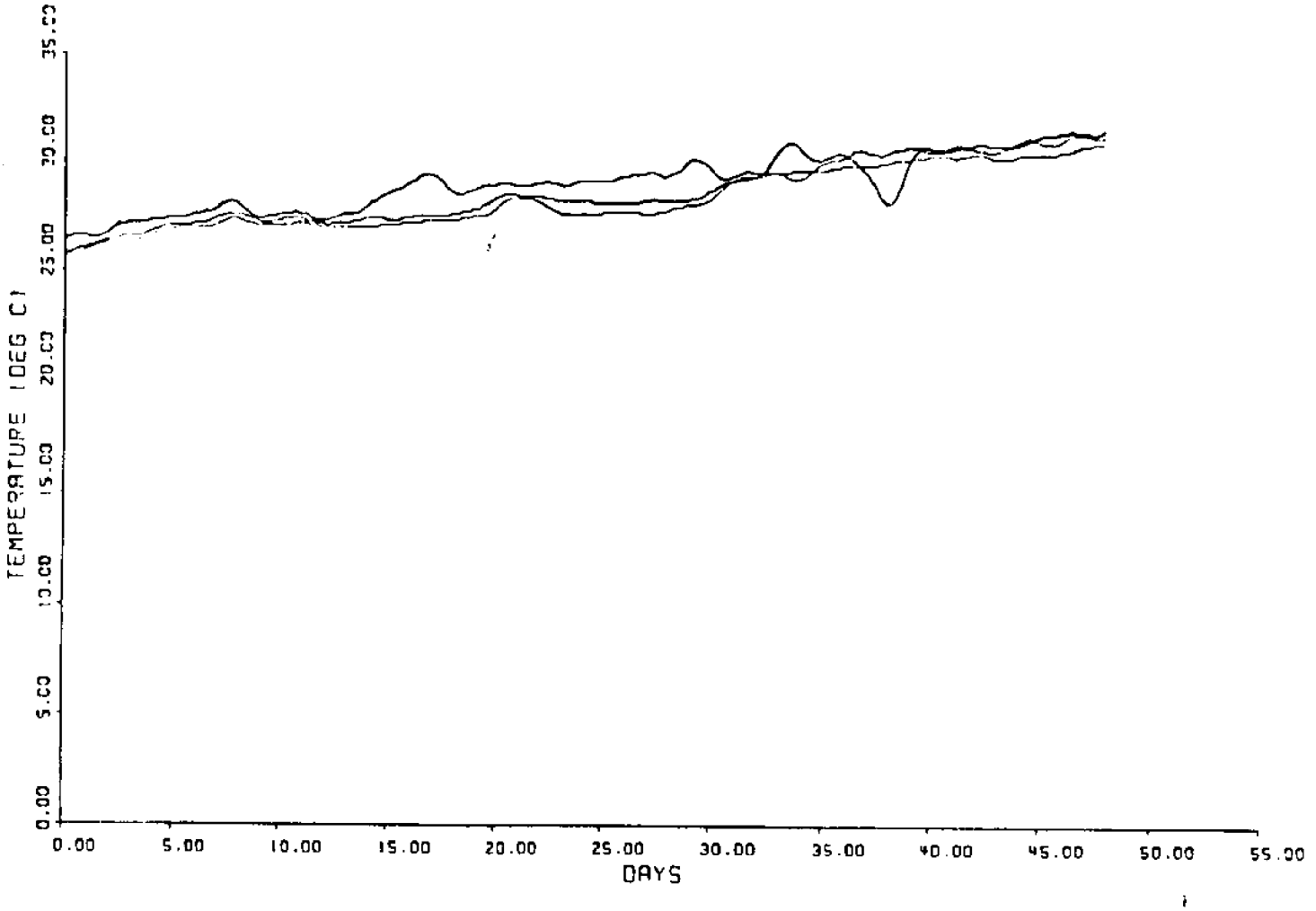

Figure 10b. Period 2, 30 May - 17 July 1977. Time series of 40 hr low-passed water temperature at SNLT comparing temperatures at three levels.

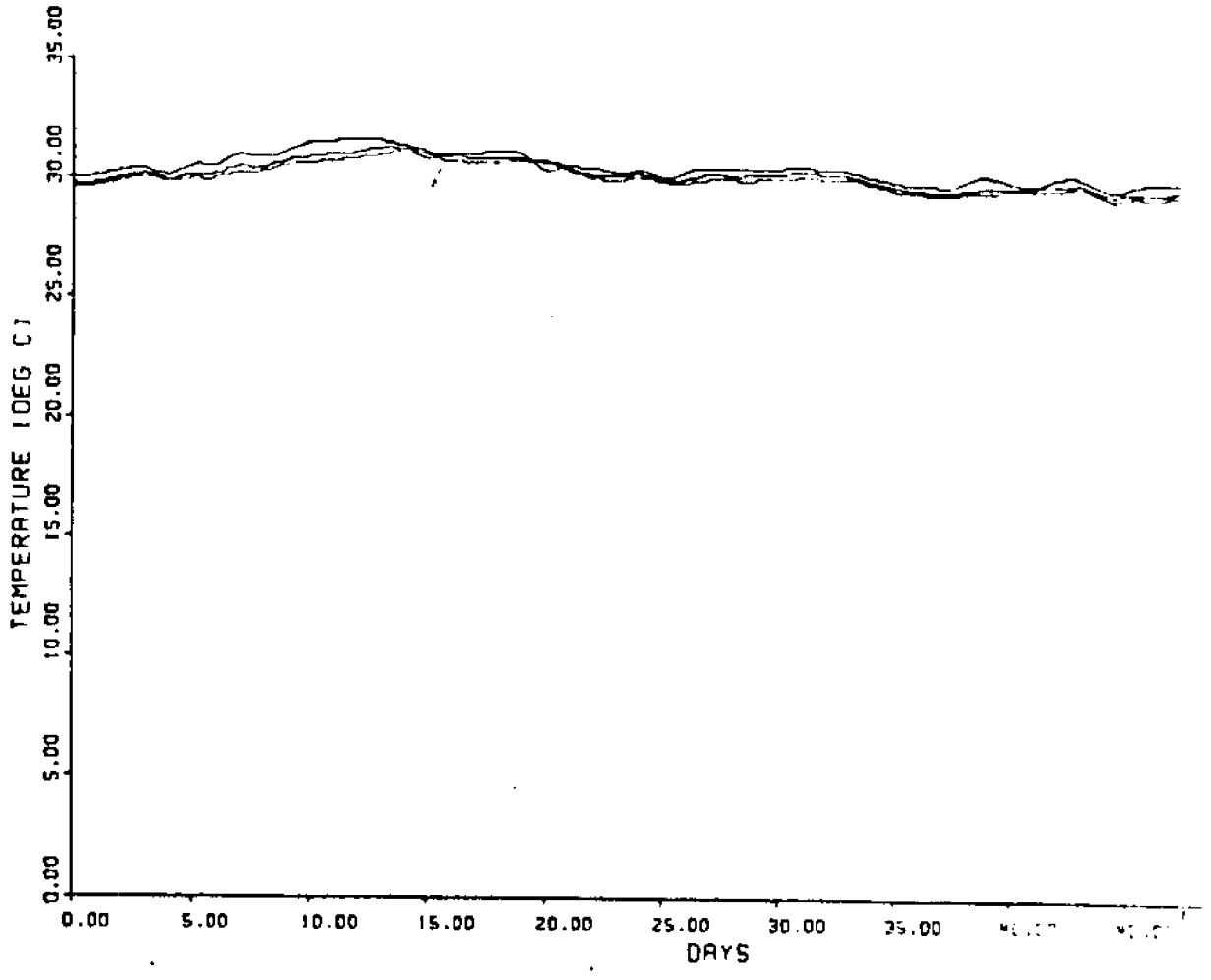

Figure 10c. Period 3, 31 July - 16 September 1977. Time series of 40 hr low-passed water temperature at SNLT comparing temperatures at three levels.

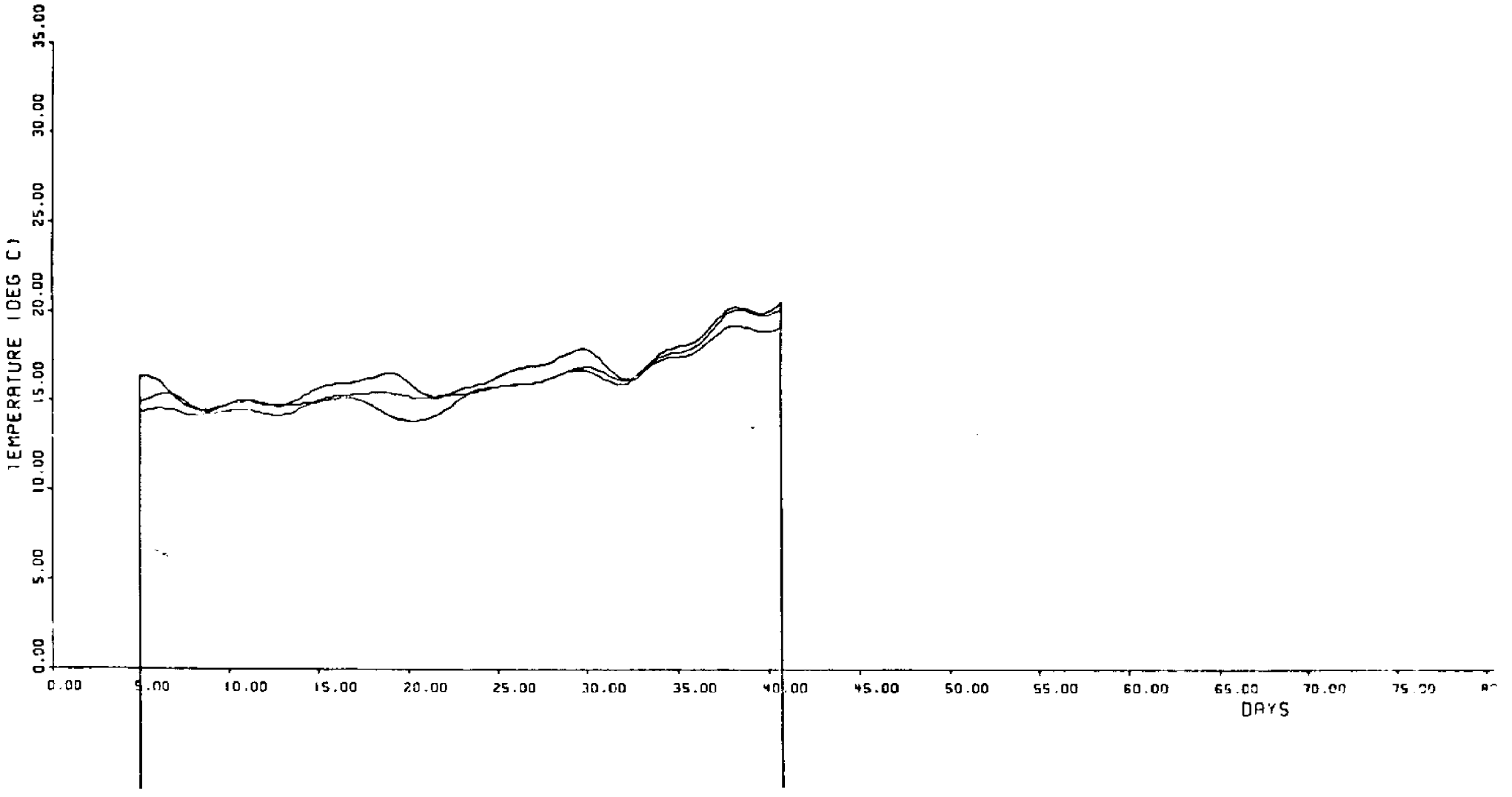

Figure 10d. Period 4, 12 April - 18 May 1980. Time series of 40 hr low-passed water temperature at SNLT comparing temperatures at three levels.

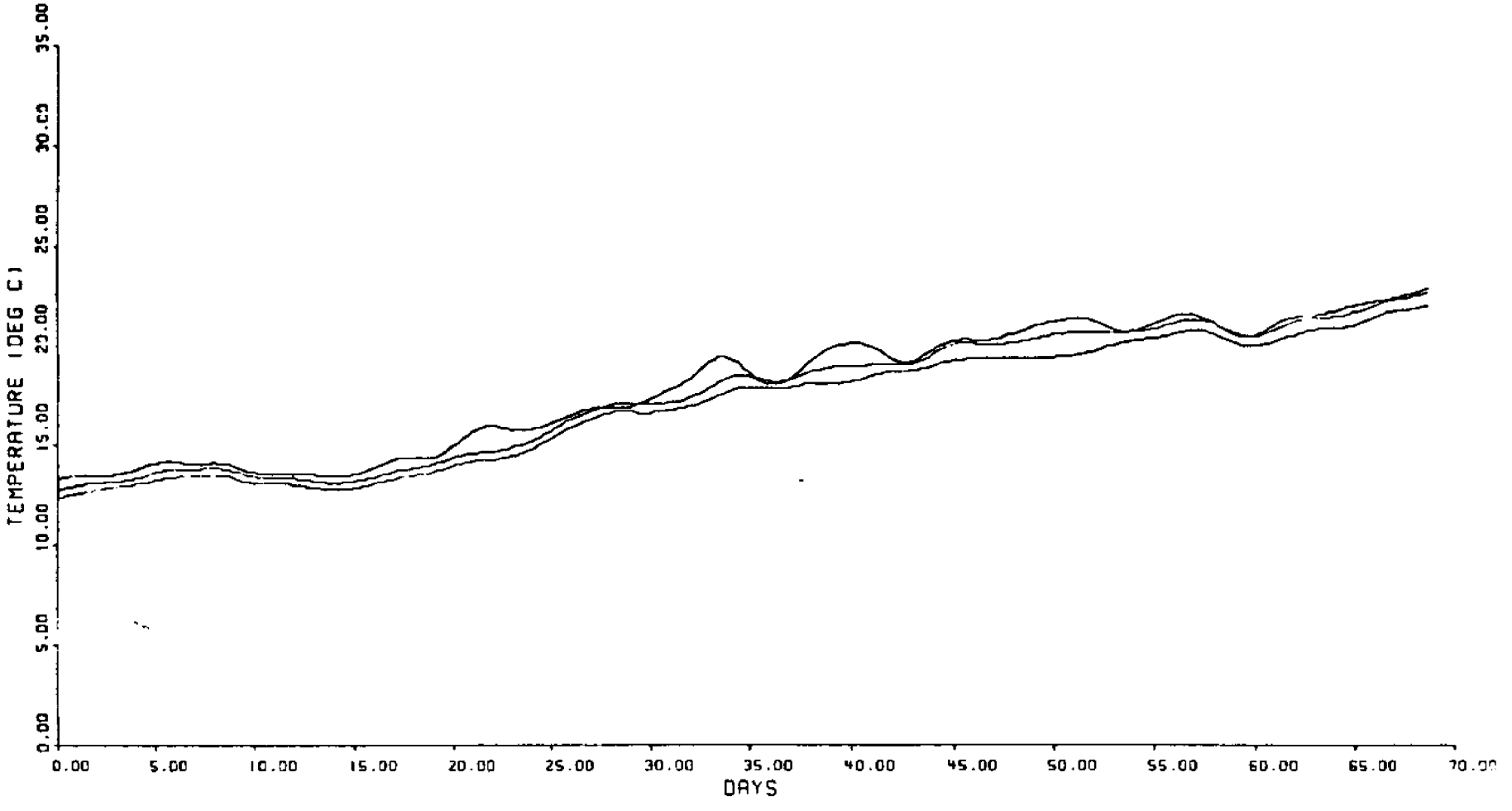

Figure 10e. Period 5, 10 March - 18 May 1981. Time series of 40 hr low-passed water temperature at SNLT comparing temperatures at three levels.

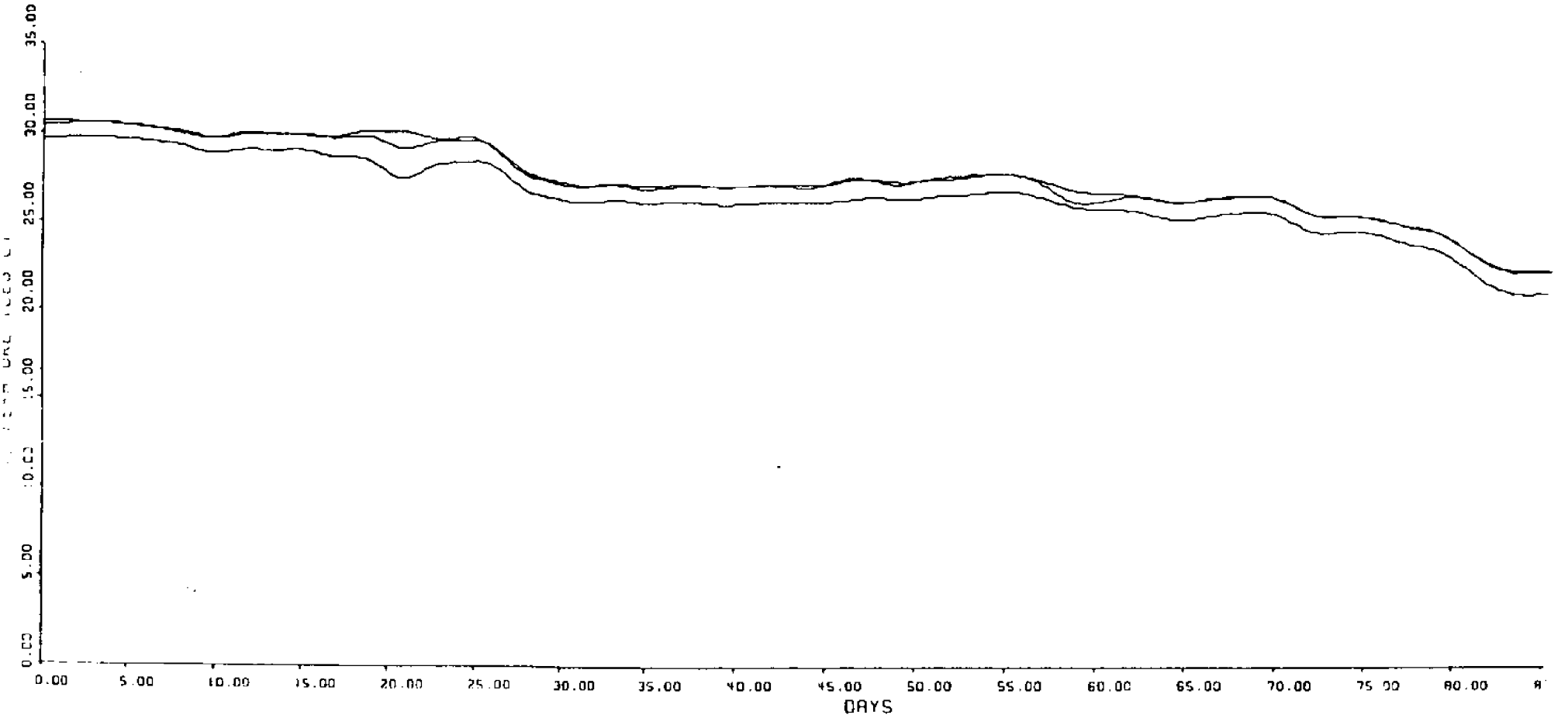

Figure 10f. Period 6, 23 July - 19 October 1981. Time series of 40 hr low-passed water temperature at SNLT comparing temperatures at three levels.

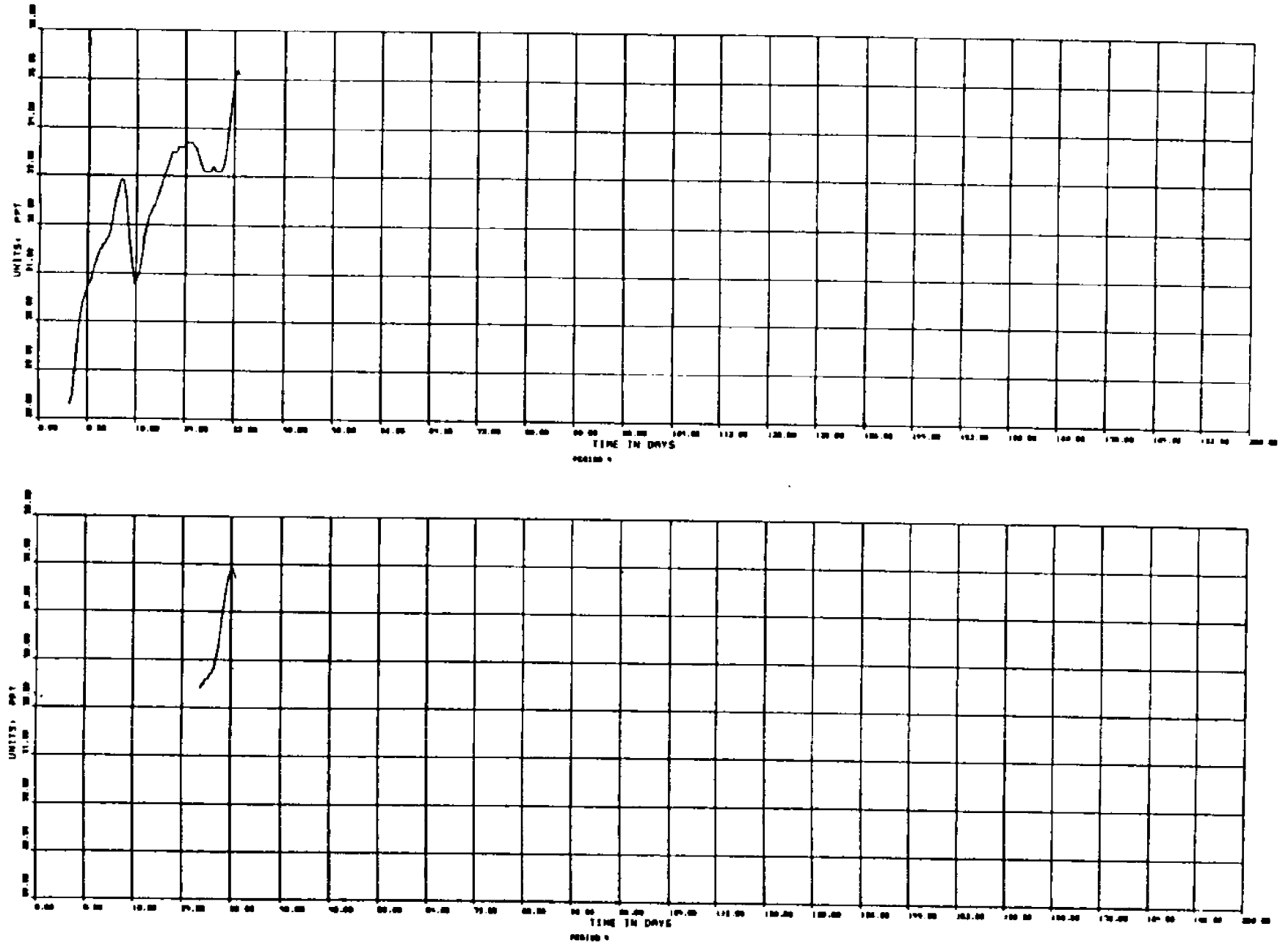

Figure 11a. Period 4, 7 April - 14 May 1980 (surface, upper plot), 1 - 14 May 1980 (bottom, lower plot). Time series of 40 hr low-passed salinity at SNLT.

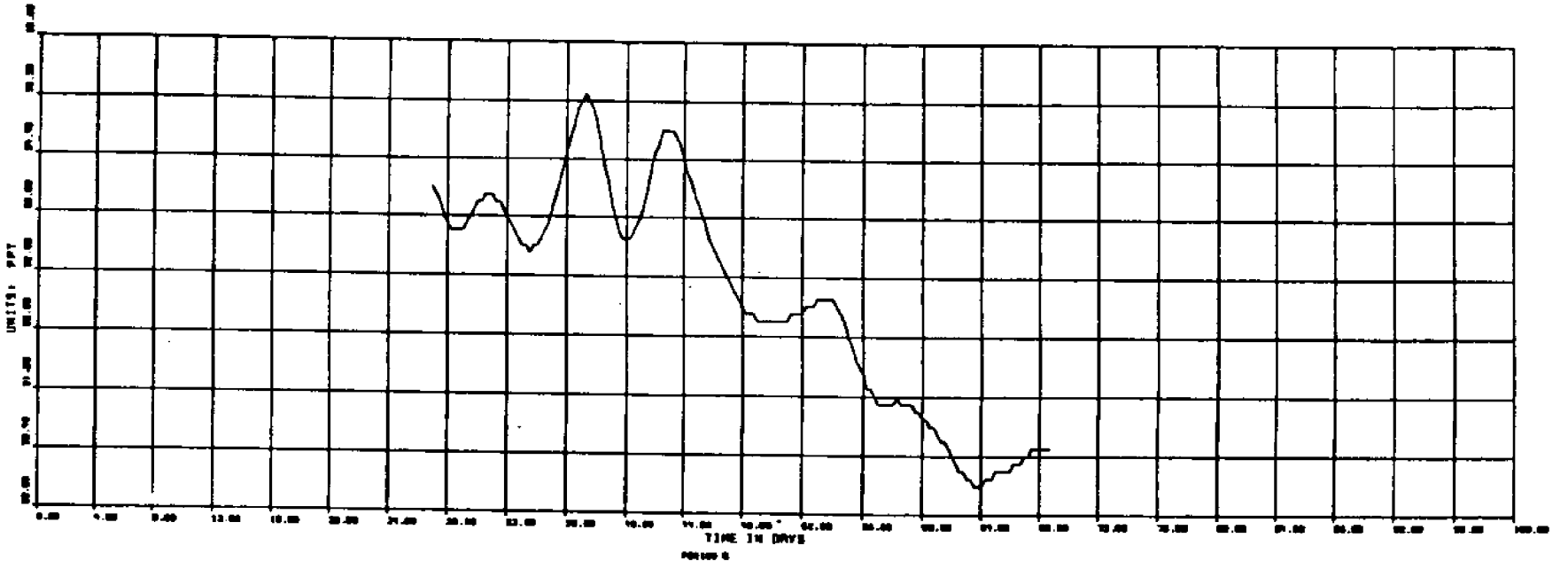

Figure 11b. Period 5, 7 April - 18 May 1981 (surface). Time series of 40 hr low-passed salinity at SNLT.

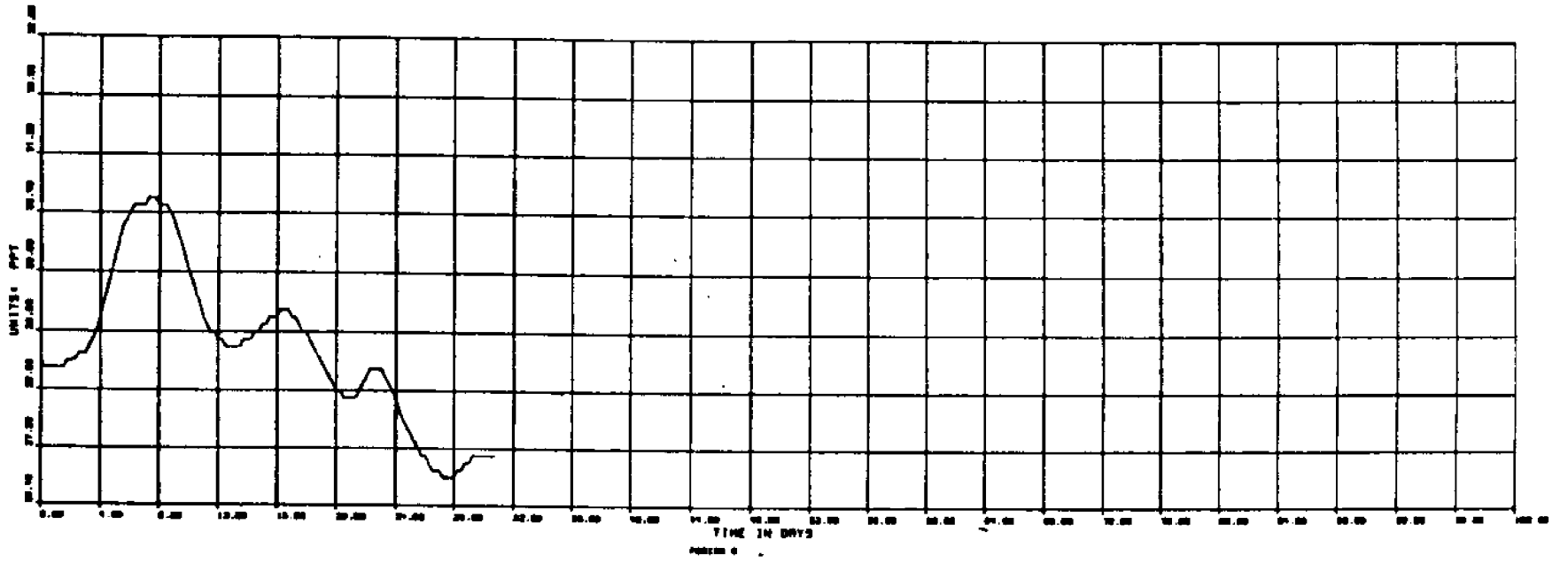

Figure 11c. Period 6, 23 July - 22 August 1981 (bottom). Time series of 40 hr low-passed salinity at SNLT.

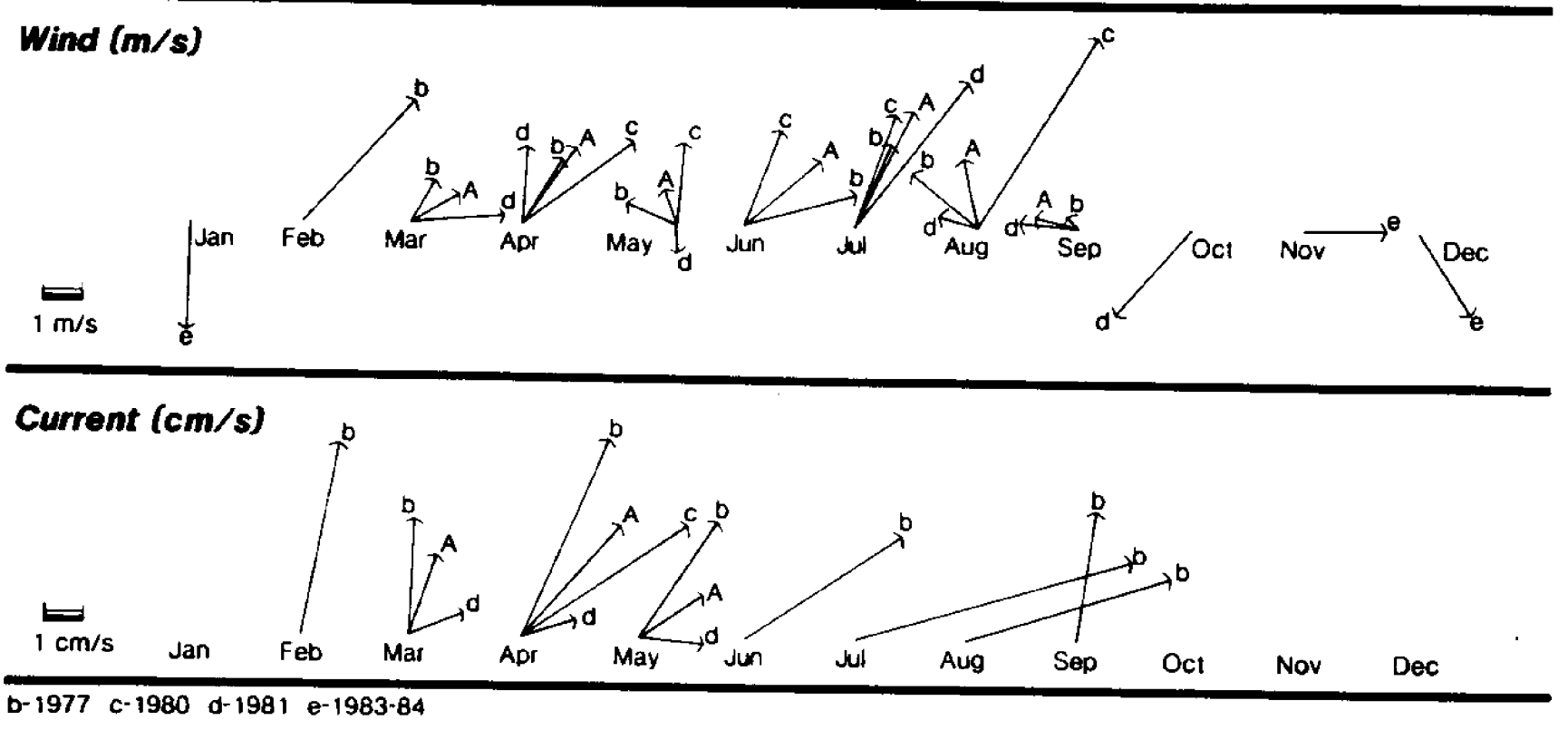

Figure 12. Monthly mean vectors of SNLT winds and currents. Vector A denotes the mean for that month for all values from all years of data. Vectors b, c, d, and e define monthly means from 1977, 1980, 1981, and 1983-84, respectively. North is toward top of figure.

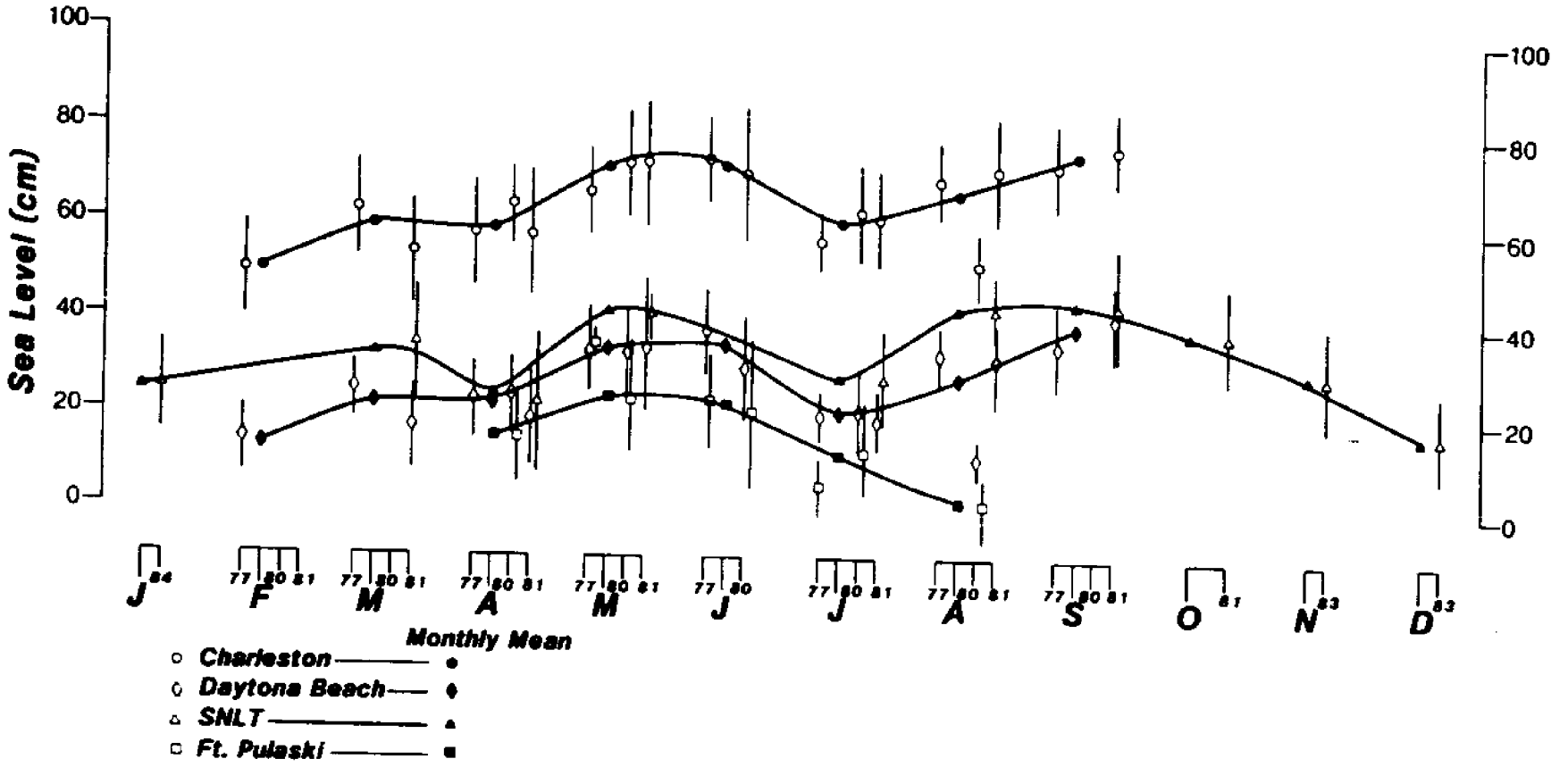

Figure 13. Monthly means and standard deviations of sea-level from SNLT, with data from Ft. Pulaski (Savannah), Charleston, and Daytona Beach included as reference. Monthly means from 1977, 1980, 1981, and 1983-84 are represented by open symbols. Means are relative to an arbitrary datum plane unique to each location. Vertical lines represent one standard deviation from mean. Means for all years combined are represented by closed symbols connected by an oscillating line.

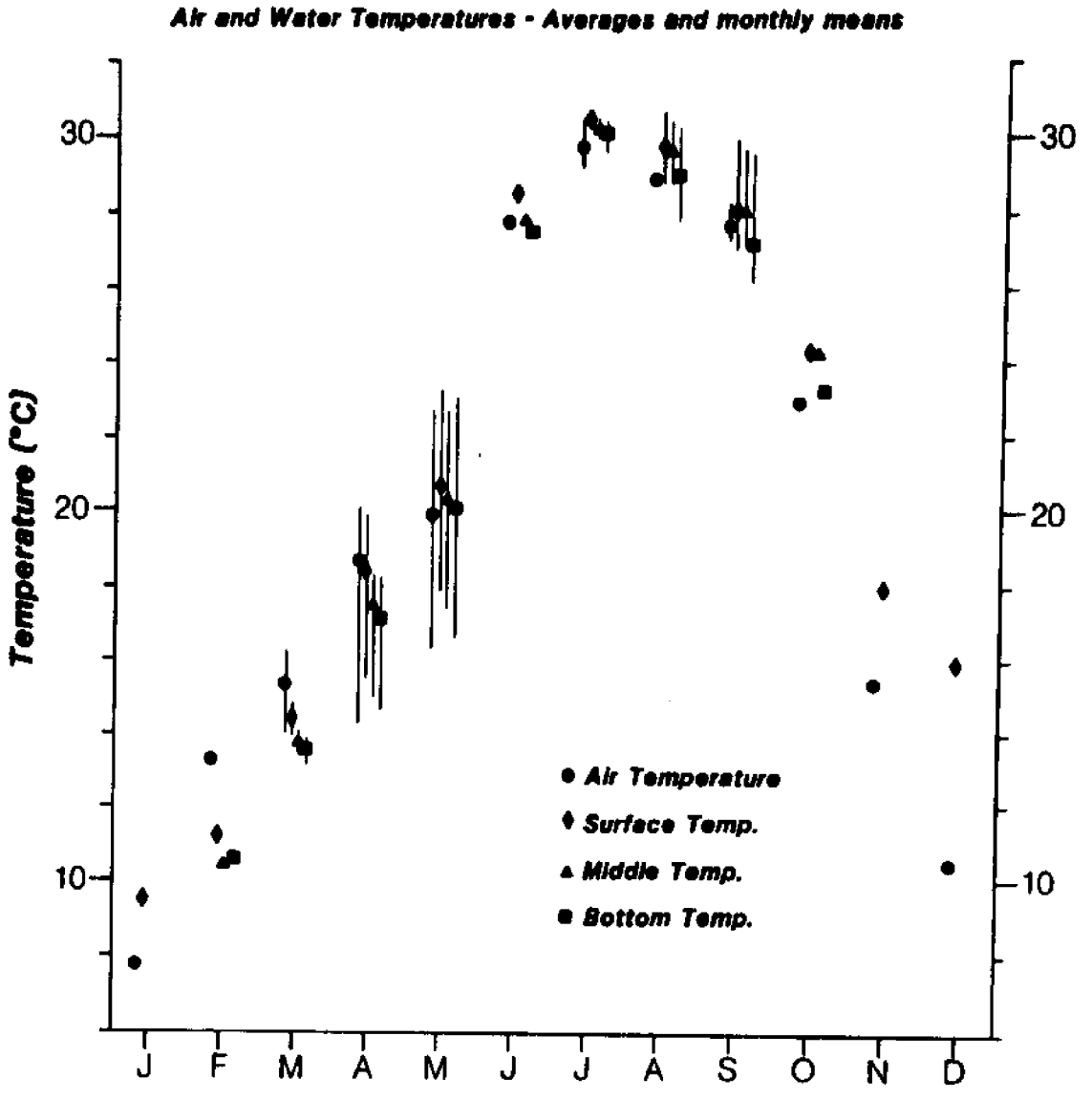

Figure 14. Means for each month for all air and water temperature data collected for SNLT. Vertical lines define ranges of monthly mean temperatures for each month. Temperature was recorded during only one year for January, February, June, October, November, and December.

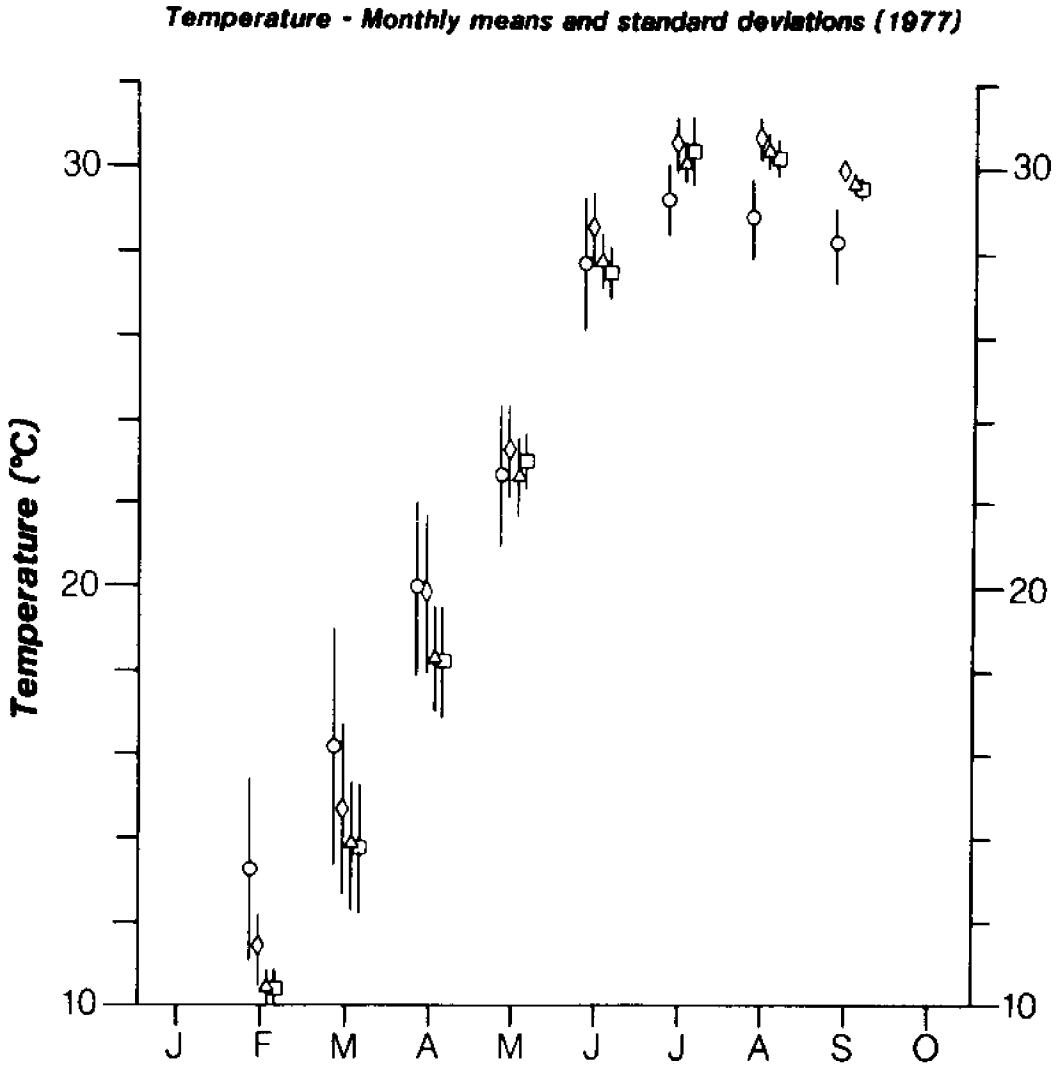

Figure 15a. Monthly means and standard deviations of SNLT air and water temperature during 1977. The legend is the same as that for Figure 14.

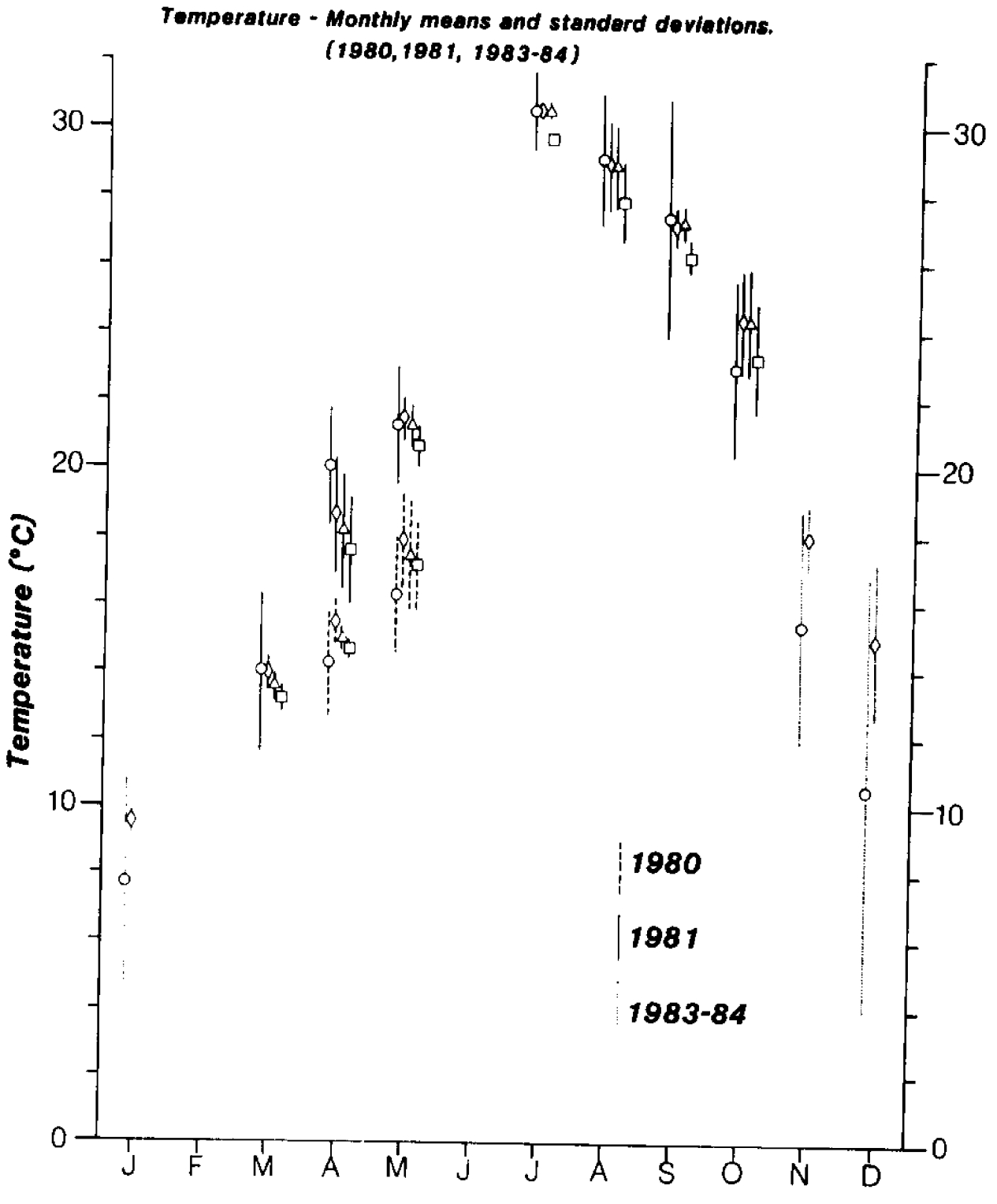

Figure 15b. Monthly means and standard deviations of SNLT air and water temperature for 1980 (defined by broken standard deviation lines) 1981 (defined by solid standard deviation lines), and 1983-84 (defined by dotted standard deviation lines). The legend is same as that for Figure 14.

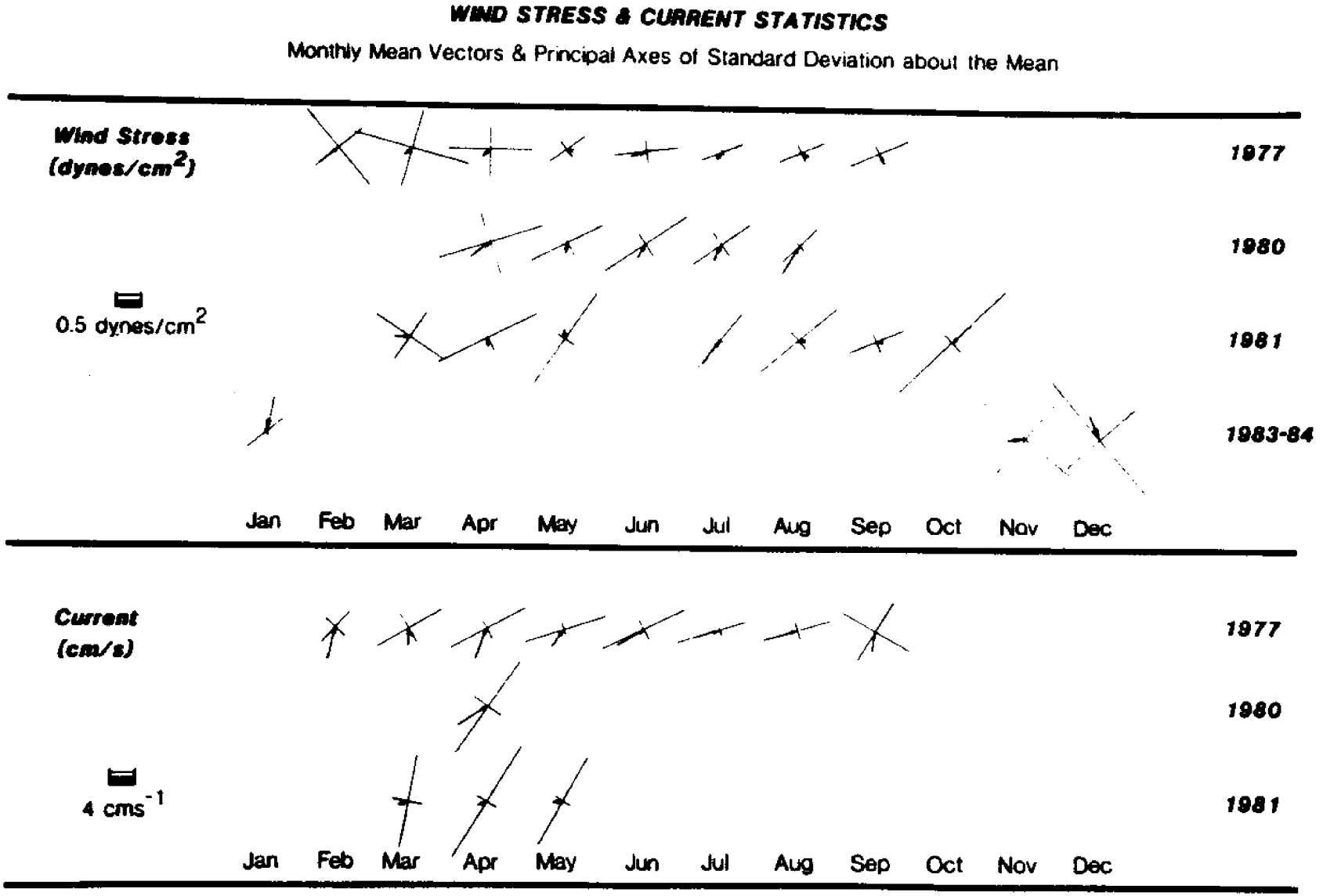

Figure 16. Monthly mean vectors and principal axes of SNLT wind stress and currents. Arrows represent monthly mean vectors. Crosses denote major and minor axes of standard deviation about the mean. North is toward top of figure. Currents from 1977 were obtained 1 m from bottom; 1980 and 1981 currents were obtained 8 m from bottom.

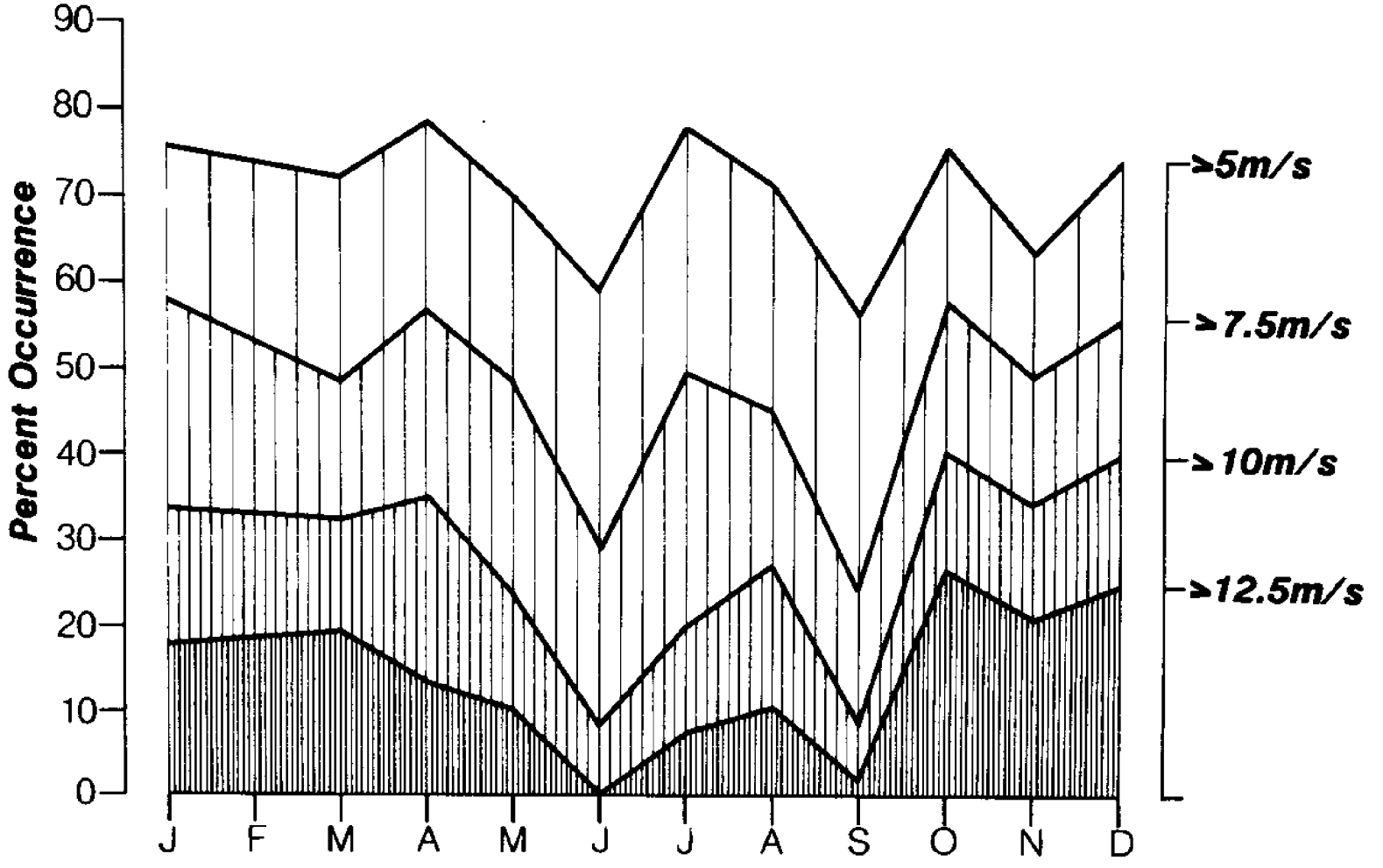

Figure 17. Monthly variations in intensity of wind speed at SNLT. Shaded areas represent percentage of monthly wind speeds greater than 5, 7.5, 10, and 12.5 m/s, respectively. For example, winds during January blew greater than 5 m/s 75% of the time, greater than 7.5 m/s 58% of the time, greater than 10 m/s 33% of the time, and greater than 12.5 m/s 18% of the time. Unshaded area represents percentage of wind speeds less than 5 m/s. All wind data at SNLT during 1977 - January 1984 (Periods 1-8) were used in the analysis.

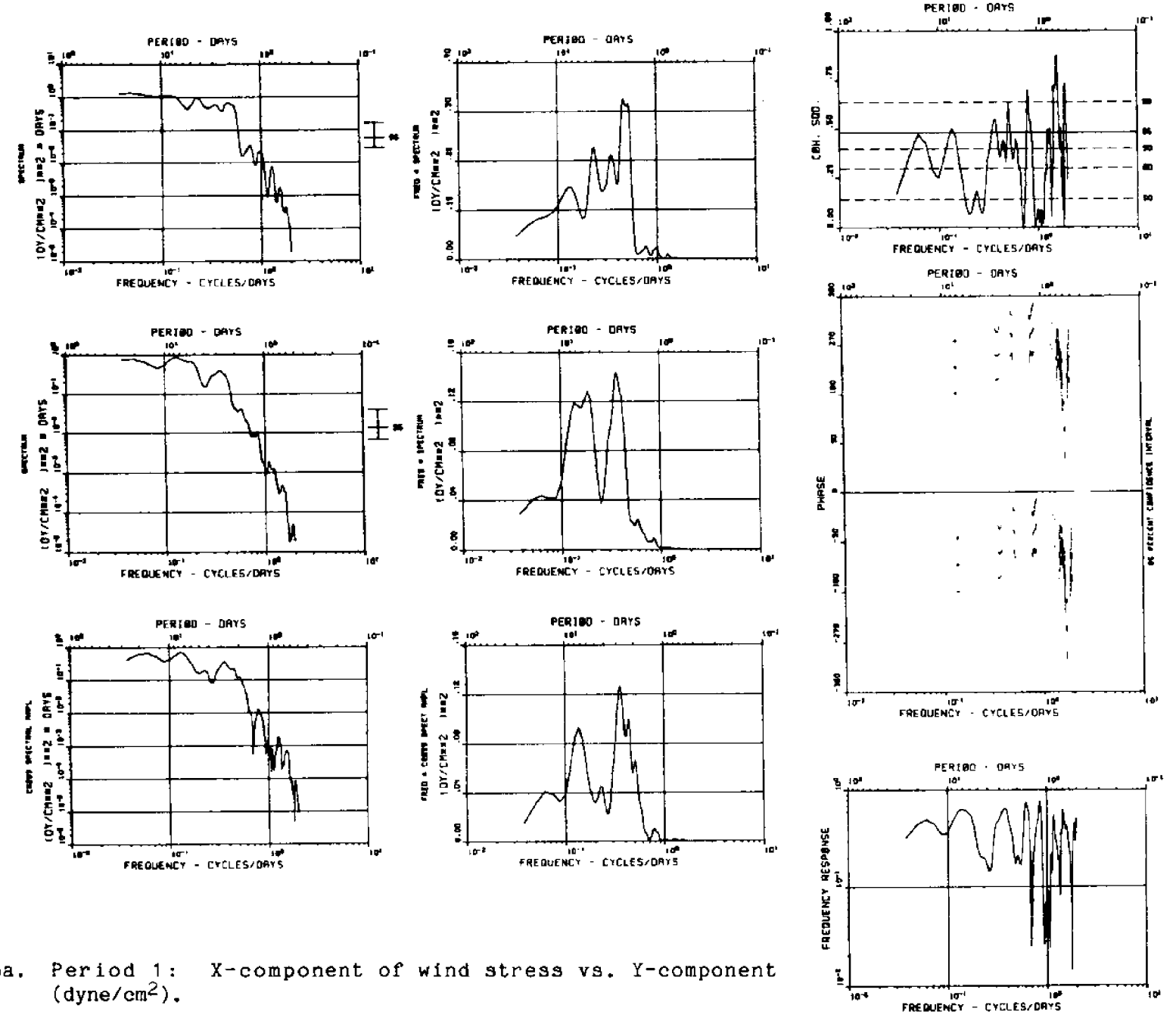

Figure 18a. Period 1: X-component of wind stress vs. Y-component (dyne/cm^2).

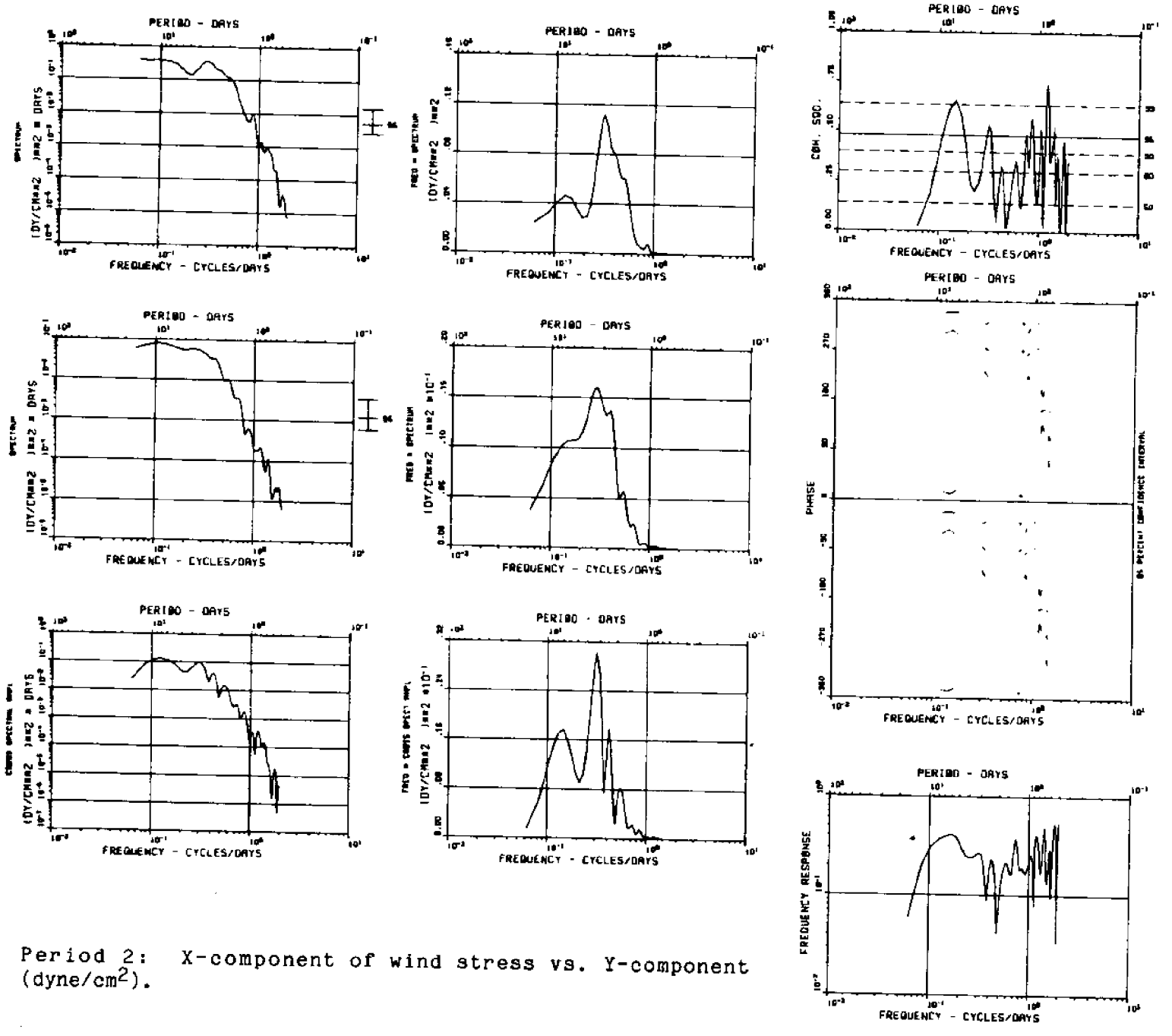

Figure 18b. Period 2: X-component of wind stress vs. Y-component (dyne/cm^2).

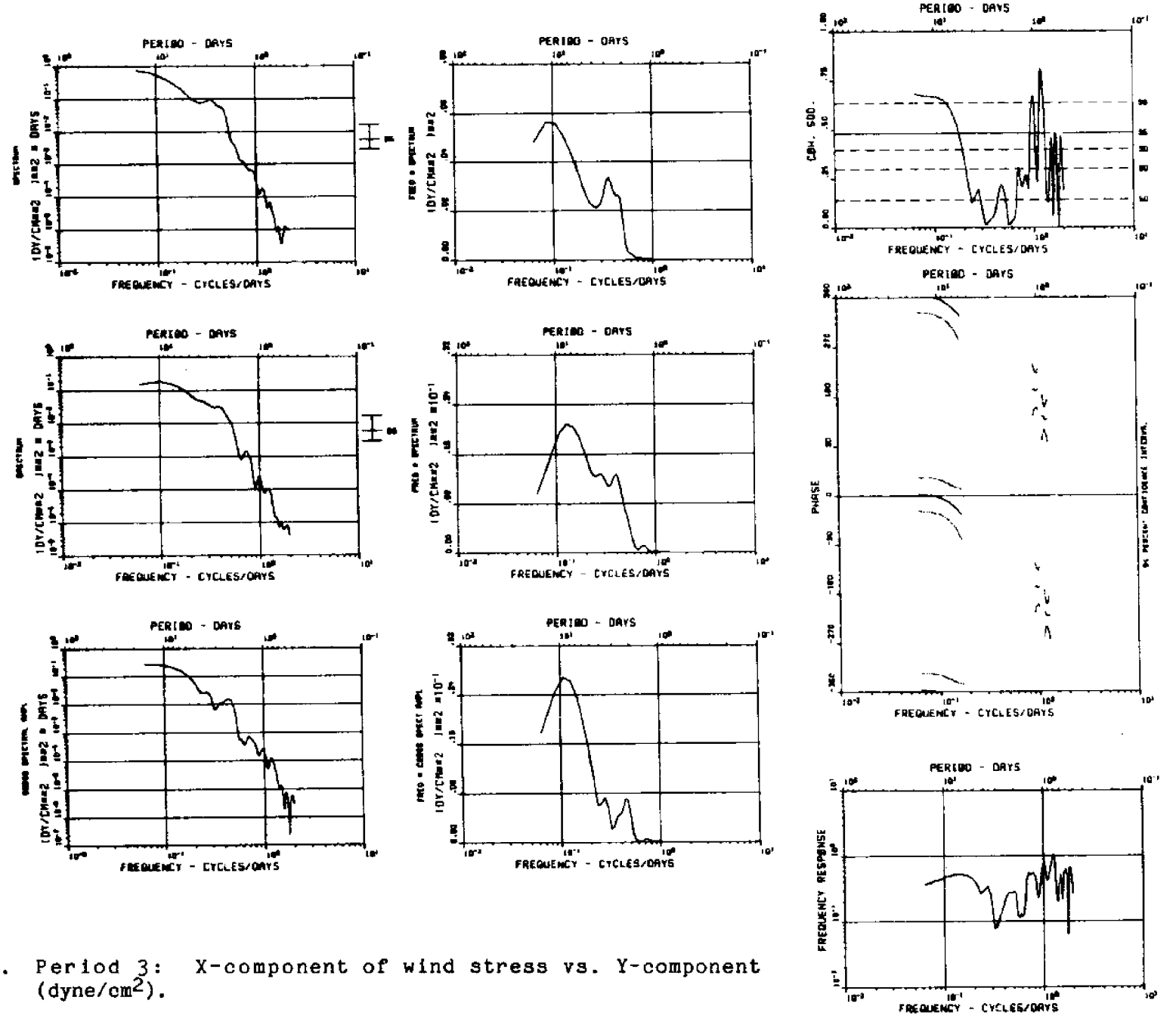

Figure 18c. Period 3: X-component of wind stress vs. Y-component (dyne/cm^2).

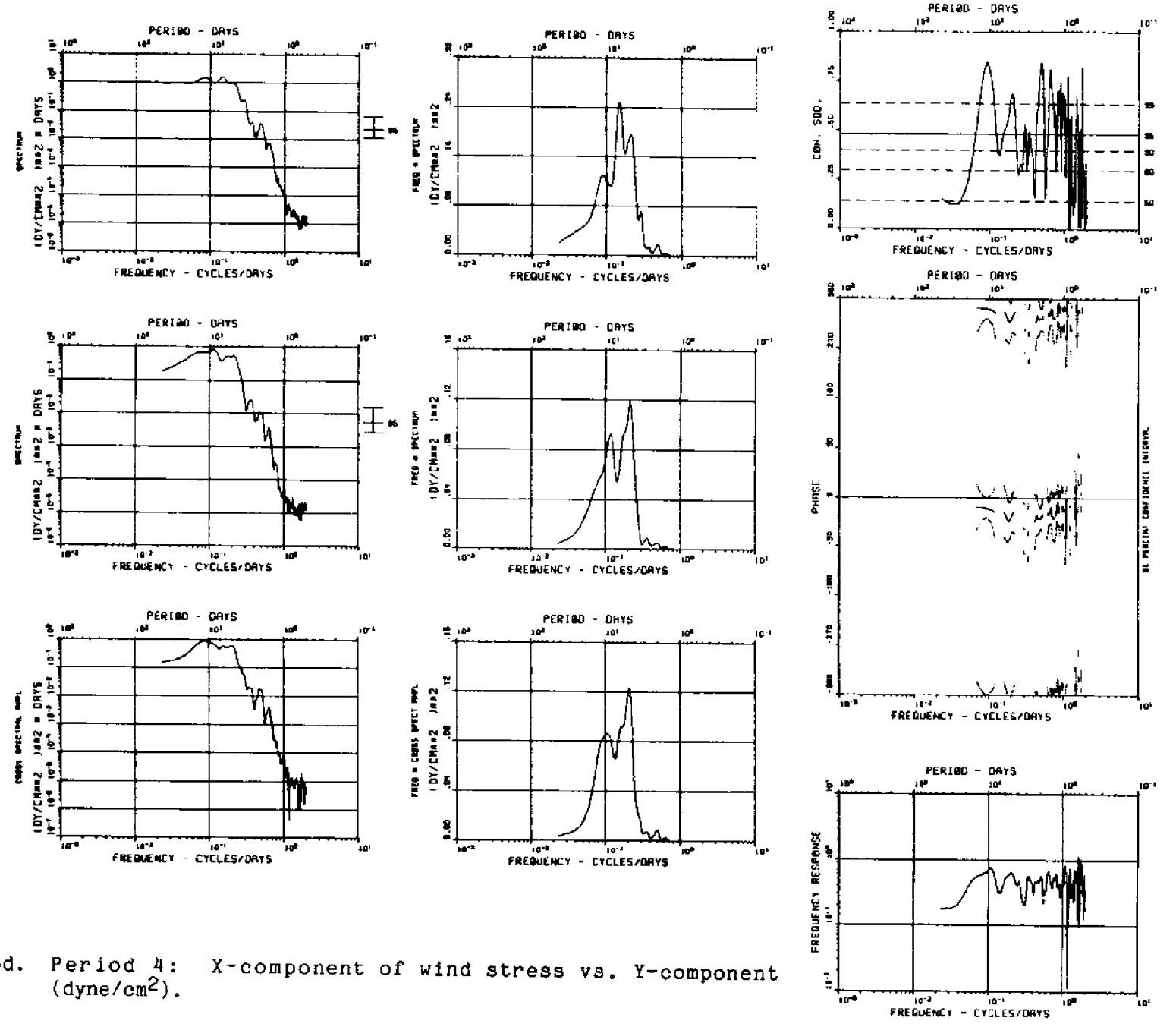

Figure 18d. Period 4: X-component of wind stress vs. Y-component (dyne/cm^2).

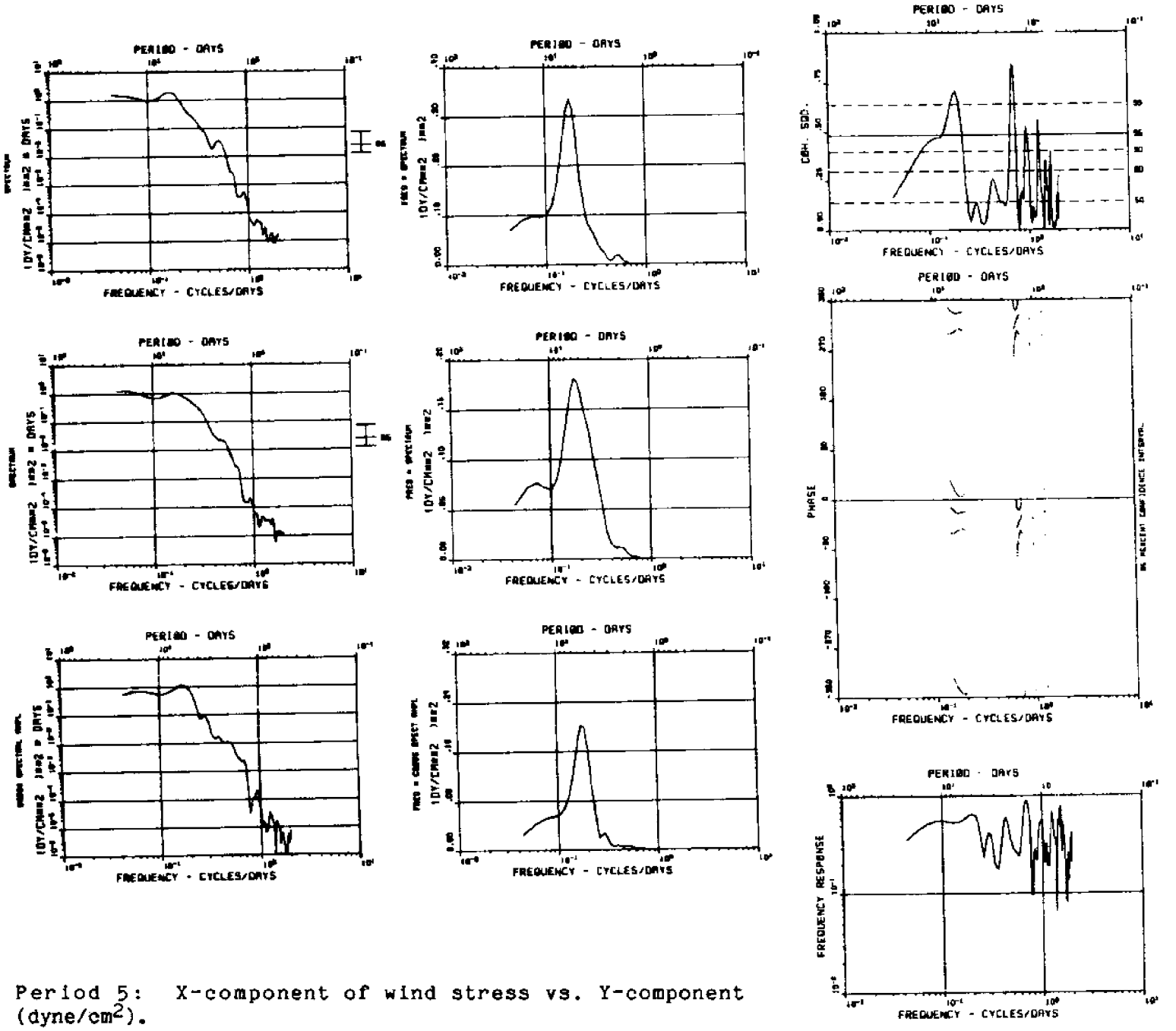

Figure 18e. Period 5: X-component of wind stress vs. Y-component (dyne/cm^2).

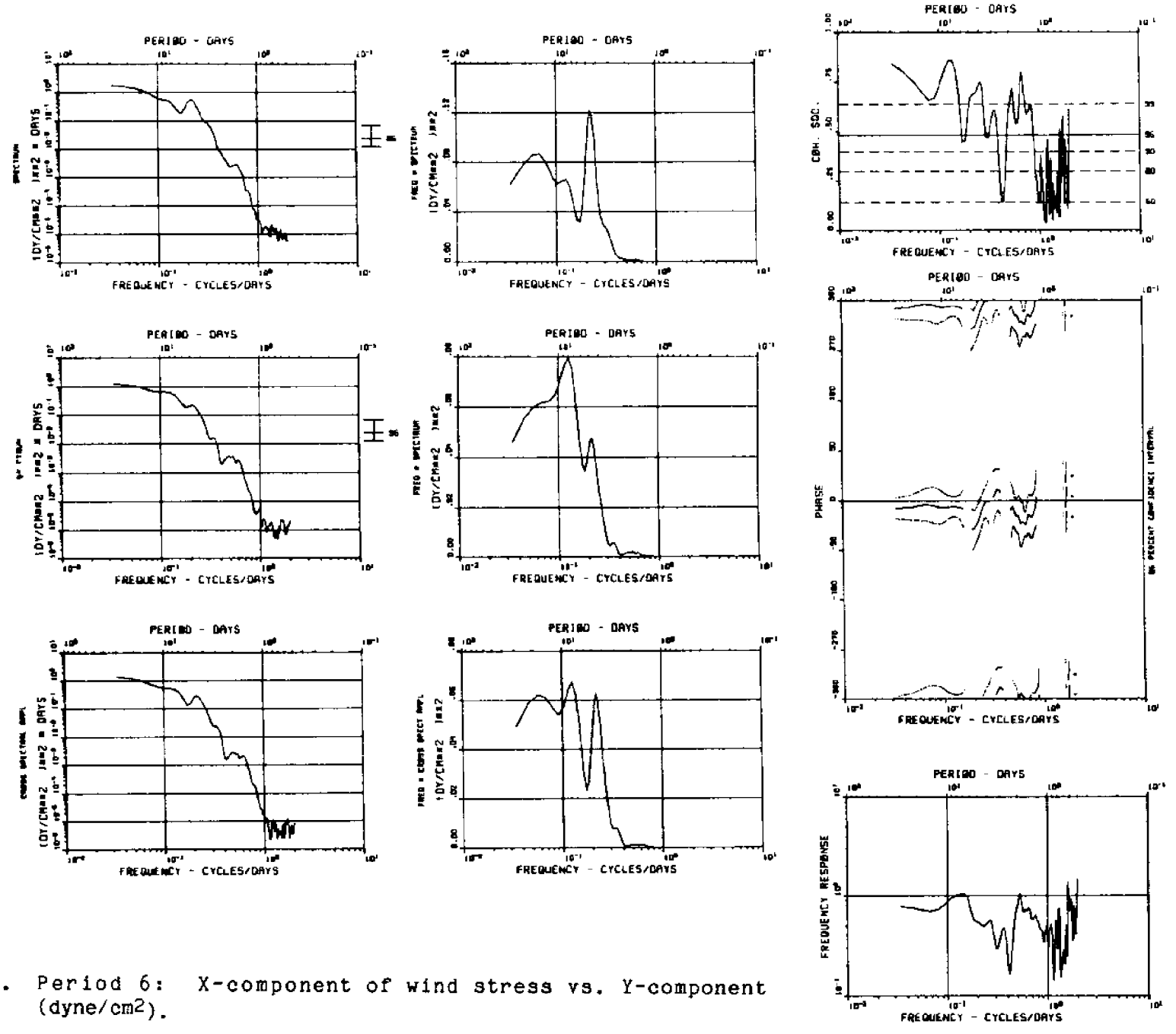

Figure 18f. Period 6: X-component of wind stress vs. Y-component (dyne/cm2).

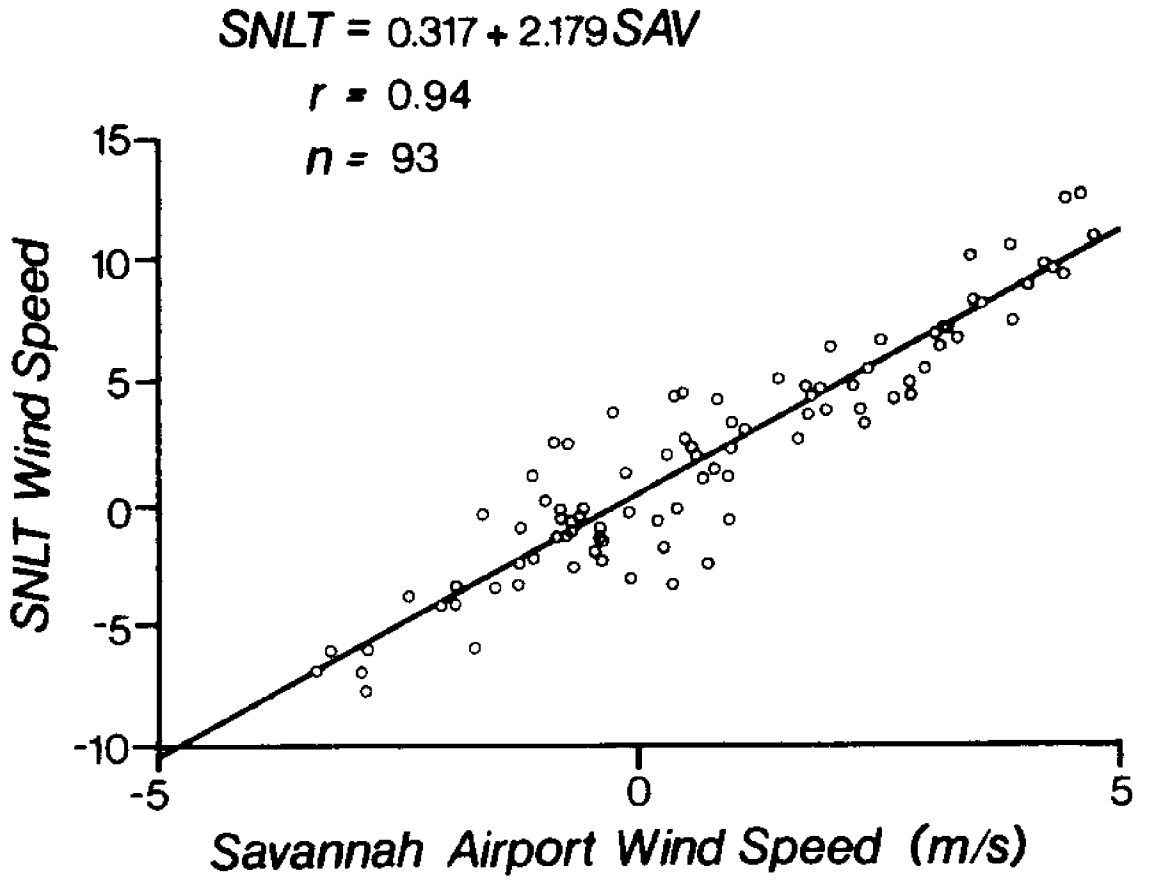

Figure 19. Regression of land-based (Travis Field, Savannah Airport) wind speed on SNLT wind speed, showing approximate 2:1 ratio between ocean and land winds. Data from Period 1 (21 February-16 March 1977).

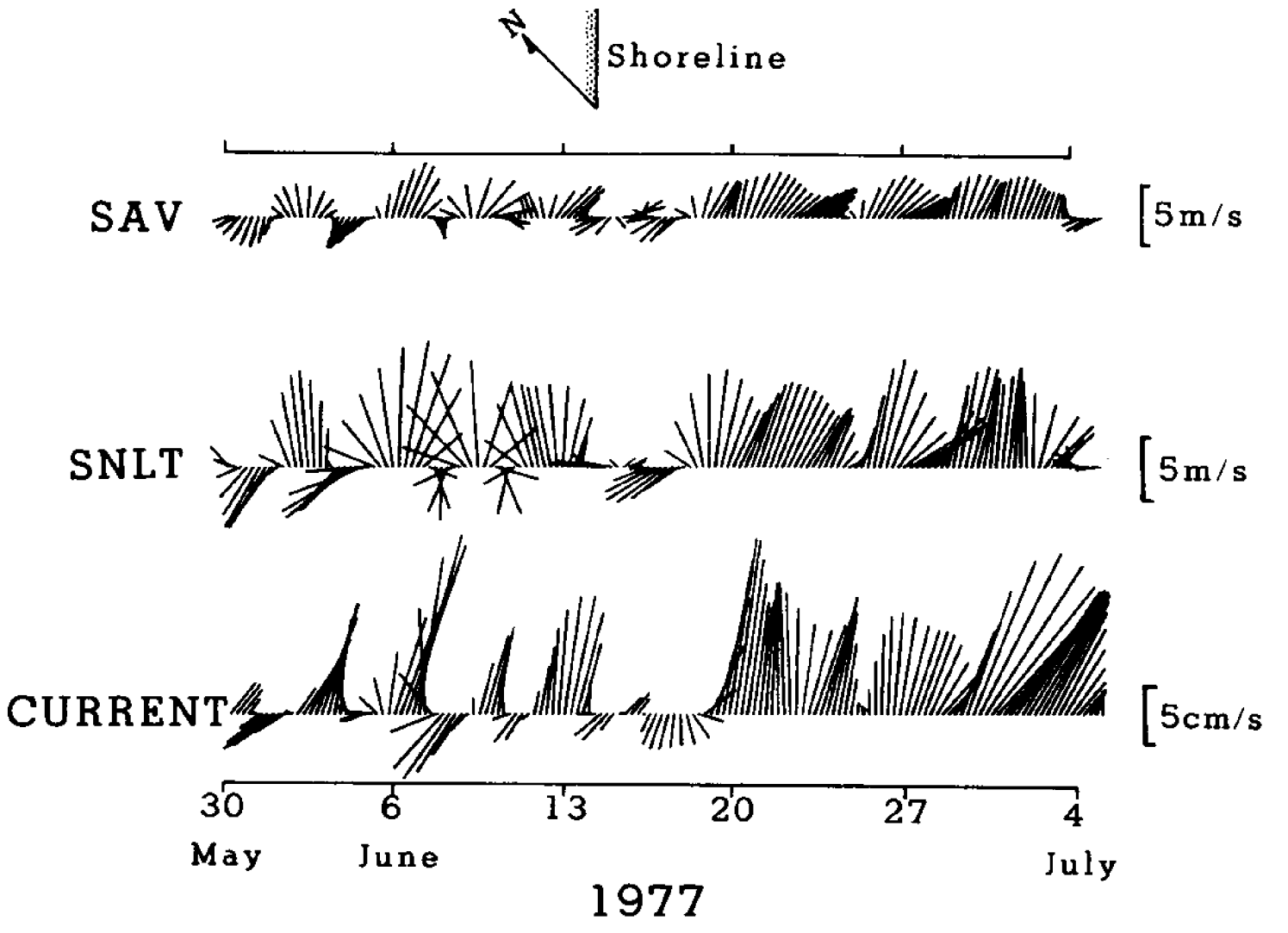

Figure 20. Stick vector diagrams of 40 hr low-passed time series, Period 2, 30 May-4 July 1977. SAV represents land wind from Travis Field, and SNLT represents ocean wind from SNLT. Currents obtained 1 m above bottom at SNLT. All data are in oceanographic convention; i.e., wind vectors point downwind. Vectors are plotted for every six hours.

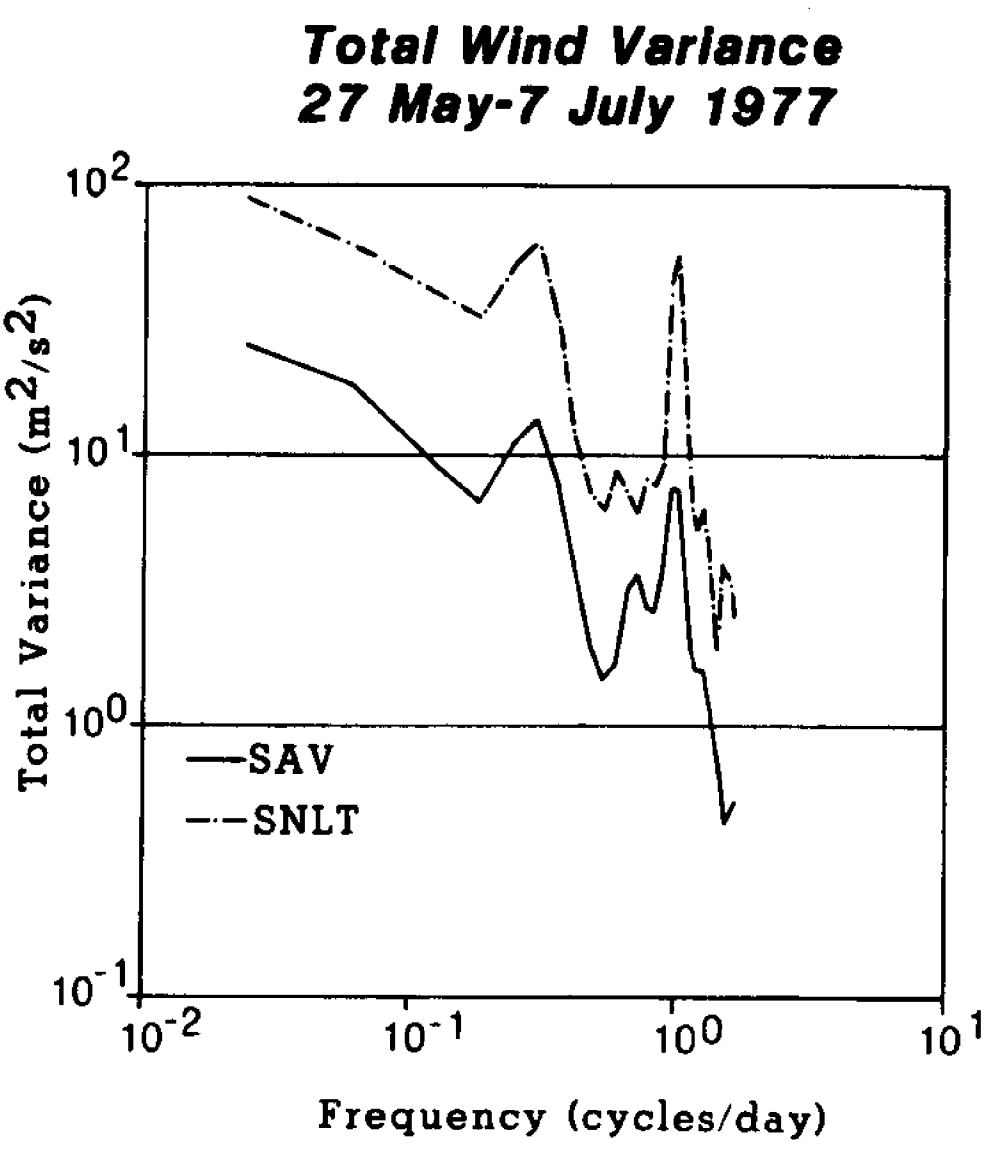

Figure 21. Autospectra of 10 hr low-passed land (SAV) and ocean (SNLT) wind time series, Period 2, 27 May-7 July 1977. The total energy in vectors is expressed in variance units.

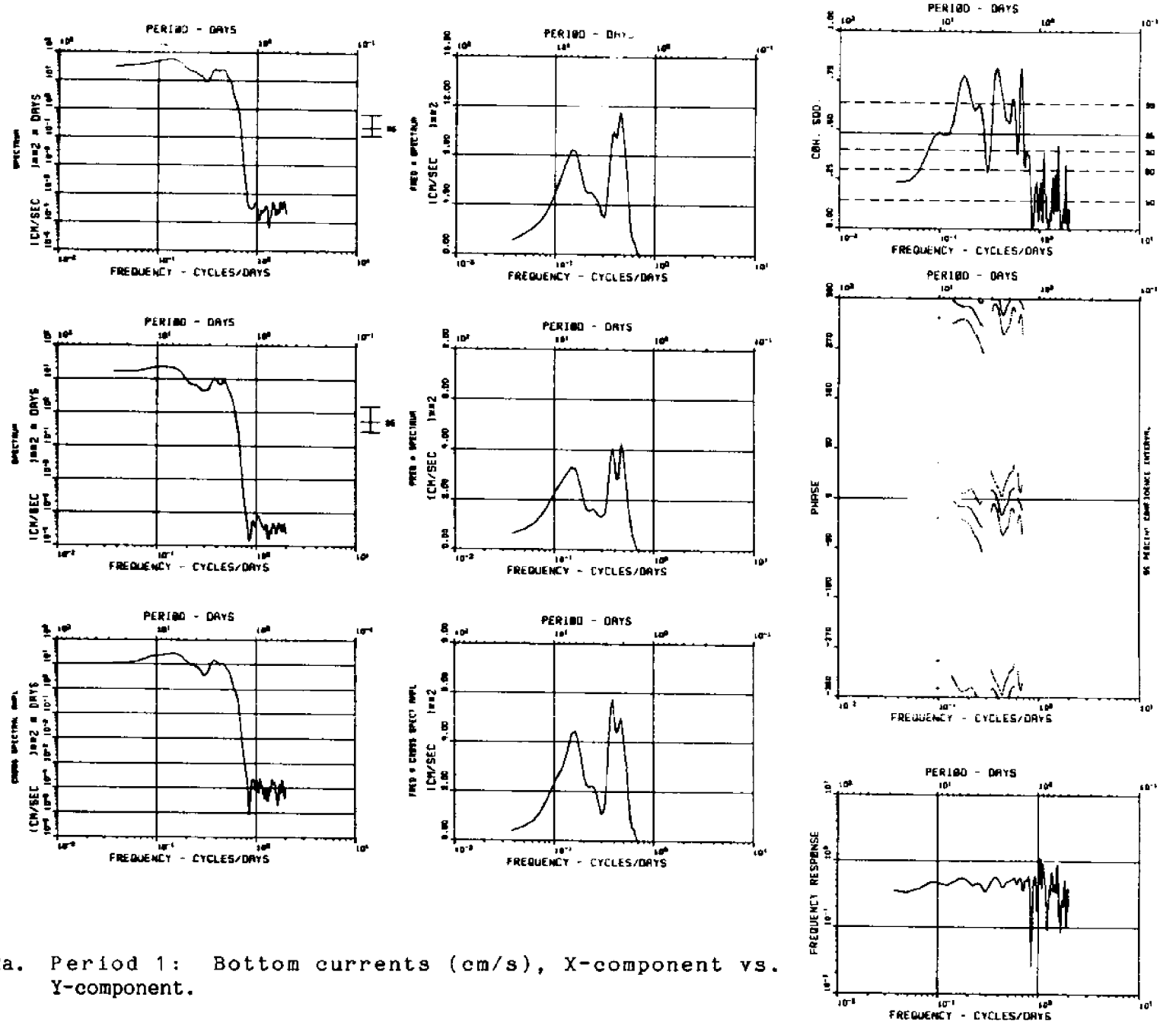

Figure 22a. Period 1: Bottom currents (cm/s), X-component vs. Y-component.

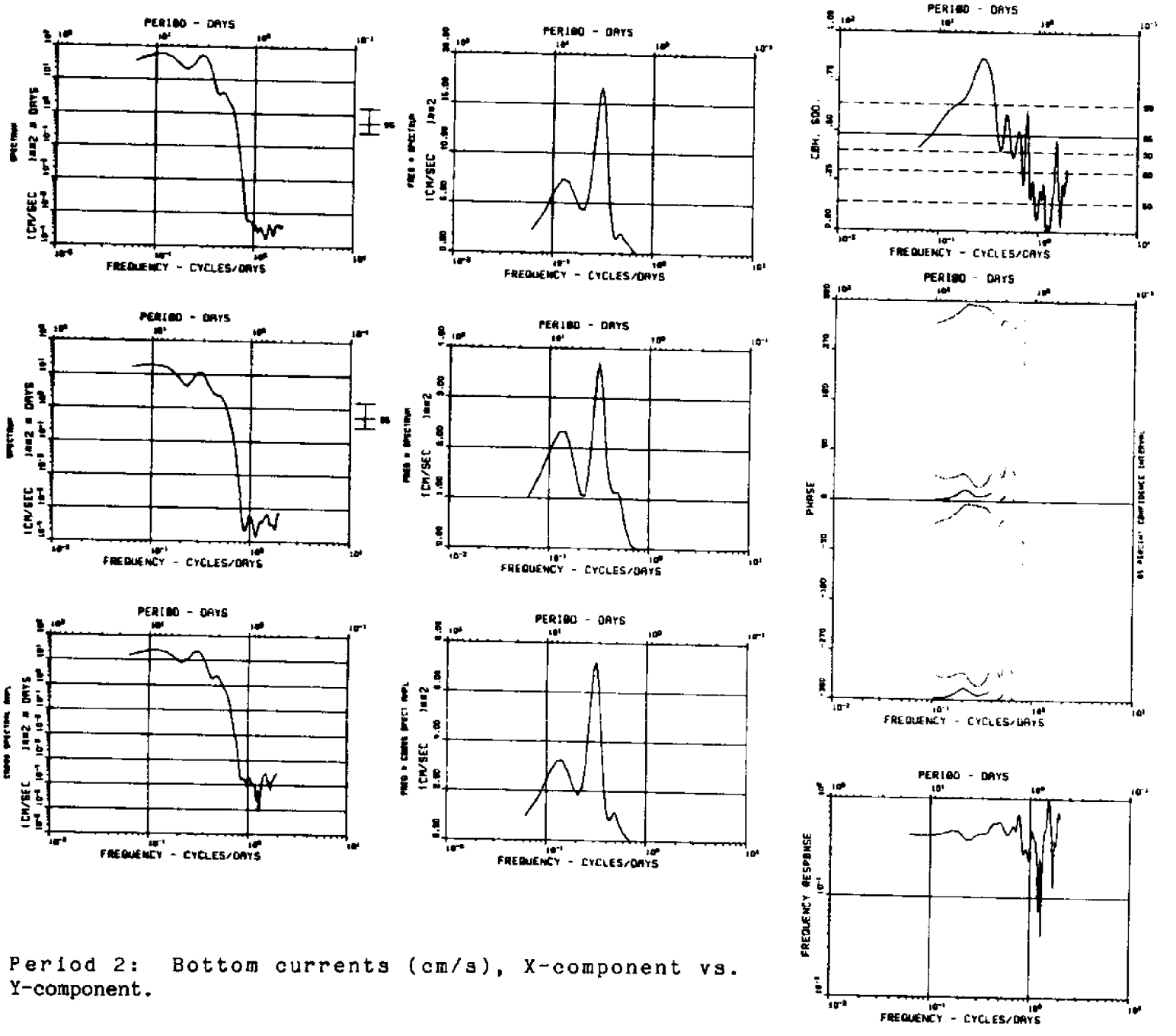

Figure 22b. Period 2: Bottom currents (cm/s), X-component vs. Y-component.

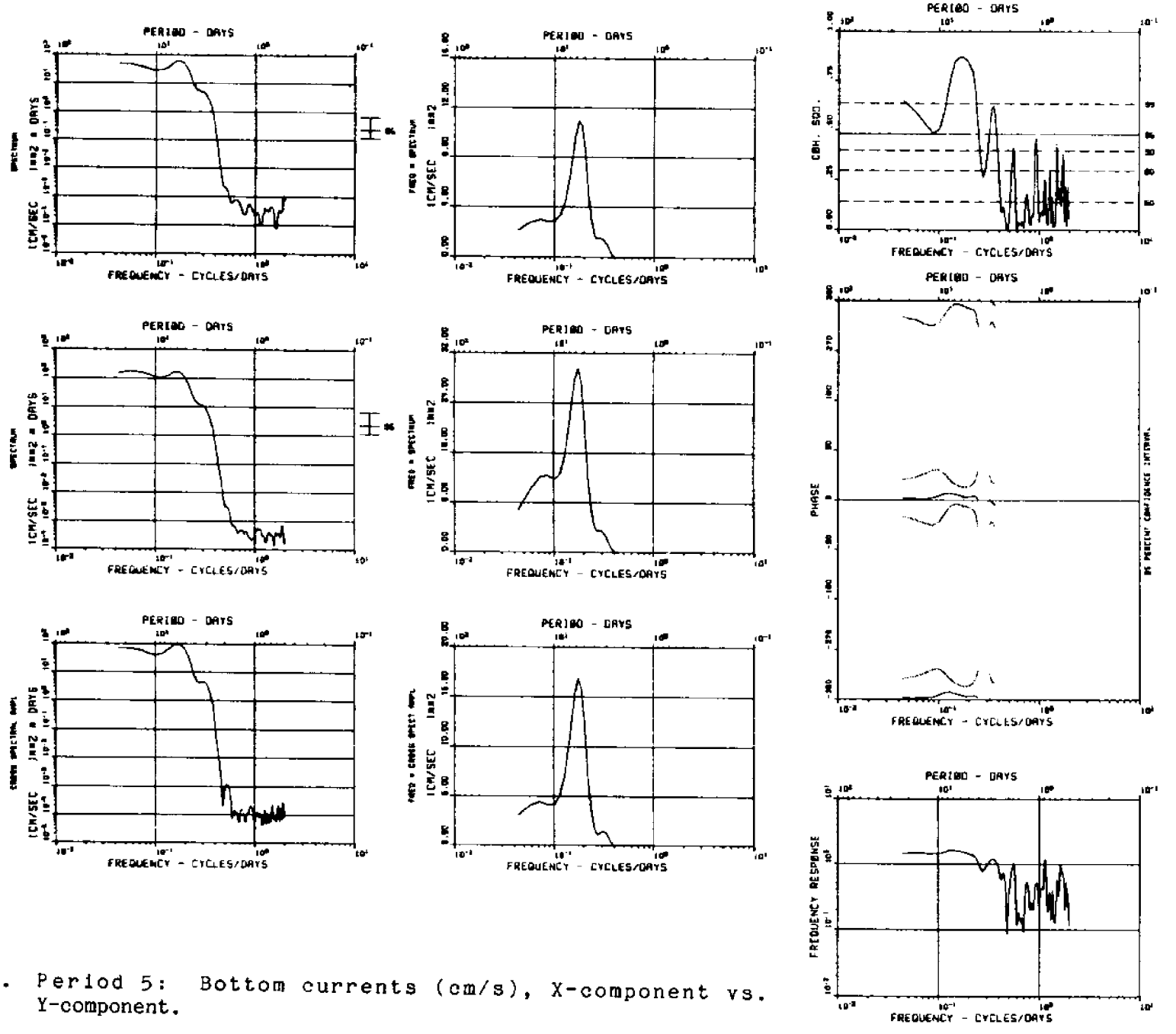

Figure 22c. Period 5: Bottom currents (cm/s), X-component vs. Y-component.

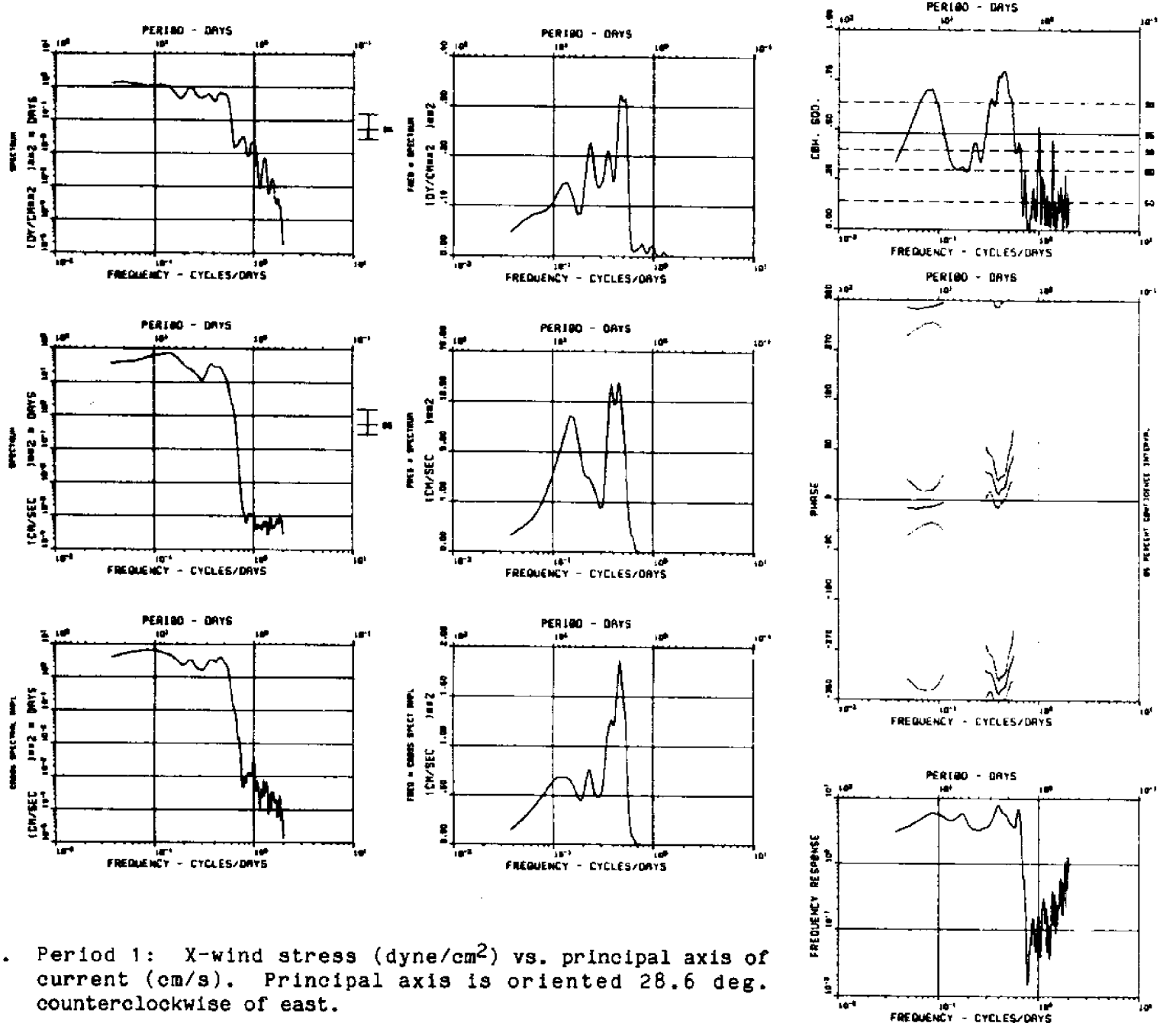

Figure 23a. Period 1: X-wind stress (dyne/cm^2) vs. principal axis of current (cm/s). Principal axis is oriented 28.6 deg. counterclockwise of east.

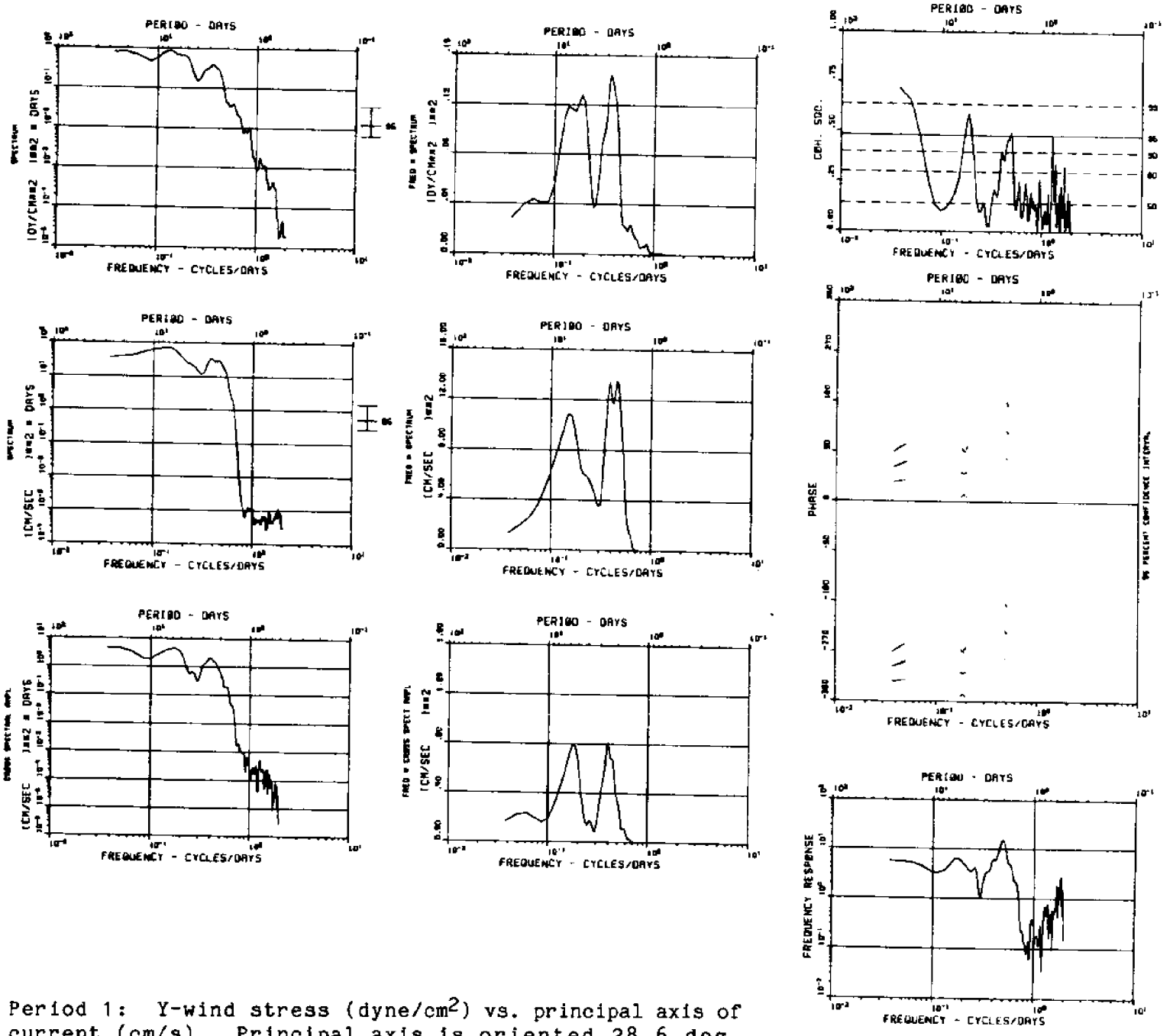

Figure 23b. Period 1: Y-wind stress (dyne/cm^2) vs. principal axis of current (cm/s). Principal axis is oriented 28.6 deg. counterclockwise of east.

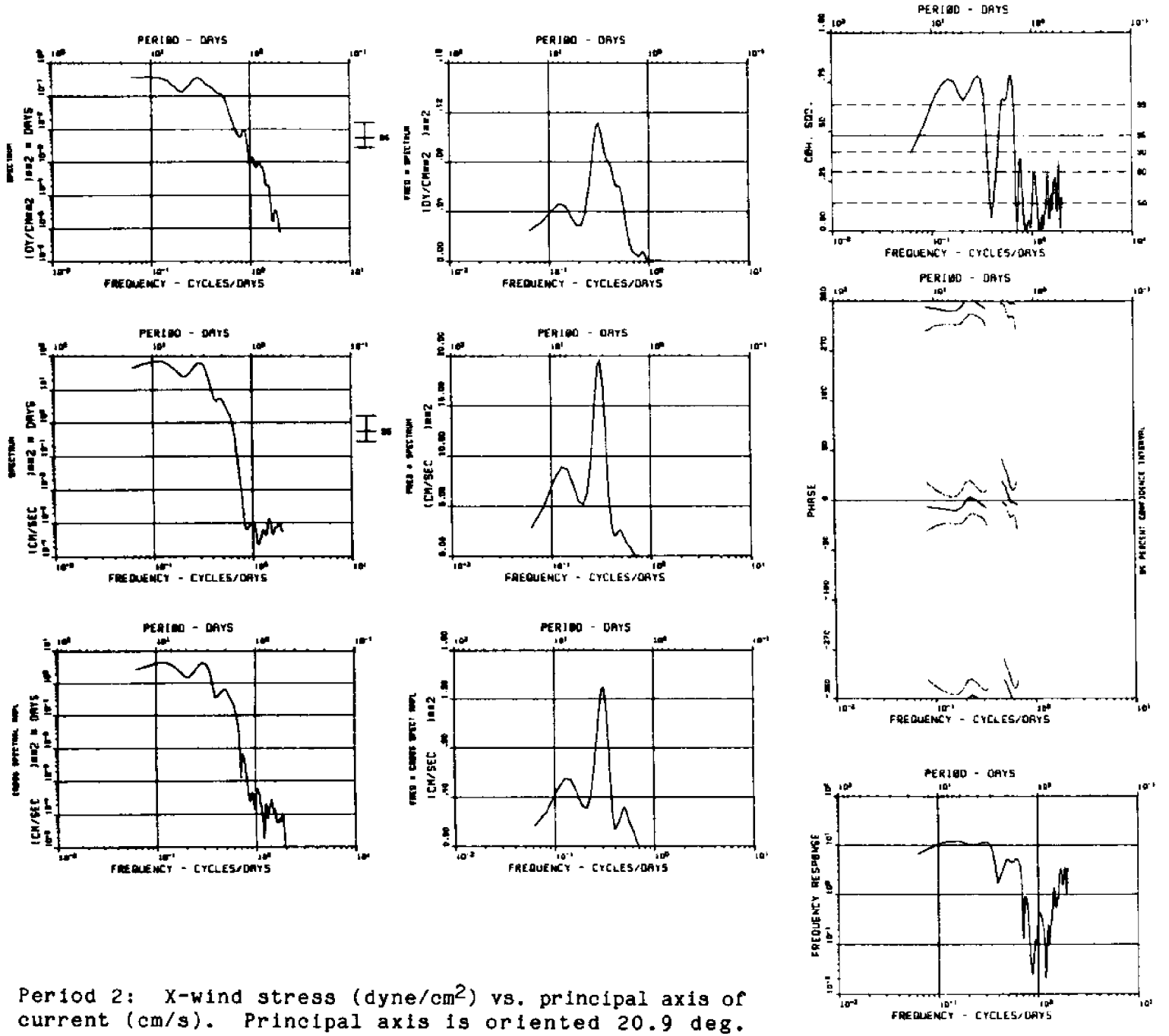

Figure 23c. Period 2: X-wind stress (dyne/cm^2) vs. principal axis of current (cm/s). Principal axis is oriented 20.9 deg. counterclockwise of east.

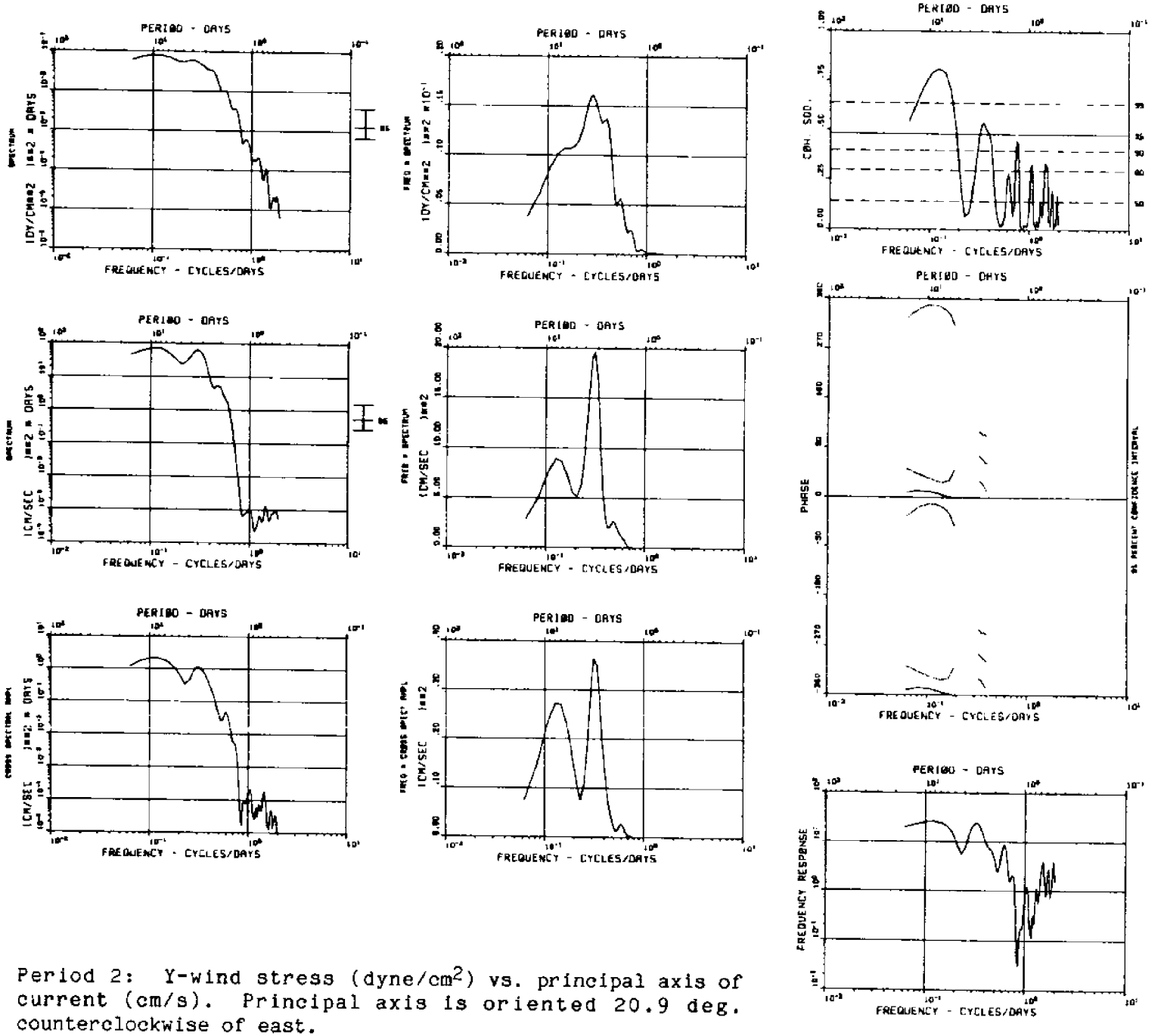

Figure 23d. Period 2: Y-wind stress (dyne/cm^2) vs. principal axis of current (cm/s). Principal axis is oriented 20.9 deg. counterclockwise of east.

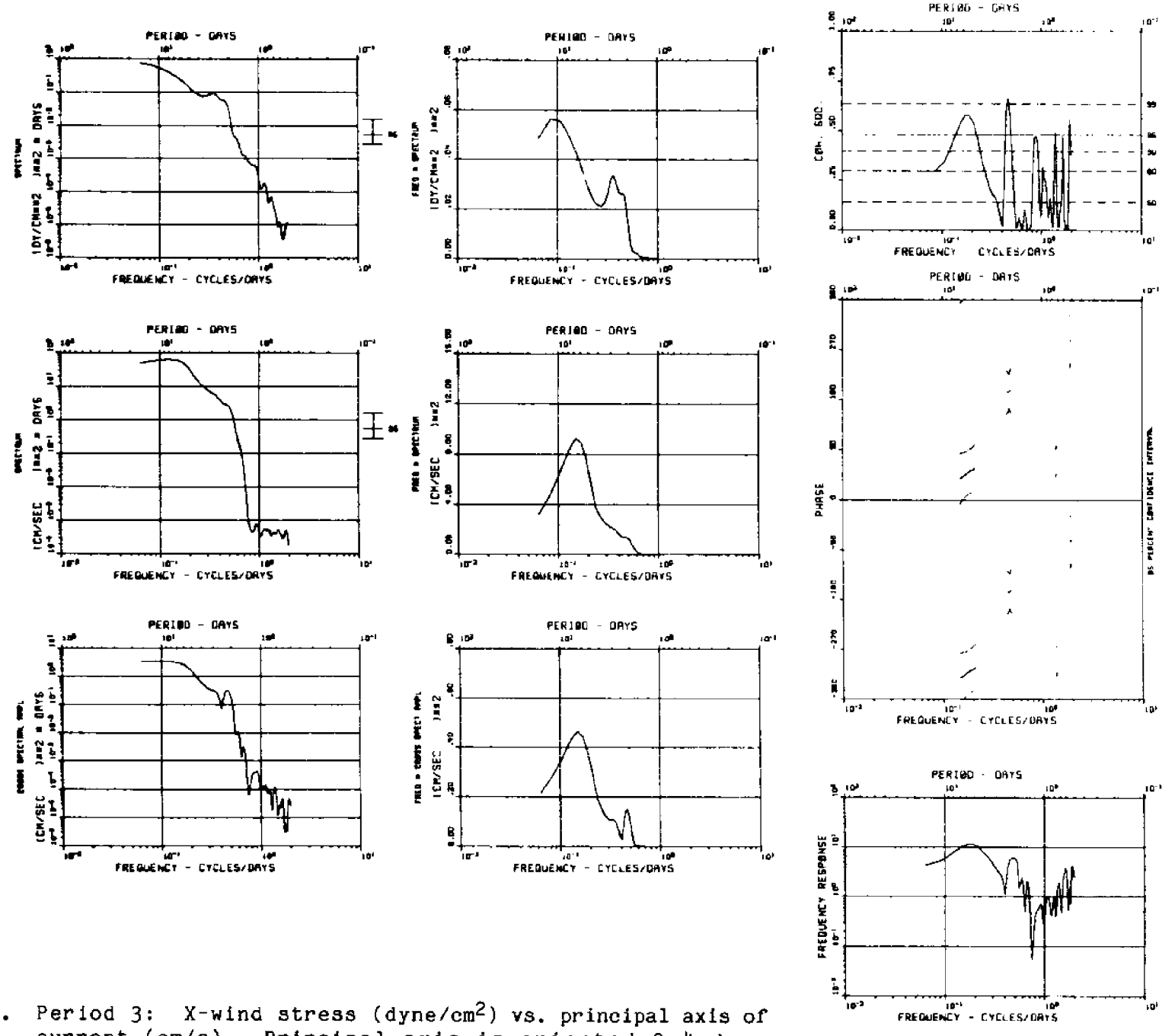

Figure 23e. Period 3: X-wind stress (dyne/cm^2) vs. principal axis of current (cm/s). Principal axis is oriented 0.4 deg. counterclockwise of east.

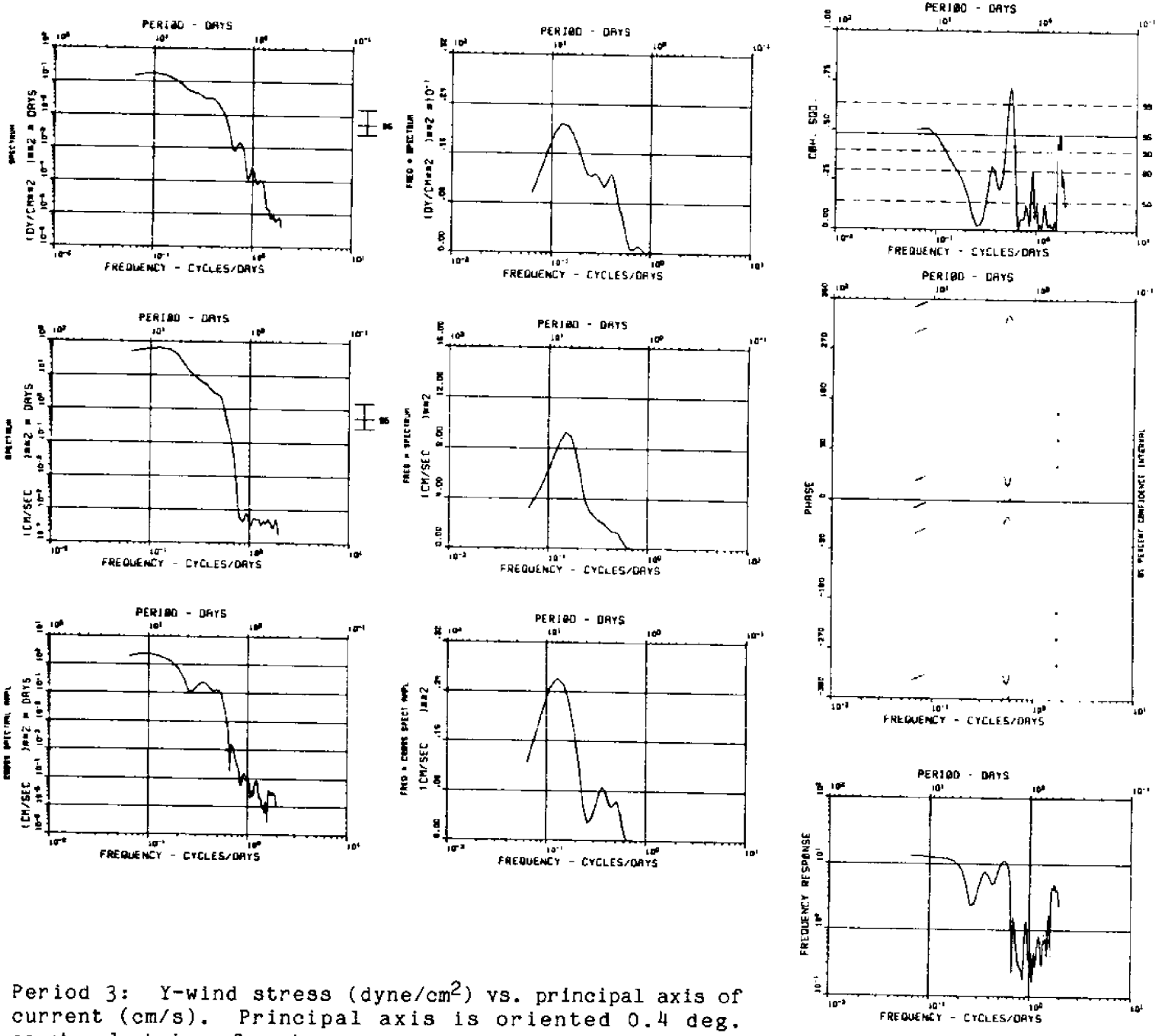

Figure 23f. Period 3: Y-wind stress (dyne/cm^2) vs. principal axis of current (cm/s). Principal axis is oriented 0.4 deg. counterclockwise of east.

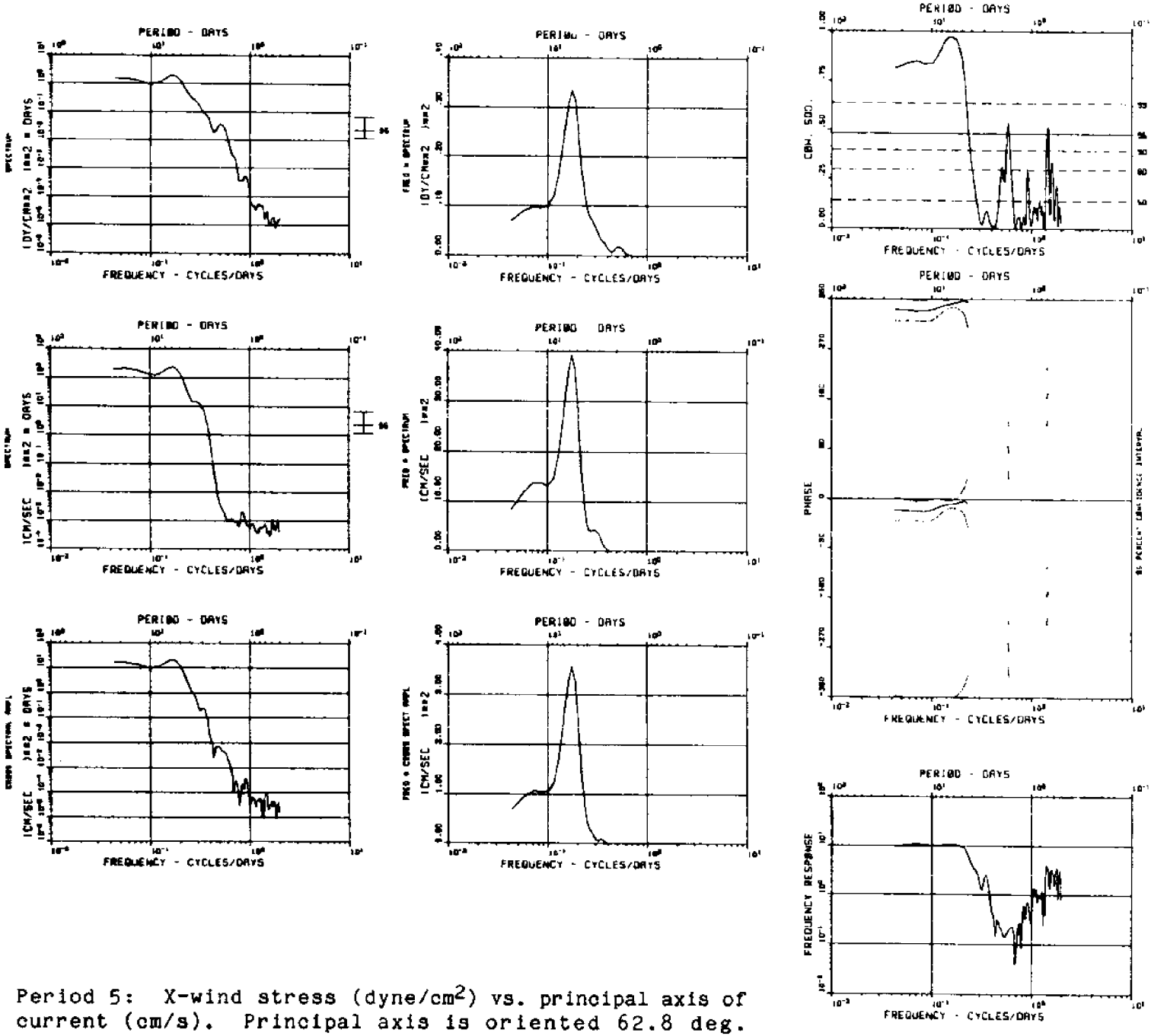

Figure 23g. Period 5: X-wind stress (dyne/cm^2) vs. principal axis of current (cm/s). Principal axis is oriented 62.8 deg. counterclockwise of east.

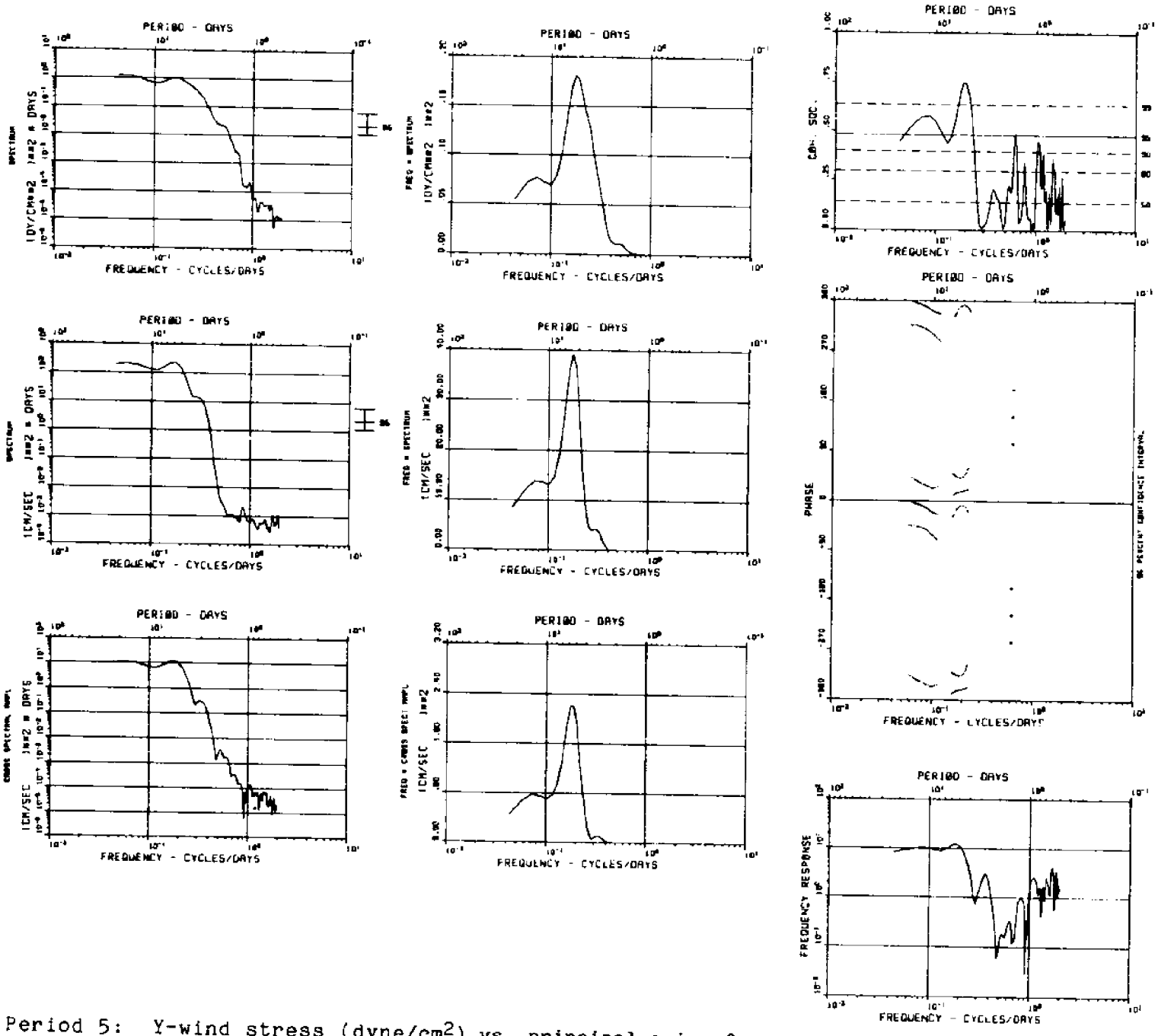

Figure 23h. Period 5: Y-wind stress (dyne/cm^2) vs. principal axis of current (cm/s). Principal axis is oriented 62.8 deg. counterclockwise of east.

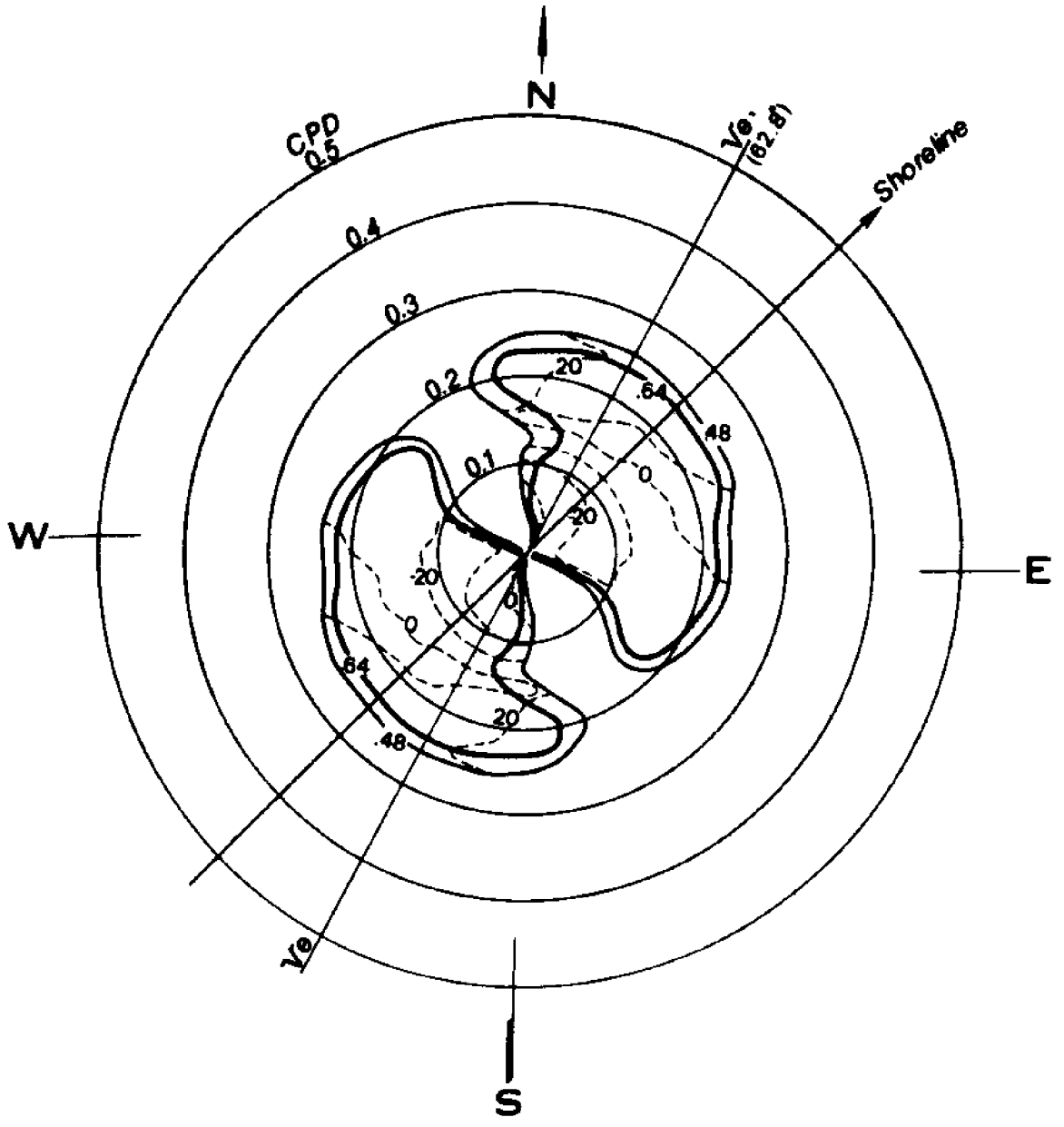

Figure 24. Rotary spectral correlation between 40 hr low-passed wind stress and principal current component ($V_{\theta'}$ = 62.8° from east) at SNLT, for Period 5. Solid lines enclose wind directions and frequencies at which current was coherent with wind at 90% (.48) and 95% (.64) confidence levels. Broken lines represent phase, in degrees, between wind and current. Positive phase indicates wind lags current. Concentric circles represent frequency in cycles per day. Compass directions and current-and-shoreline orientation are included.

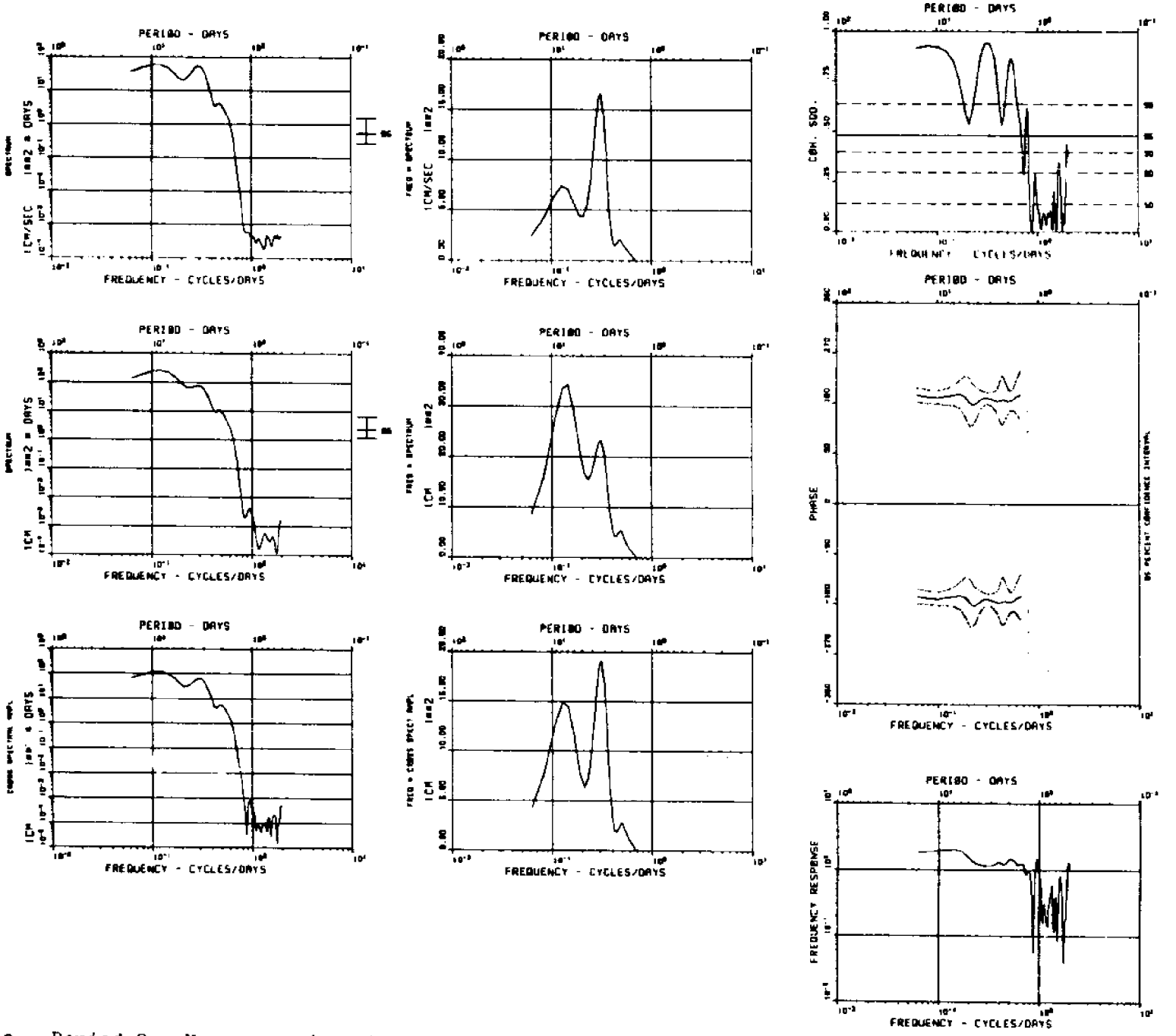

Figure 25a. Period 2: X-current (cm/s) vs. sea level (cm).

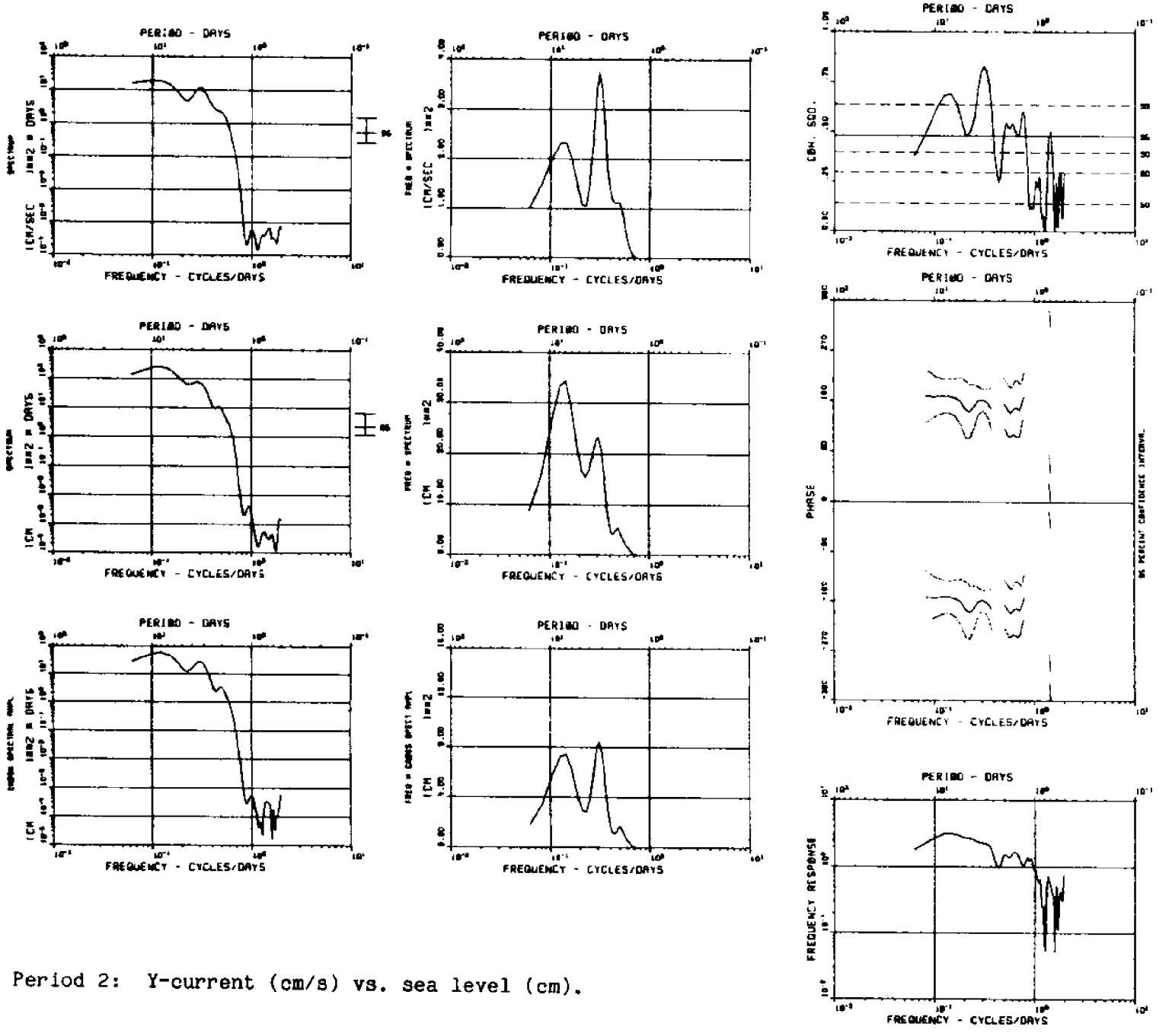

Figure 25b. Period 2: Y-current (cm/s) vs. sea level (cm).

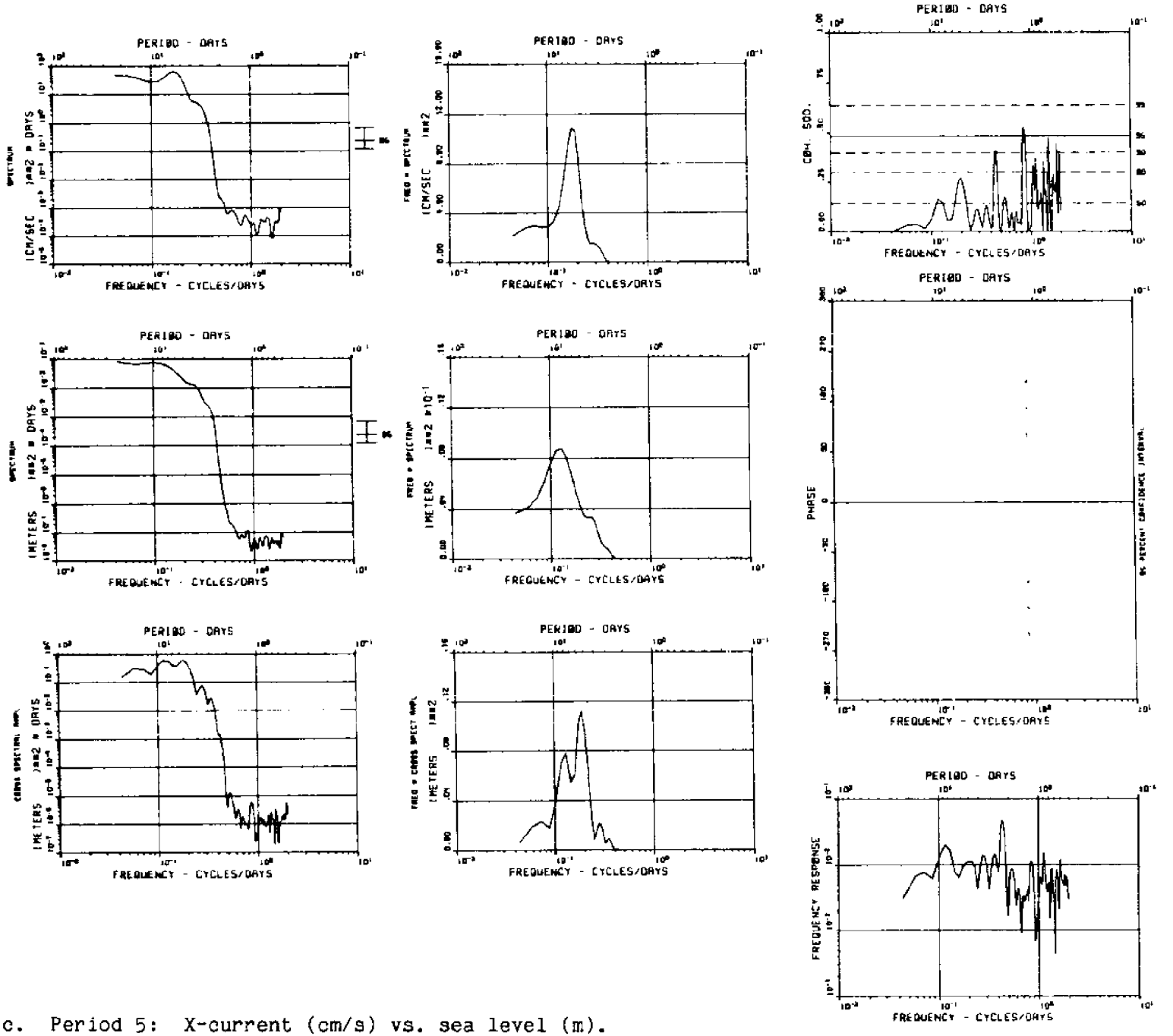

Figure 25c. Period 5: X-current (cm/s) vs. sea level (m).

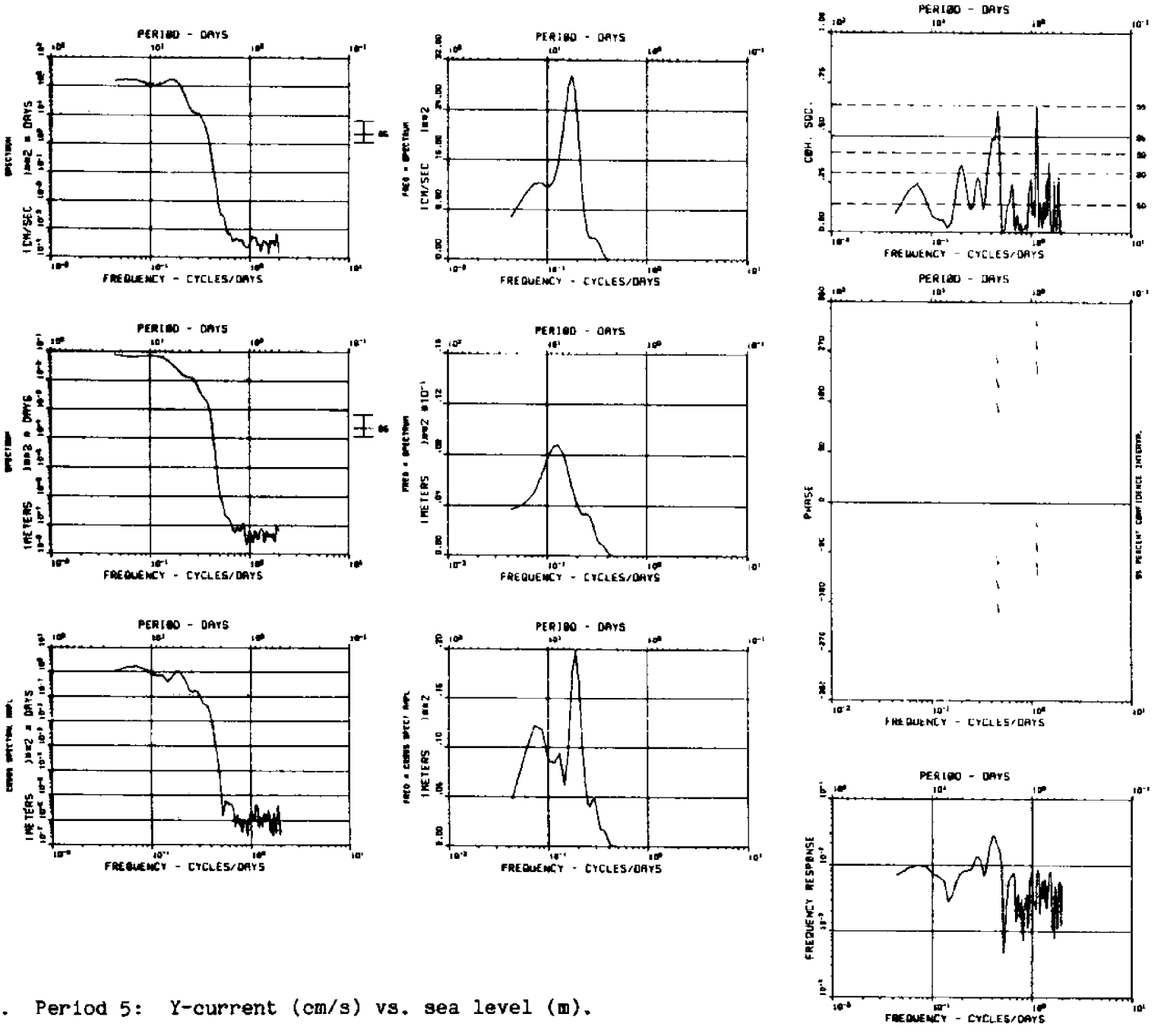

Figure 25d. Period 5: Y-current (cm/s) vs. sea level (m).

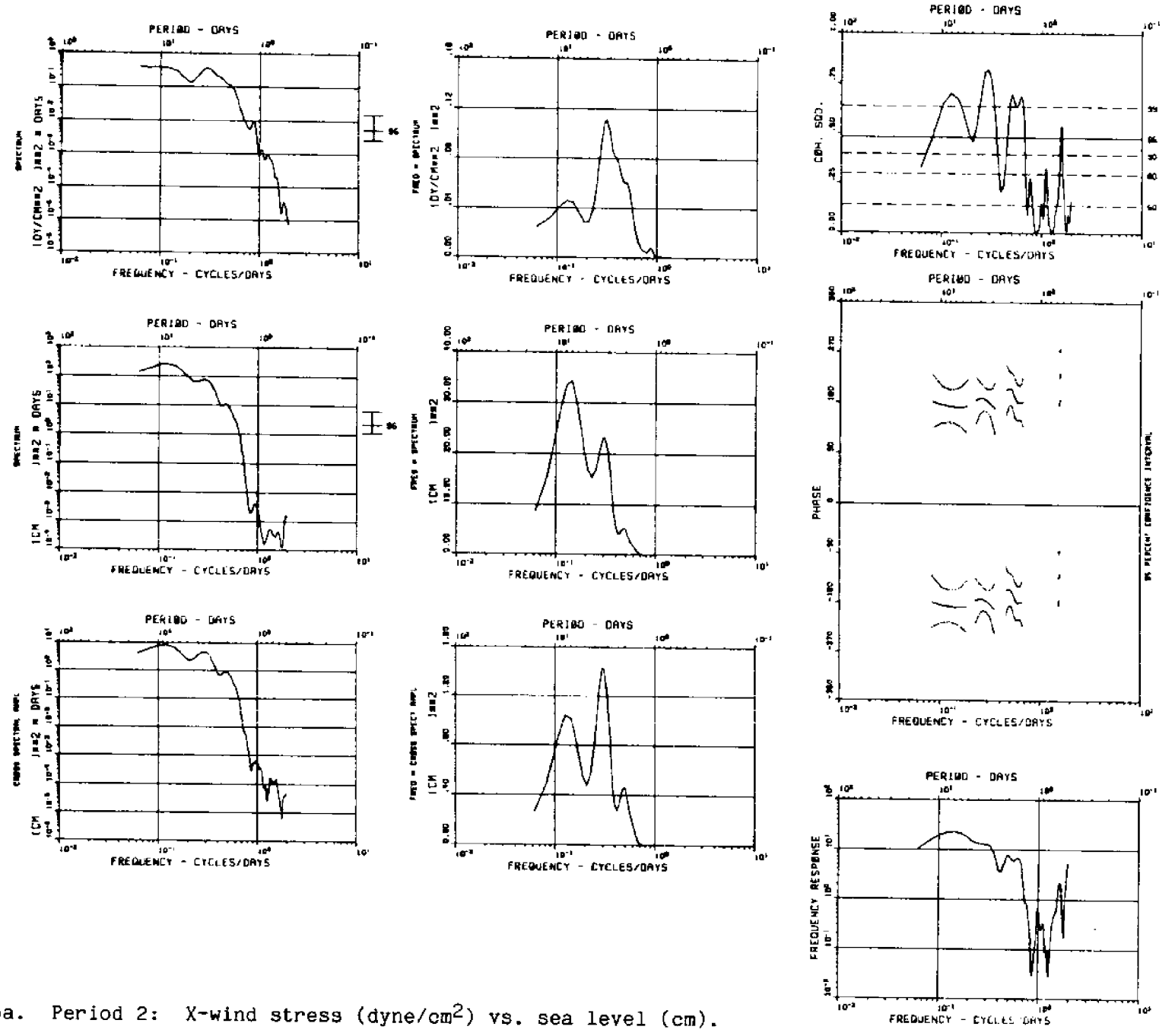

Figure 26a. Period 2: X-wind stress (dyne/cm^2) vs. sea level (cm).

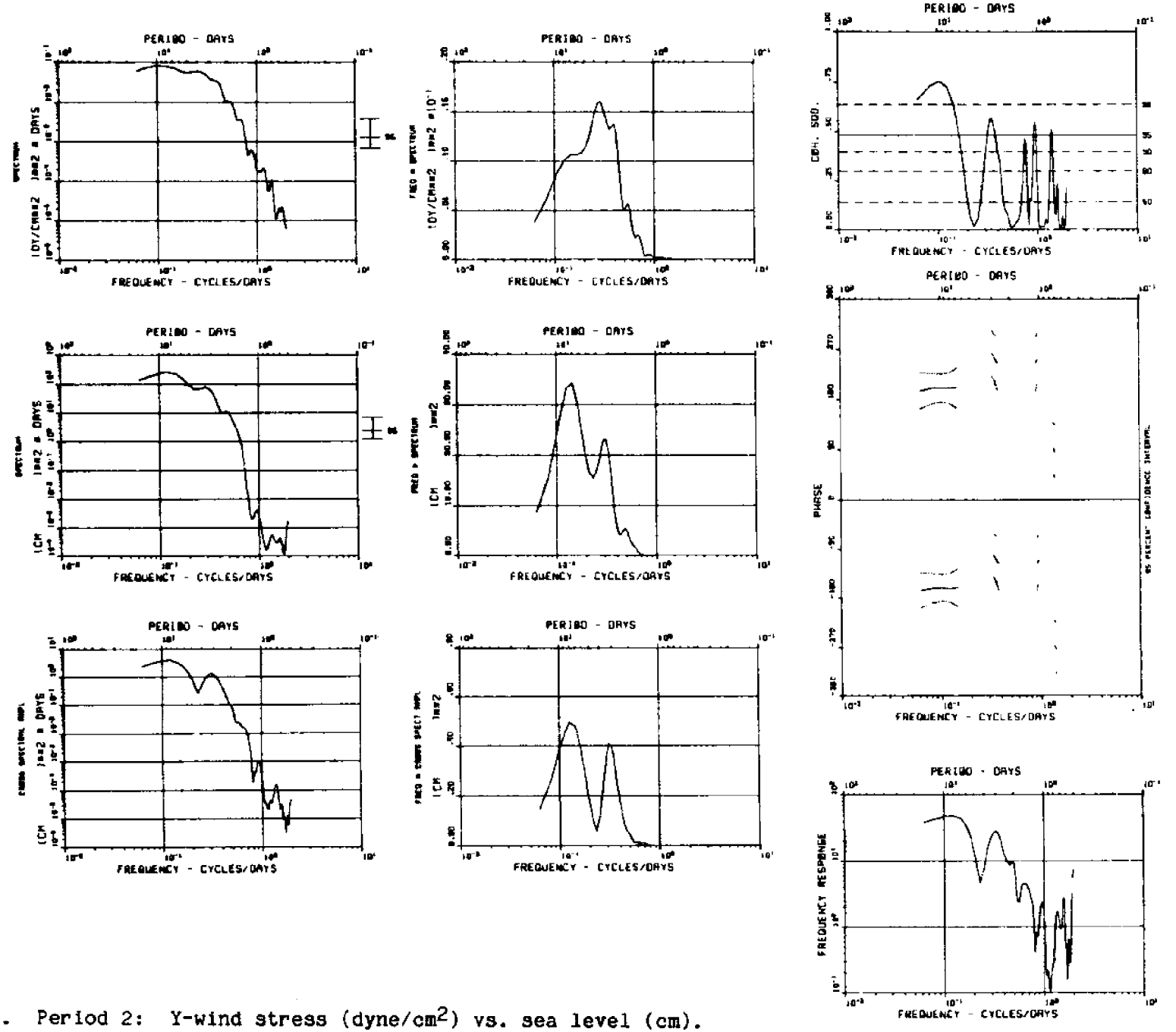

Figure 26b. Period 2: Y-wind stress (dyne/cm^2) vs. sea level (cm).

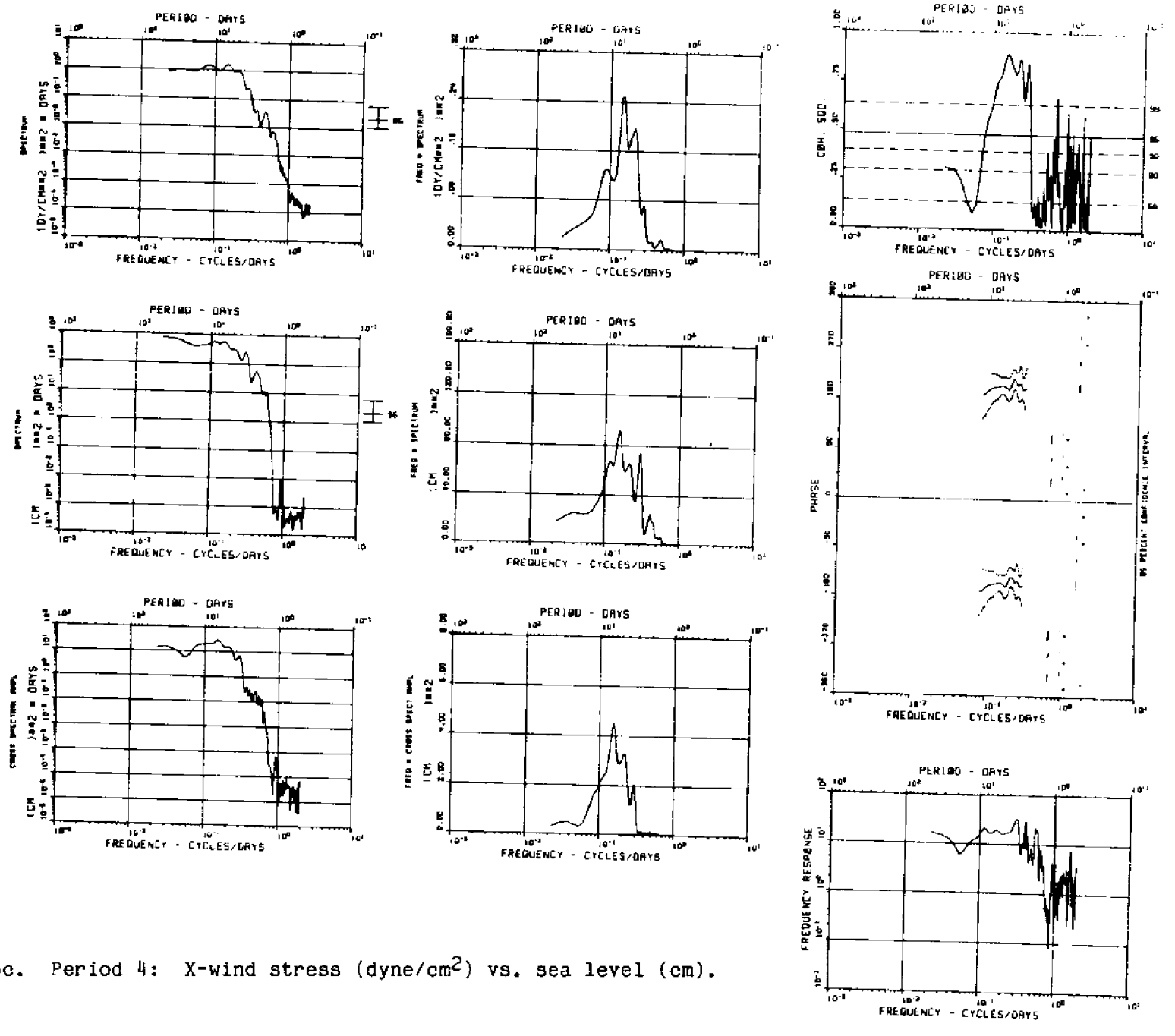

Figure 26c. Period 4: X-wind stress (dyne/cm^2) vs. sea level (cm).

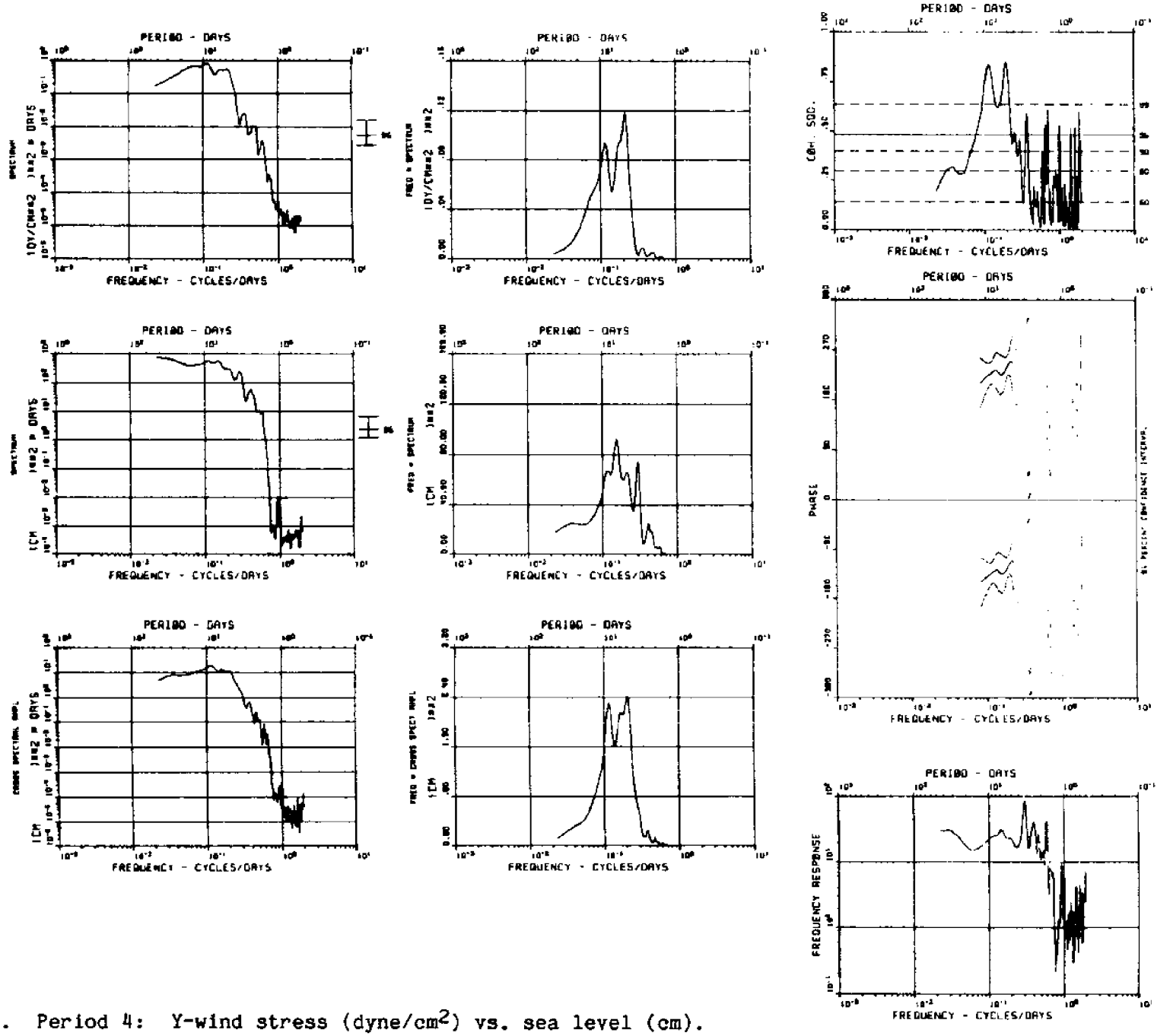

Figure 26d. Period 4: Y-wind stress (dyne/cm^2) vs. sea level (cm).

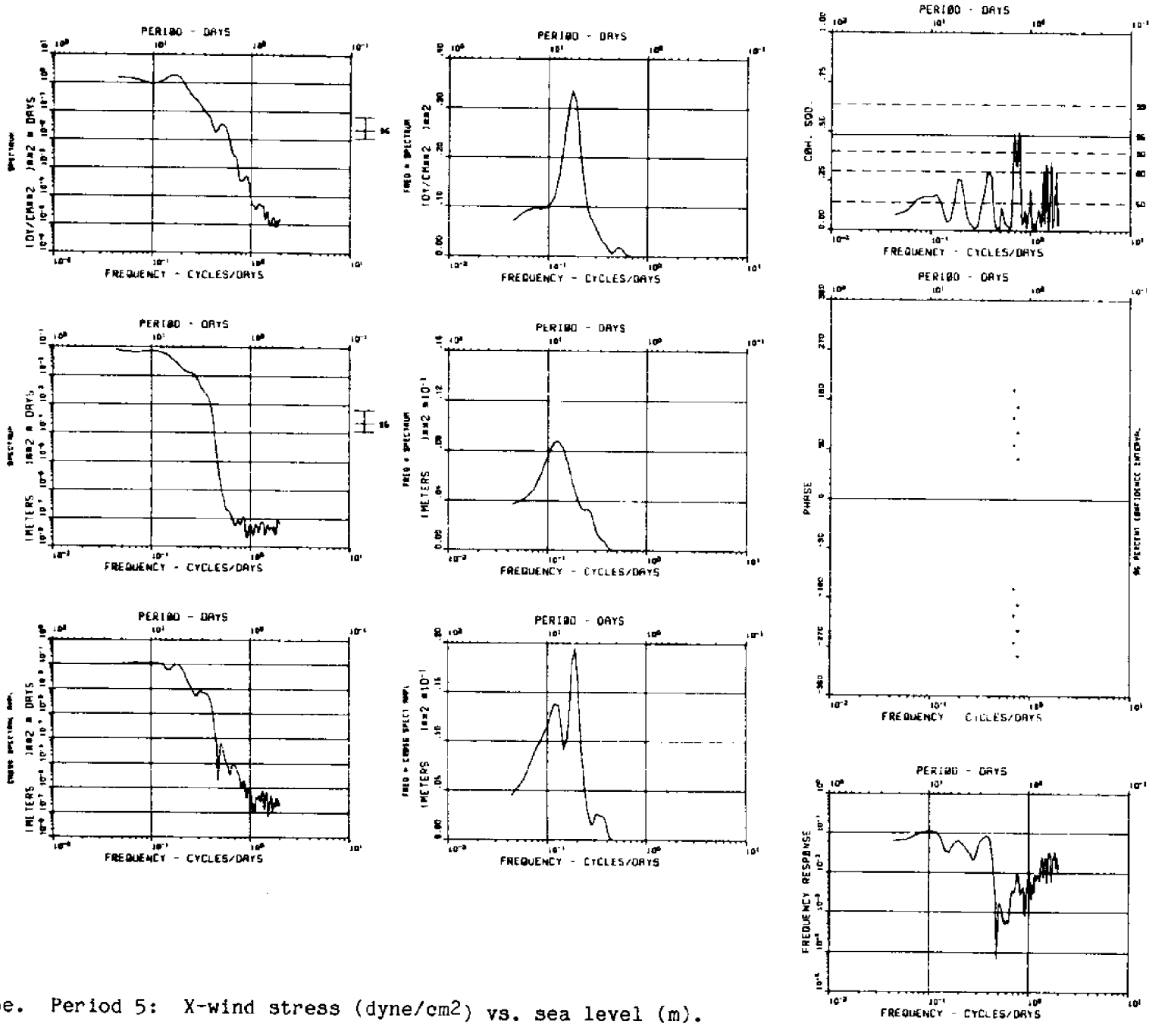

Figure 26e. Period 5: X-wind stress (dyne/cm2) vs. sea level (m).

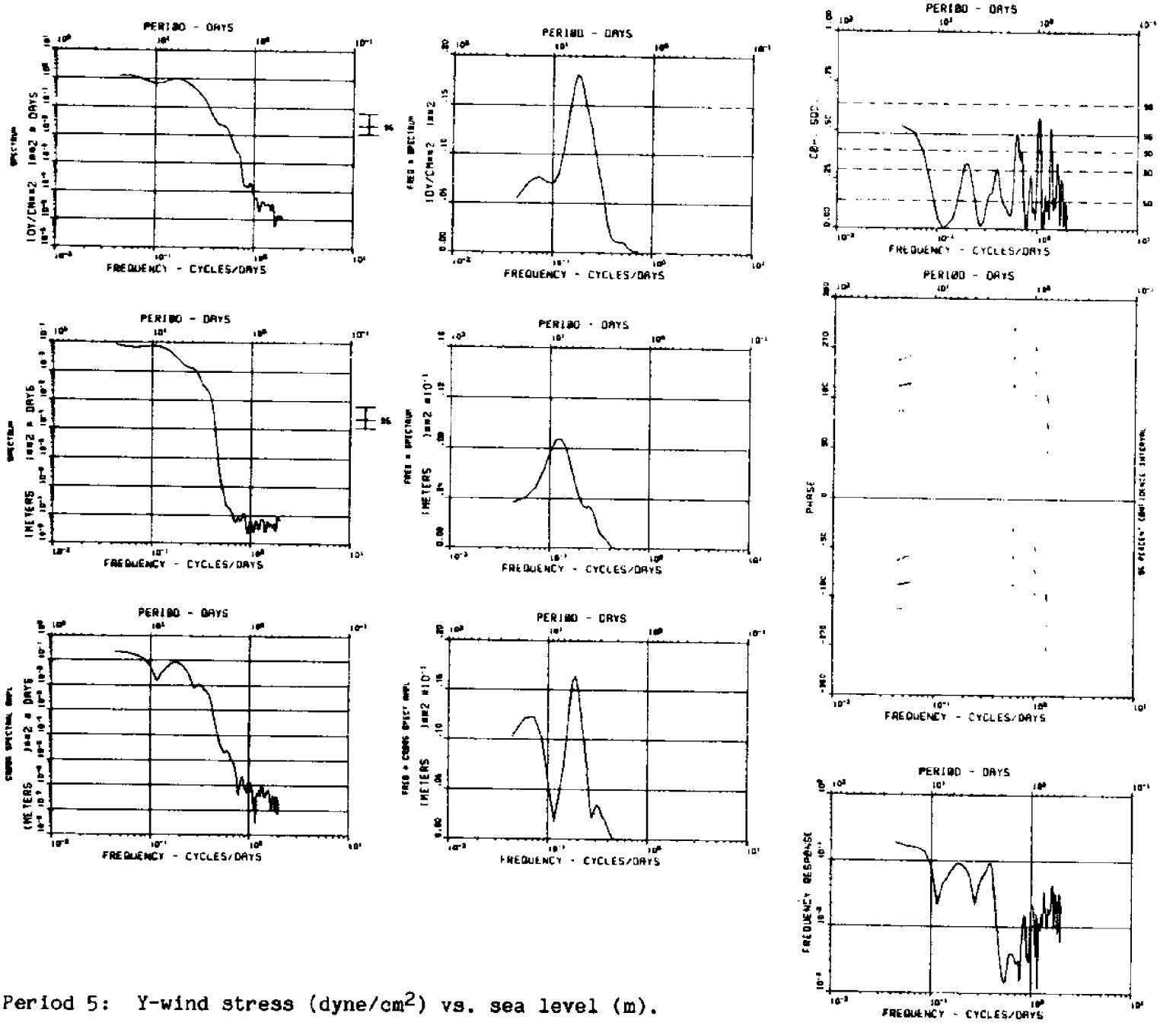

Figure 26f. Period 5: Y-wind stress (dyne/cm^2) vs. sea level (m).

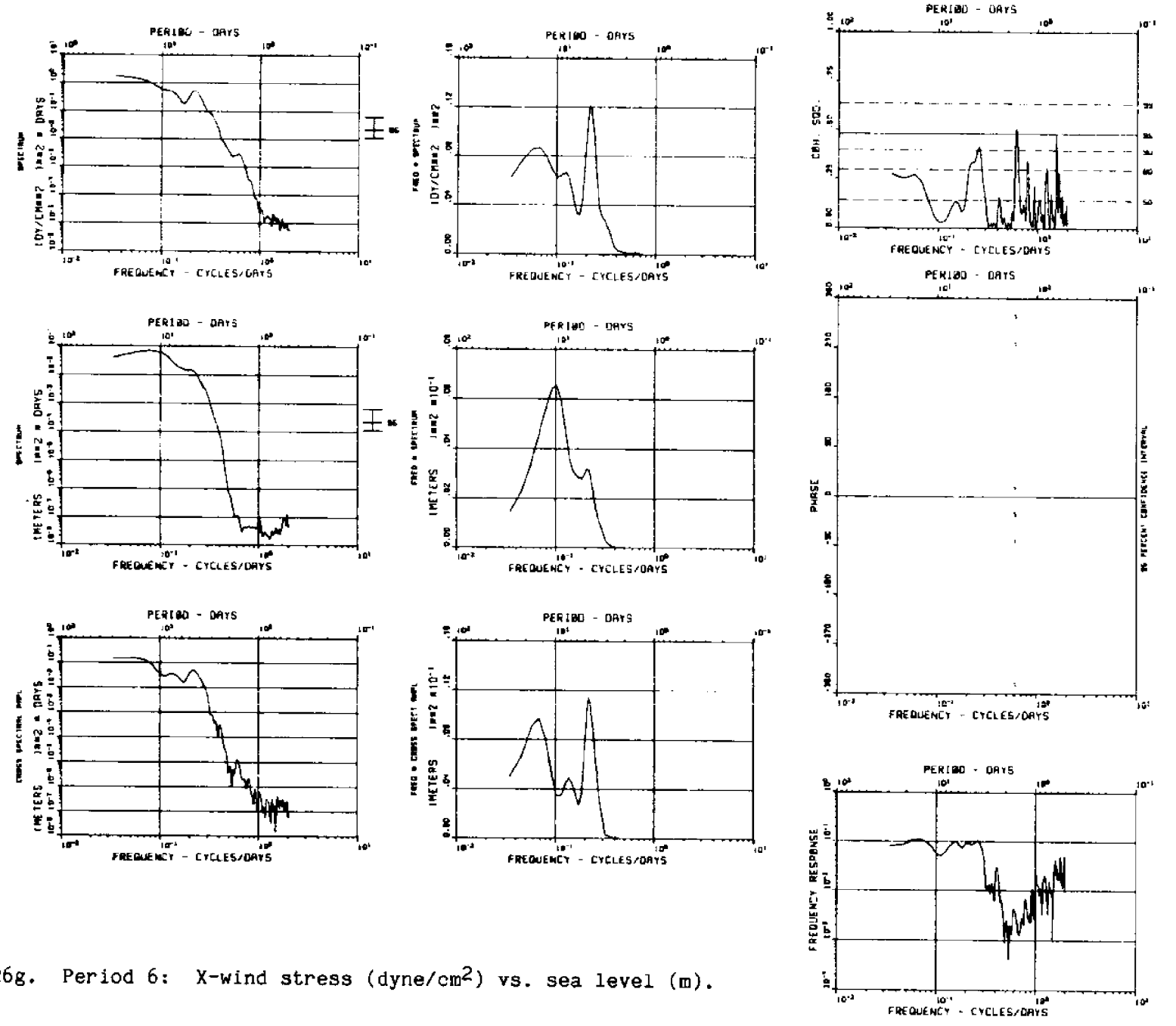

Figure 26g. Period 6: X-wind stress (dyne/cm^2) vs. sea level (m).

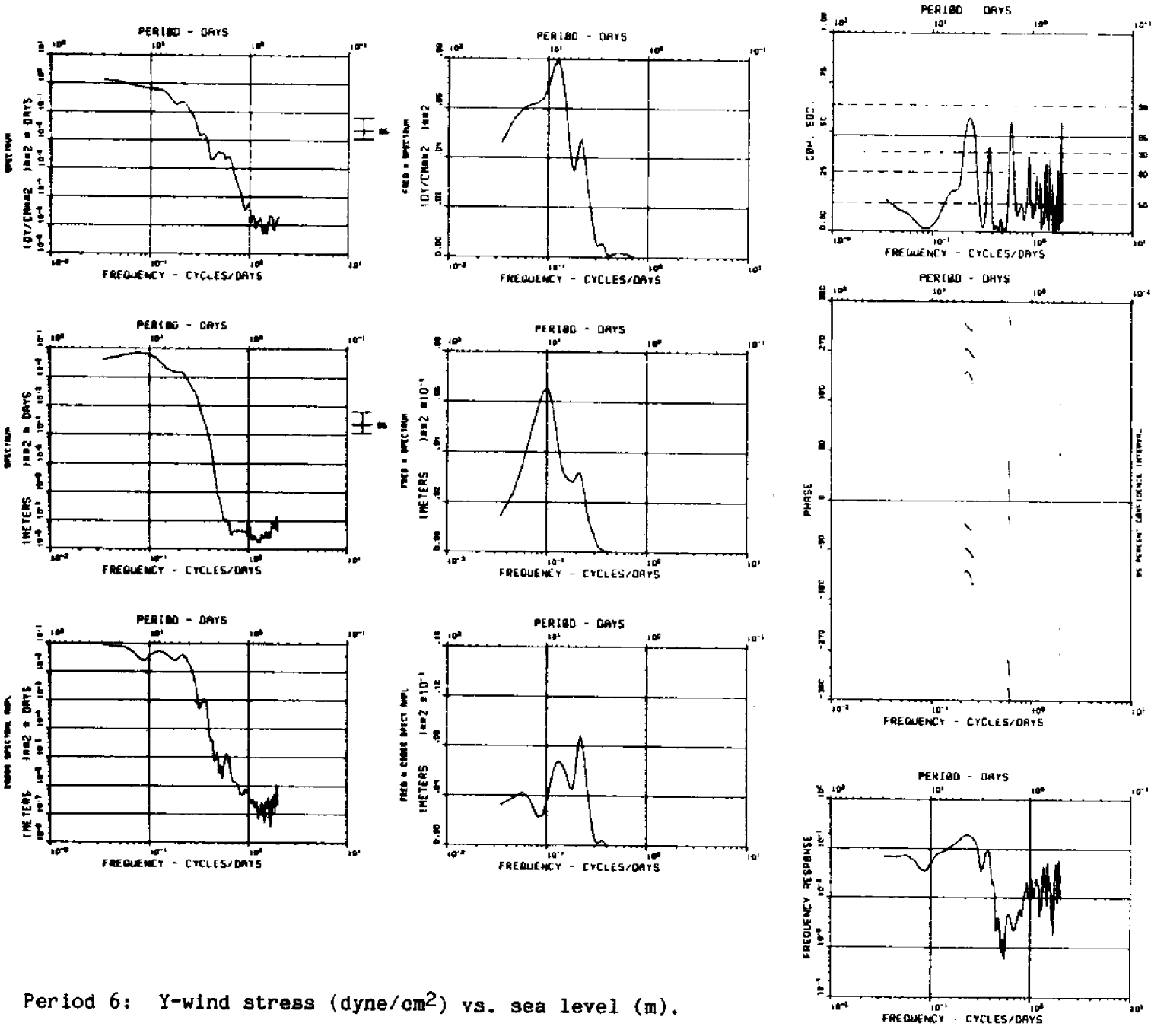

Figure 26h. Period 6: Y-wind stress (dyne/cm^2) vs. sea level (m).

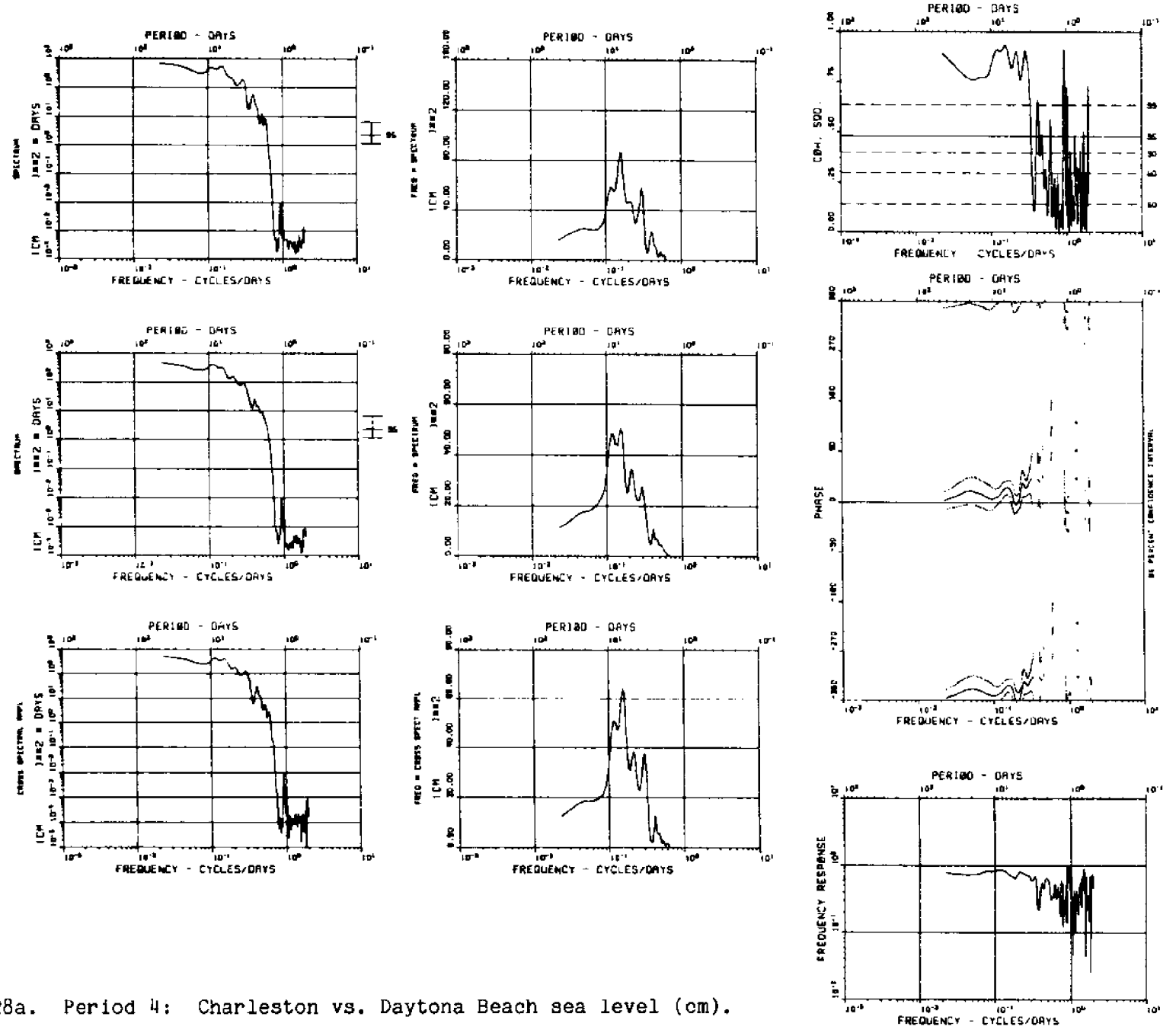

Figure 28a. Period 4: Charleston vs. Daytona Beach sea level (cm).

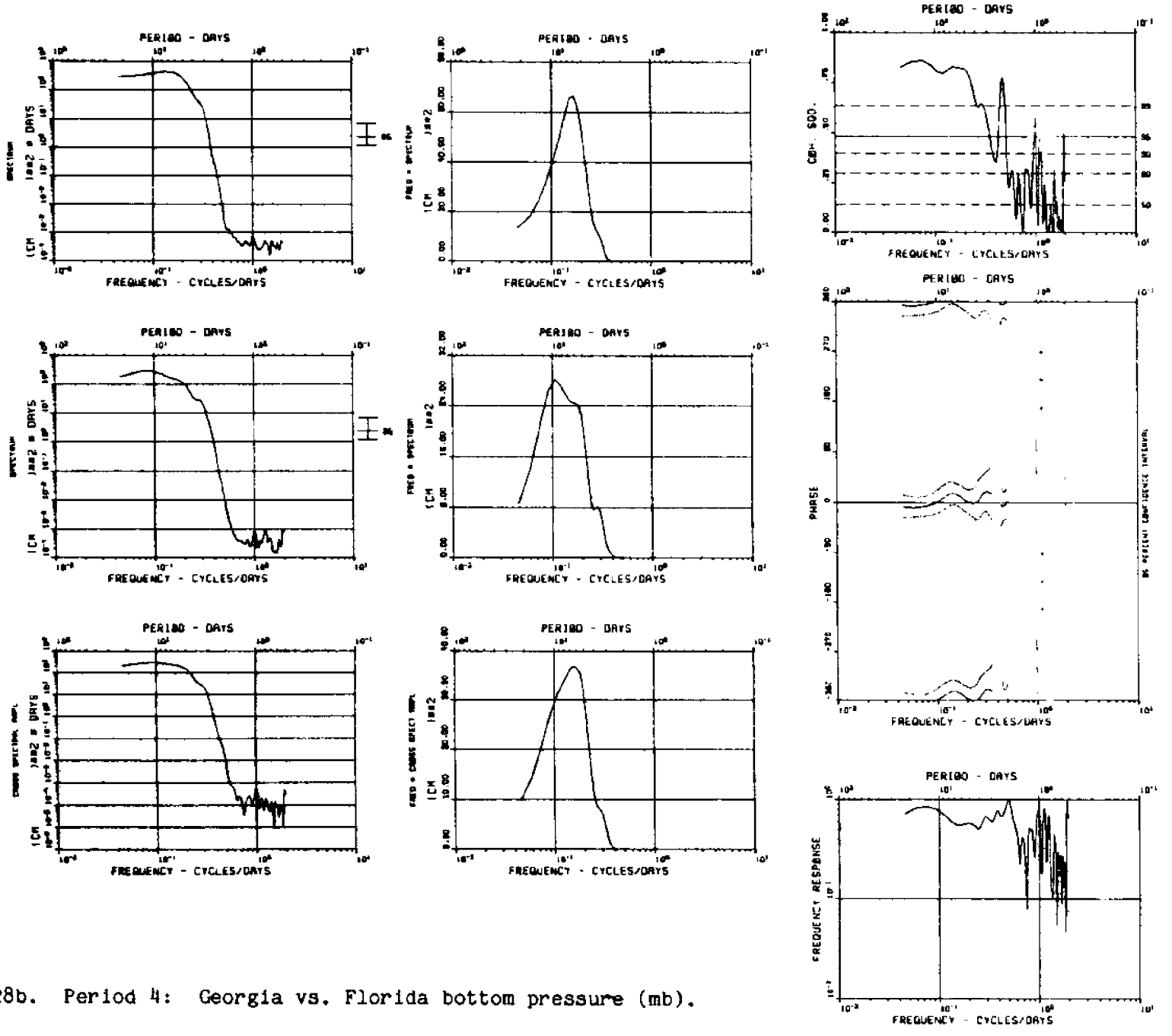

Figure 28b. Period 4: Georgia vs. Florida bottom pressure (mb).

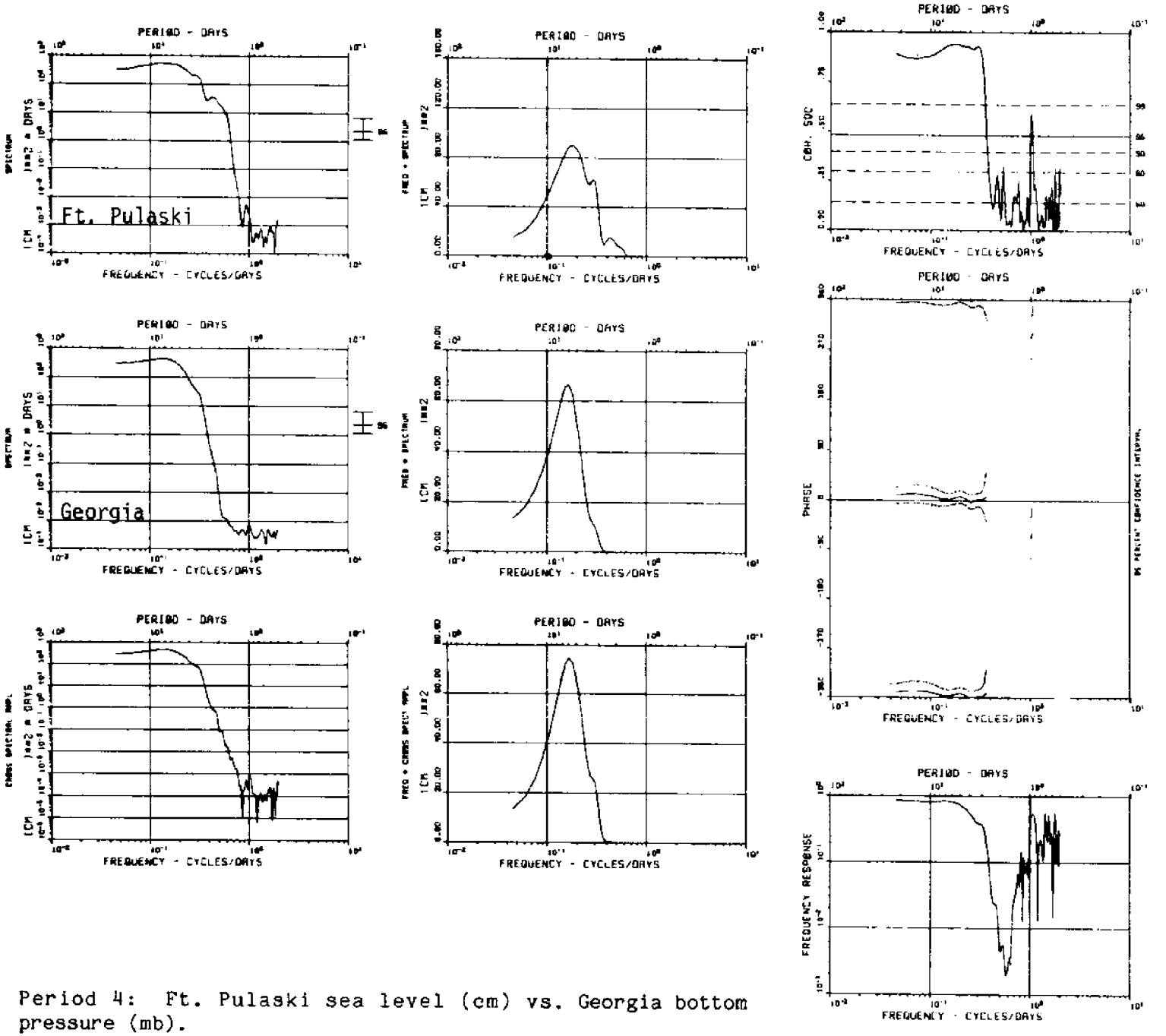

Figure 28c. Period 4: Ft. Pulaski sea level (cm) vs. Georgia bottom pressure (mb).

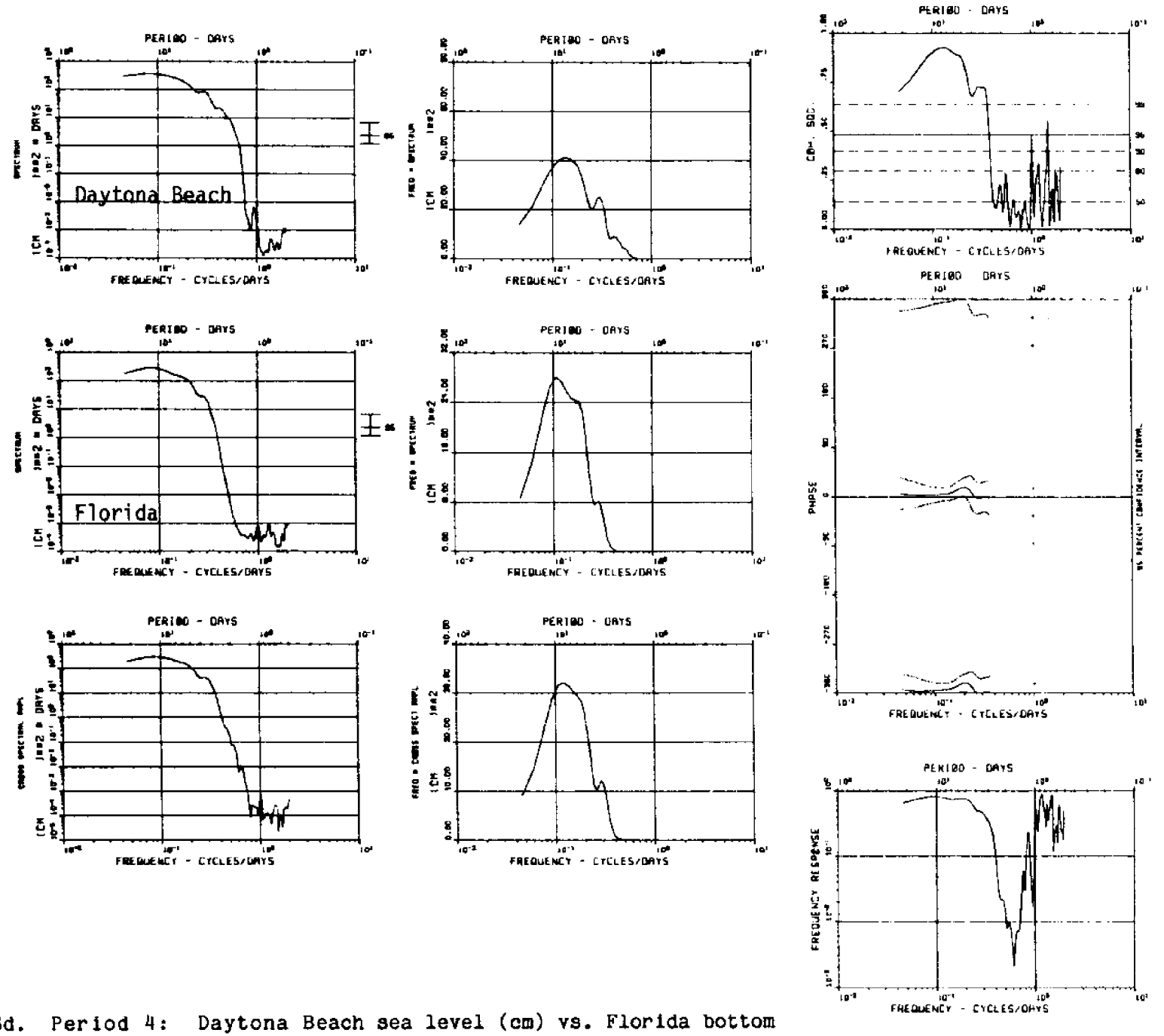

Figure 28d. Period 4: Daytona Beach sea level (cm) vs. Florida bottom pressure (mb).

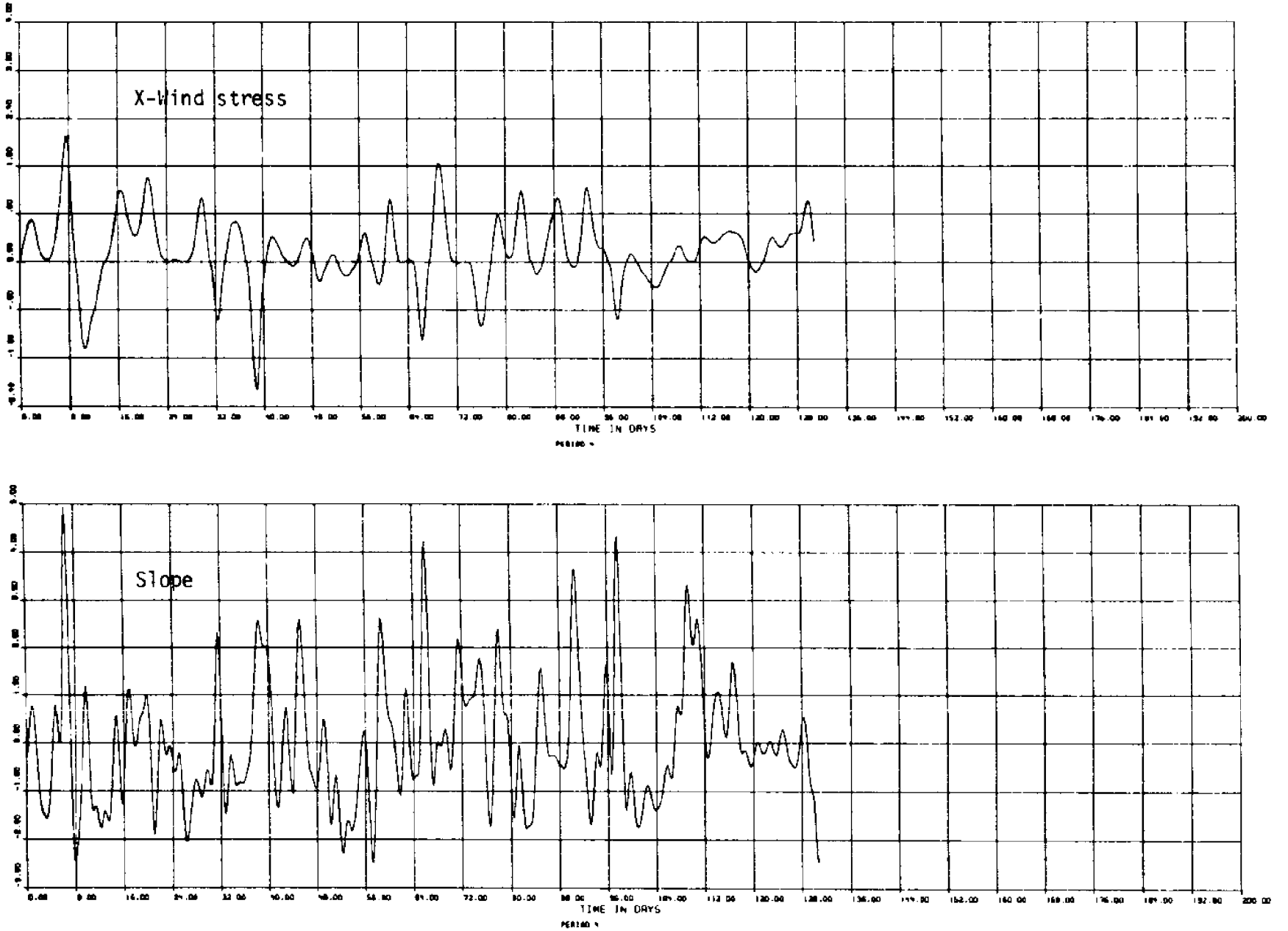

Figure 29a. Period 4: X-wind stress (dyne/cm^2) vs. Charleston-Daytona sea level slope (cm/100 km).

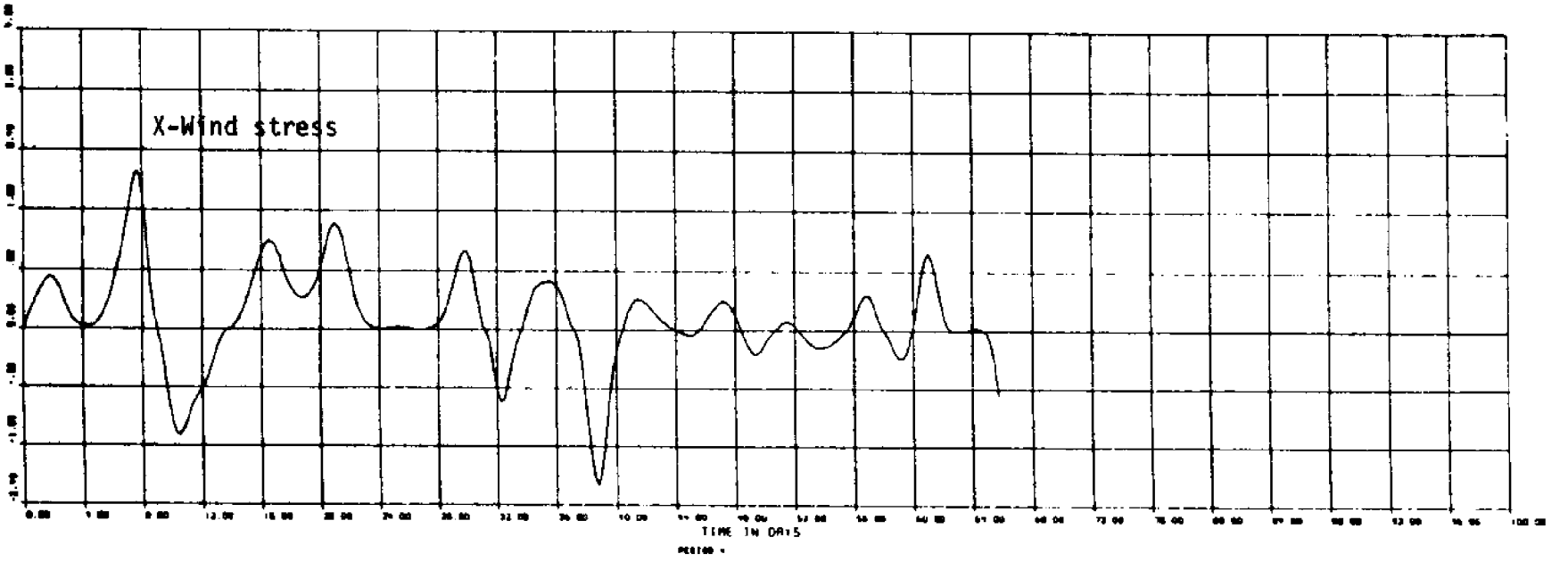

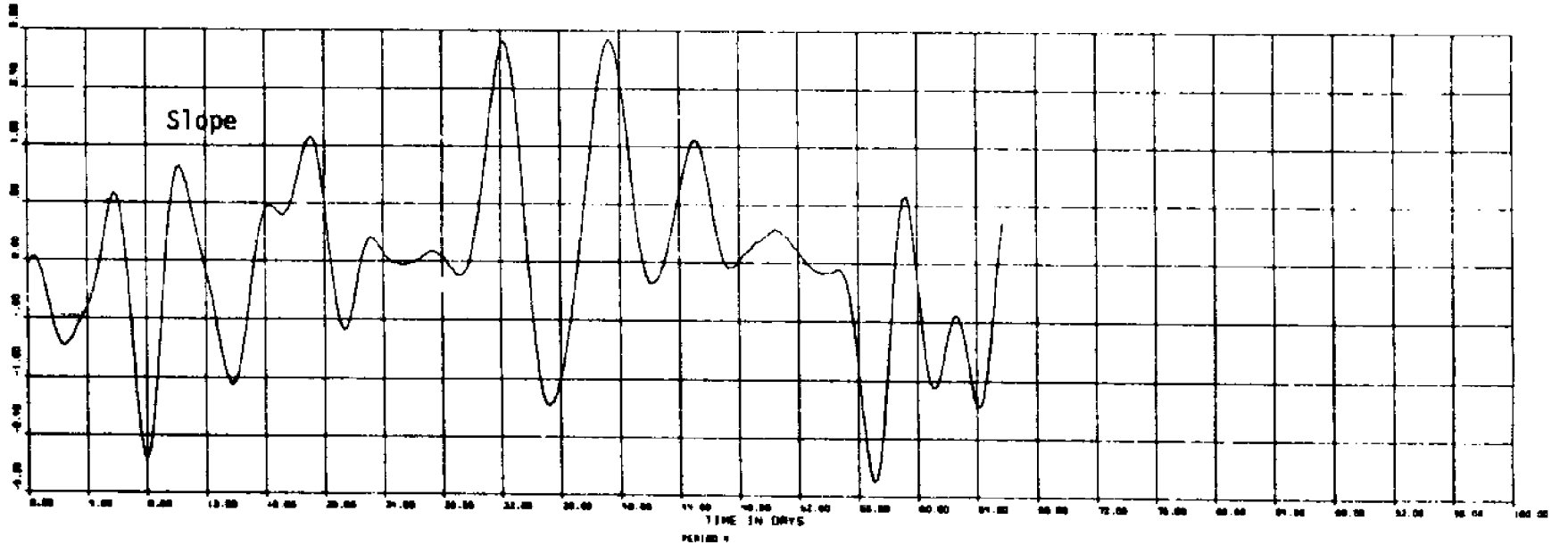

Figure 29b. Period 4: X-wind stress (dyne/cm2) vs. Georgia-Florida sea level slope (cm/100 km).

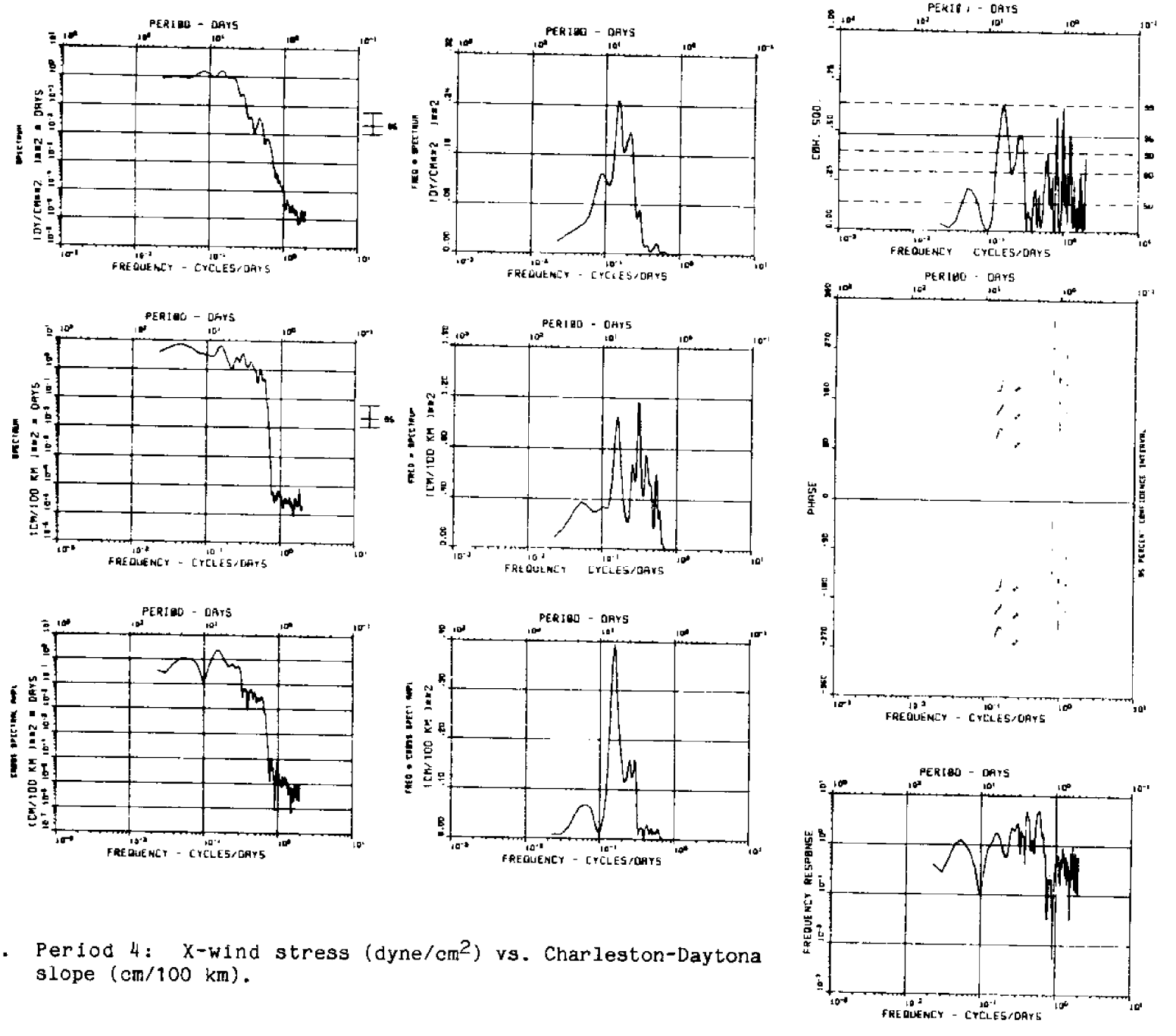

Figure 30a. Period 4: X-wind stress (dyne/cm^2) vs. Charleston-Daytona slope (cm/100 km).

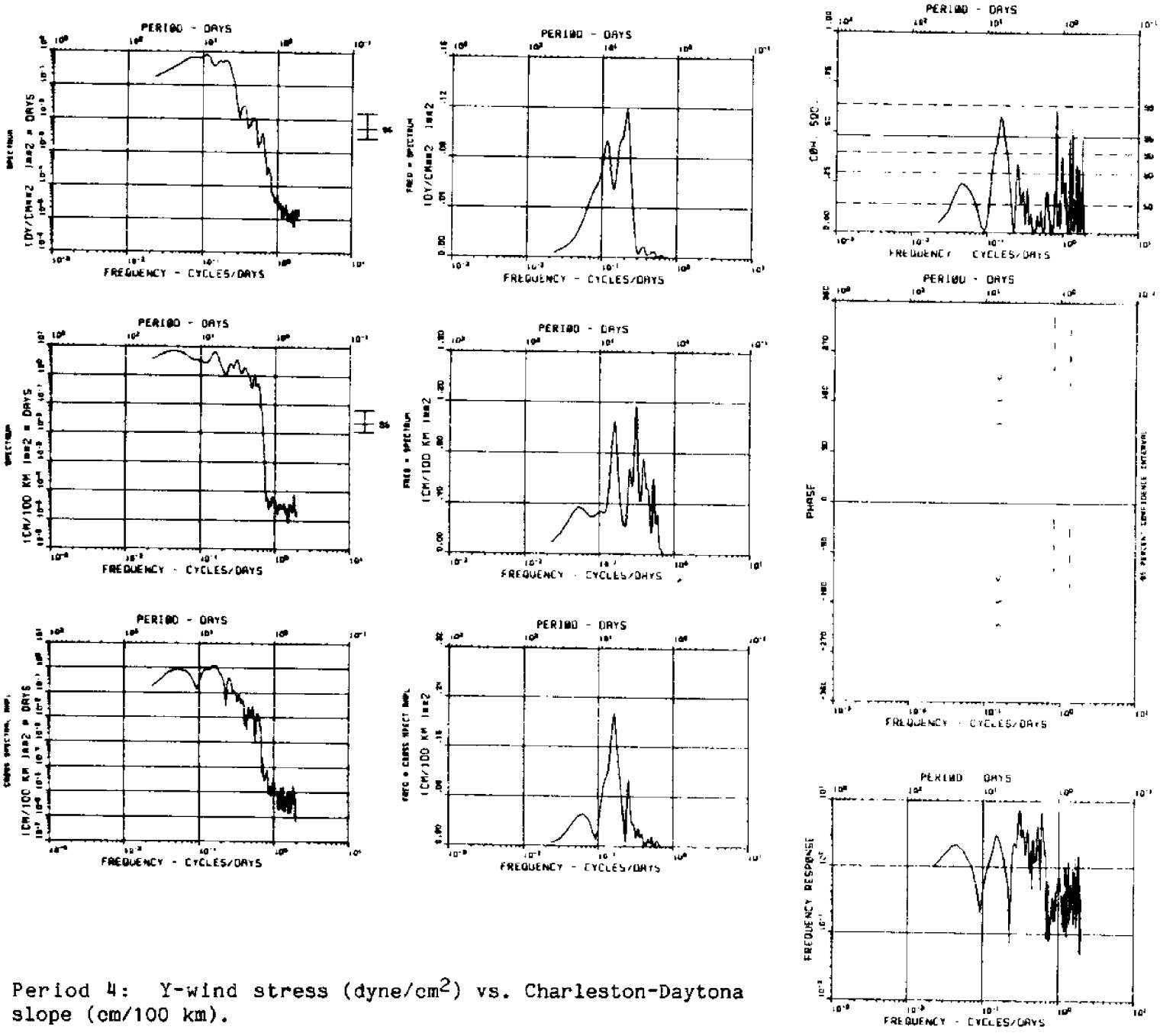

Figure 30b. Period 4: Y-wind stress (dyne/cm^2) vs. Charleston-Daytona slope (cm/100 km).

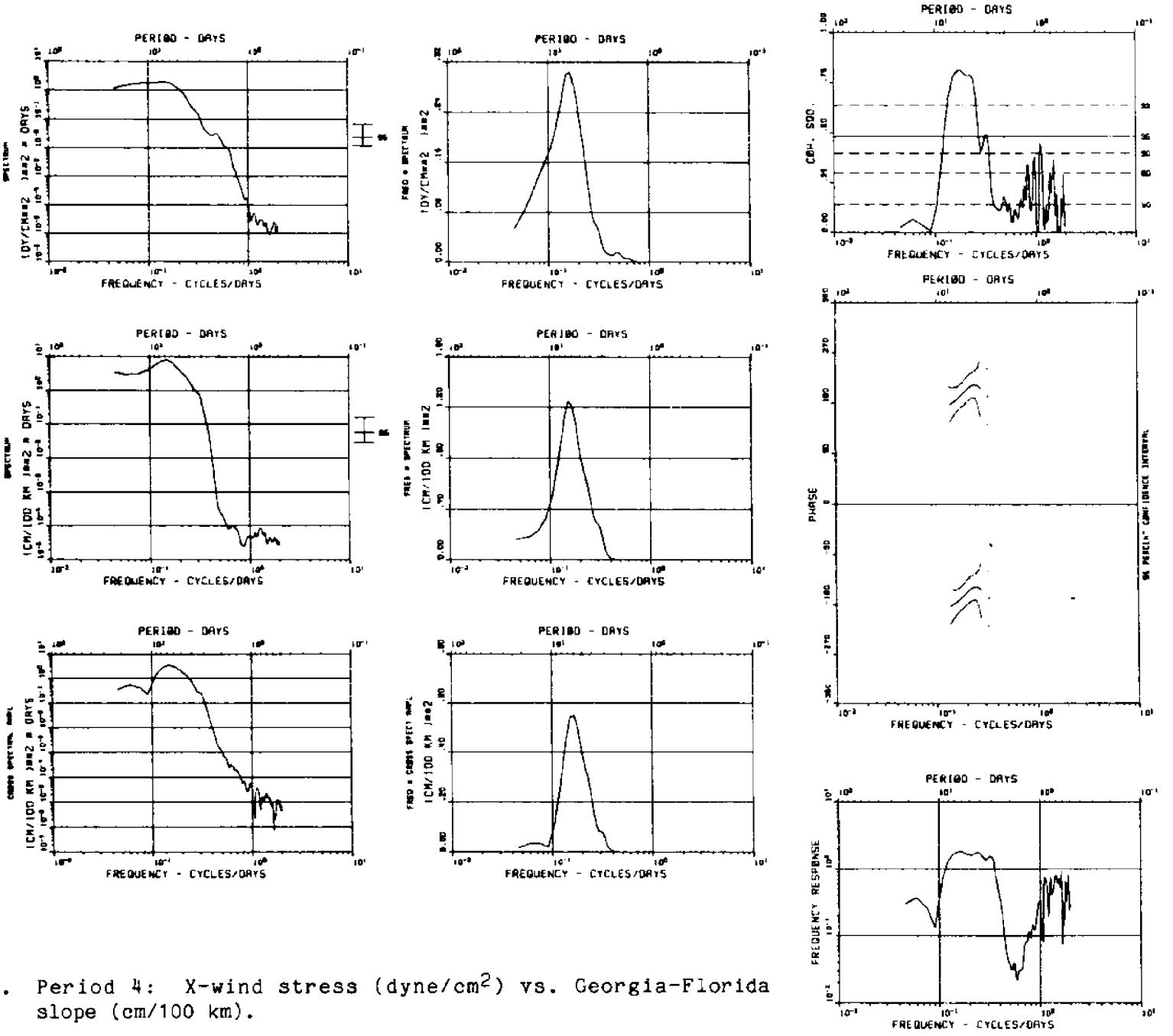

Figure 30c. Period 4: X-wind stress (dyne/cm^2) vs. Georgia-Florida slope (cm/100 km).

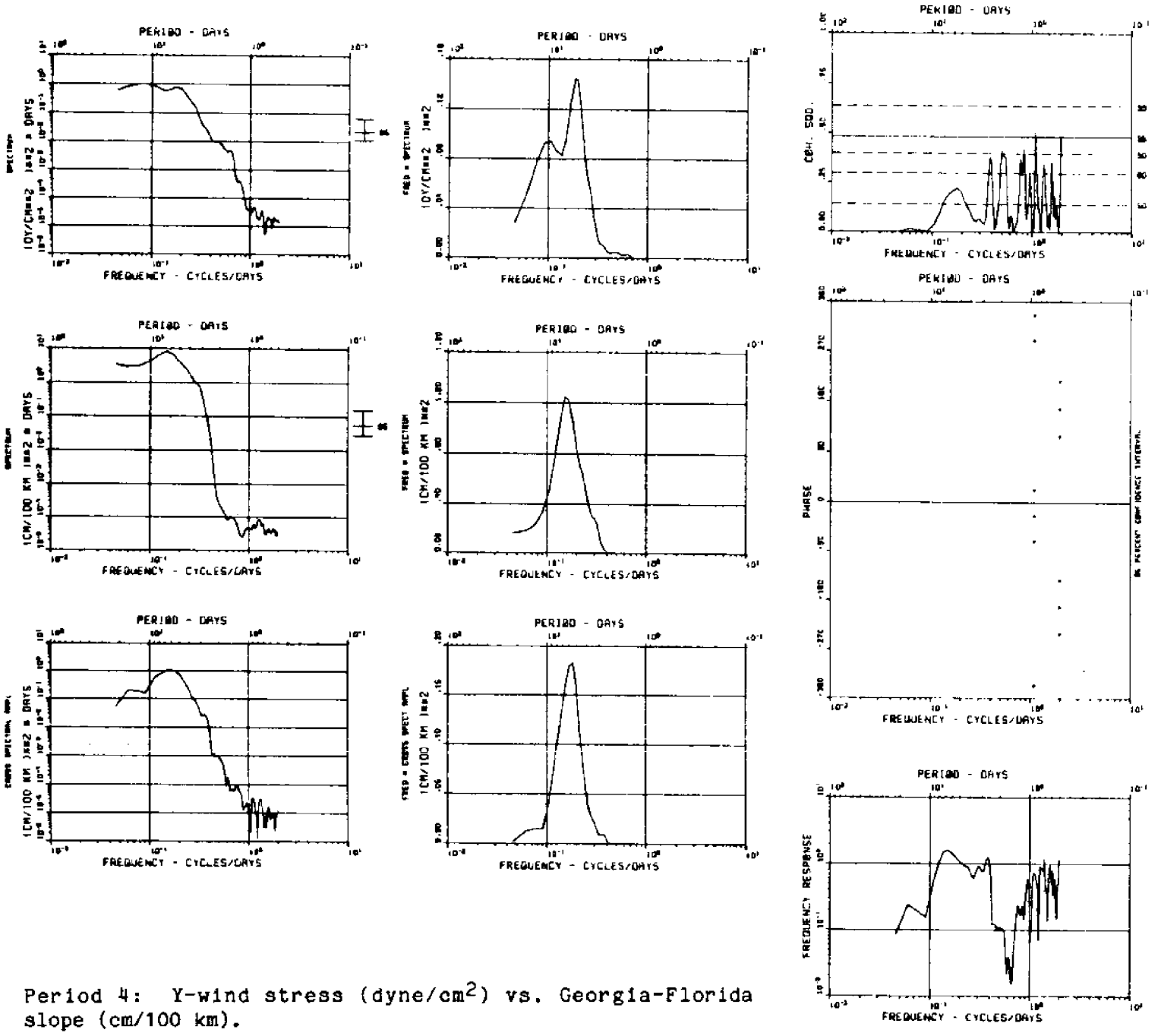

Figure 30d. Period 4: Y-wind stress (dyne/cm^2) vs. Georgia-Florida slope (cm/100 km).

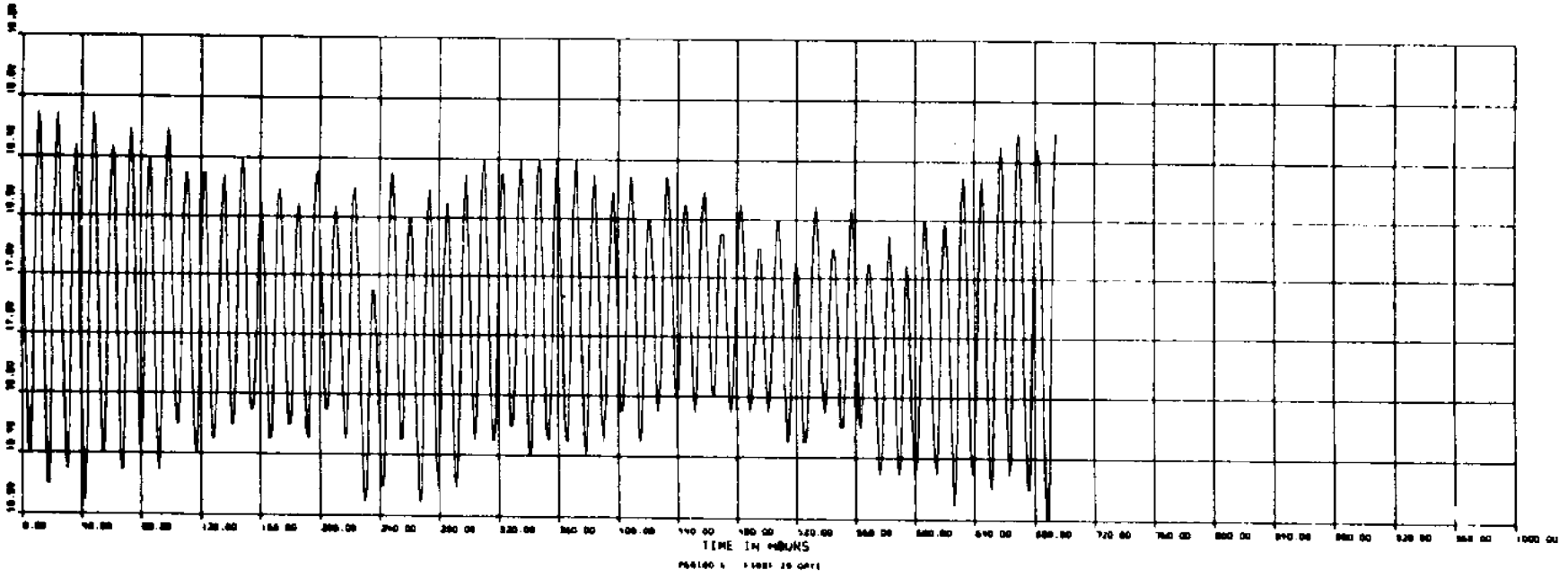

Figure 31a. Period 5: SNLT sea level (m) (3 hr low-passed data).

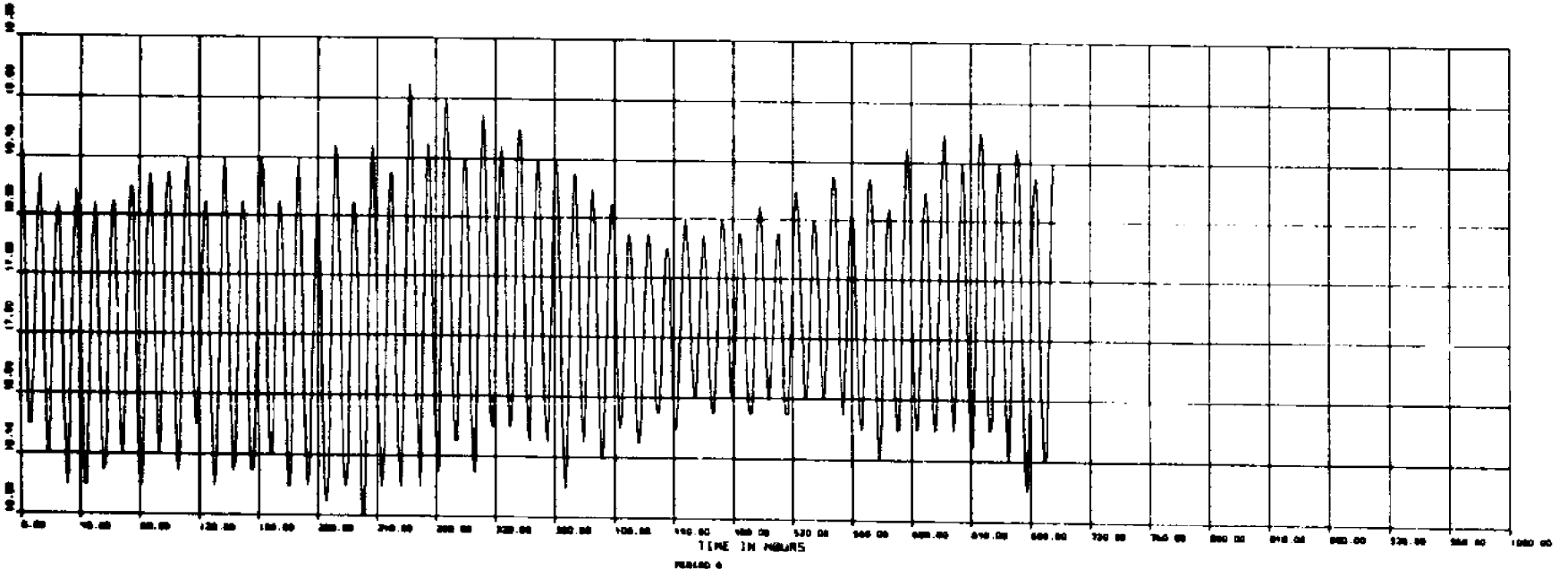

Figure 31b. Period 6: SNLT sea level (m) (3 hr low-passed data).

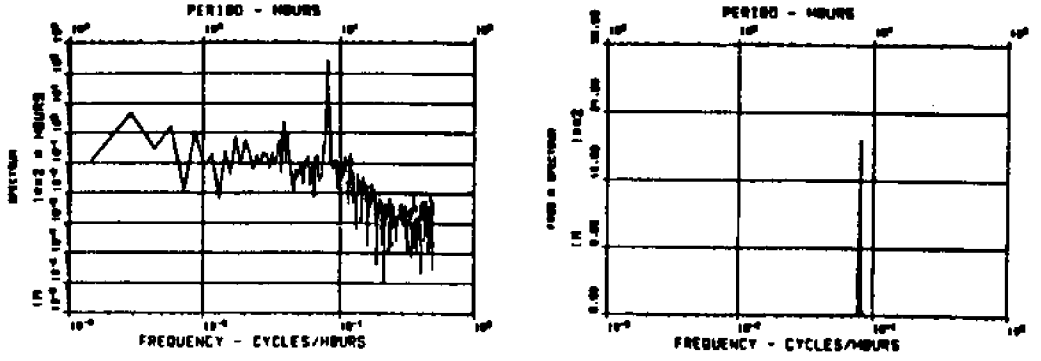

Figure 32a. Period 5: Autospectral plots of 3 hr low-passed sea level at SNLT showing variance and variance preserved.

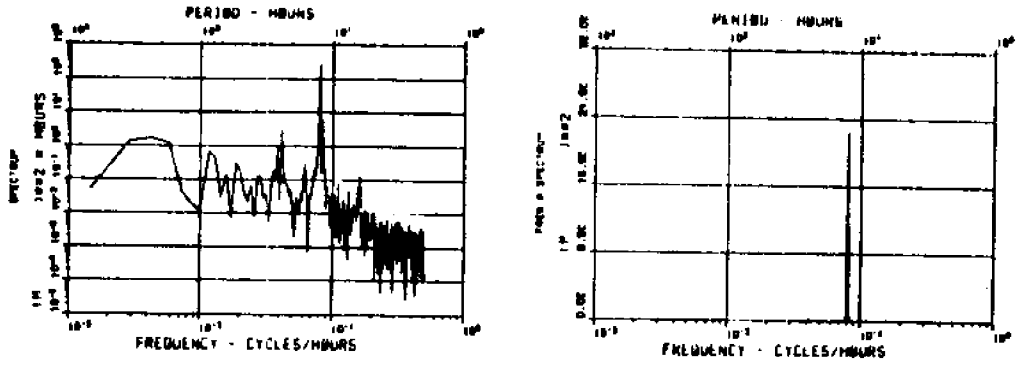

Figure 32b. Period 6: Autospectral plots of 3 hr low-passed sea level at SNLT showing variance and variance preserved.

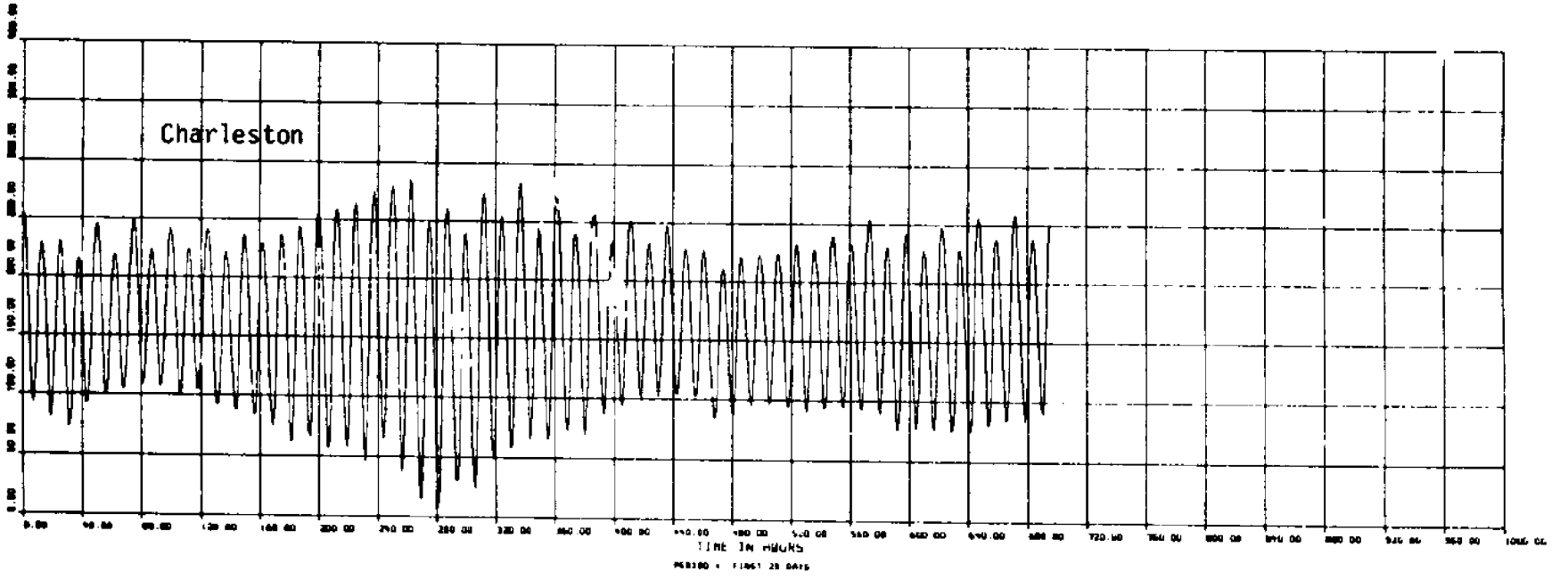

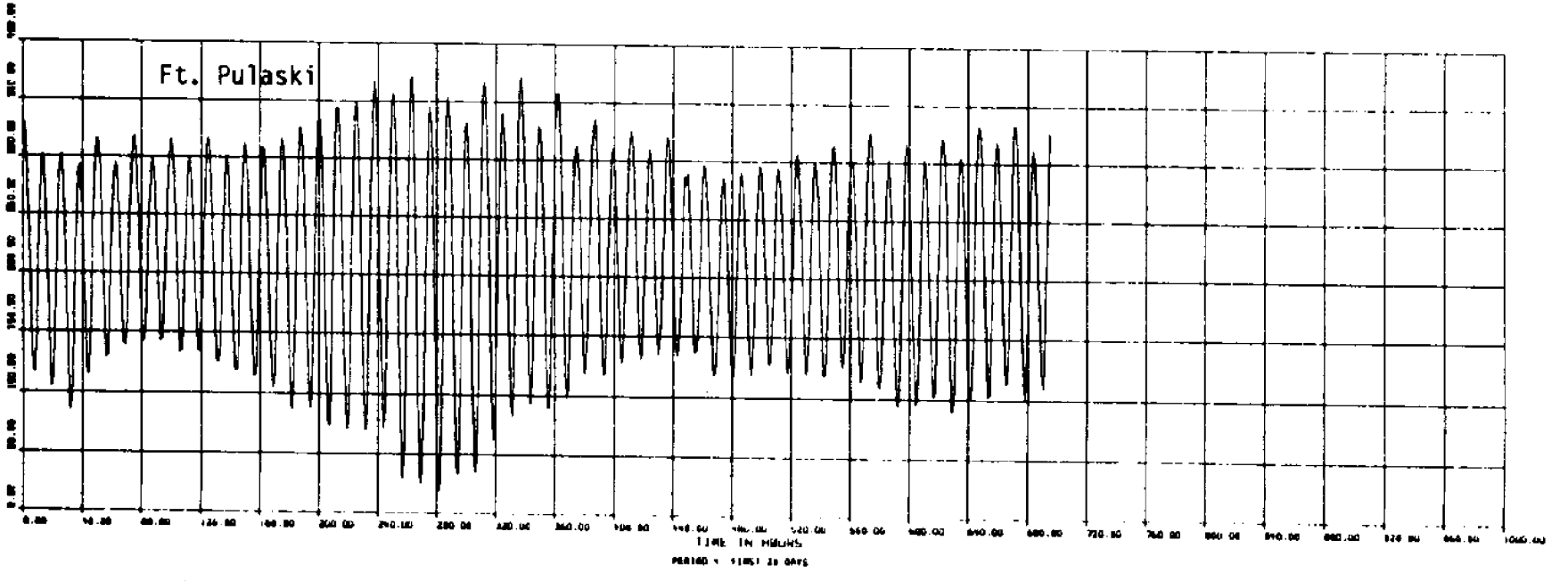

Figure 33a. Period 4: Charleston vs. Ft. Pulaski sea level (cm) (3 hr low-passed data).

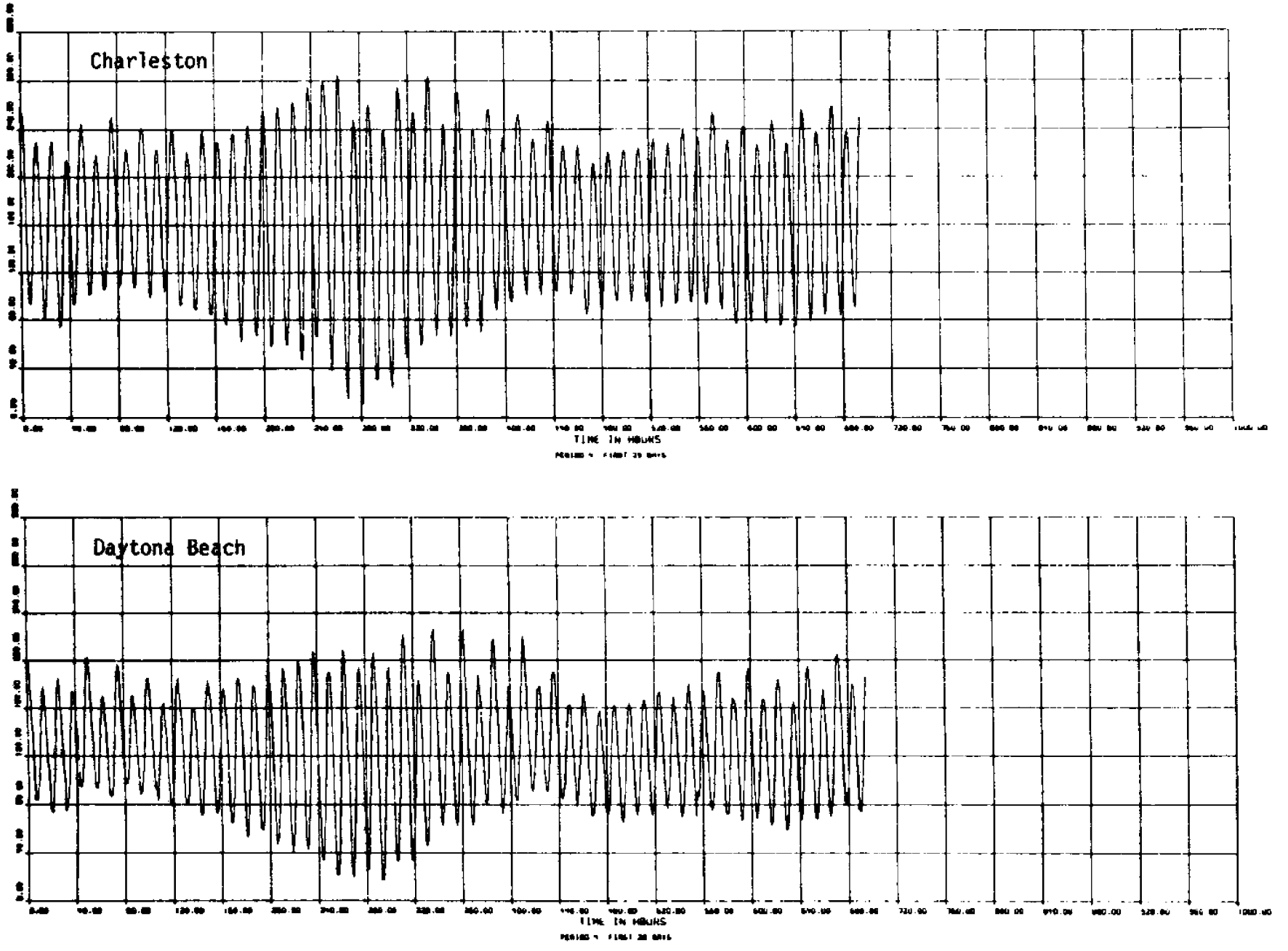

Figure 33b. Period 4: Charleston vs. Daytona Beach sea levels (cm) (3 hr low-passed data).

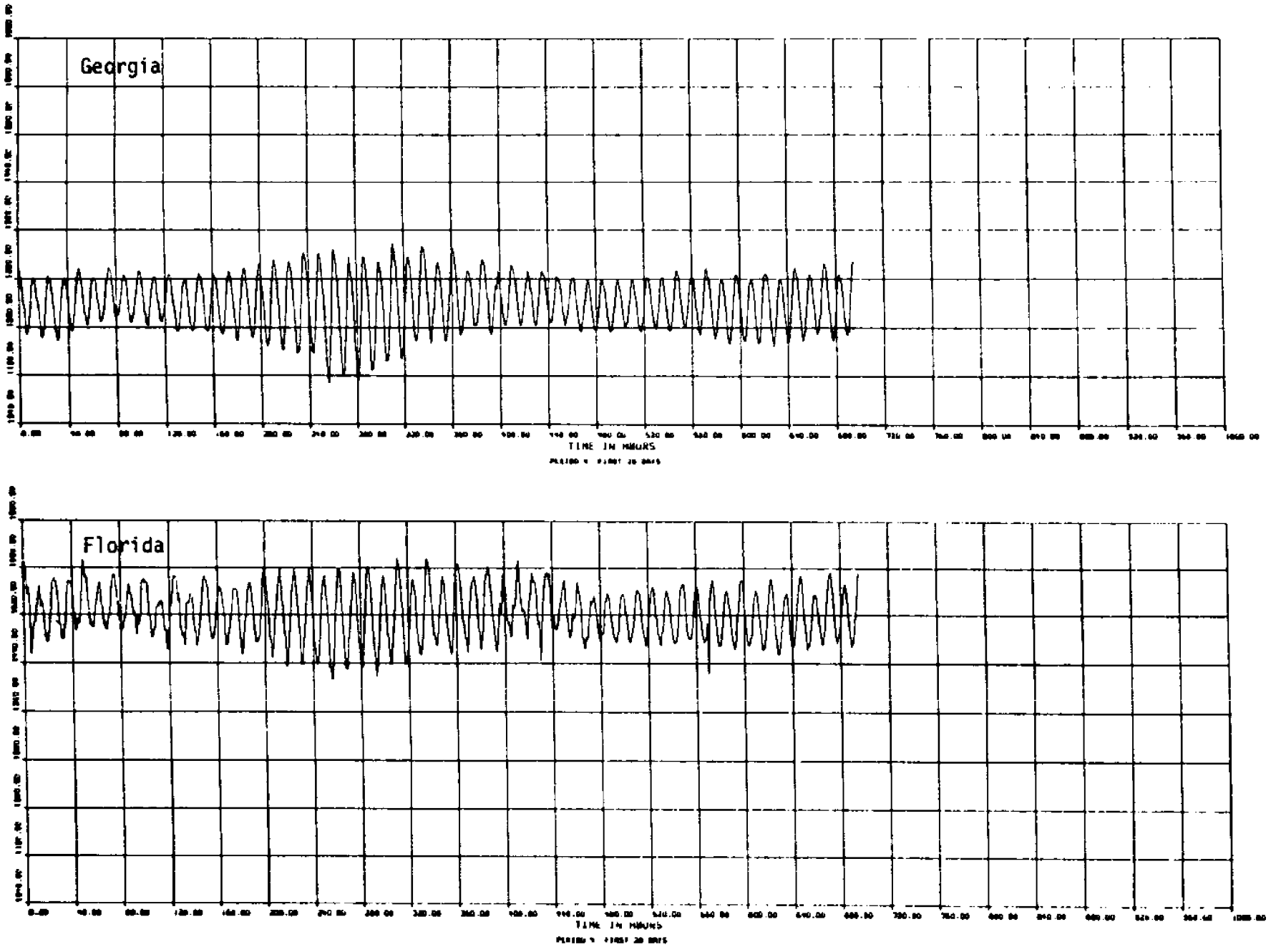

Figure 33c. Period 4: Georgia vs. Florida bottom pressures (mb) (3 hr low-passed data).

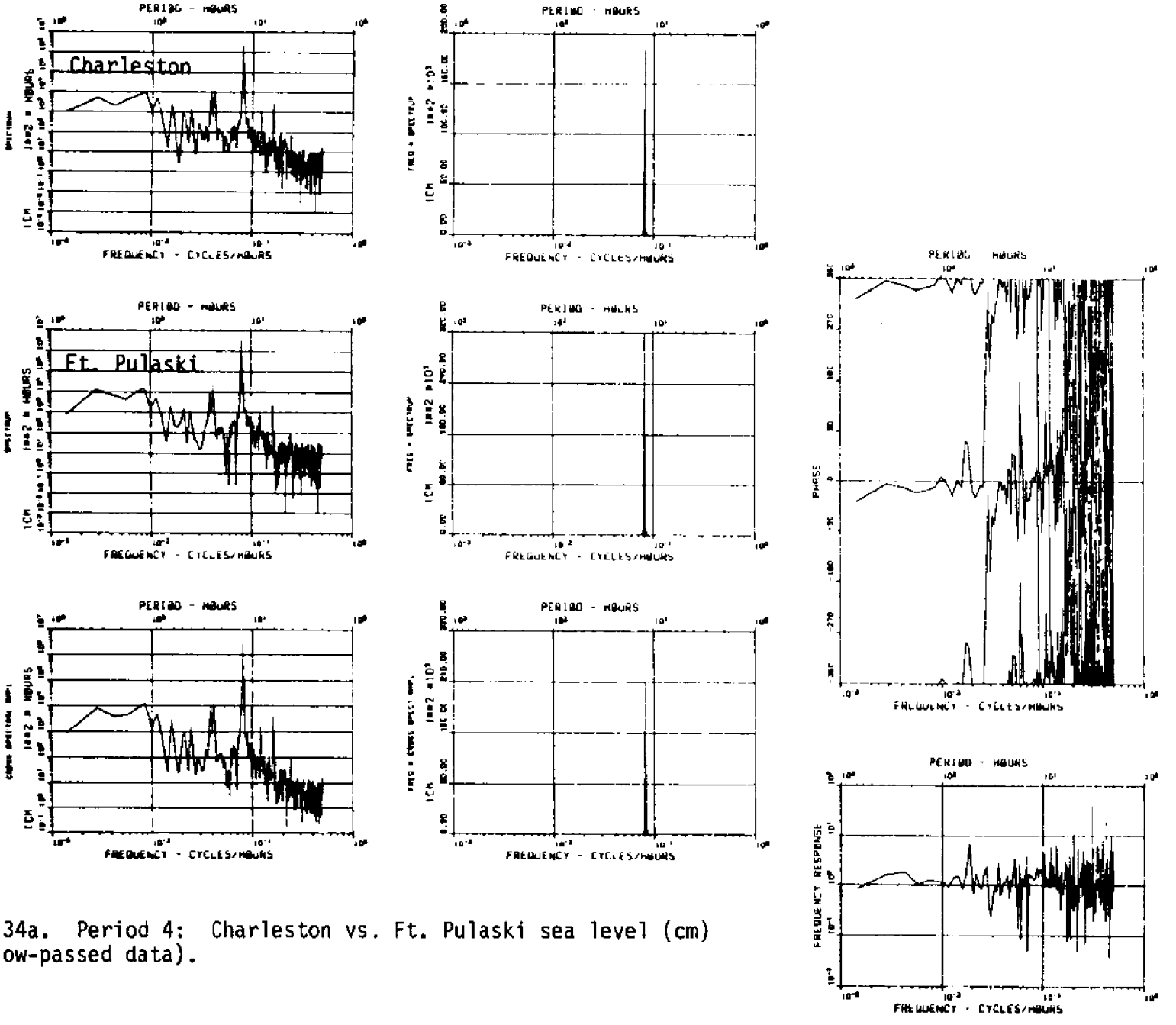

Figure 34a. Period 4: Charleston vs. Ft. Pulaski sea level (cm) (3 hr low-passed data).

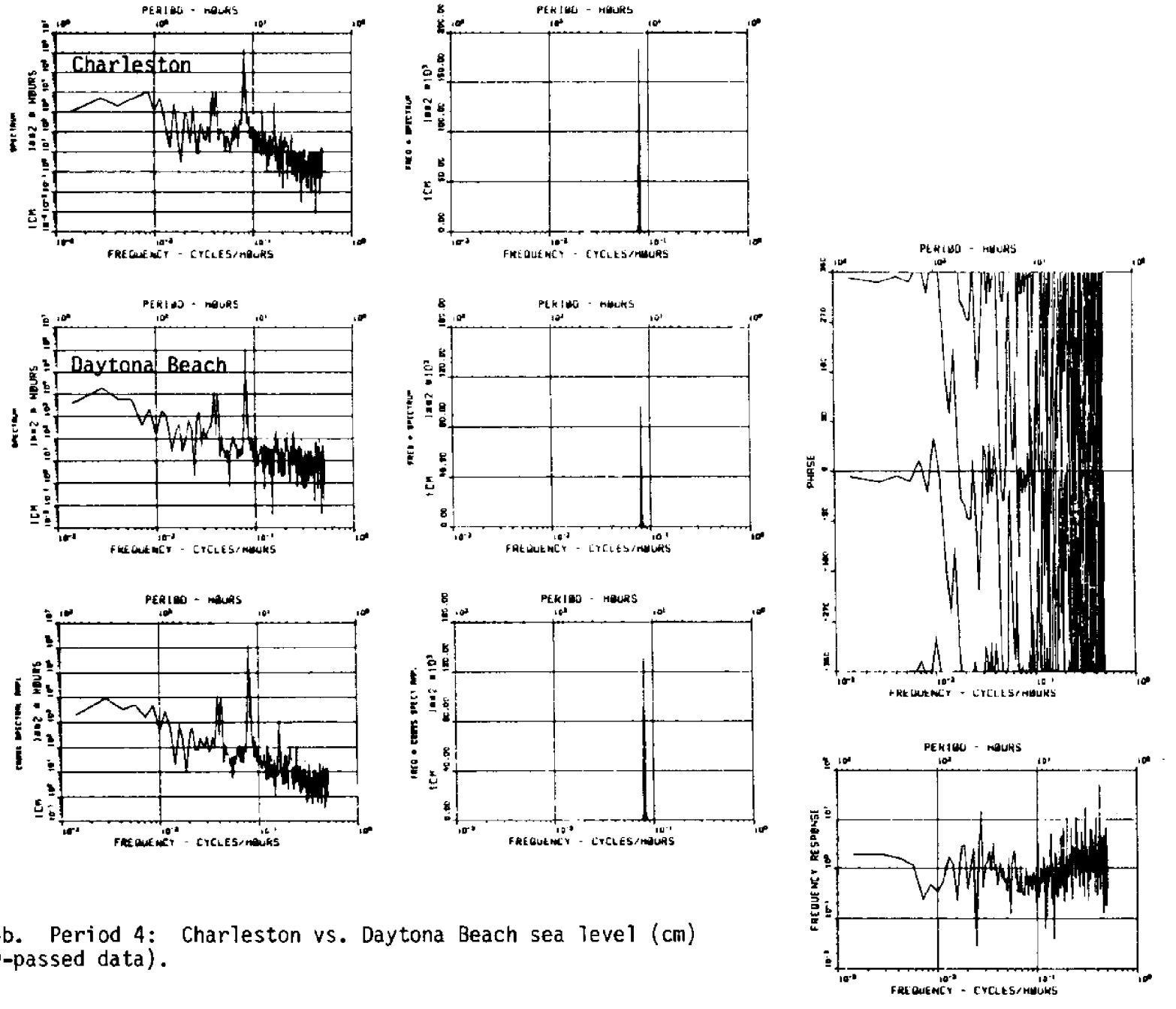

Figure 34b. Period 4: Charleston vs. Daytona Beach sea level (cm) (3 hr low-passed data).

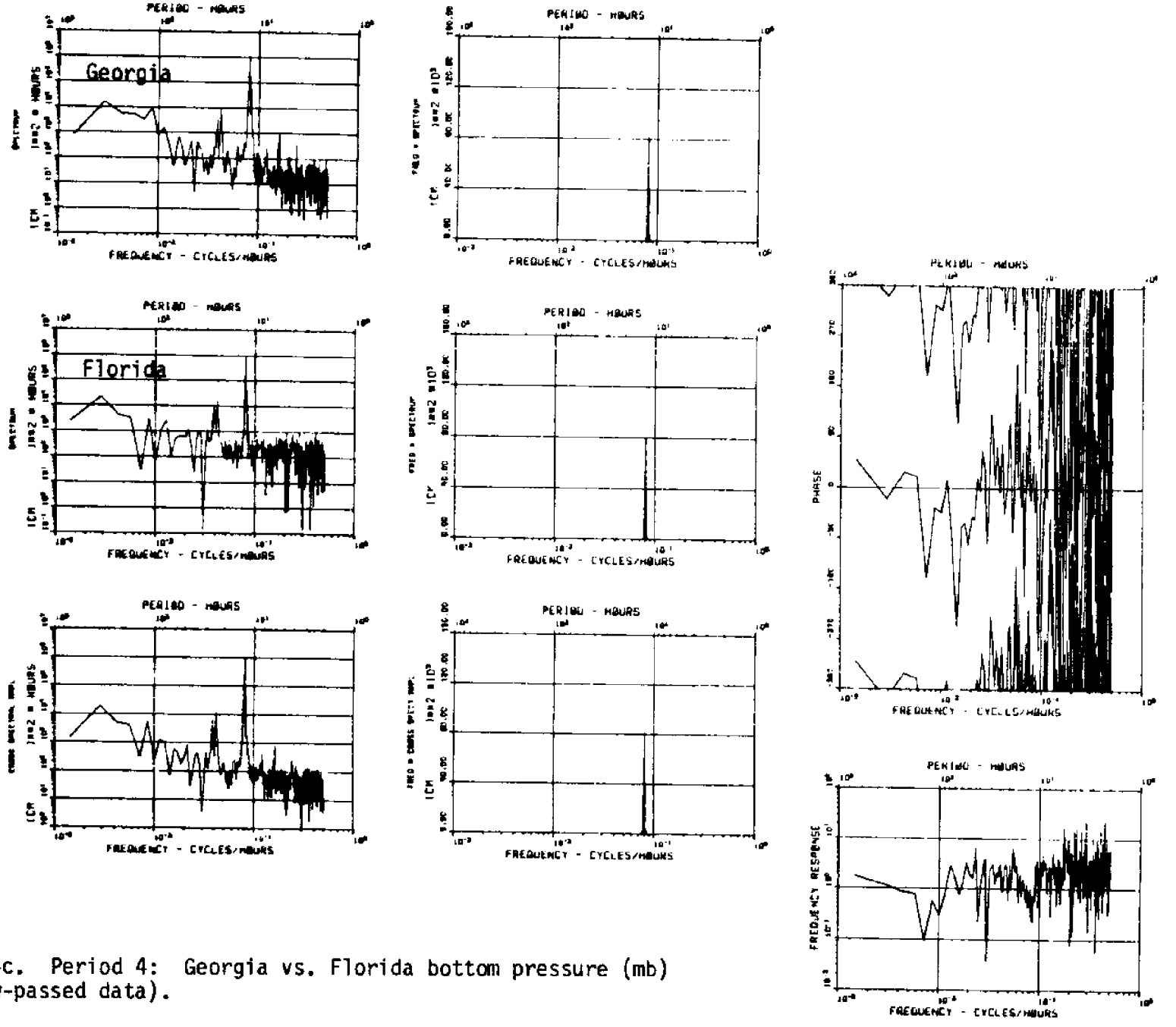

Figure 34c. Period 4: Georgia vs. Florida bottom pressure (mb) (3 hr low-passed data).

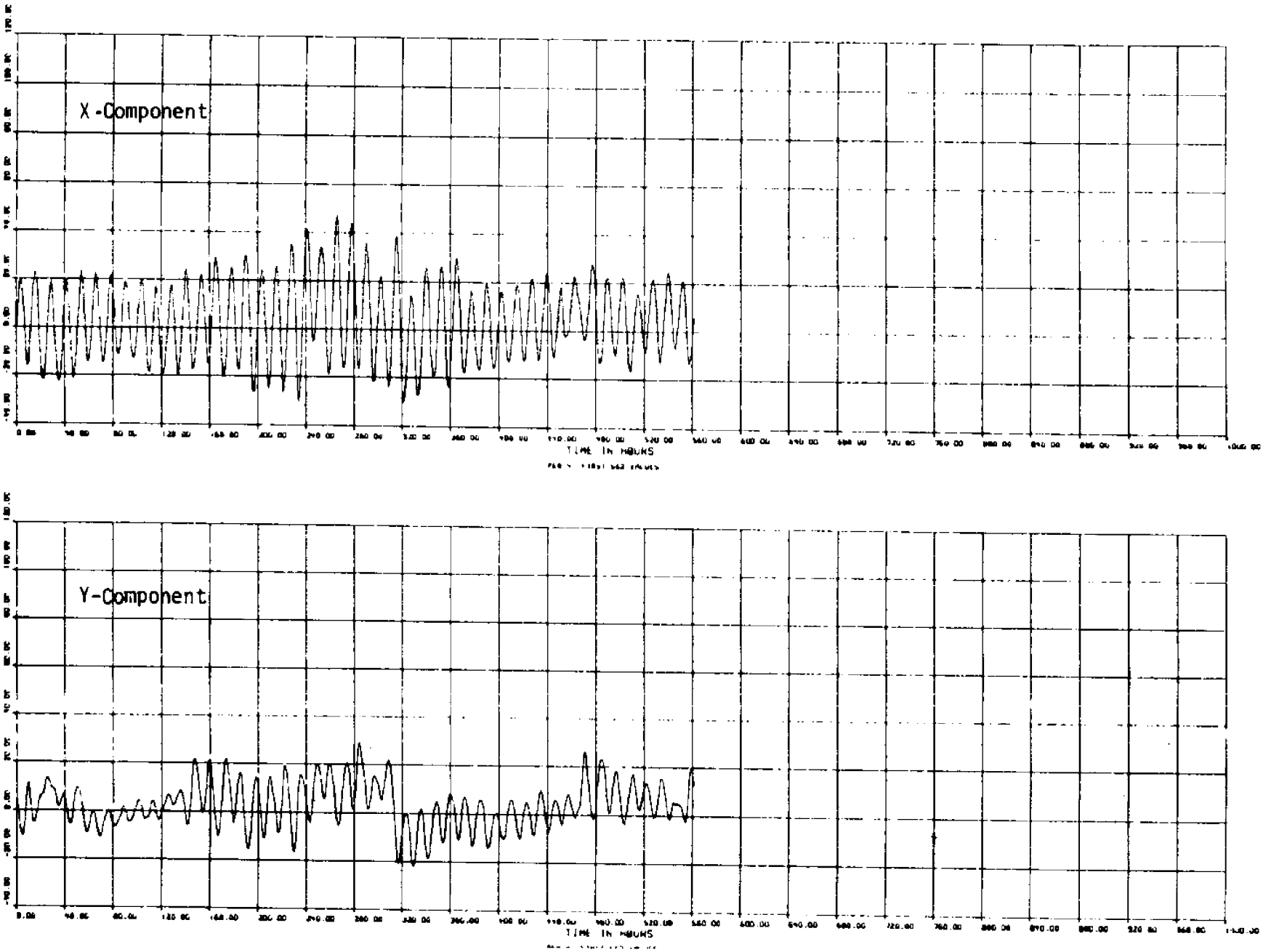

Figure 35a. Period 1: SNLT currents (cm/s) (3 hr low-passed data).

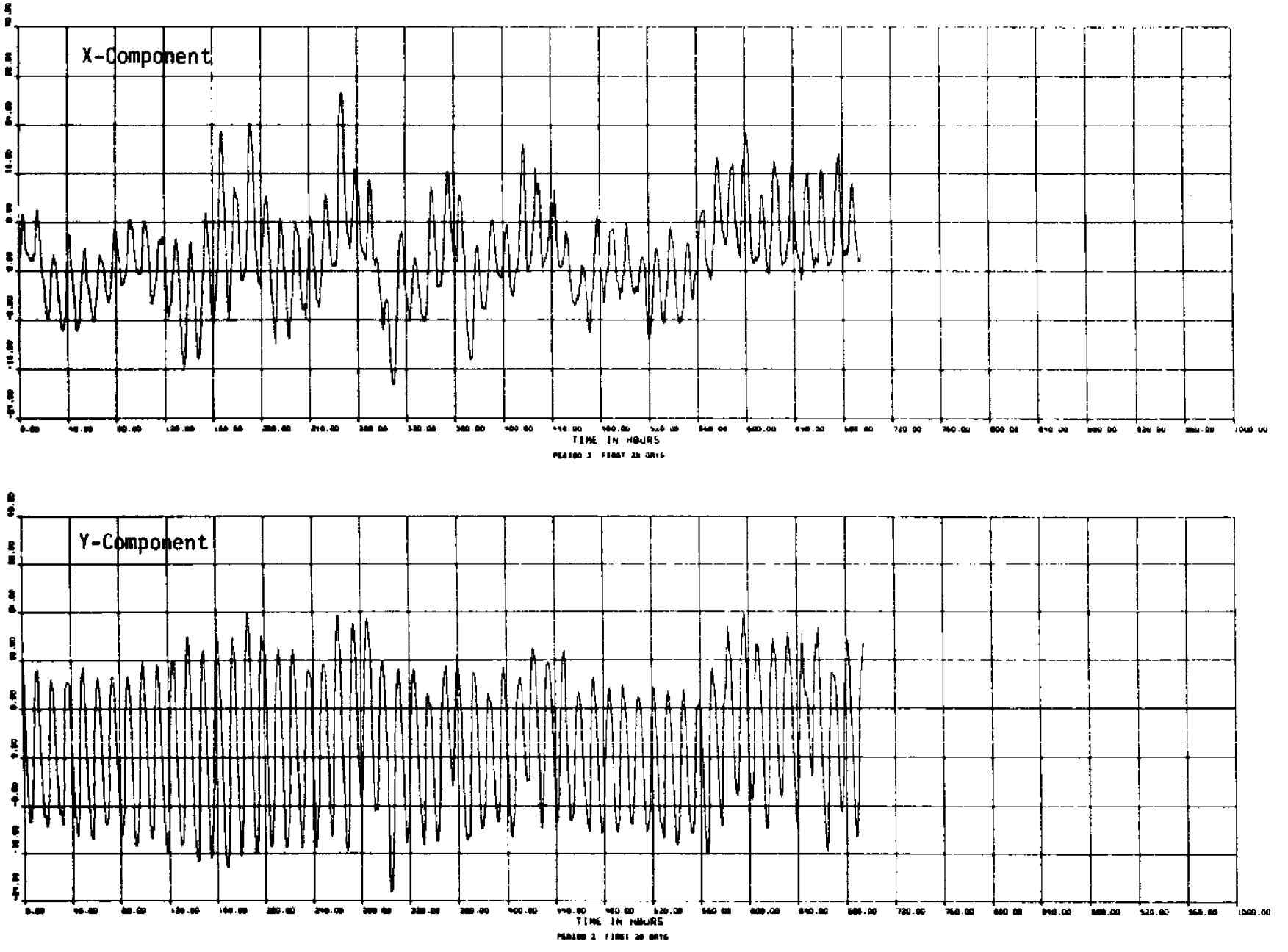

Figure 35b. Period 2: SNLT currents (cm/s) (3 hr low-passed data).

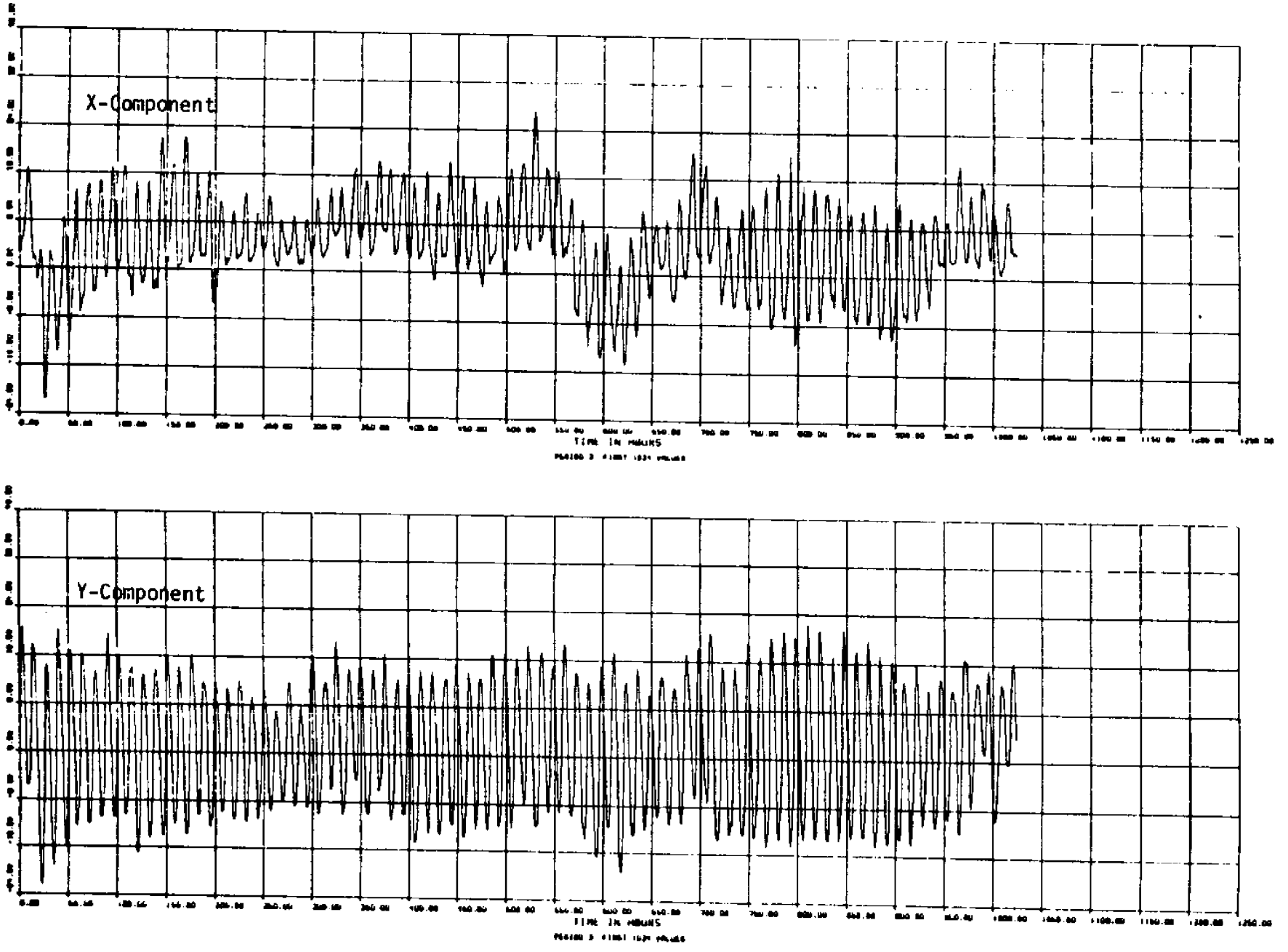

Figure 35c. Period 3: SNLT currents (cm/s). X-Y coordinates rotated -33 deg.

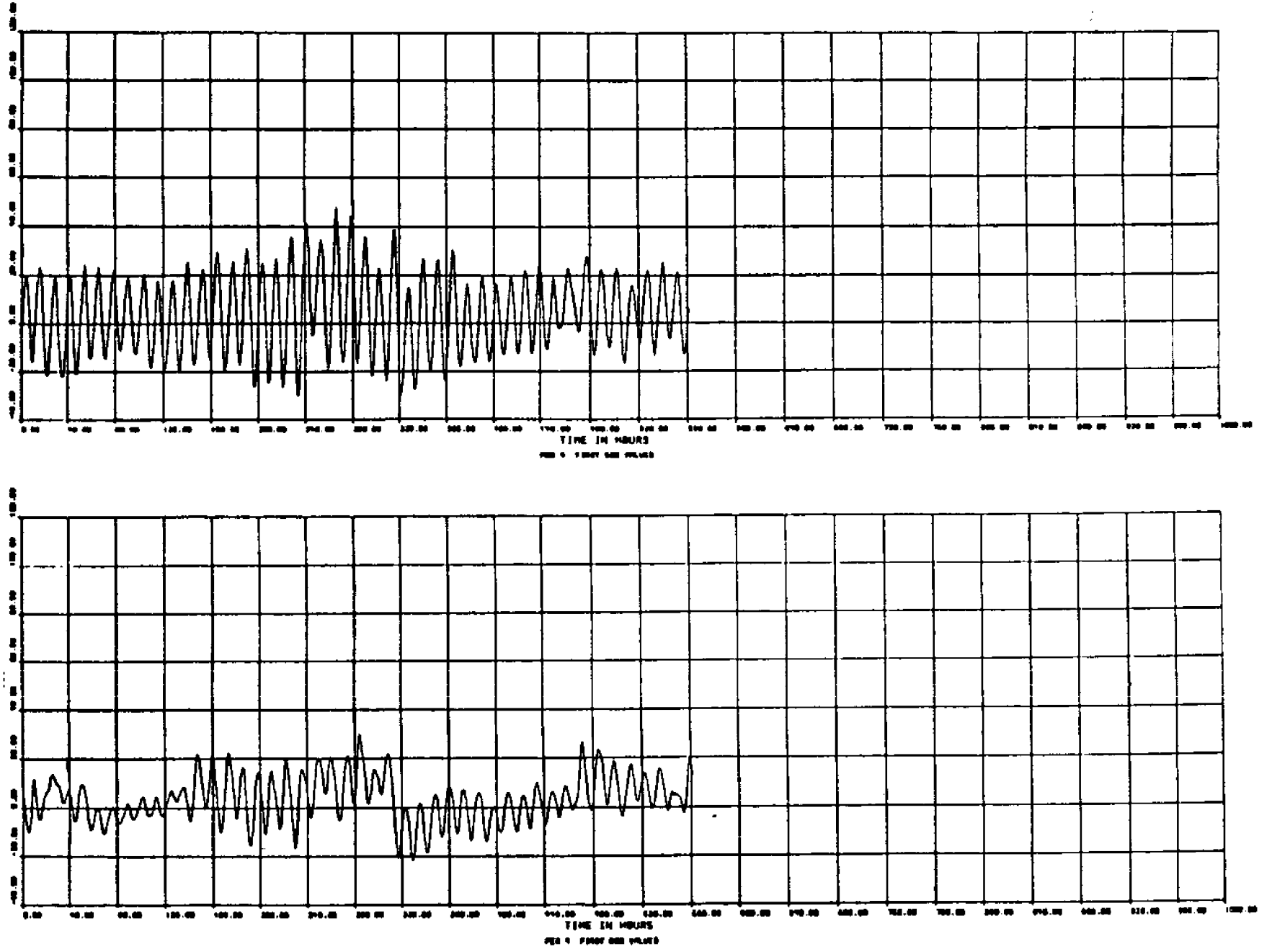

Figure 35d. Period 4: SNLT currents (cm/s) (3 hr low-passed data).

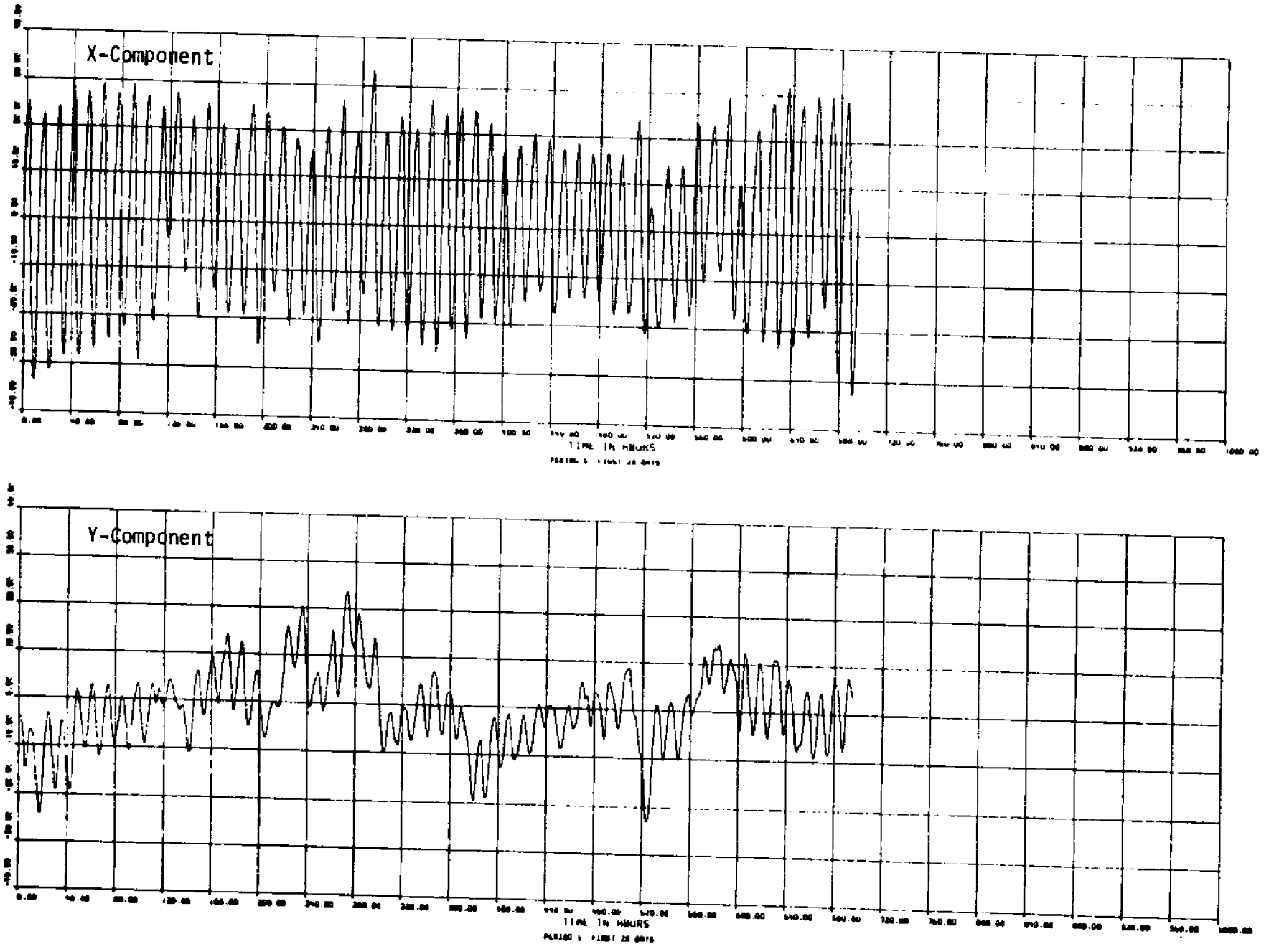

Figure 35e. Period 5: SNLT currents (cm/s) (3 hr low-passed data).

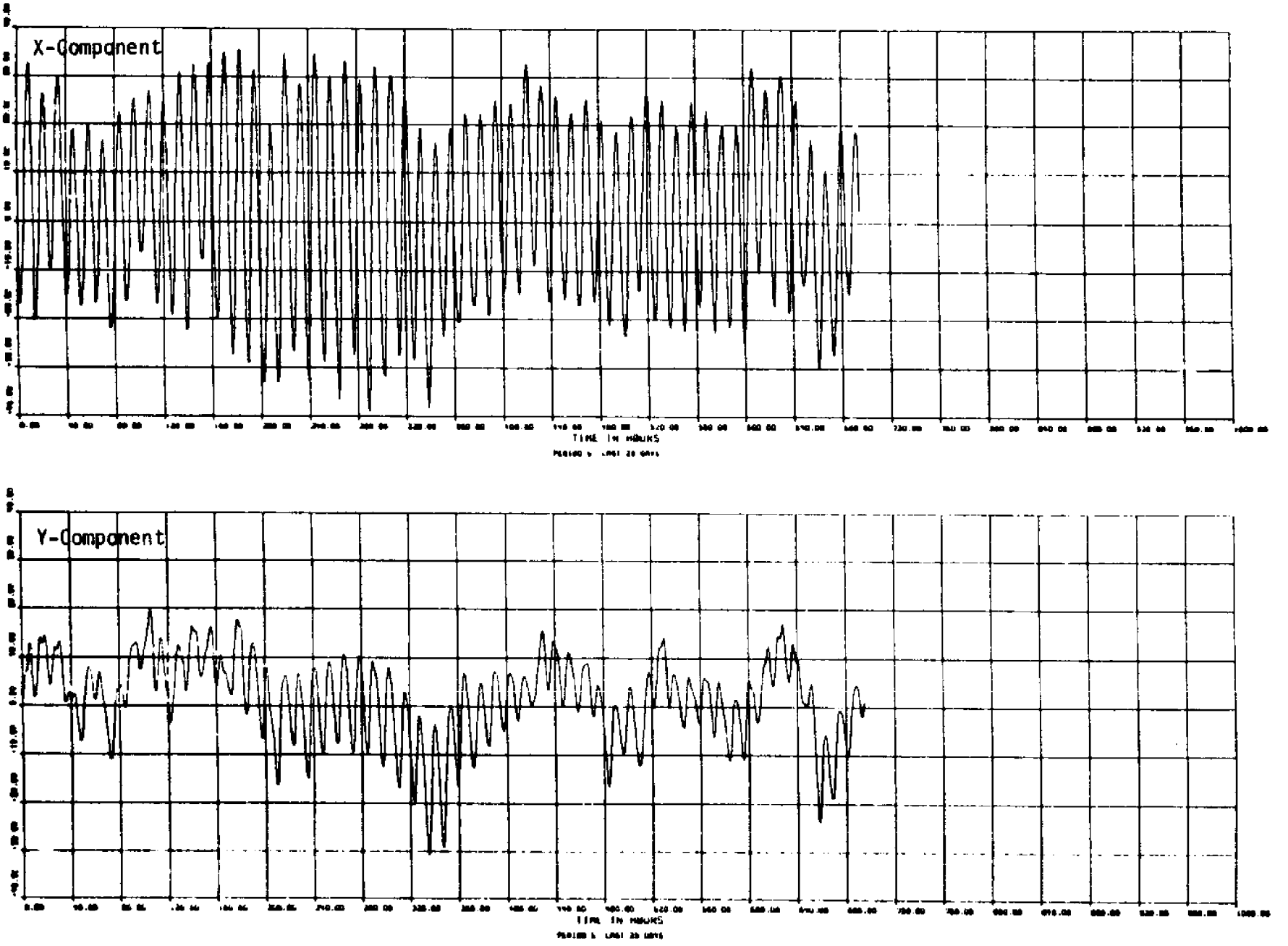

Figure 35f. Period 5: SNLT currents (cm/s) (3 hr low-passed data).

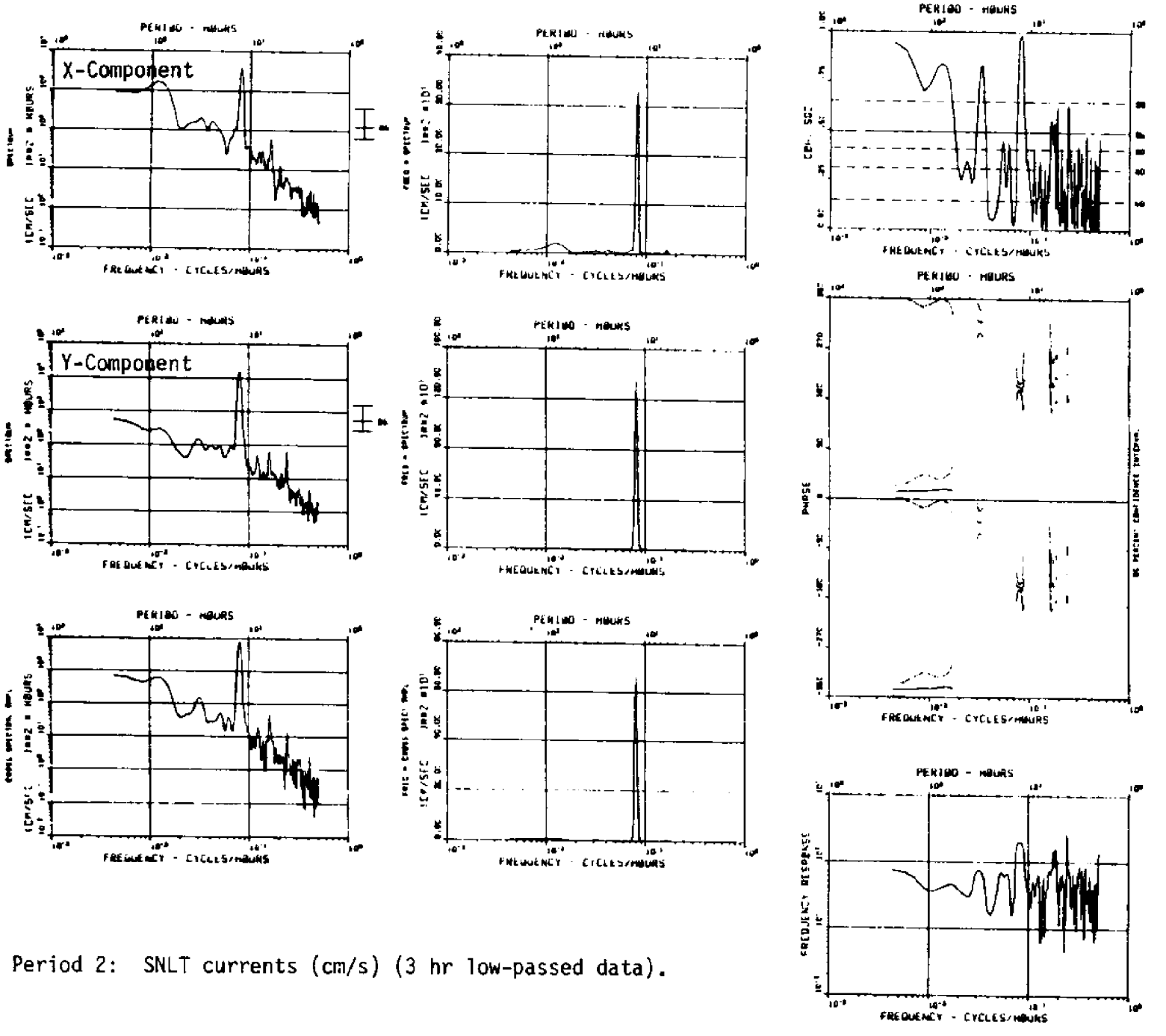

Figure 36a. Period 2: SNLT currents (cm/s) (3 hr low-passed data).

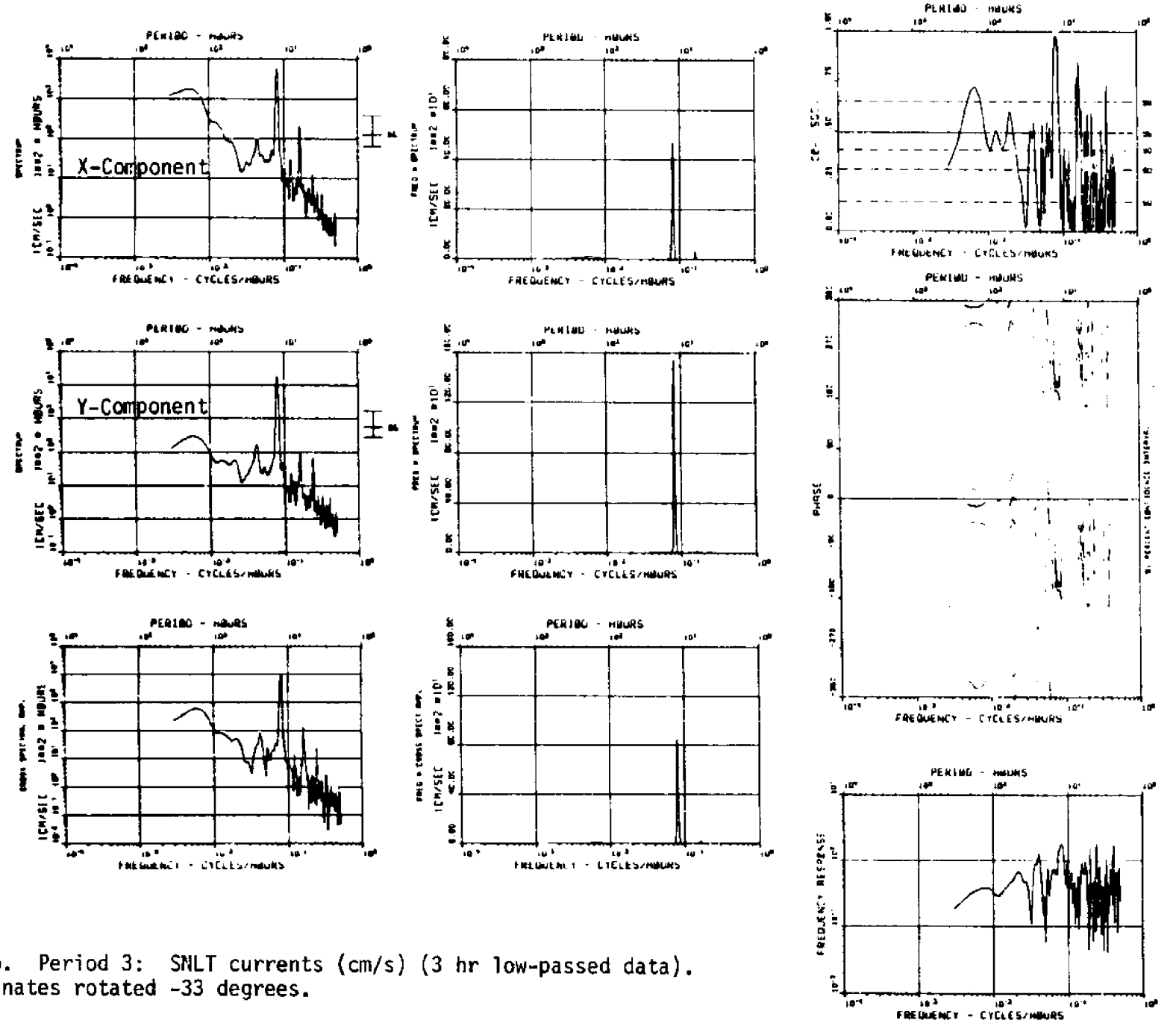

Figure 36b. Period 3: SNLT currents (cm/s) (3 hr low-passed data). X-Y coordinates rotated -33 degrees.

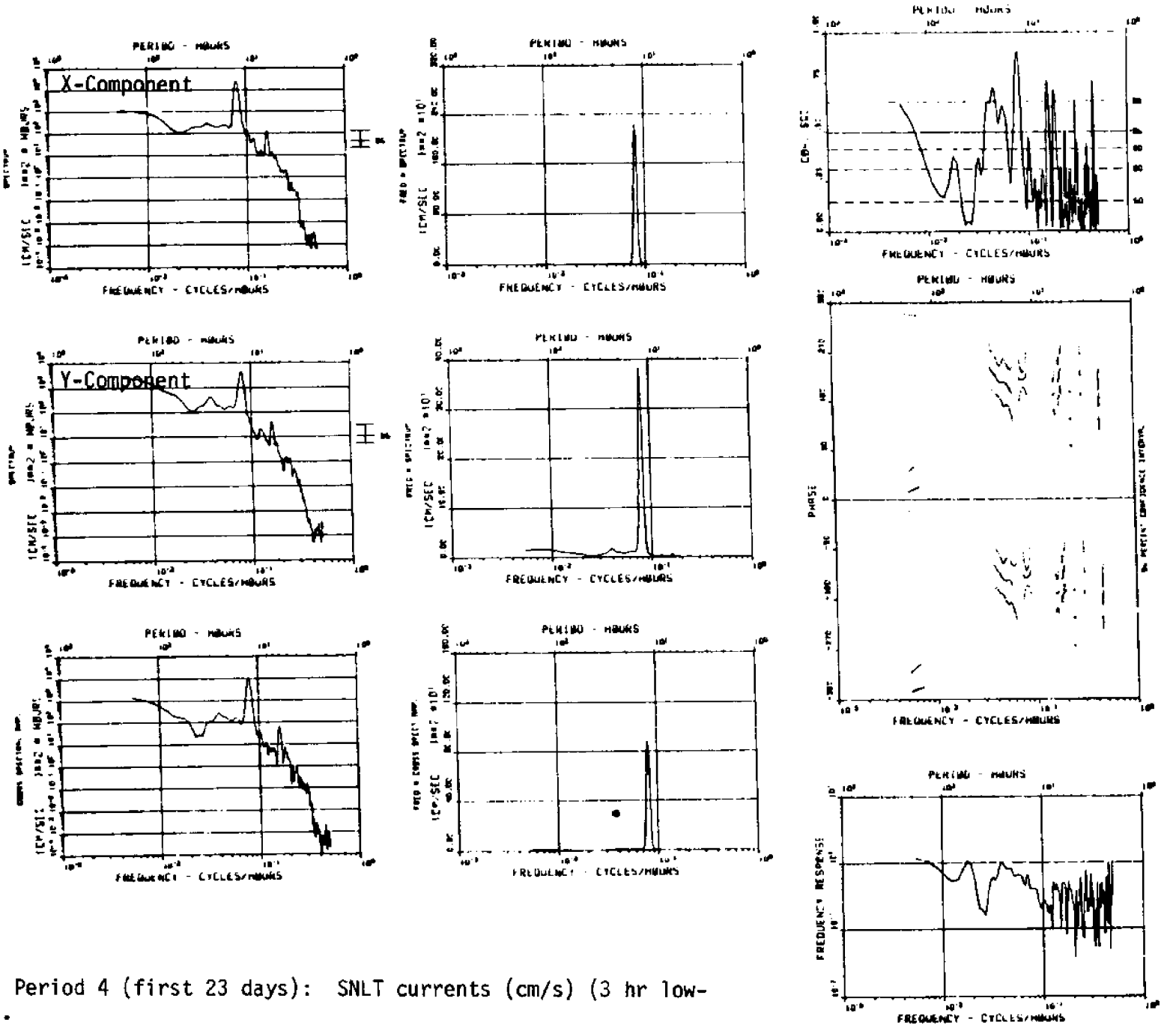

Figure 36c. Period 4 (first 23 days): SNLT currents (cm/s) (3 hr low-passed data).

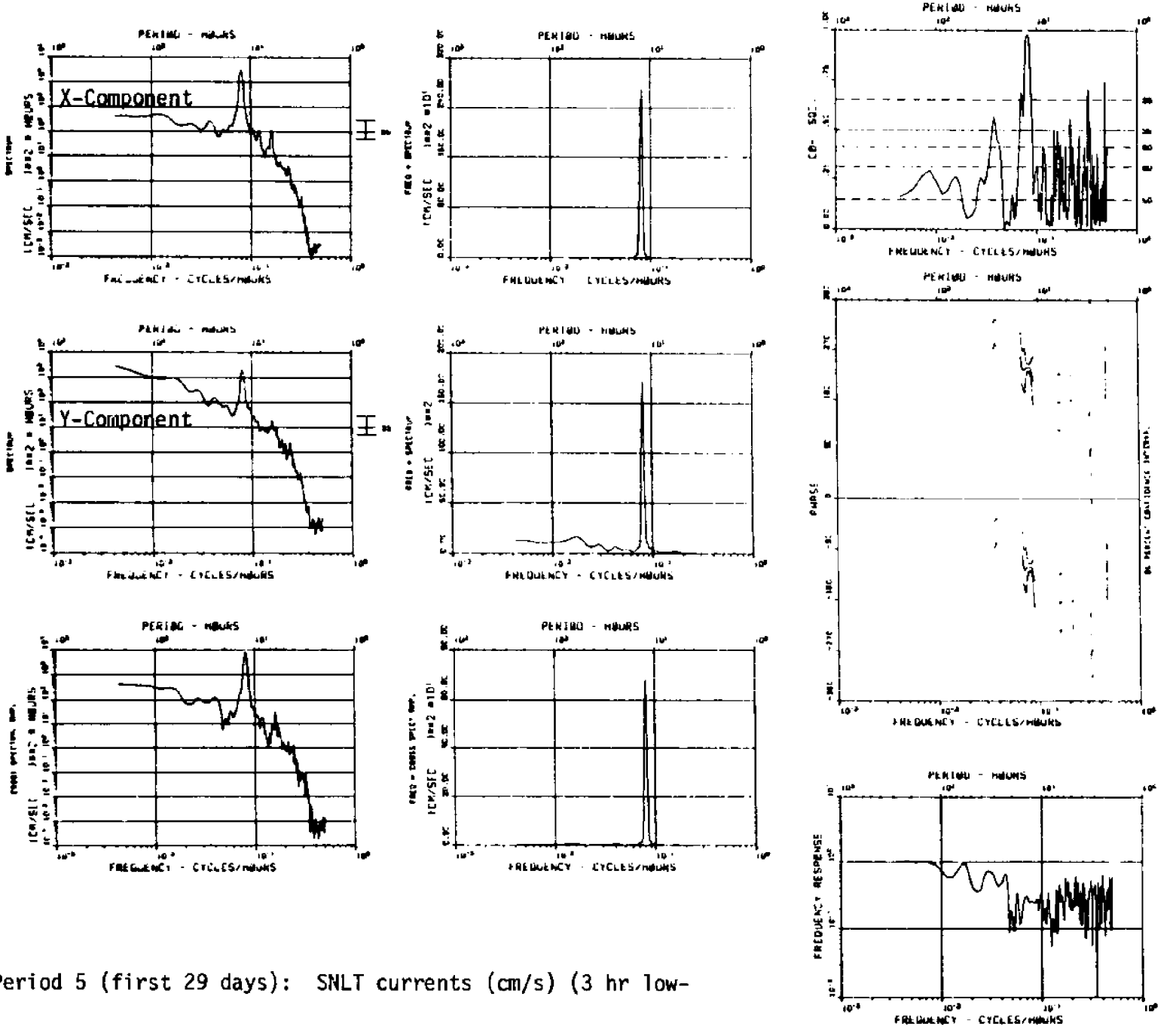

Figure 36d. Period 5 (first 29 days): SNLT currents (cm/s) (3 hr low-passed data).

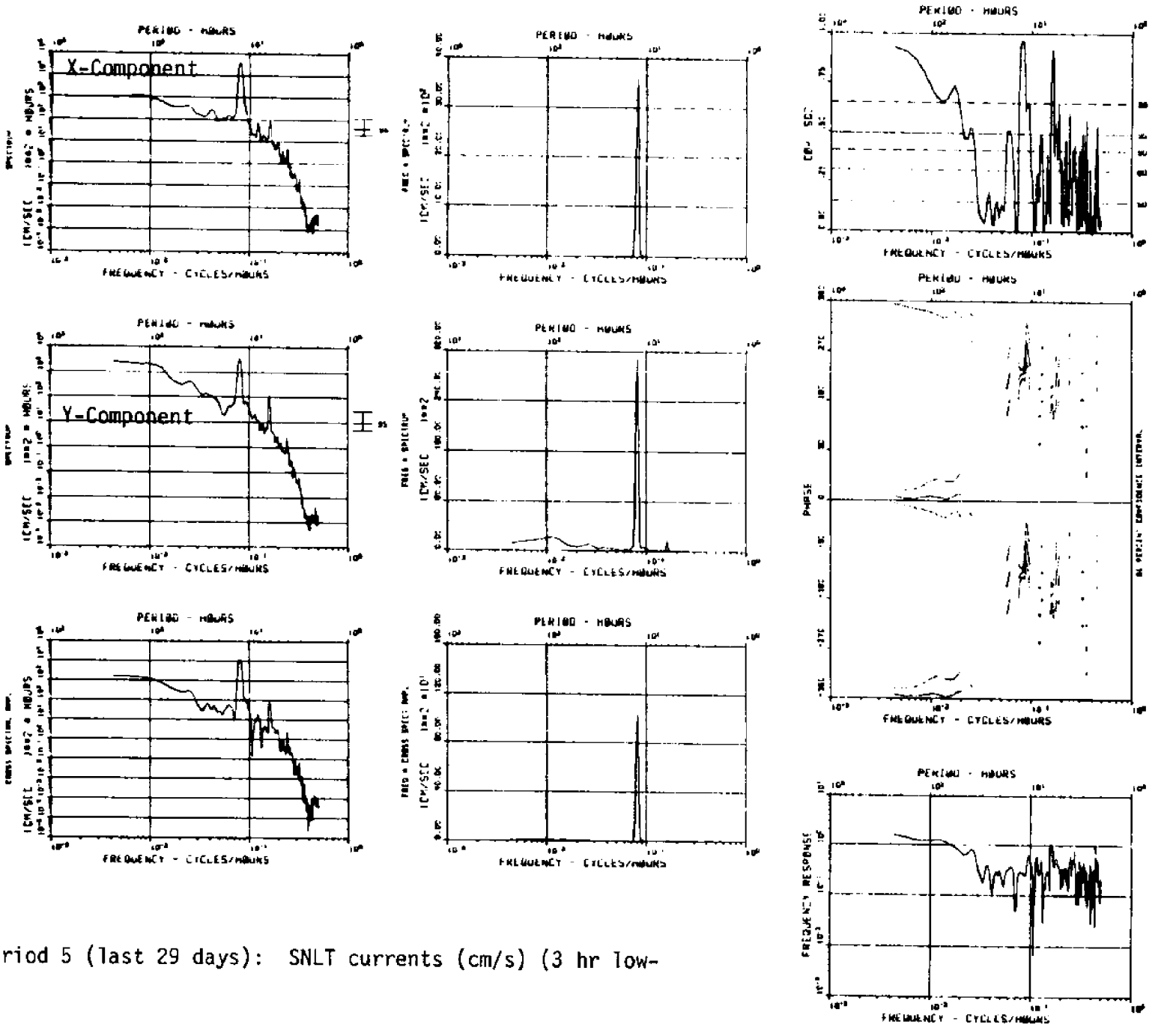

Figure 36e. Period 5 (last 29 days): SNLT currents (cm/s) (3 hr low-passed data).

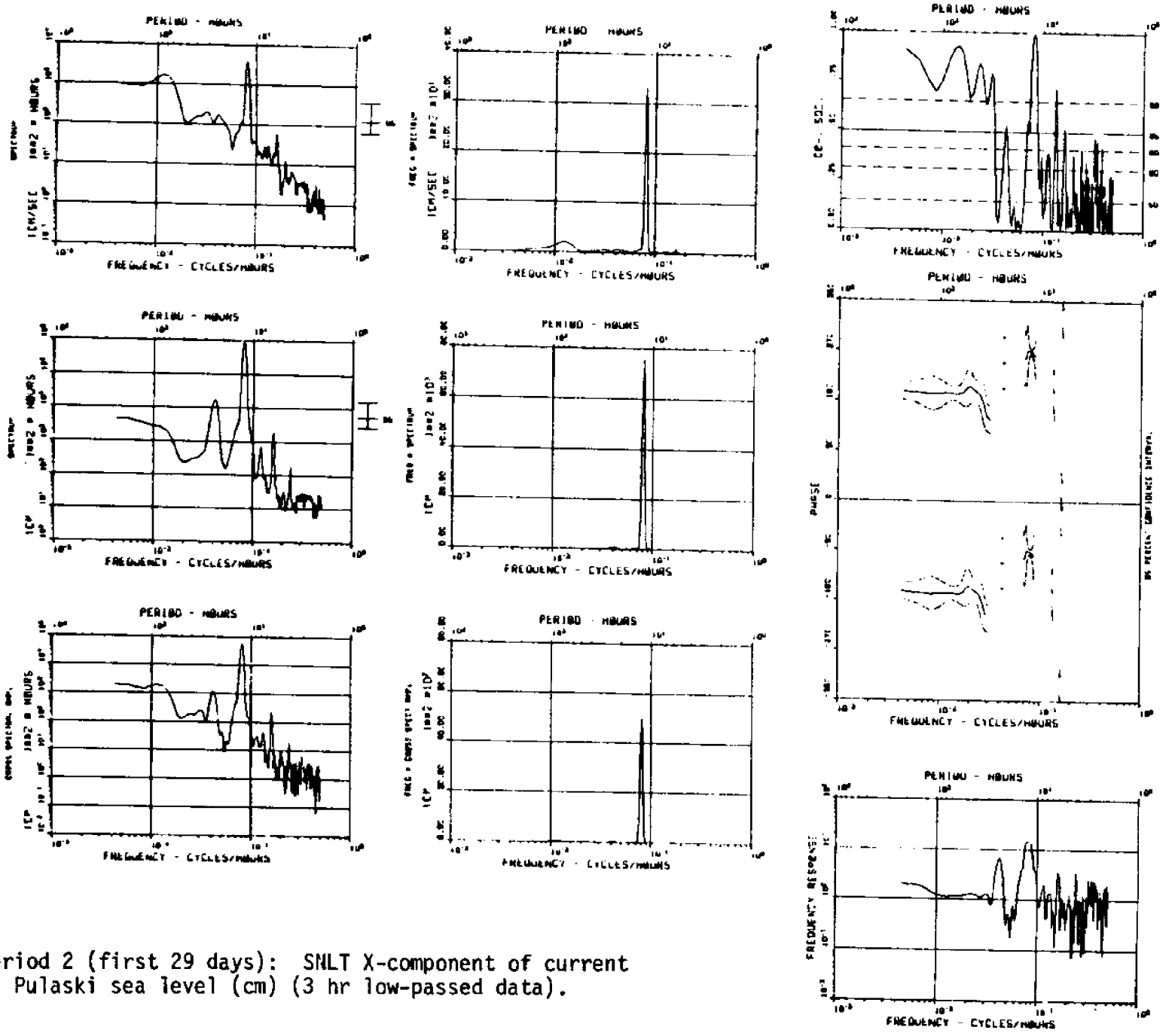

Figure 37a. Period 2 (first 29 days): SNLT X-component of current (cm/s) vs. Ft. Pulaski sea level (cm) (3 hr low-passed data).

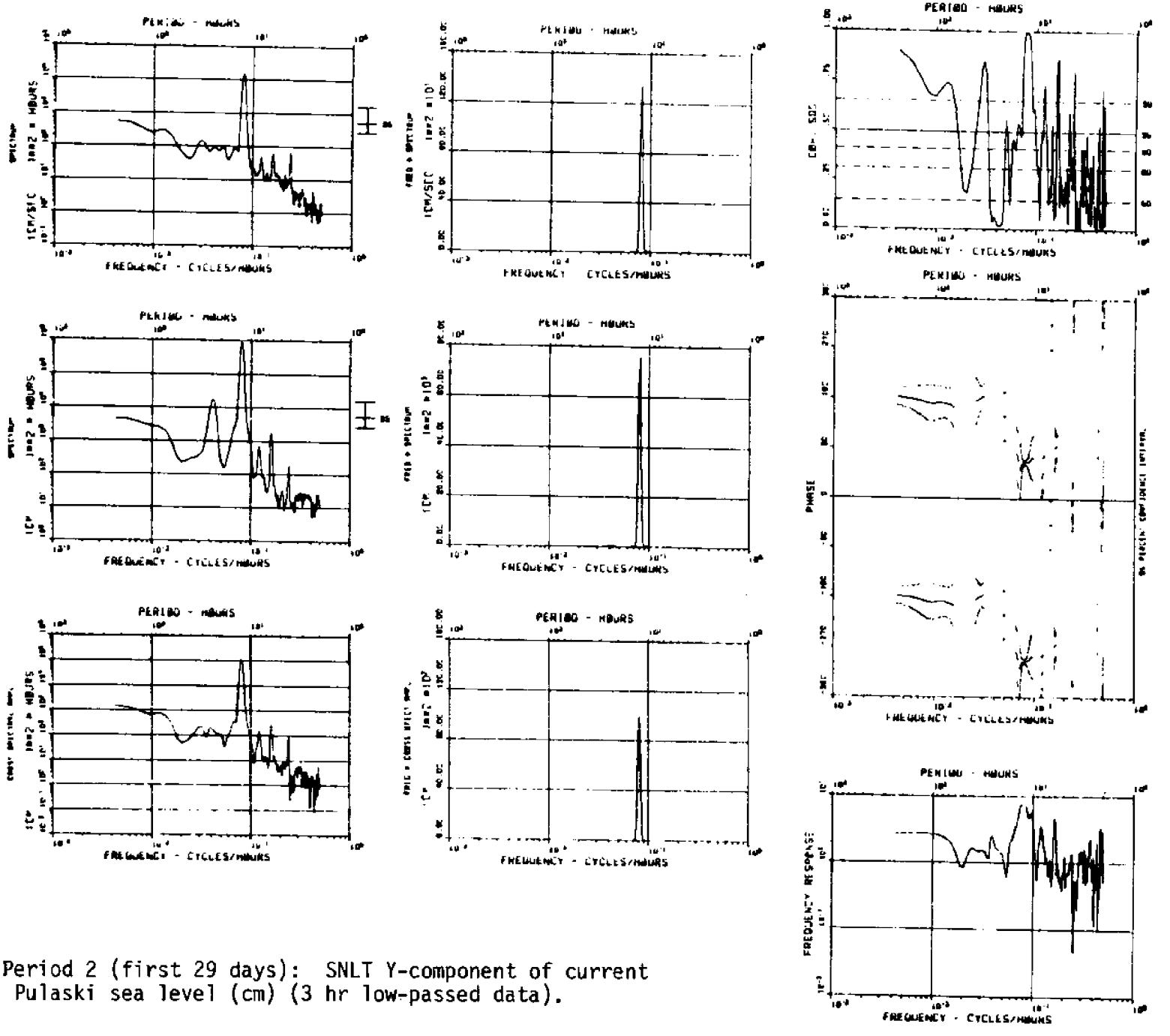

Figure 37b. Period 2 (first 29 days): SNLT Y-component of current (cm/s) vs. Ft. Pulaski sea level (cm) (3 hr low-passed data).

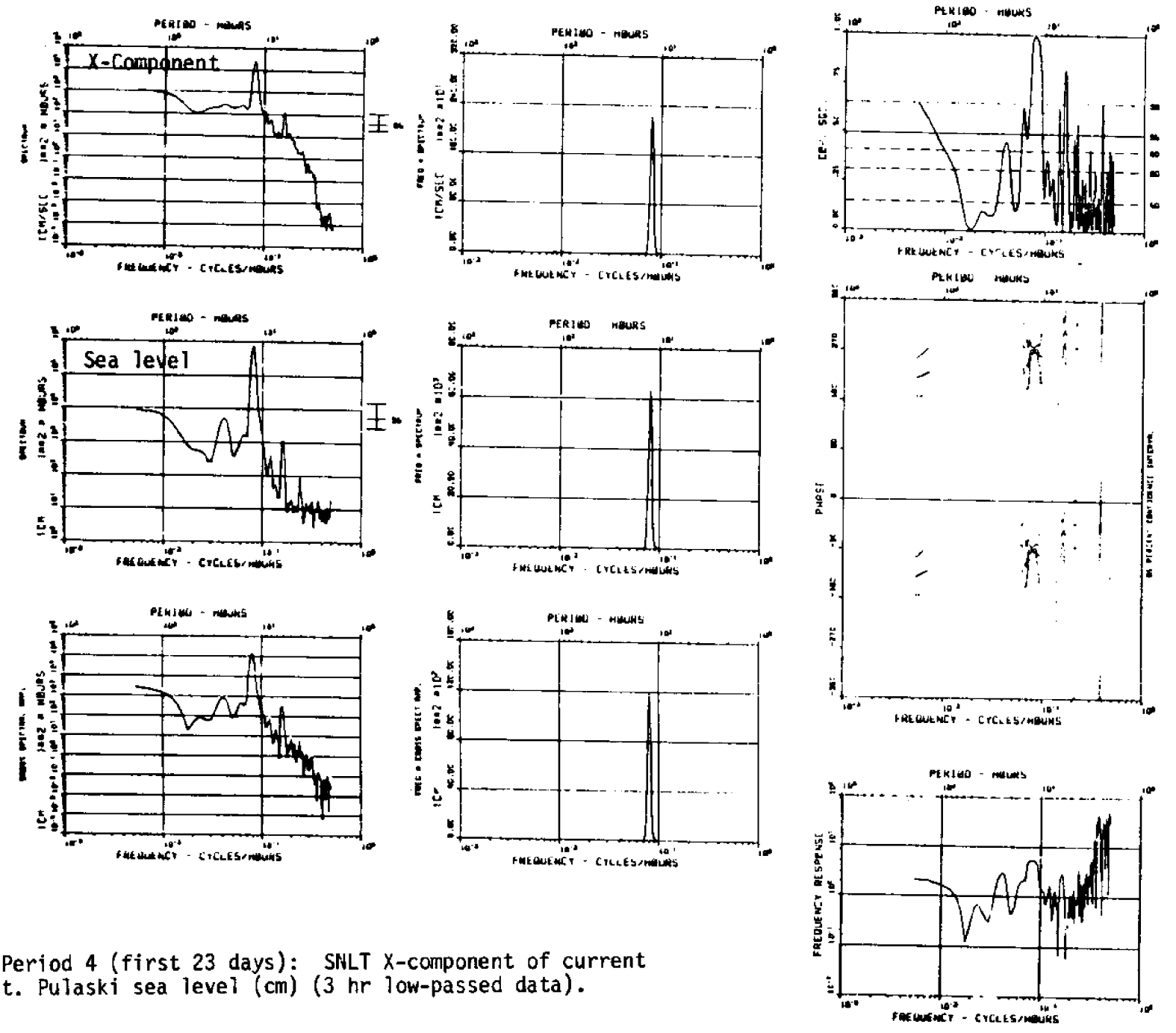

Figure 37c. Period 4 (first 23 days): SNLT X-component of current (cm/s) vs. Ft. Pulaski sea level (cm) (3 hr low-passed data).

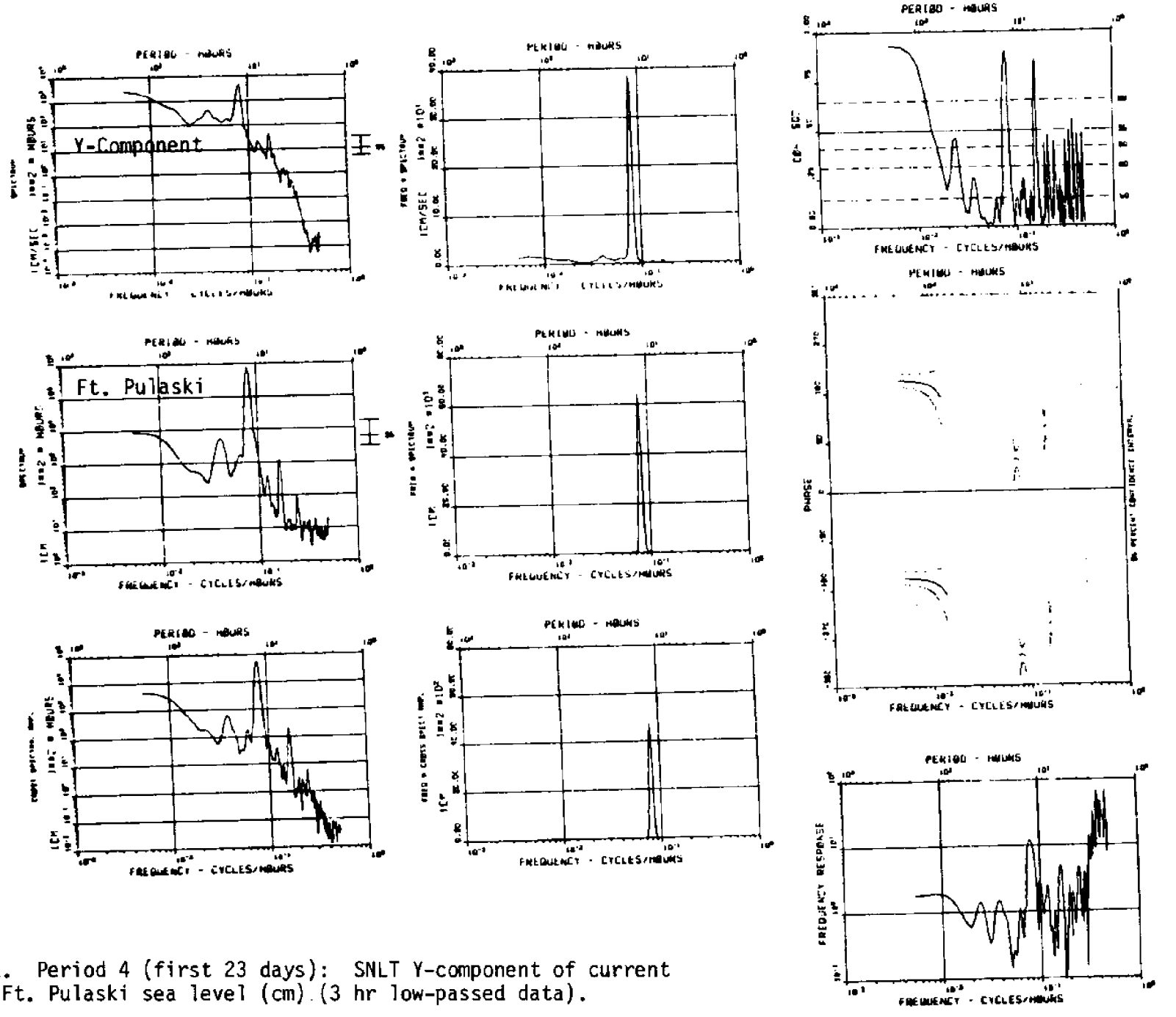

Figure 37d. Period 4 (first 23 days): SNLT Y-component of current (cm/s) vs. Ft. Pulaski sea level (cm) (3 hr low-passed data).

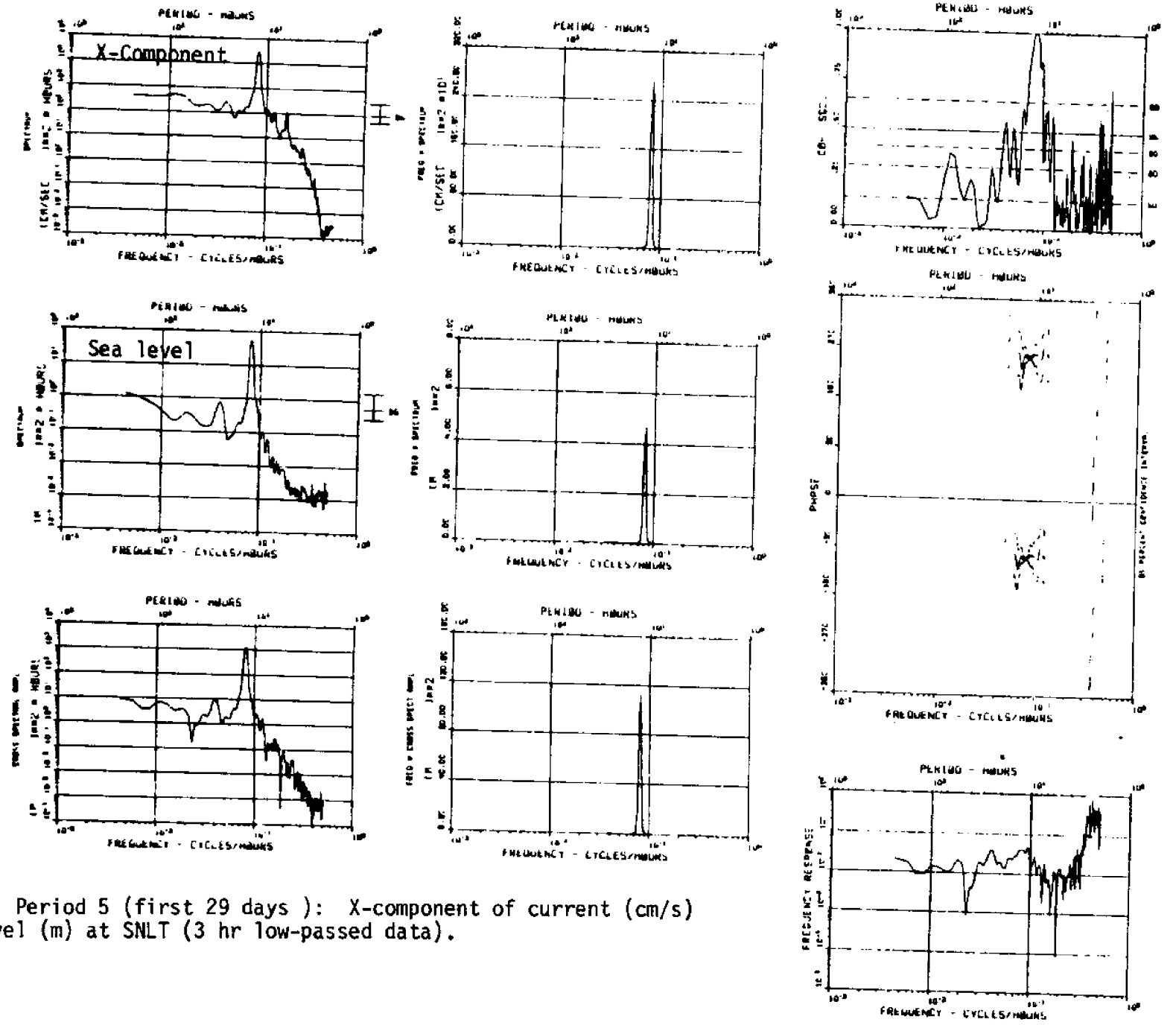

Figure 37e. Period 5 (first 29 days): X-component of current (cm/s) vs. sea level (m) at SNLT (3 hr low-passed data).

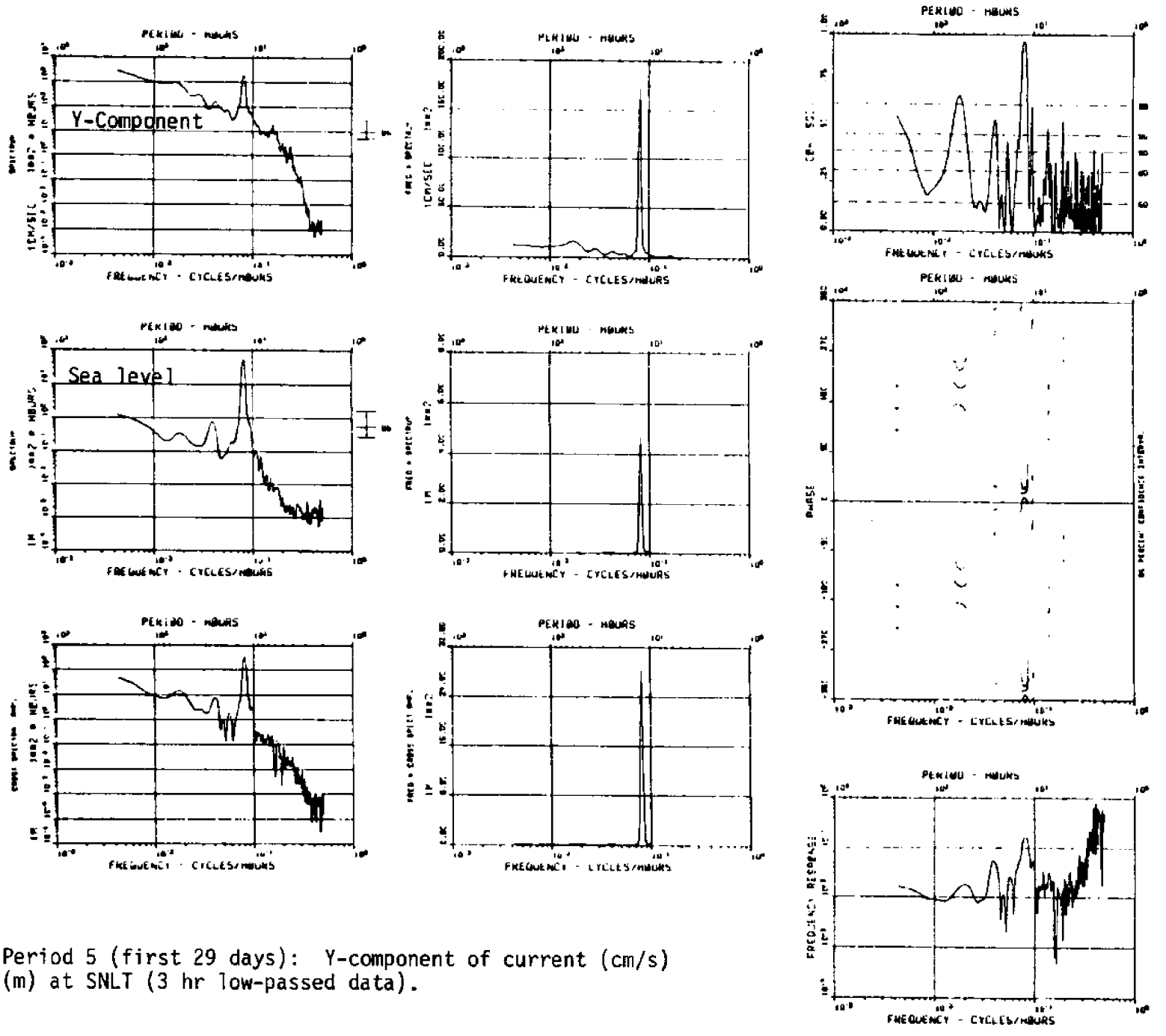

Figure 37 f. Period 5 (first 29 days): Y-component of current (cm/s) vs. sea level (m) at SNLT (3 hr low-passed data).

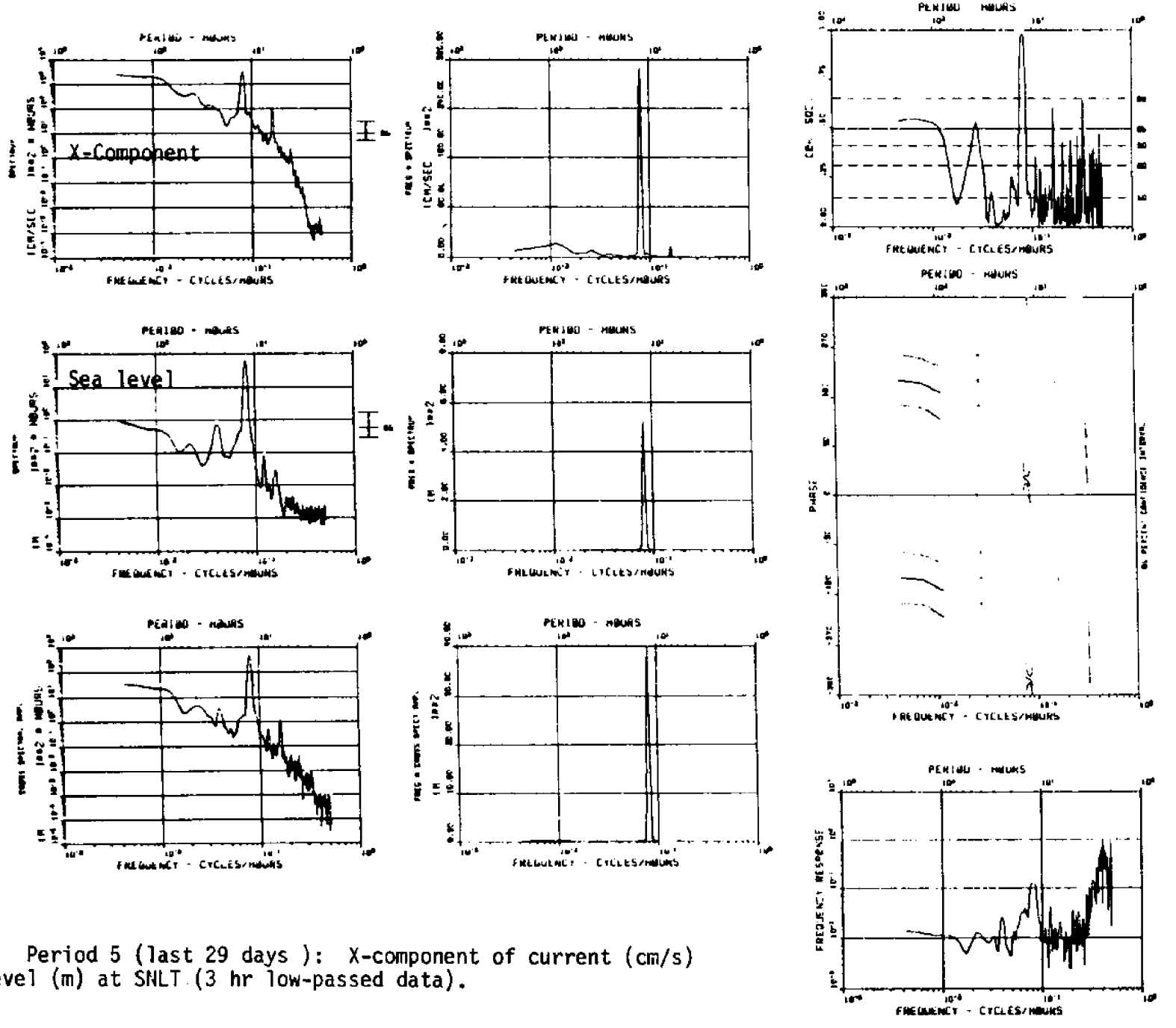

Figure 37g. Period 5 (last 29 days): X-component of current (cm/s) vs. sea level (m) at SNLT (3 hr low-passed data).

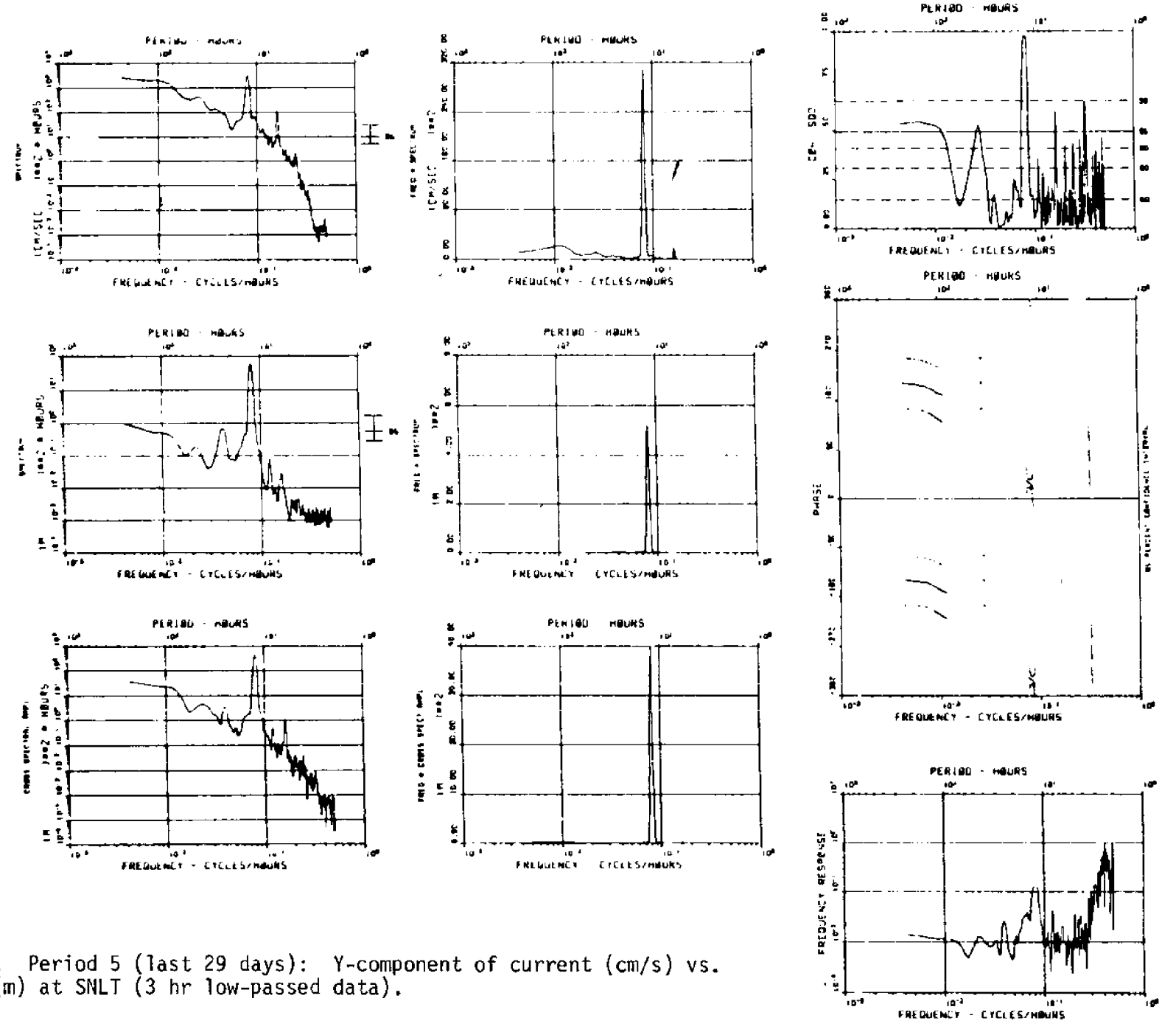

Figure 37h. Period 5 (last 29 days): Y-component of current (cm/s) vs. sea level (m) at SNLT (3 hr low-passed data).

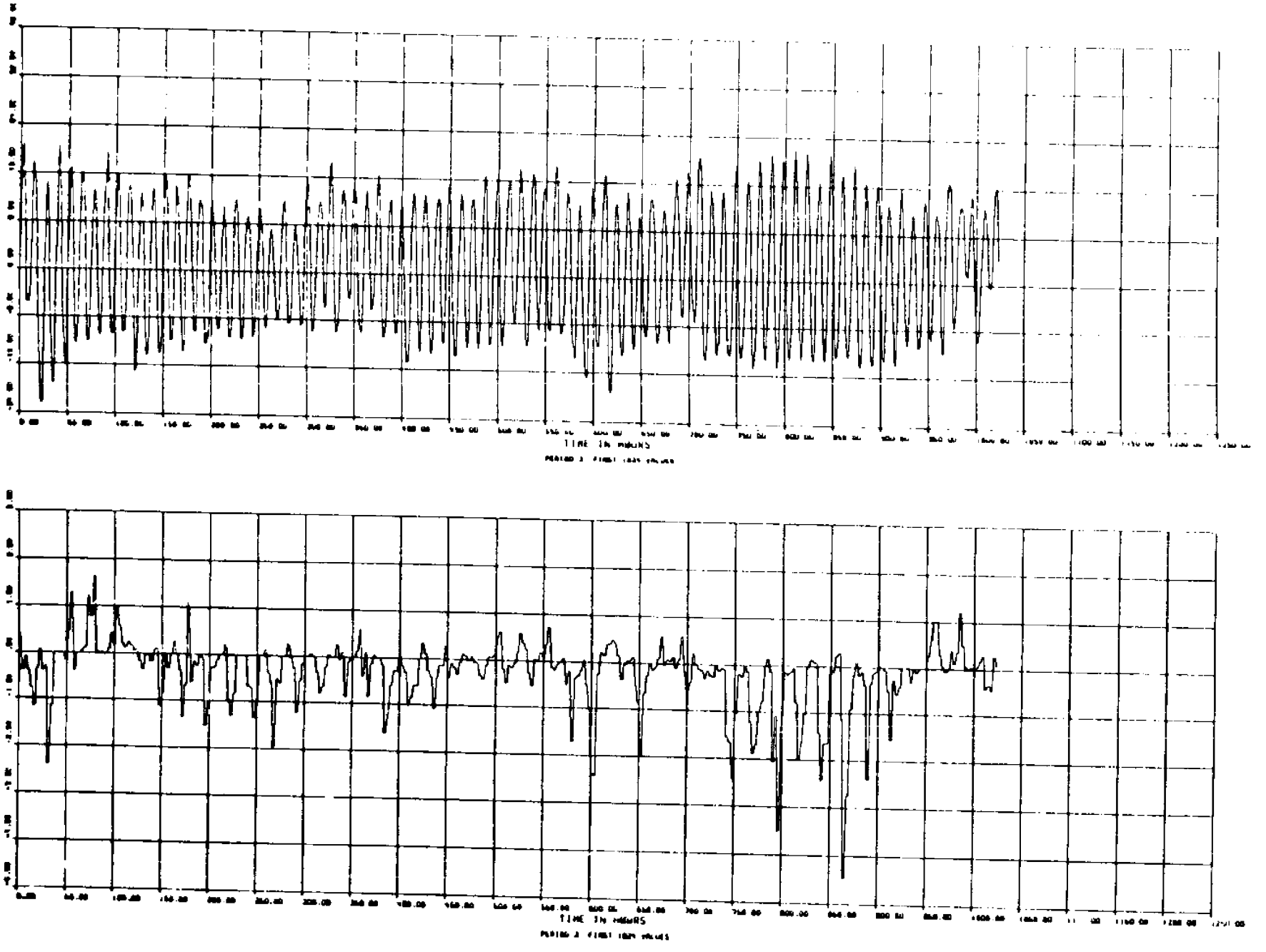

Figure 38. Period 3: North component of current (cm/s) vs. alongshore wind stress (dyne/cm^2) at SNLT. Alongshore wind directed 33 deg. east of north (3 hr low-passed data).

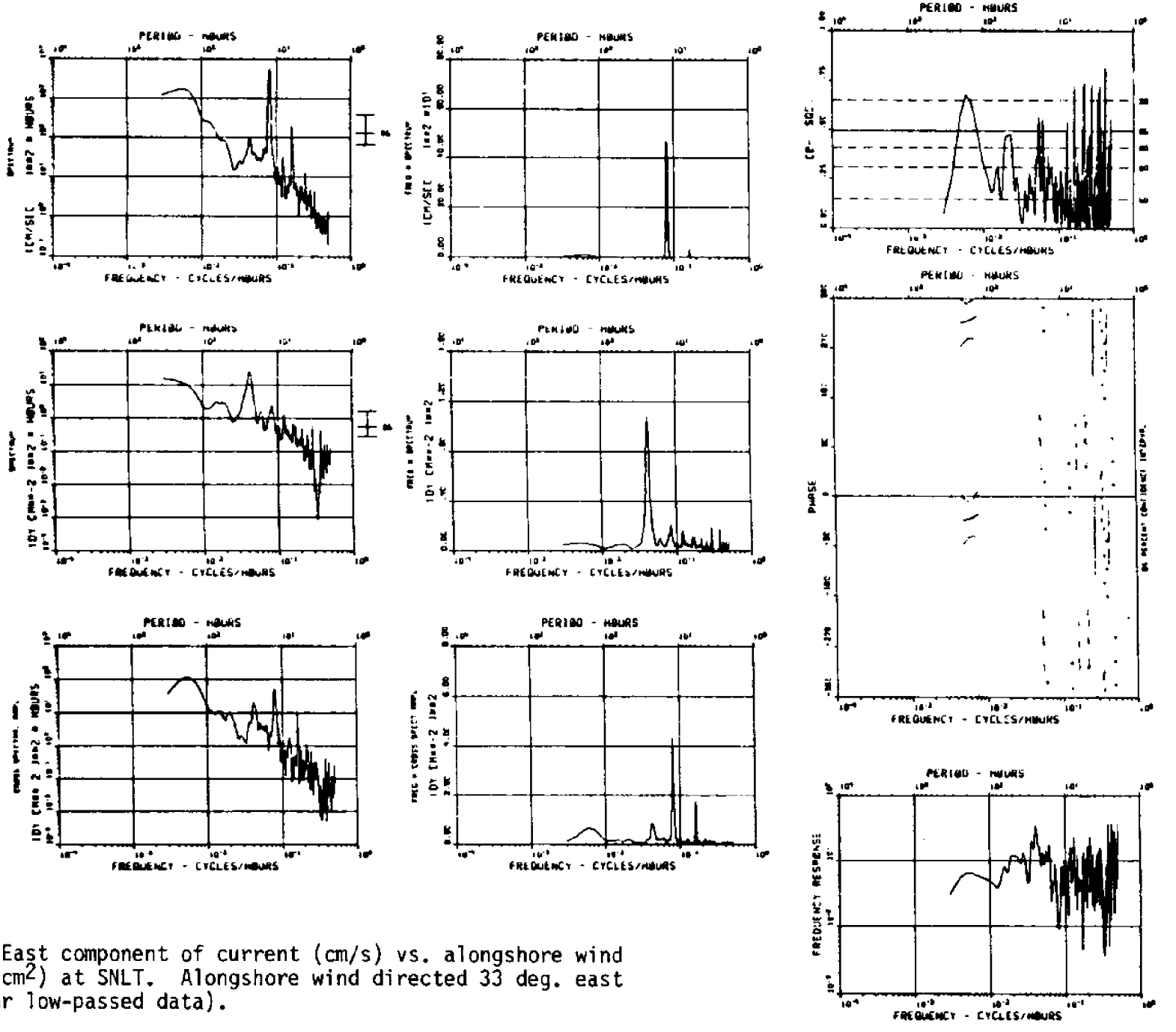

Figure 39a. East component of current (cm/s) vs. alongshore wind stress (dyne/cm^2) at SNLT. Alongshore wind directed 33 deg. east of north (3 hr low-passed data).

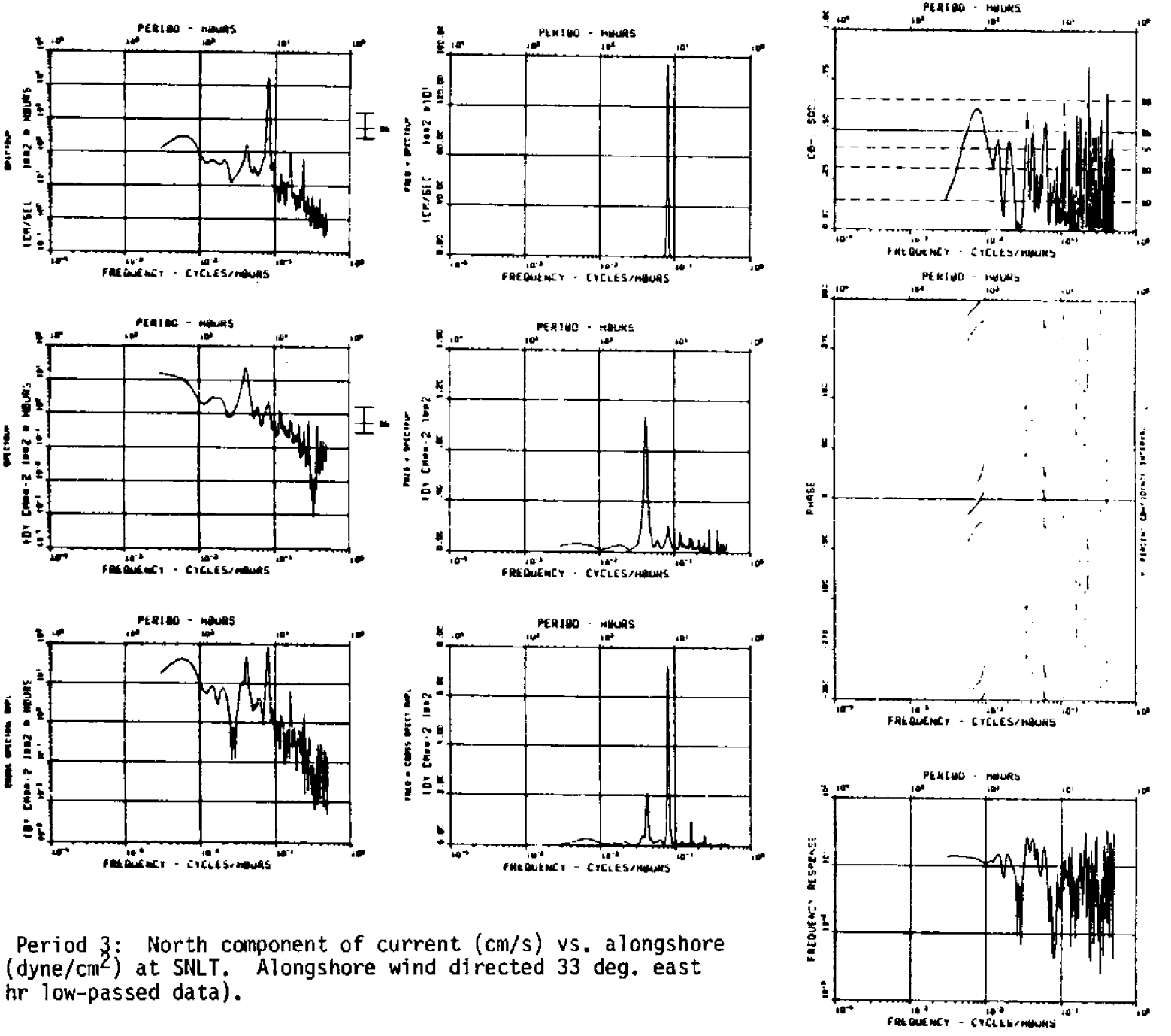

Figure 39b. Period 3: North component of current (cm/s) vs. alongshore wind stress (dyne/cm^2) at SNLT. Alongshore wind directed 33 deg. east of north (3 hr low-passed data).

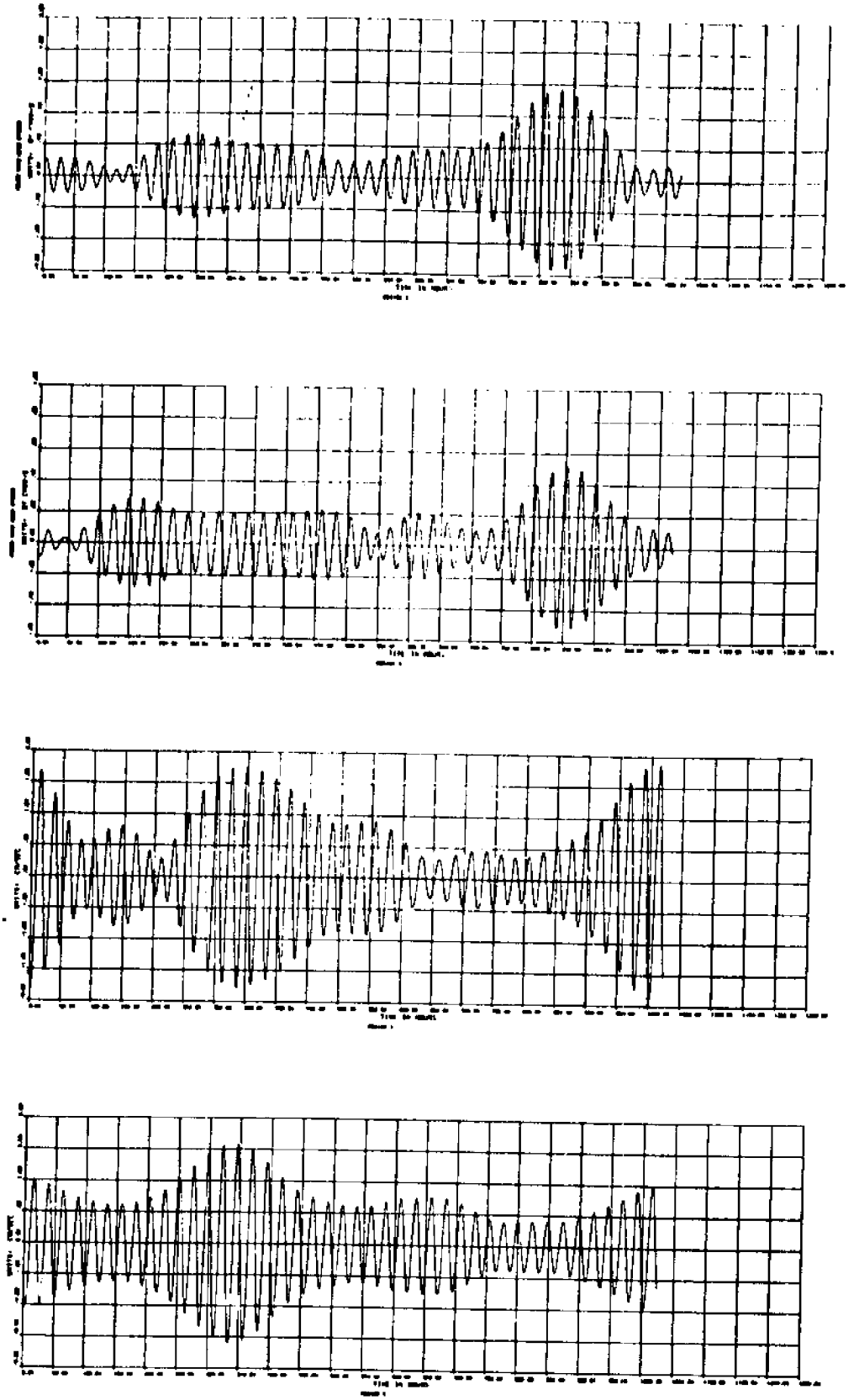

Figure 40. Time series of wind stress and current at SNLT during Period 3, band-passed with a filter centered about 24 hr to define daily events. Fortnightly (14-day) tidal cycle is seen in series. From top to bottom, time series are wind stress major axis, wind stress minor axis, east current, and north current.

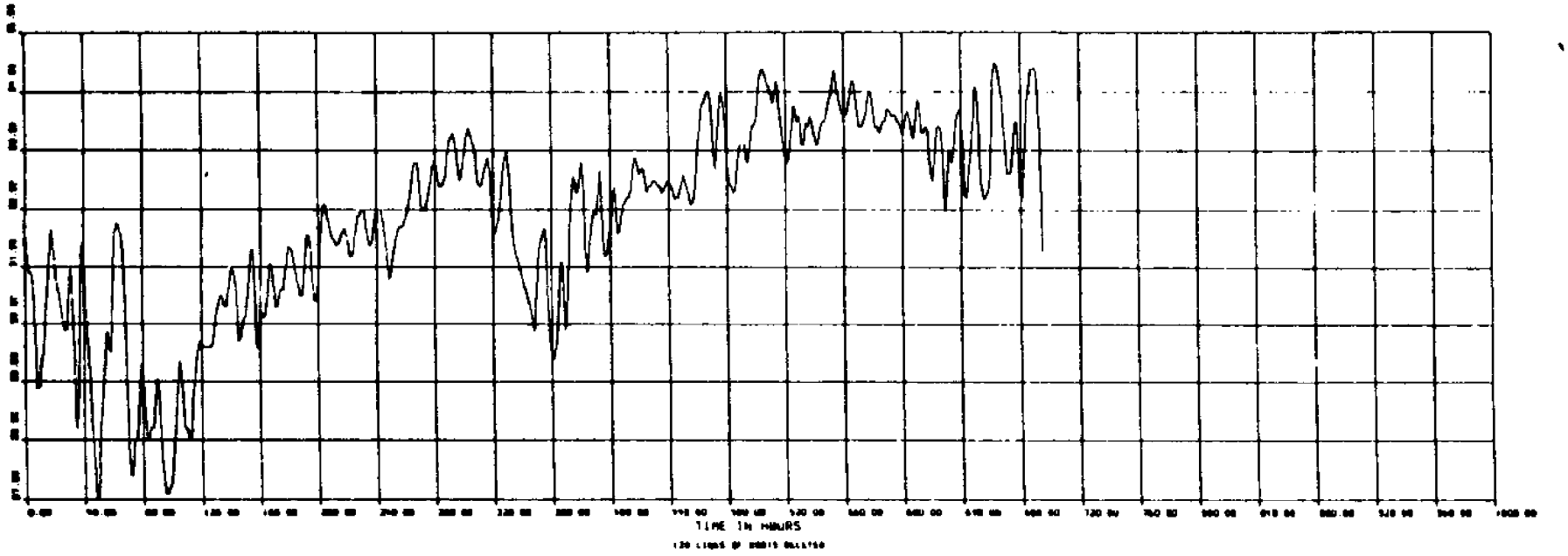

Figure 41a. Period 4: Salinity at level 3 (ppt.) at SNLT.(3 hr low-passed data).

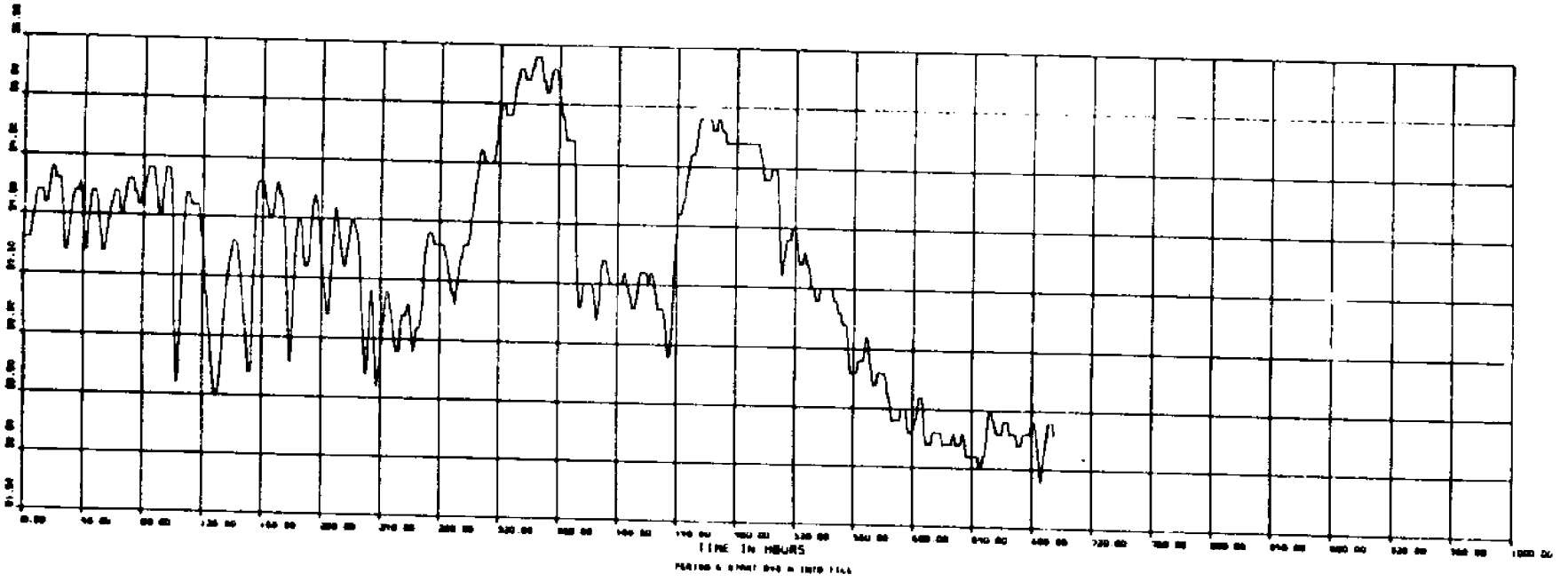

Figure 41b. Period 5: Salinity at level 3 (ppt.) at SNLT (3 hr low-passed data).

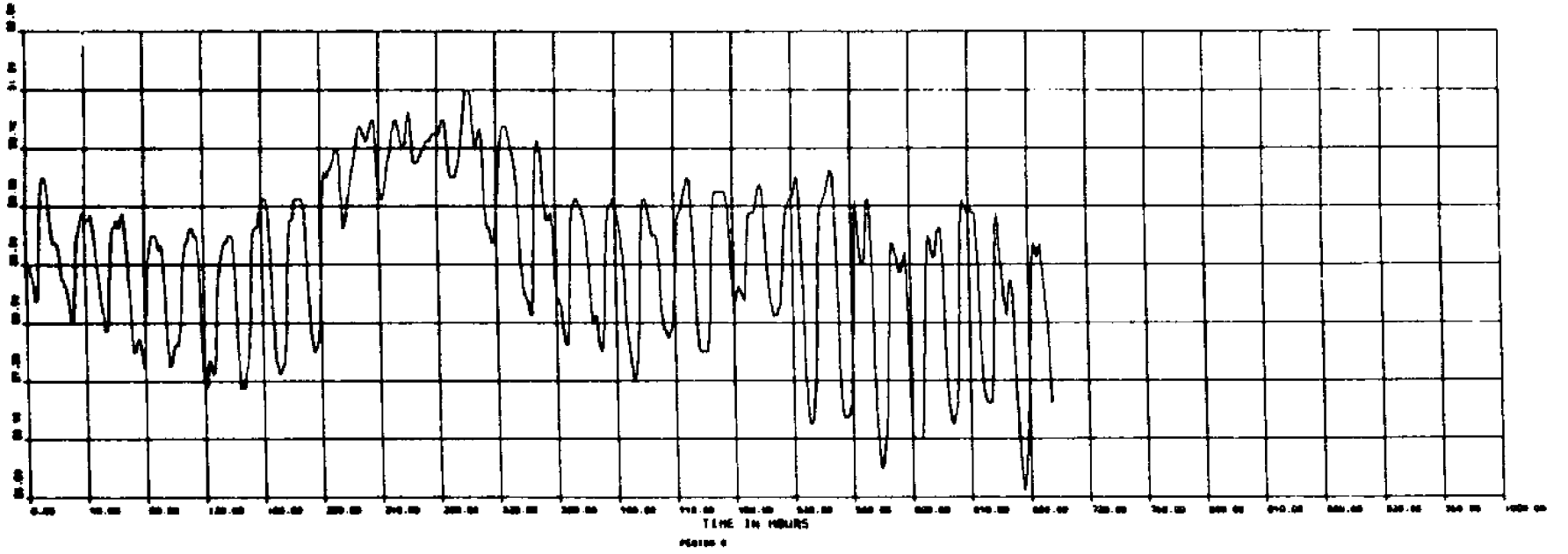

Figure 41c. Period 6: Salinity at level 3 (ppt.) at SNLT (3 hr low-passed data).

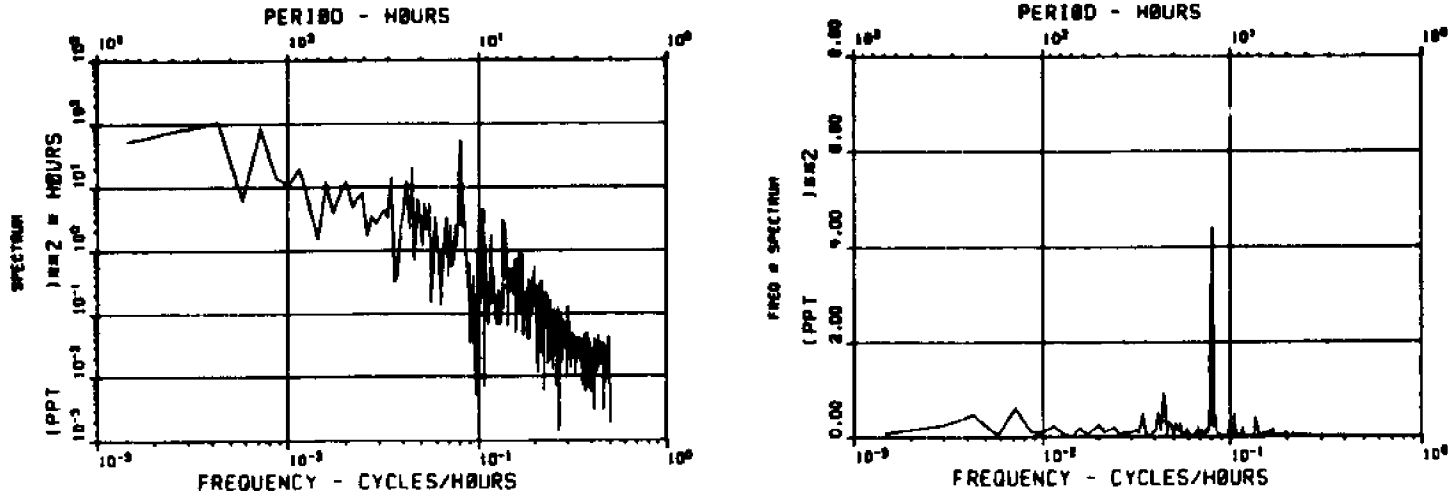

Figure 42a. Period 4: Salinity spectra (3 hr low-passed data).

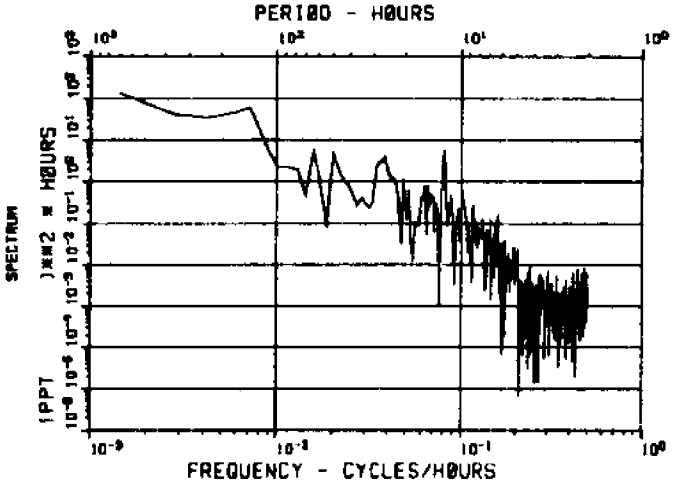

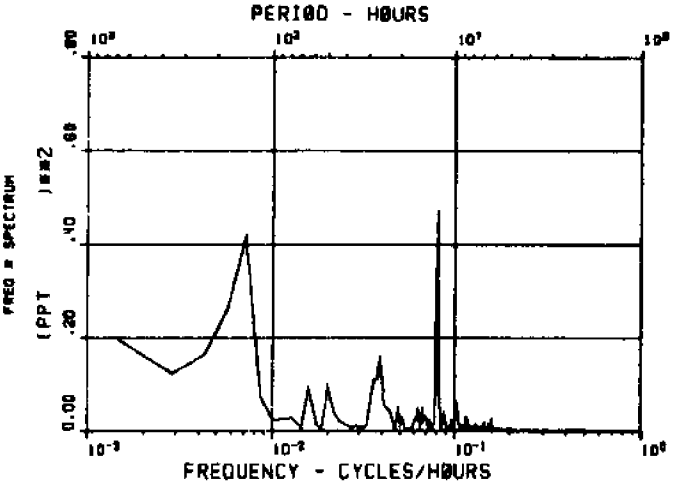

Figure 42b. Period 5: Salinity spectra. Unfiltered data.

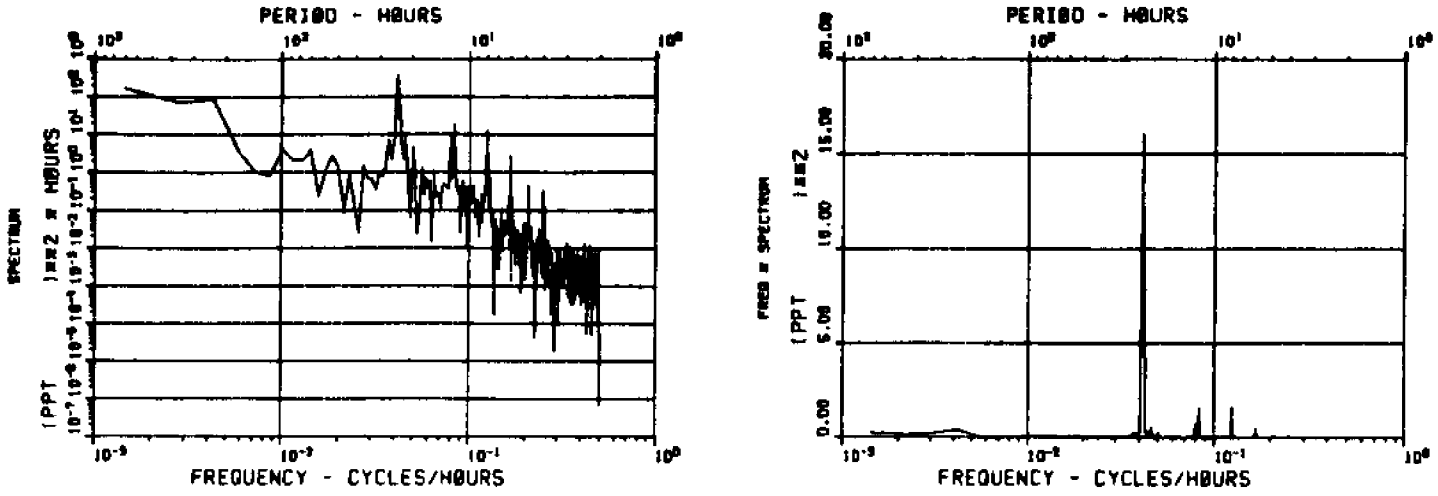

Figure 42c. Period 6: Salinity spectra (3 hr low-passed data).

APPENDIX

Plots of Weekly Data Summaries of SNLT Data Collected During 1984

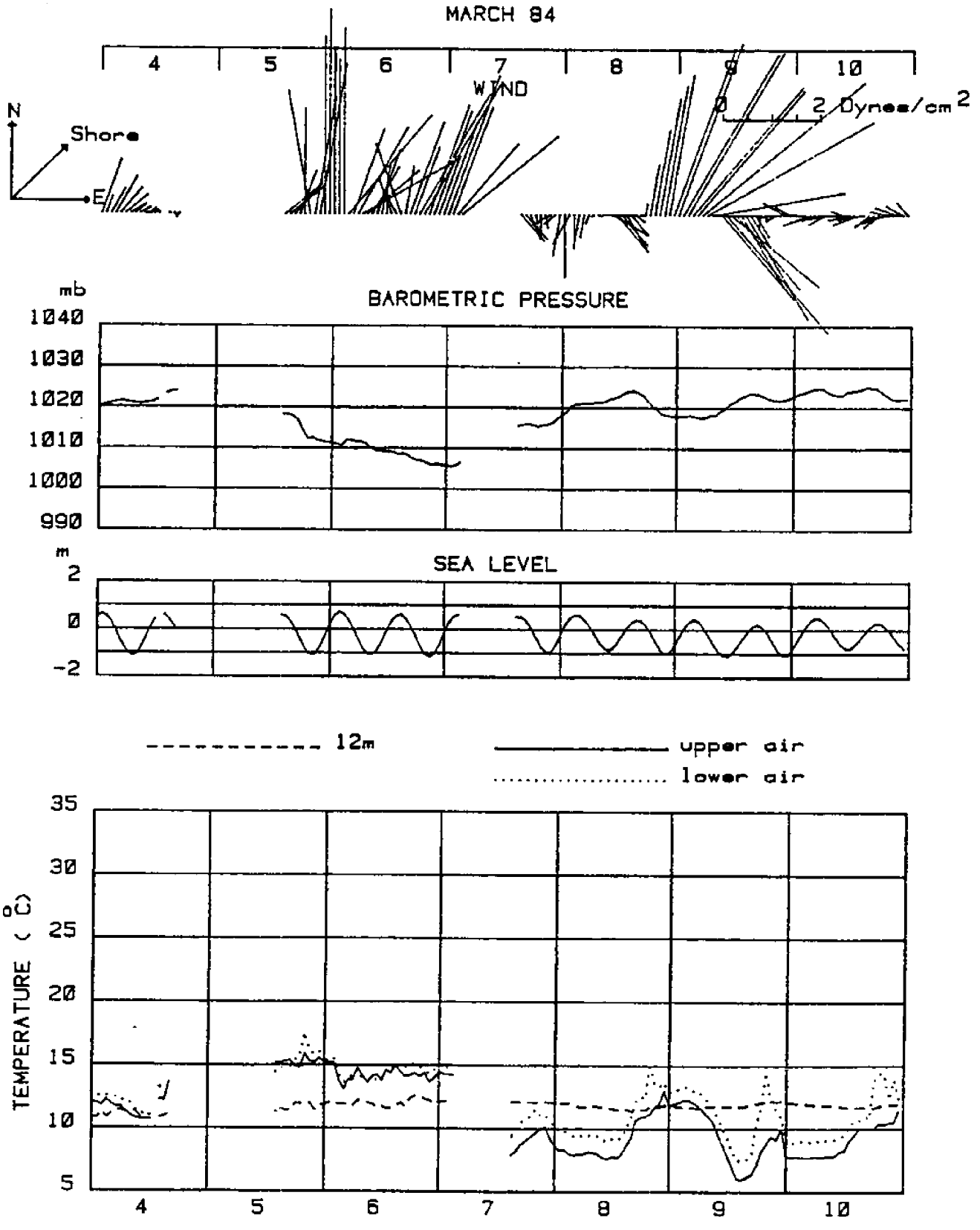
MARCH 84
4
5
6
7
8
9
10
WIND
N
Shore
E
0
2 Dynes/cm 2
mb
BAROMETRIC PRESSURE
1040
1030
1020
1010
1000
990
m
SEA LEVEL
2
0
-2
12m
upper air
lower air
TEMPERATURE (°C)
35
30
25
20
15
10
5
4
5
6
7
8
9
10

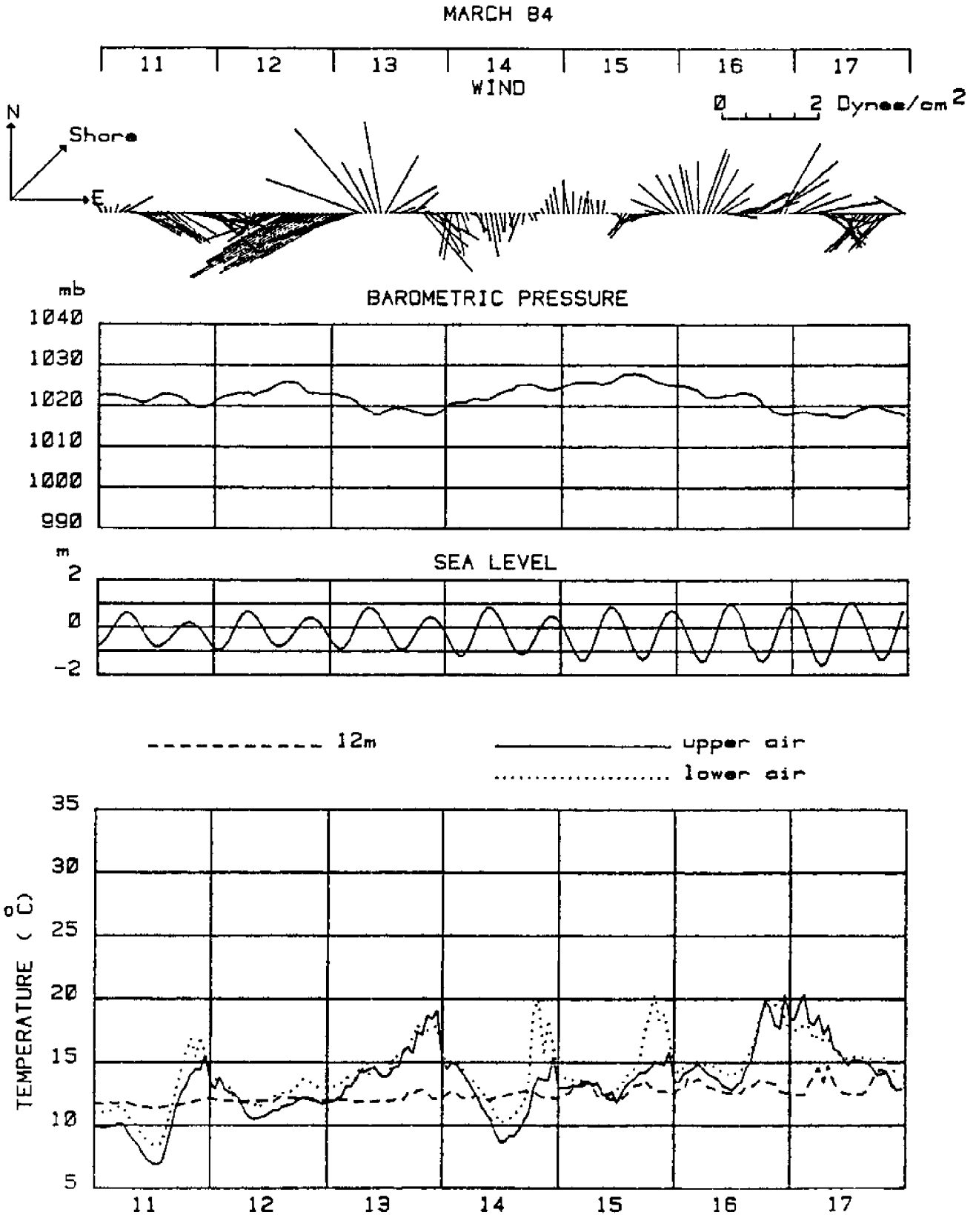
MARCH 84
11
12
13
14
15
16
17
WIND
0 2 Dynes/cm 2
N
Shore
E
mb
BAROMETRIC PRESSURE
1040
1030
1020
1010
1000
990
m
SEA LEVEL
2
0
-2
12m
upper air
lower air
TEMPERATURE (°C)
35
30
25
20
15
10
5
11
12
13
14
15
16
17

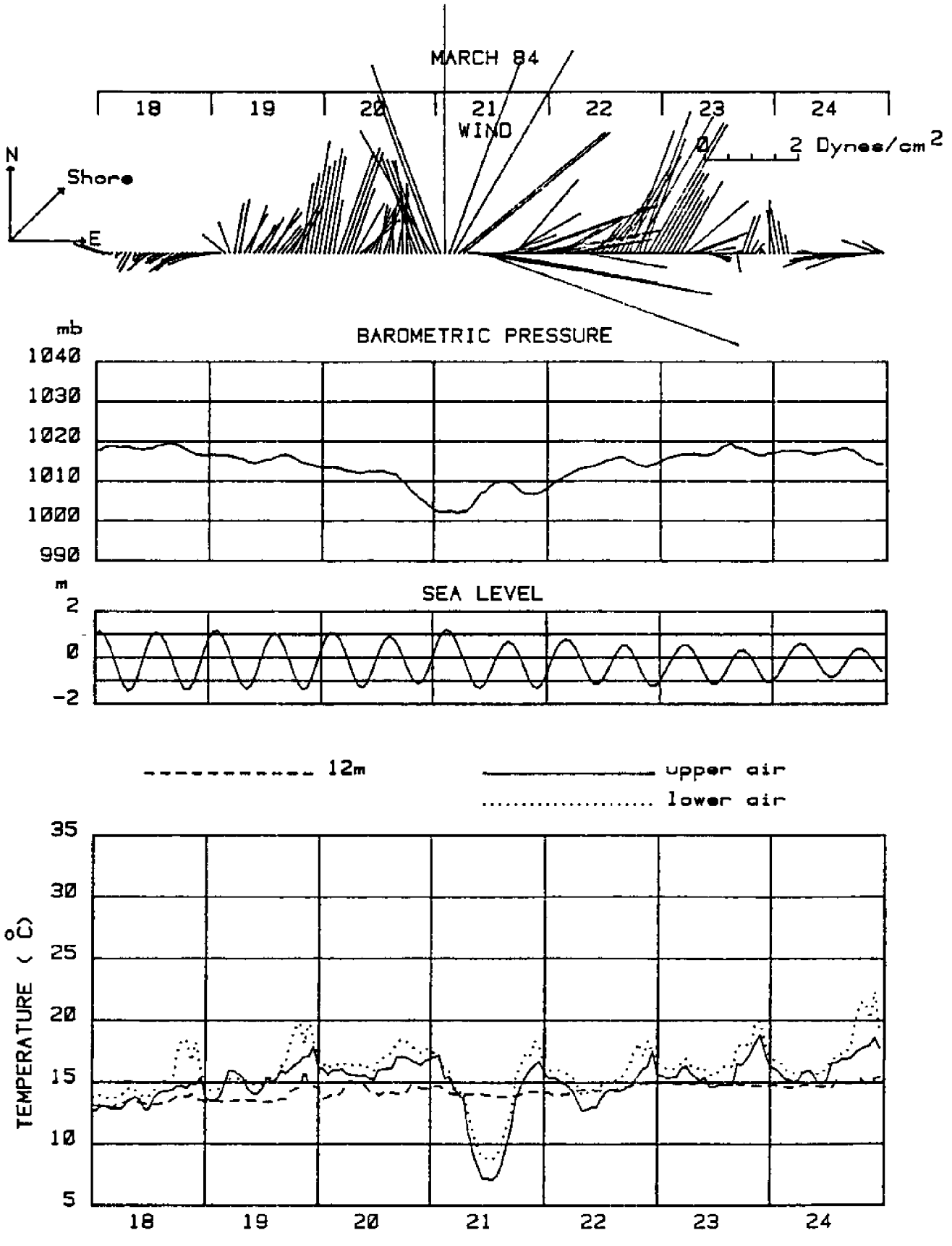
MARCH 84
18
19
20
21
22
23
24
WIND
2 Dynes/cm 2
N
Shore
E
mb
BAROMETRIC PRESSURE
1040
1030
1020
1010
1000
990
m
SEA LEVEL
2
0
-2
12m
upper air
lower air
TEMPERATURE (°C)
35
30
25
20
15
10
5
18
19
20
21
22
23
24

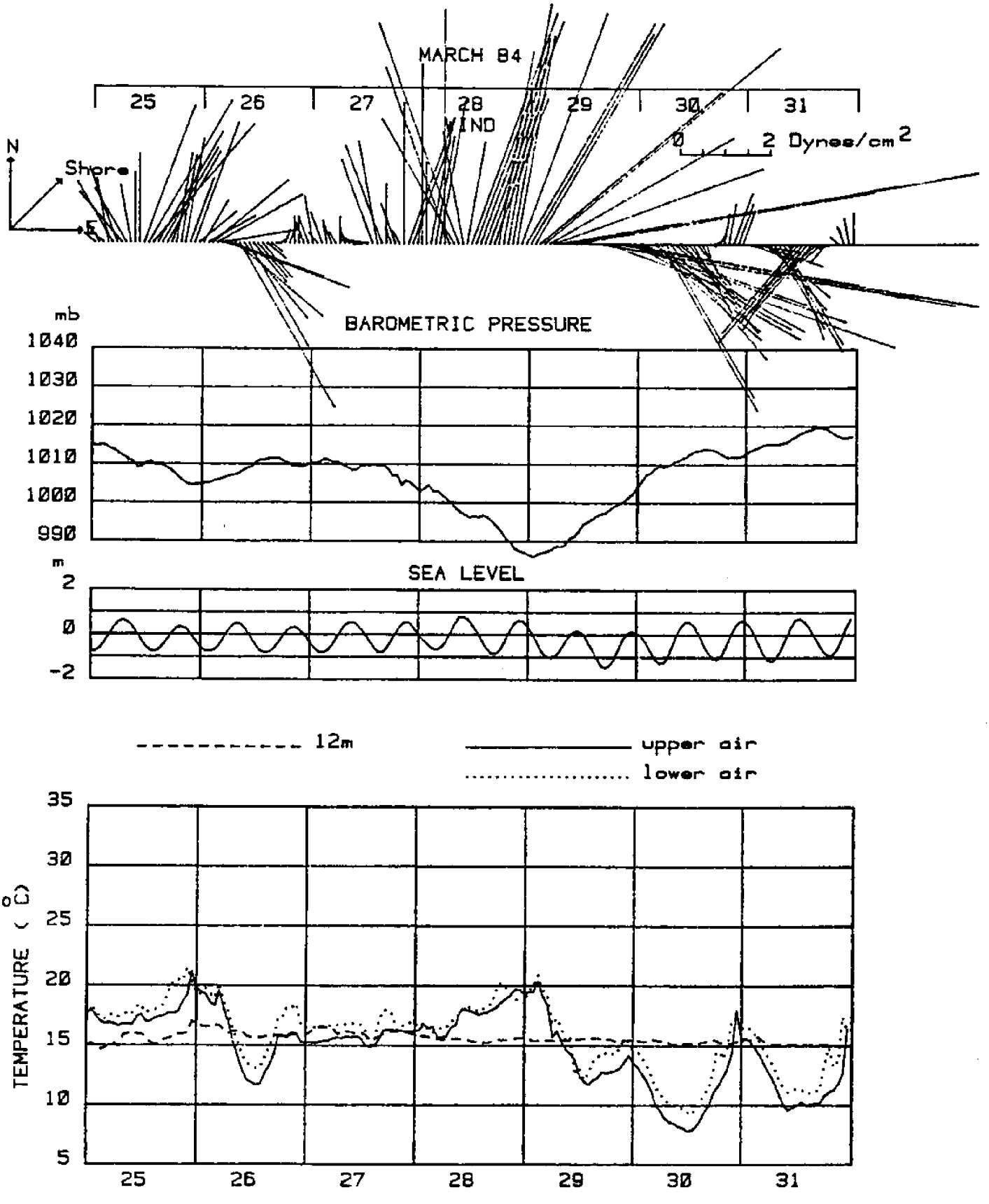
MARCH 84
25
26
27
28
29
30
31
WIND
0
2 Dynes/cm 2
N
Shore
BAROMETRIC PRESSURE
mb
1040
1030
1020
1010
1000
990
SEA LEVEL
m
2
0
-2
12m
upper air
lower air
TEMPERATURE (°C)
35
30
25
20
15
10
5
25
26
27
28
29
30
31

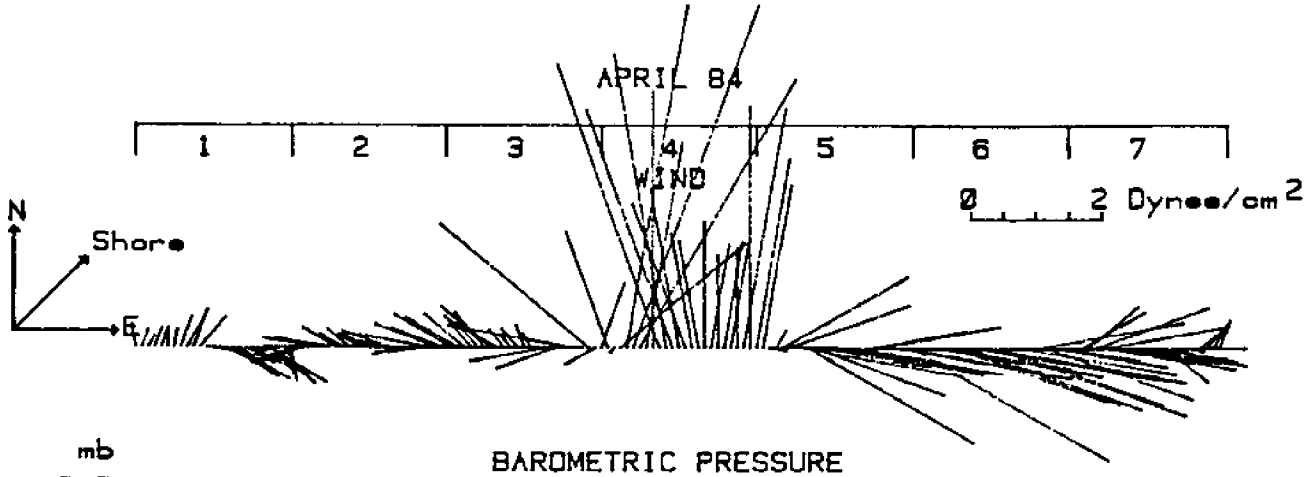
APRIL 84
1
2
3
4
5
6
7
WIND
0 2 Dynes/cm 2
N
Shore
E

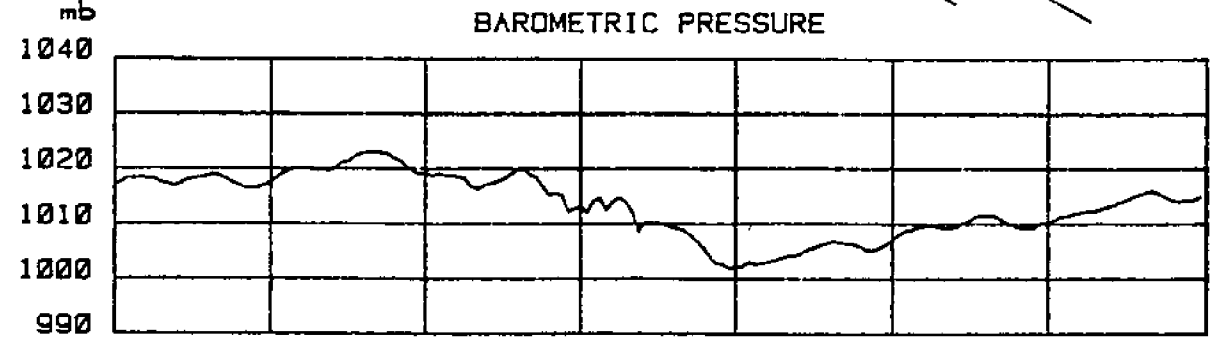
mb
BAROMETRIC PRESSURE
1040
1030
1020
1010
1000
990

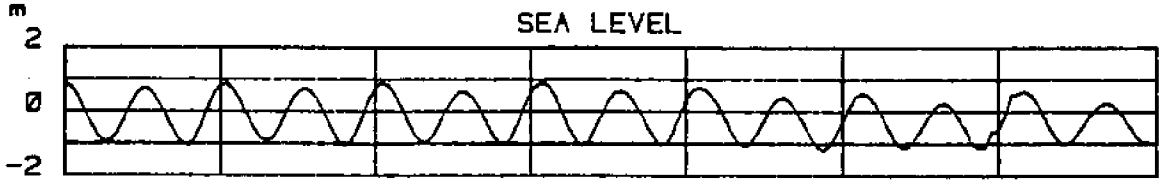
m
SEA LEVEL
2
0
-2

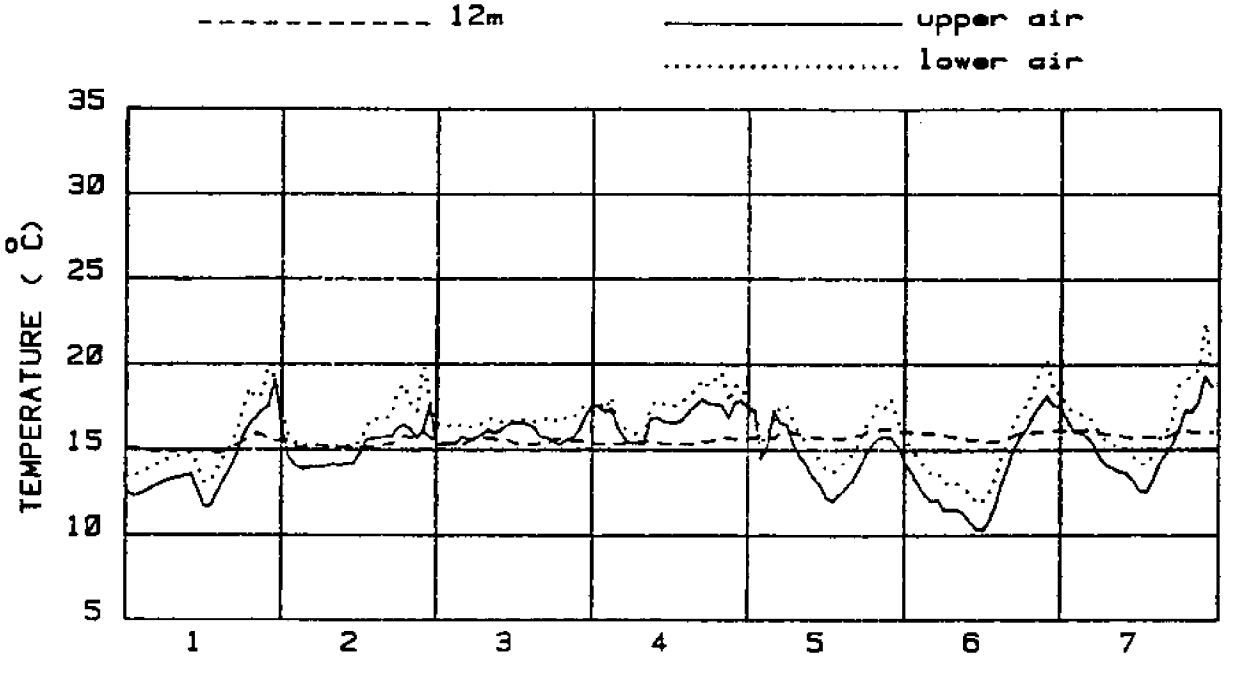
12m
upper air
lower air
TEMPERATURE (°C)
35
30
25
20
15
10
5
1
2
3
4
5
6
7

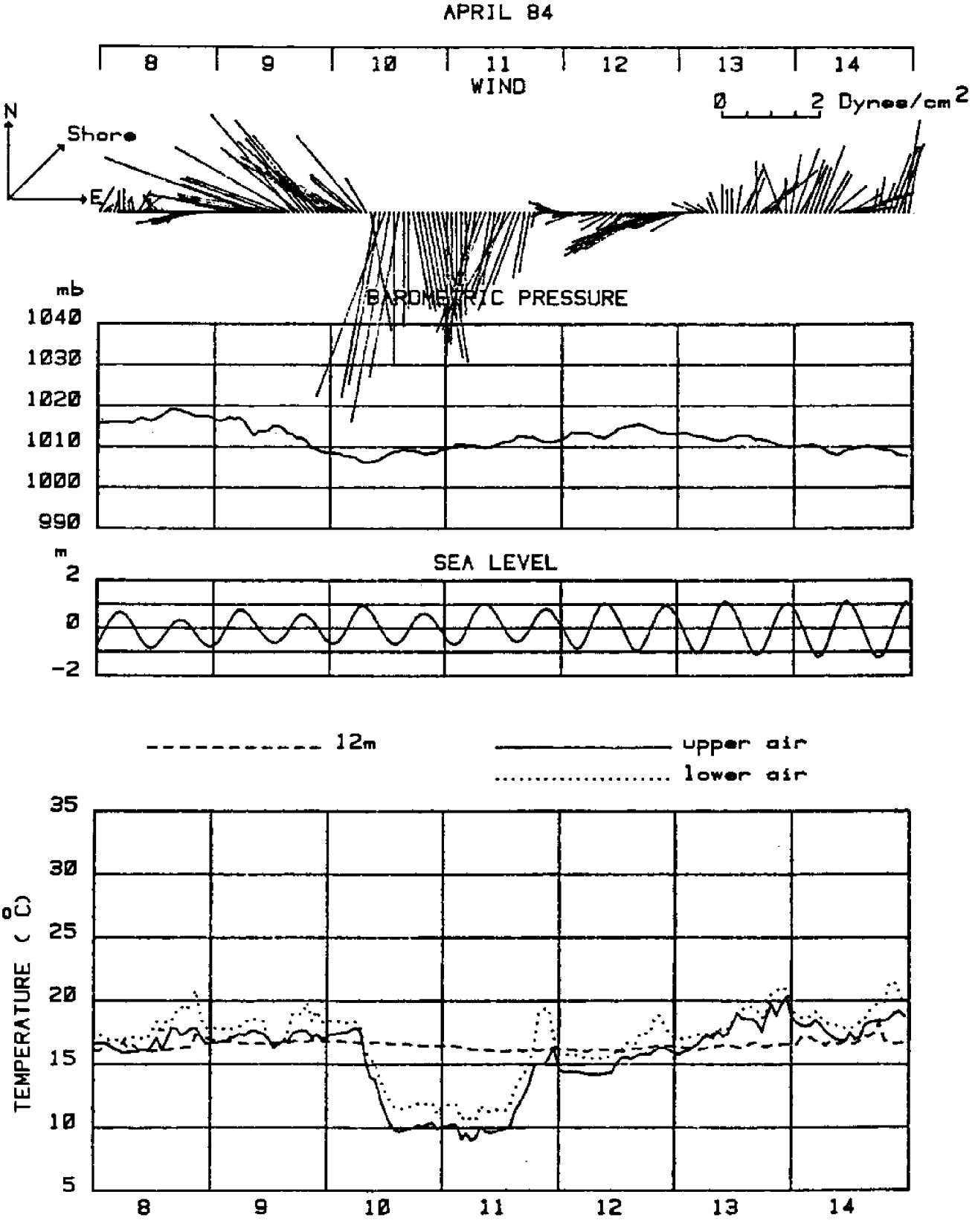
APRIL 84
8
9
10
11
12
13
14
WIND
0 2 Dynes/cm 2
N
Shore
E
mb
BAROMETRIC PRESSURE
1040
1030
1020
1010
1000
990
m
SEA LEVEL
2
0
-2
12m
upper air
lower air
TEMPERATURE (°C)
35
30
25
20
15
10
5
8
9
10
11
12
13
14

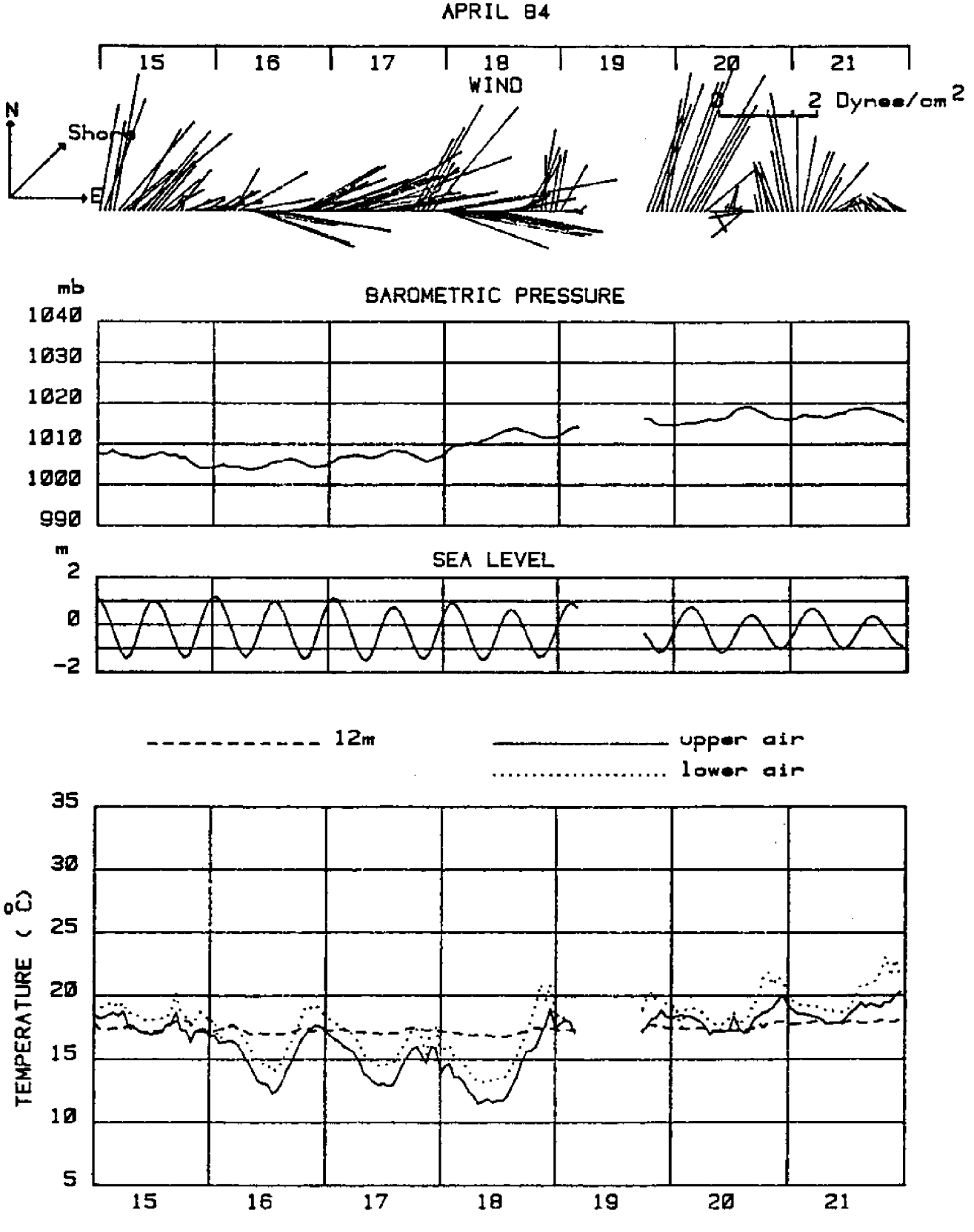
APRIL 84
15
16
17
18
19
20
21
WIND
N
E
Sho
2 Dynes/cm 2
mb
BAROMETRIC PRESSURE
1040
1030
1020
1010
1000
990
m
SEA LEVEL
2
0
-2
12m
upper air
lower air
TEMPERATURE (°C)
35
30
25
20
15
10
5
15
16
17
18
19
20
21

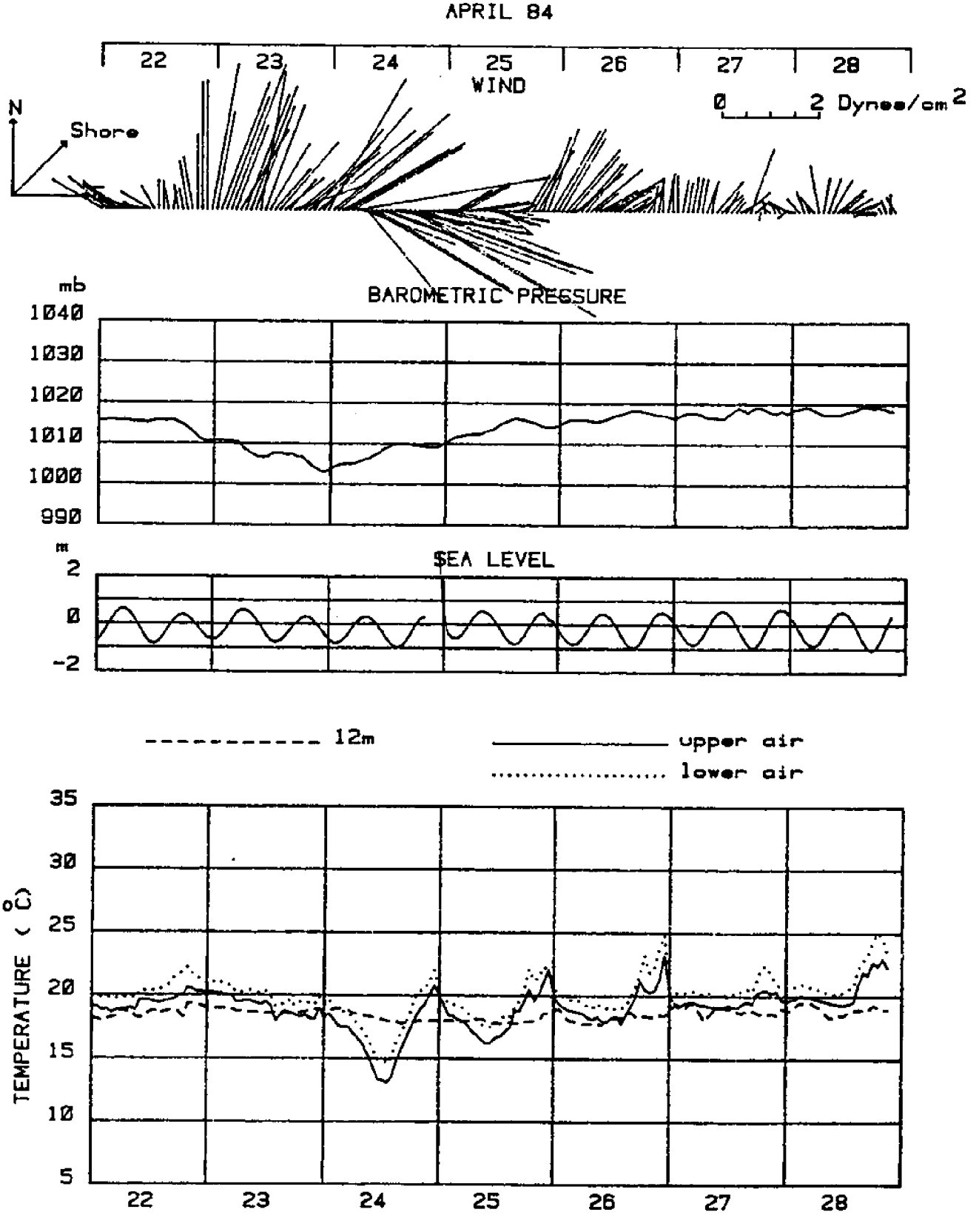
APRIL 84
22
23
24
25
26
27
28
WIND
0 2 Dynes/cm 2
N
Shore
mb
BAROMETRIC PRESSURE
1040
1030
1020
1010
1000
990
m
SEA LEVEL
2
0
-2
12m
upper air
lower air
TEMPERATURE (°C)
35
30
25
20
15
10
5
22
23
24
25
26
27
28

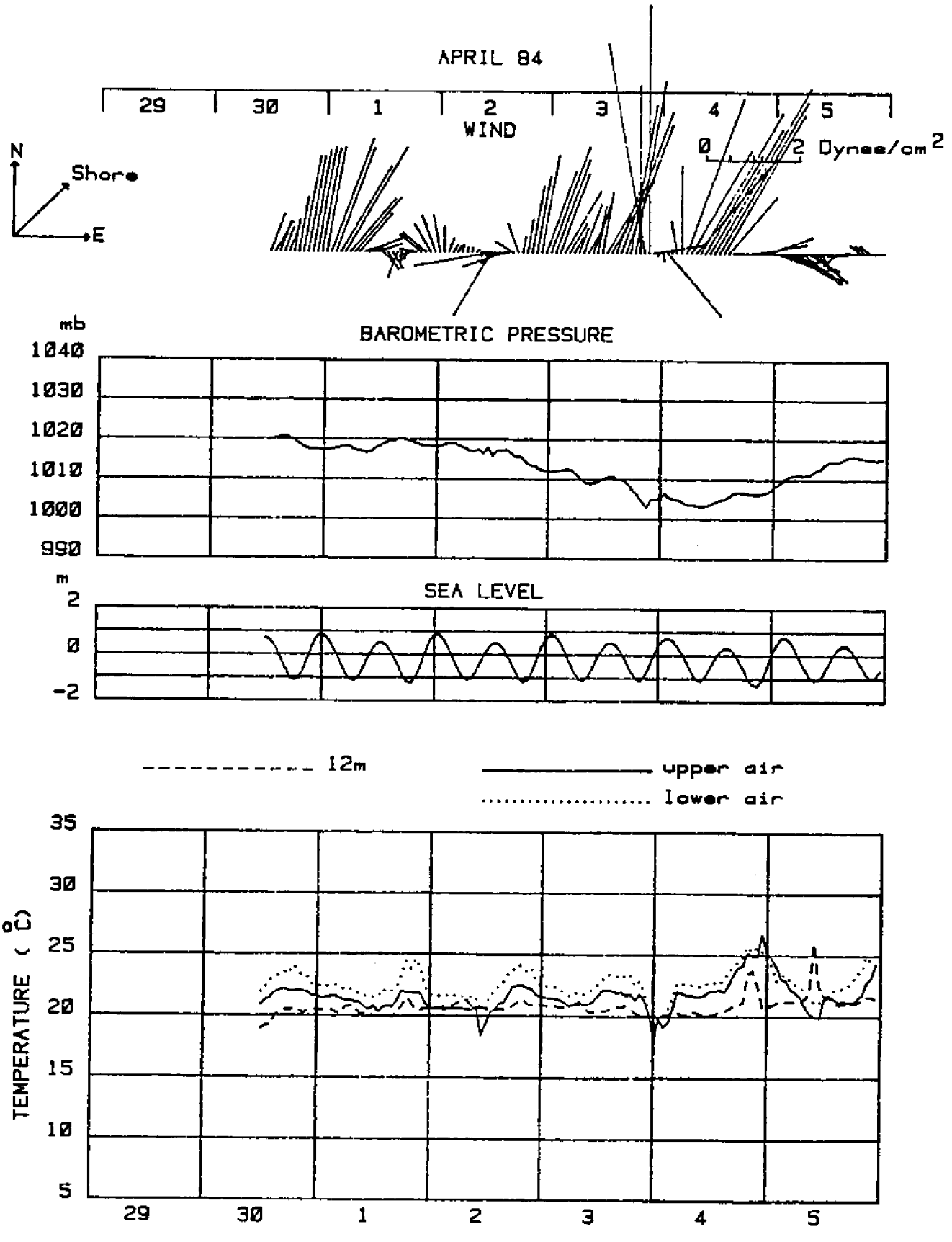
APRIL 84
29
30
1
2
3
4
5
WIND
0
2 Dynes/cm 2
N
Shore
E
mb
BAROMETRIC PRESSURE
1040
1030
1020
1010
1000
990
m
SEA LEVEL
2
0
-2
12m
upper air
lower air
TEMPERATURE (oC)
35
30
25
20
15
10
5
29
30
1
2
3
4
5

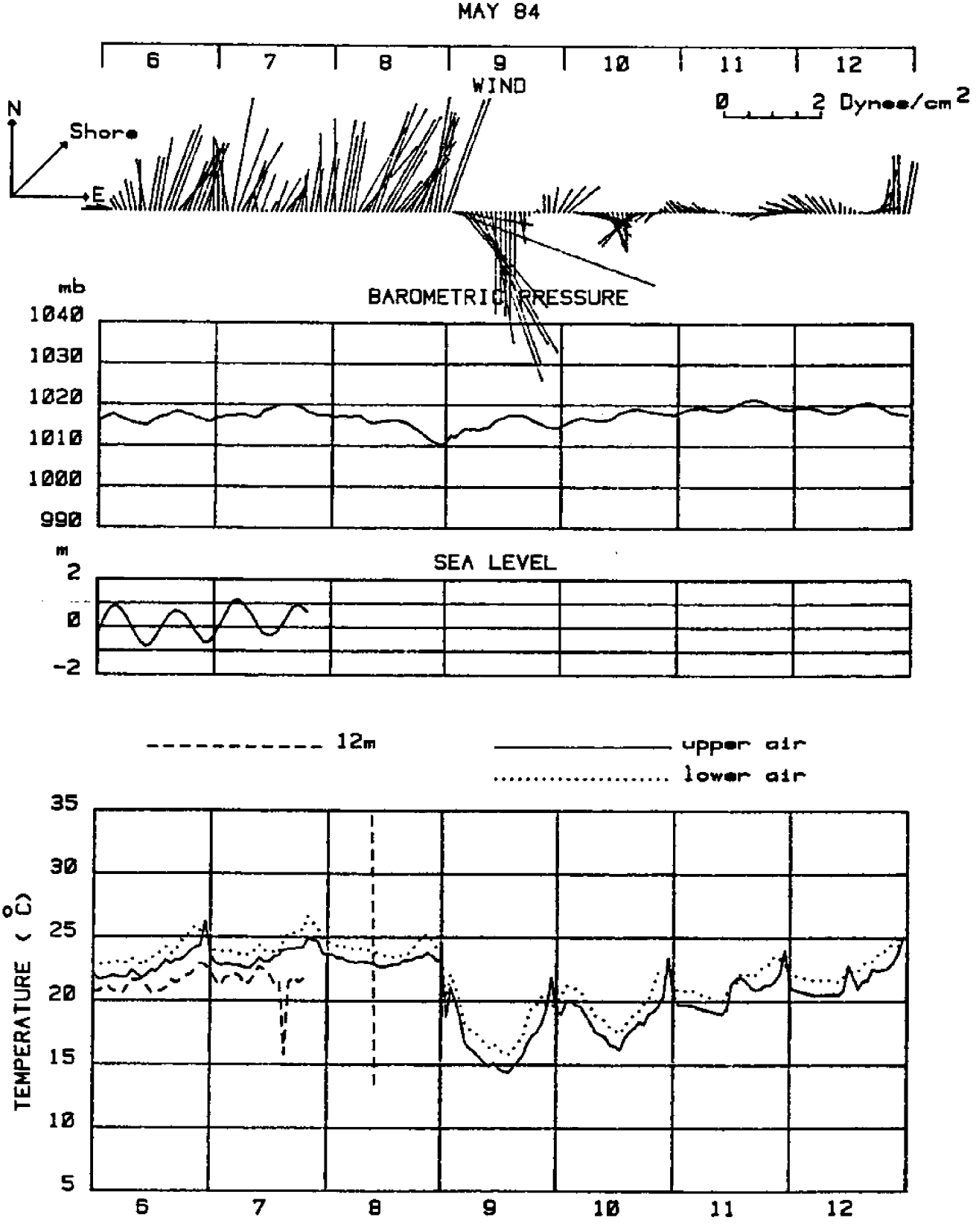
MAY 84
6
7
8
9
10
11
12
WIND
0 2 Dynes/cm 2
N
Shore
E
mb
BAROMETRIC PRESSURE
1040
1030
1020
1010
1000
990
m
SEA LEVEL
2
0
-2
12m
upper air
lower air
TEMPERATURE (°C)
35
30
25
20
15
10
5
6
7
8
9
10
11
12

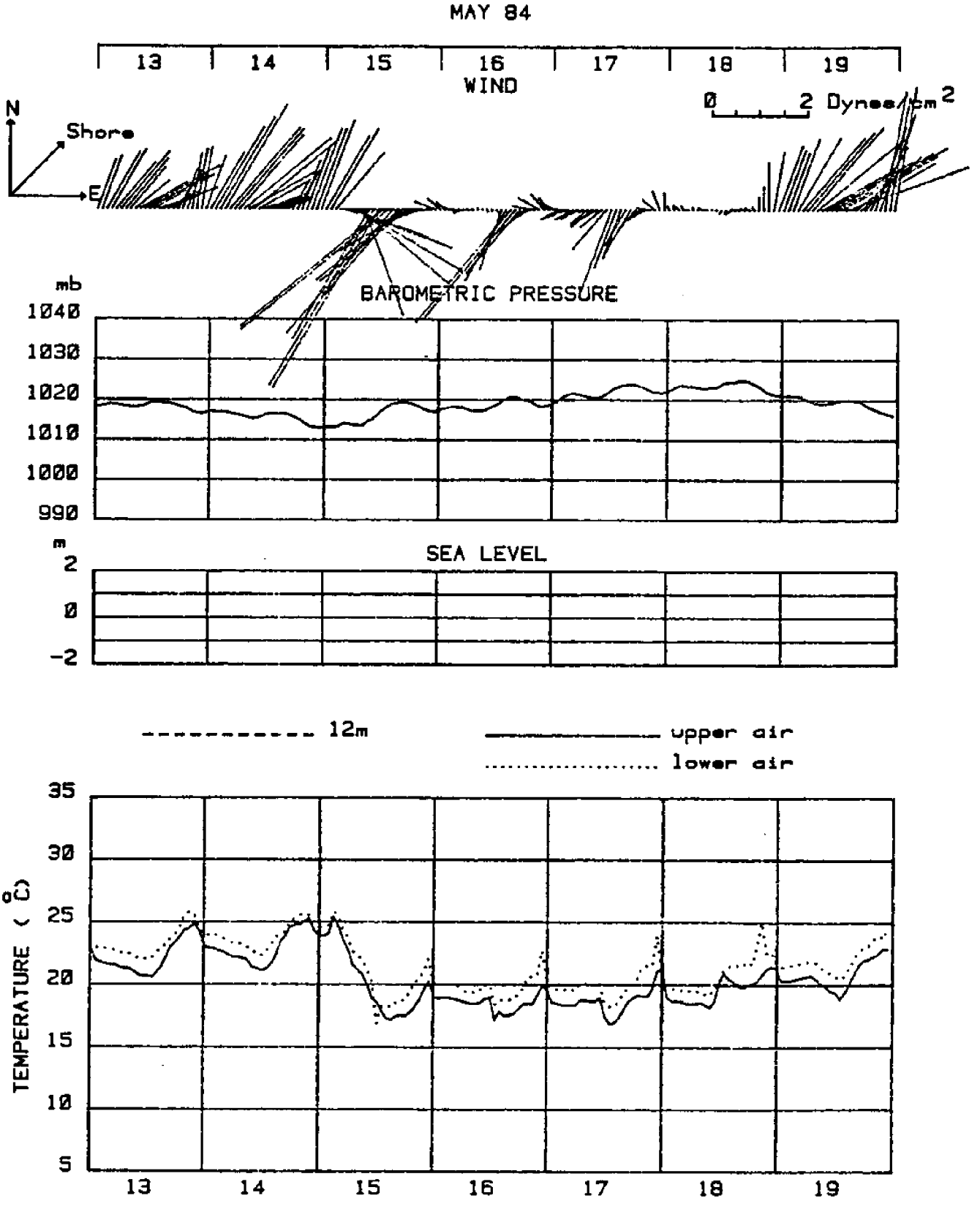
MAY 84
13
14
15
16
17
18
19
WIND
0
2 Dynes/cm 2
N
Shore
E
mb
BAROMETRIC PRESSURE
1040
1030
1020
1010
1000
990
m
SEA LEVEL
2
0
-2
12m
upper air
lower air
35
30
25
20
15
10
5
TEMPERATURE (°C)
13
14
15
16
17
18
19

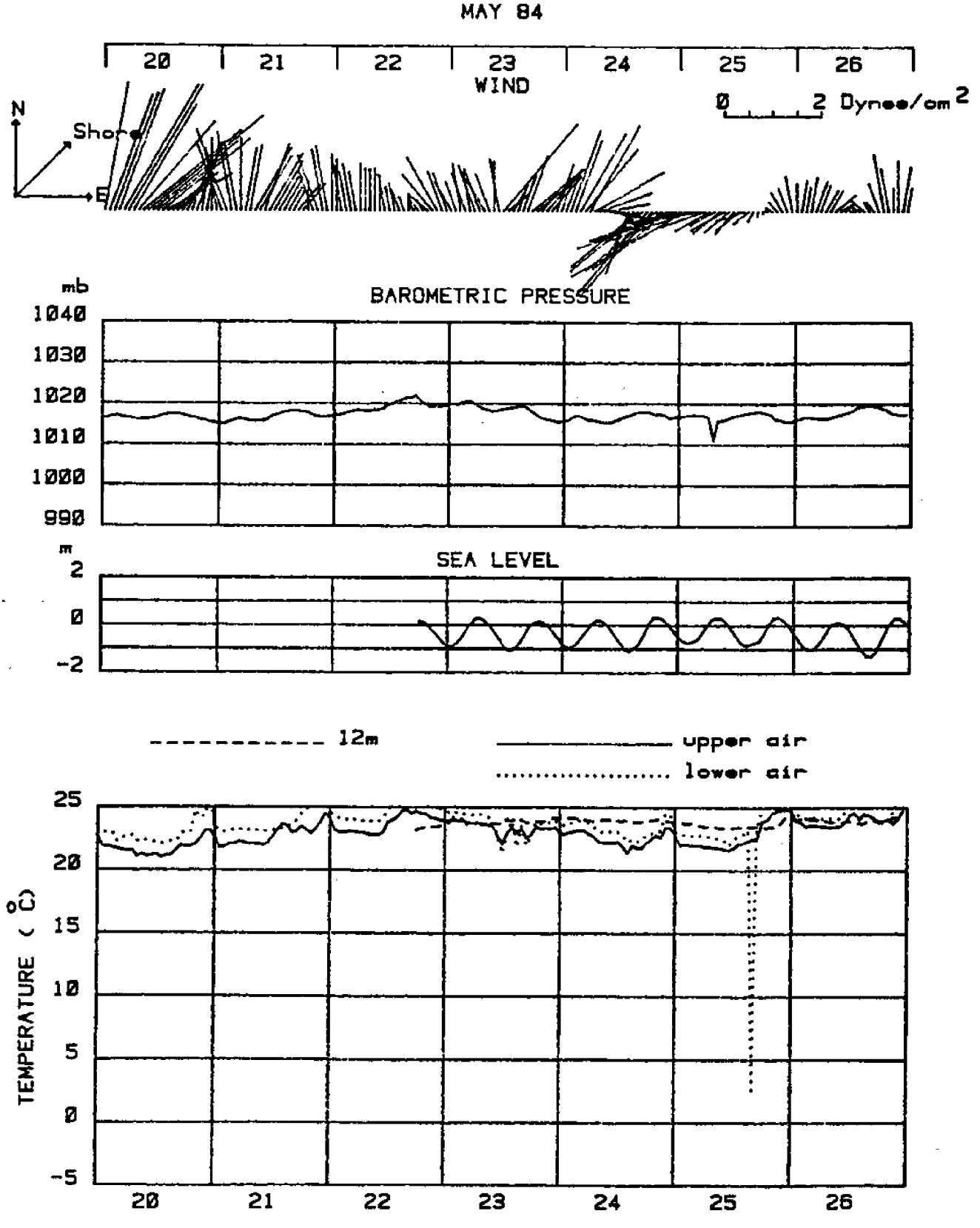
MAY 84
20
21
22
23
24
25
26
WIND
0 2 Dynes/cm 2
N
E
mb
BAROMETRIC PRESSURE
1040
1030
1020
1010
1000
990
m
SEA LEVEL
2
0
-2
12m
upper air
lower air
TEMPERATURE (°C)
25
20
15
10
5
0
-5
20
21
22
23
24
25
26

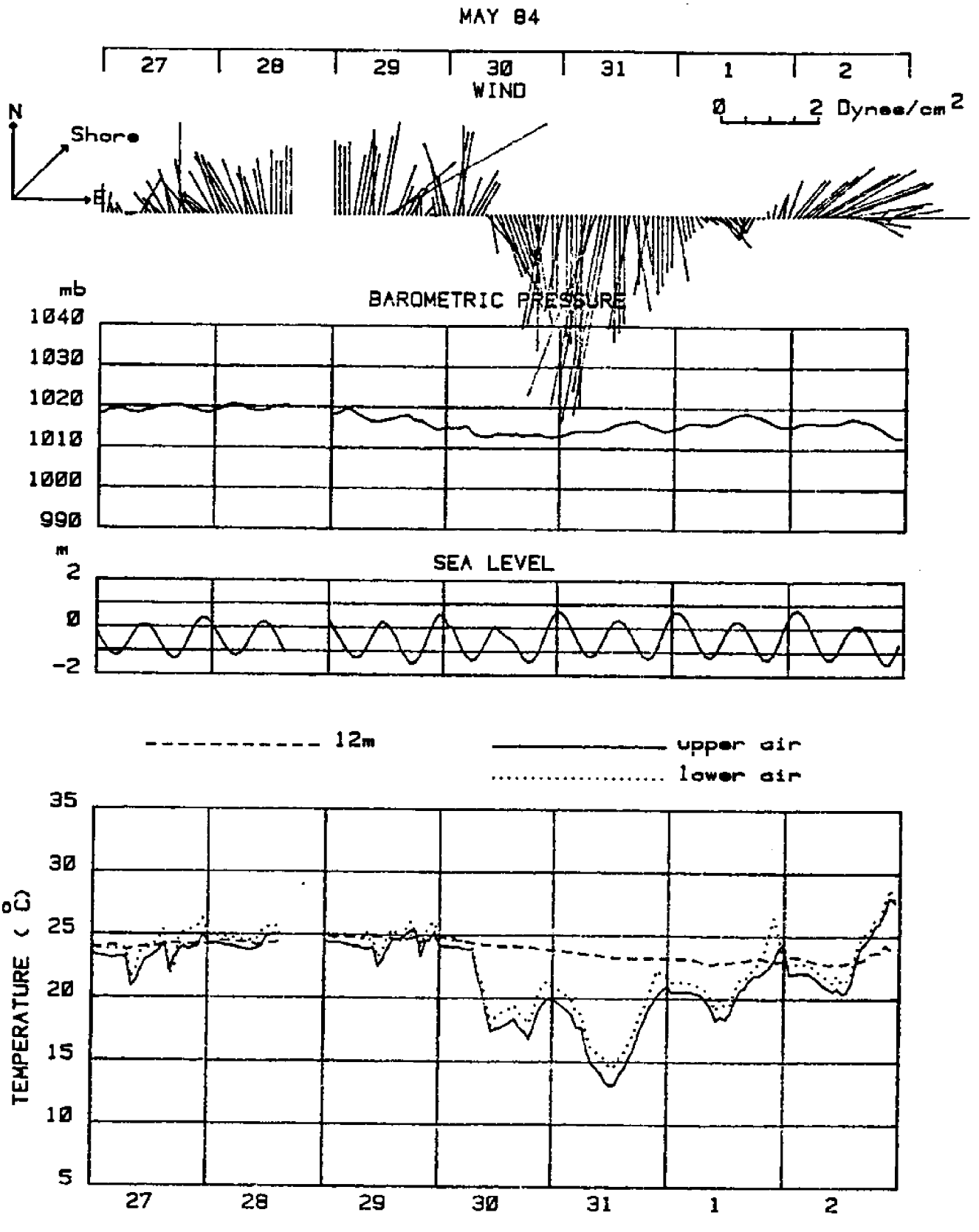
MAY 84
27
28
29
30
31
1
2
WIND
0 2 Dynes/cm 2
N
Shore
mb
BAROMETRIC PRESSURE
1040
1030
1020
1010
1000
990
m
SEA LEVEL
2
0
-2
12m
upper air
lower air
TEMPERATURE (°C)
35
30
25
20
15
10
5
27
28
29
30
31
1
2

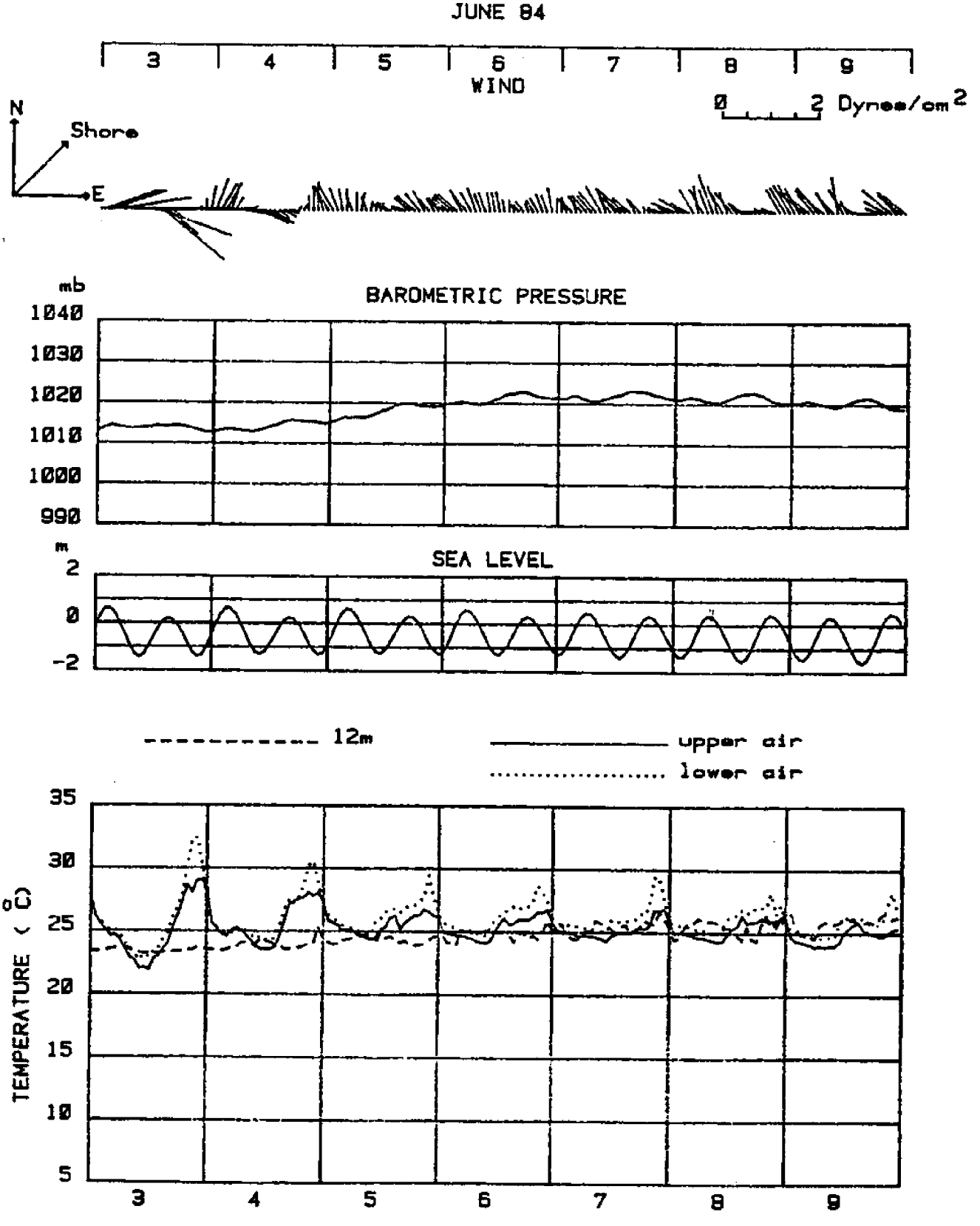
JUNE 84
3
4
5
6
7
8
9
WIND
0
2 Dynes/cm 2
N
Shore
E
mb
BAROMETRIC PRESSURE
1040
1030
1020
1010
1000
990
m
SEA LEVEL
2
0
-2
12m
upper air
lower air
TEMPERATURE (°C)
35
30
25
20
15
10
5
3
4
5
6
7
8
9

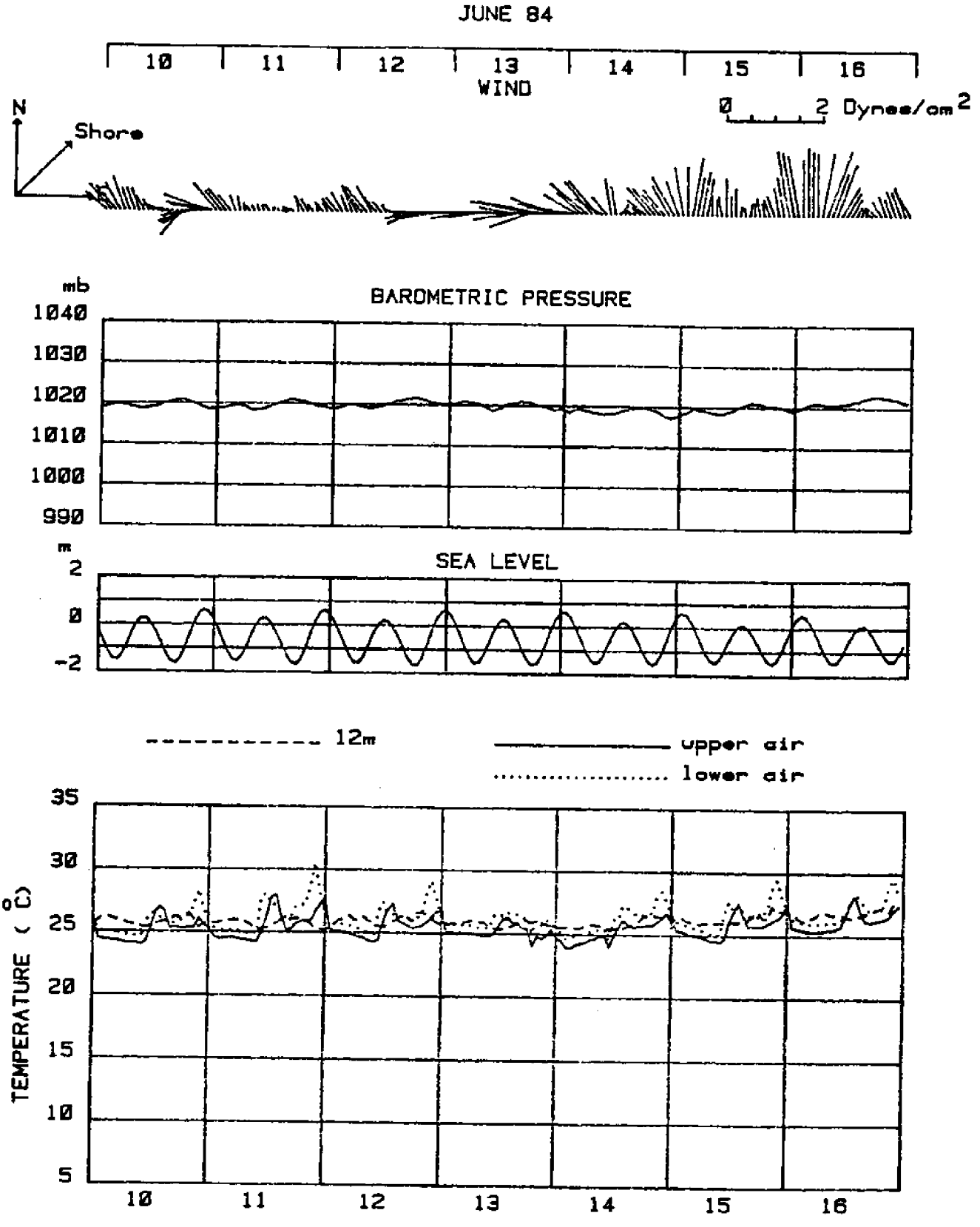
JUNE 84
10
11
12
13
14
15
16
WIND
N
Shore
0
2 Dynes/cm2
mb
BAROMETRIC PRESSURE
1040
1030
1020
1010
1000
990
m
SEA LEVEL
2
0
-2
12m
upper air
lower air
TEMPERATURE (°C)
35
30
25
20
15
10
5
10
11
12
13
14
15
16

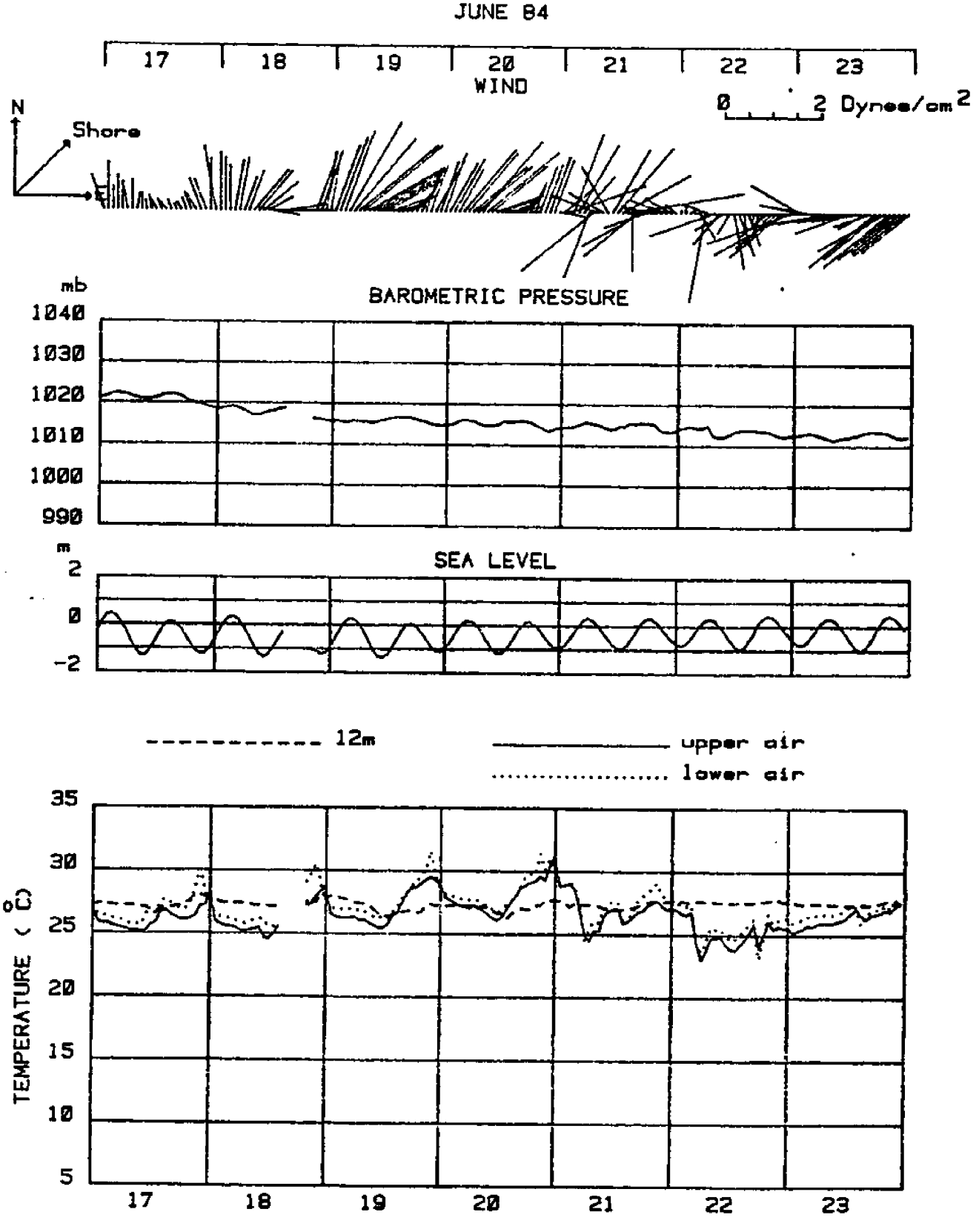
JUNE 84
17
18
19
20
21
22
23
WIND
0 2 Dynes/cm 2
N
Shore
mb
BAROMETRIC PRESSURE
1040
1030
1020
1010
1000
990
m
SEA LEVEL
2
0
-2
12m
upper air
lower air
TEMPERATURE (°C)
35
30
25
20
15
10
5
17
18
19
20
21
22
23

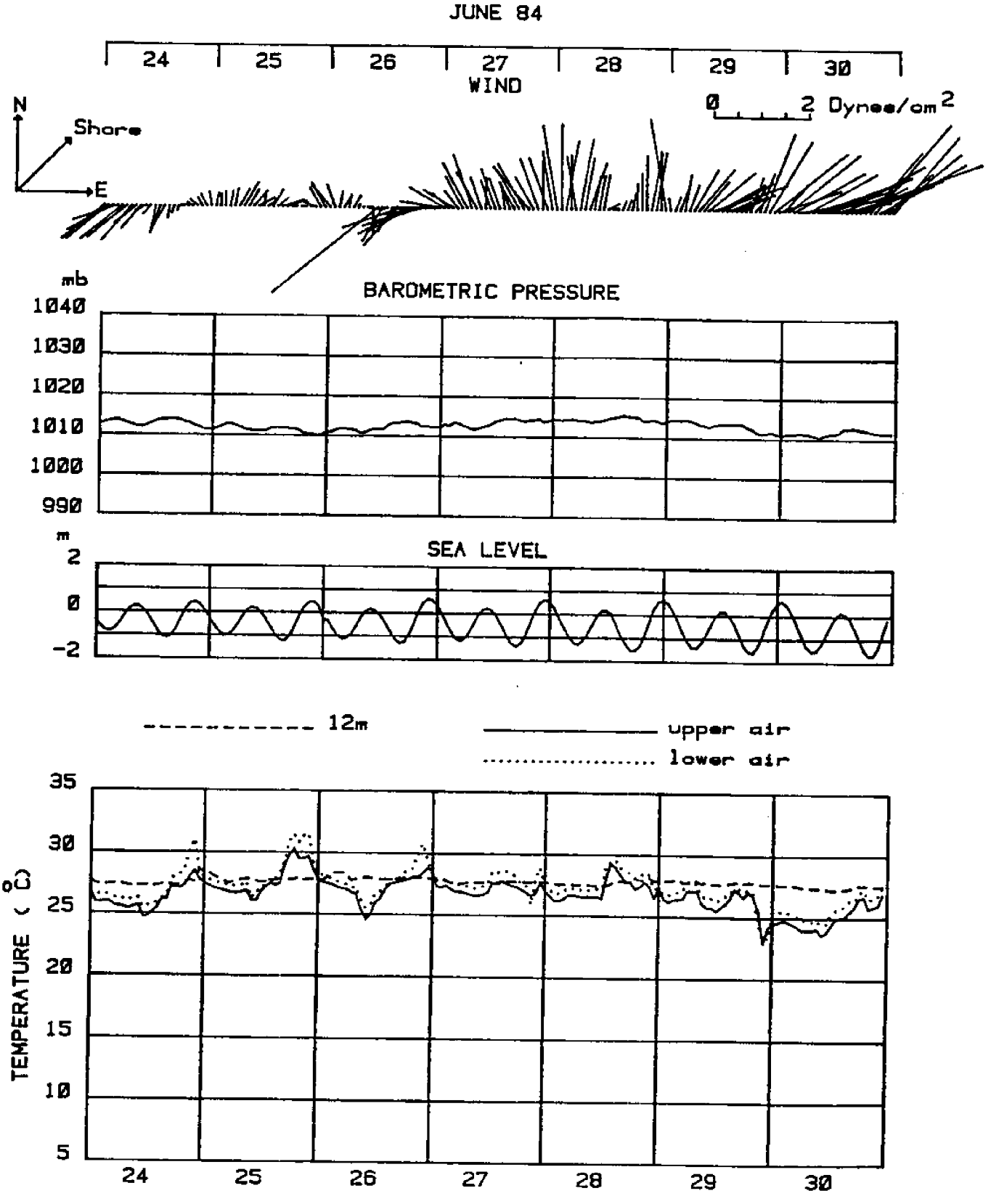
JUNE 84
24
25
26
27
28
29
30
WIND
0 2 Dynes/cm 2
N
Shore
E
mb
BAROMETRIC PRESSURE
1040
1030
1020
1010
1000
990
m
SEA LEVEL
2
0
-2
12m
upper air
lower air
TEMPERATURE (oC)
35
30
25
20
15
10
5
24
25
26
27
28
29
30

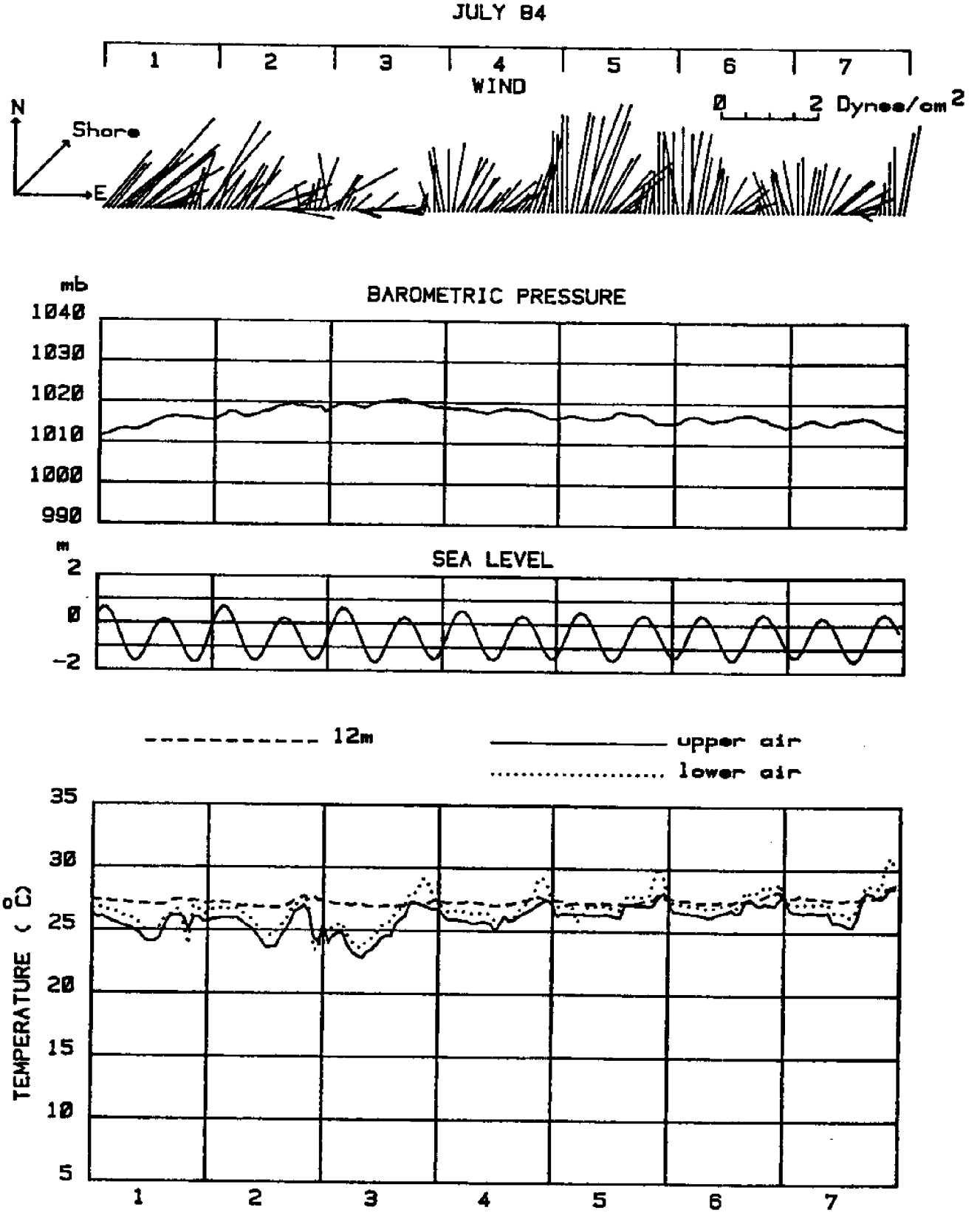
JULY 84
1
2
3
4
5
6
7
WIND
N
Shore
E
0
2 Dynes/cm 2
mb
BAROMETRIC PRESSURE
1040
1030
1020
1010
1000
990
m
SEA LEVEL
2
0
-2
12m
upper air
lower air
TEMPERATURE (oC)
35
30
25
20
15
10
5
1
2
3
4
5
6
7

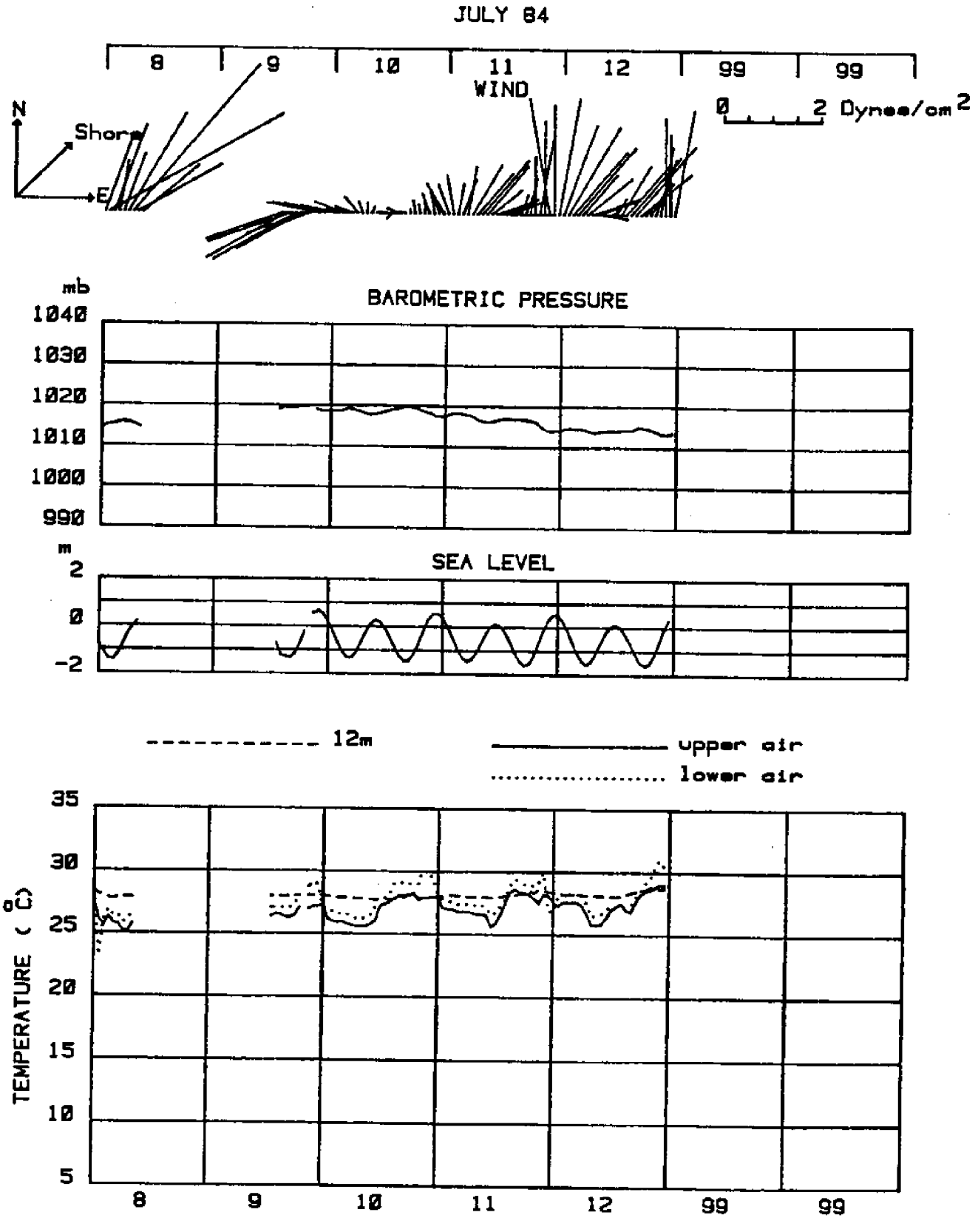
JULY 84
8
9
10
11
12
99
99
WIND
N
Shore
E
0
2 Dynes/cm 2
mb
BAROMETRIC PRESSURE
1040
1030
1020
1010
1000
990
m
SEA LEVEL
2
0
-2
12m
upper air
lower air
TEMPERATURE (°C)
35
30
25
20
15
10
5
8
9
10
11
12
99
99

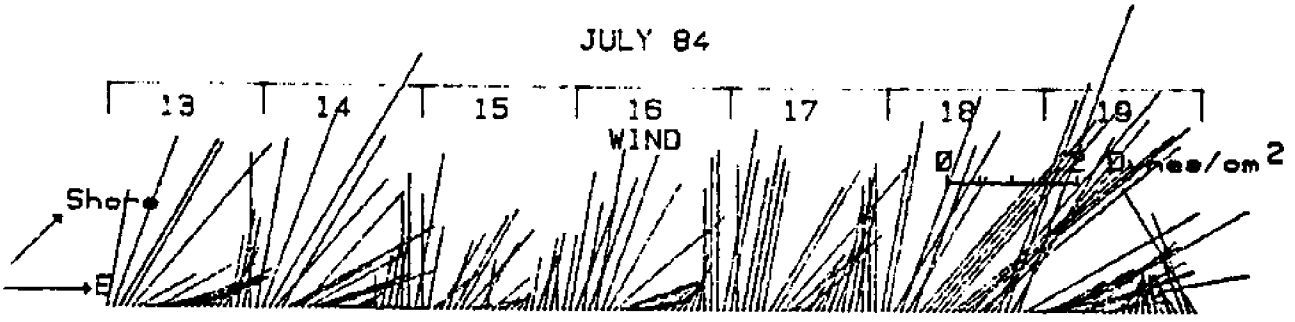
JULY 84
13
14
15
16
17
18
19
WIND
Short
0
2
m/sec/cm 2

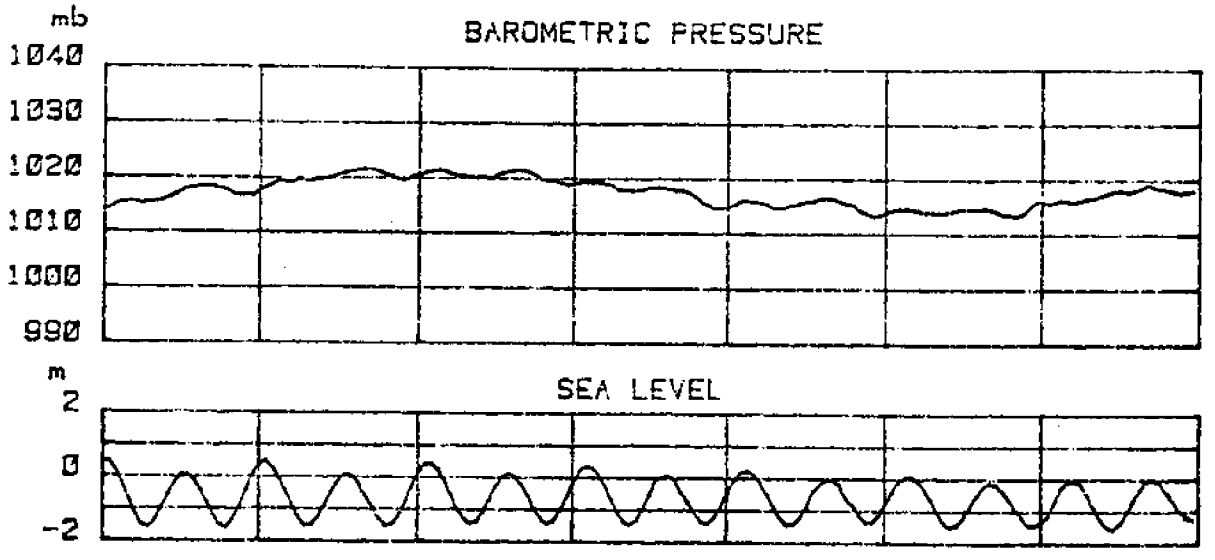
mb
BAROMETRIC PRESSURE
1040
1030
1020
1010
1000
990
m
SEA LEVEL
2
0
-2

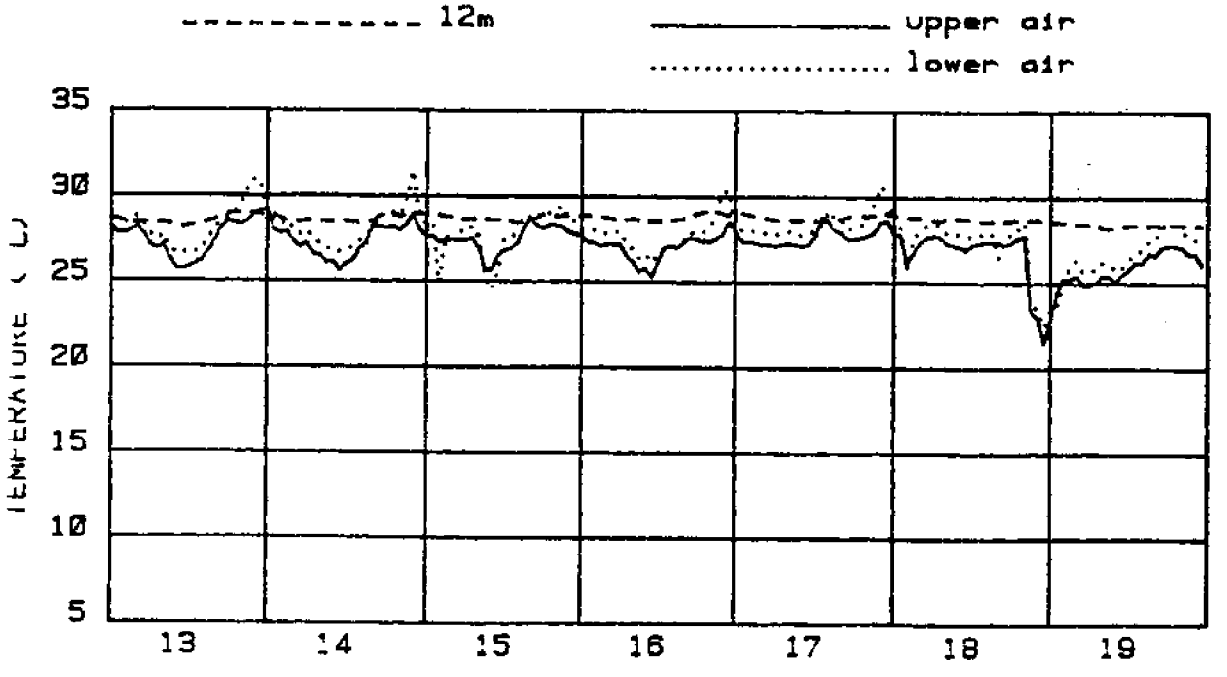
12m
upper air
lower air
35
30
25
20
15
10
5
13
14
15
16
17
18
19

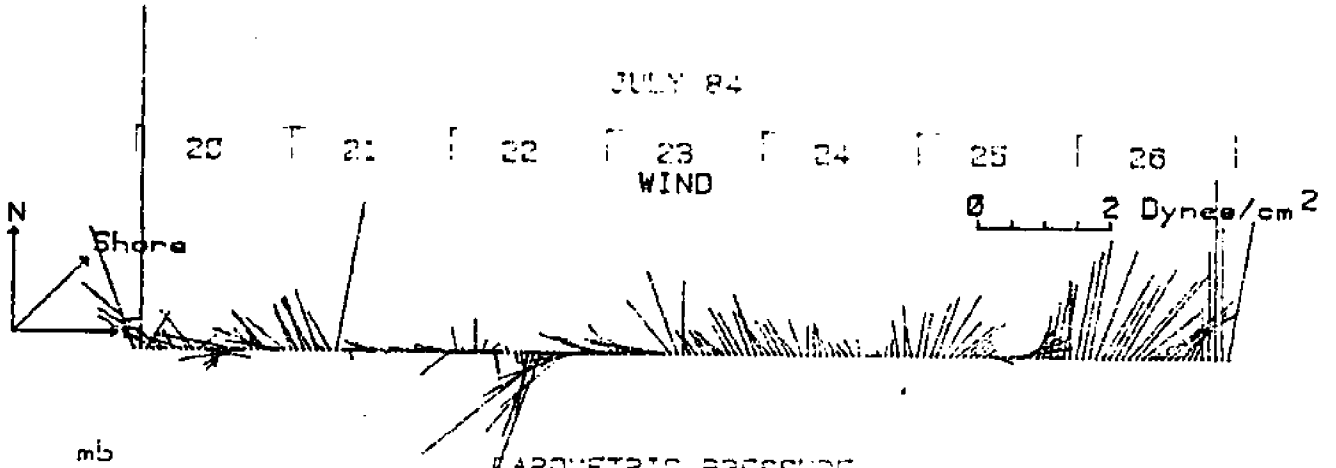
JULY 84
20
21
22
23
24
25
26
WIND
N
Shore
0
2 Dynes/cm 2

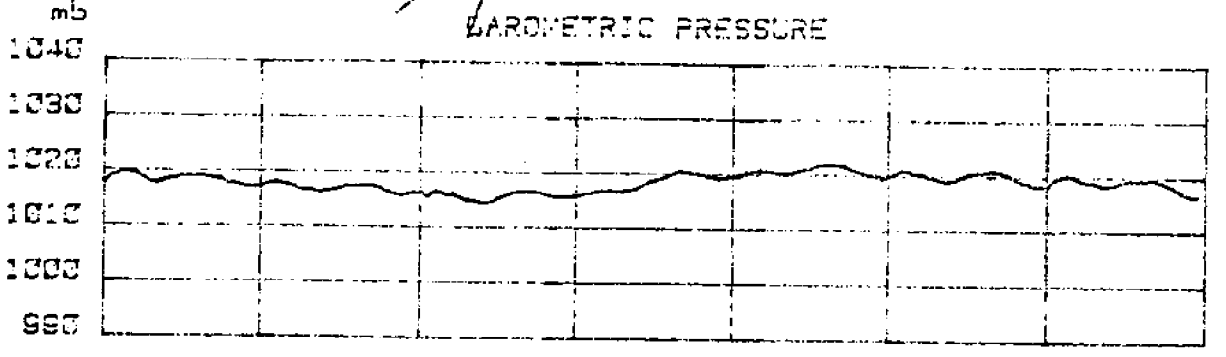
mb
BAROMETRIC PRESSURE
1040
1030
1020
1010
1000
990

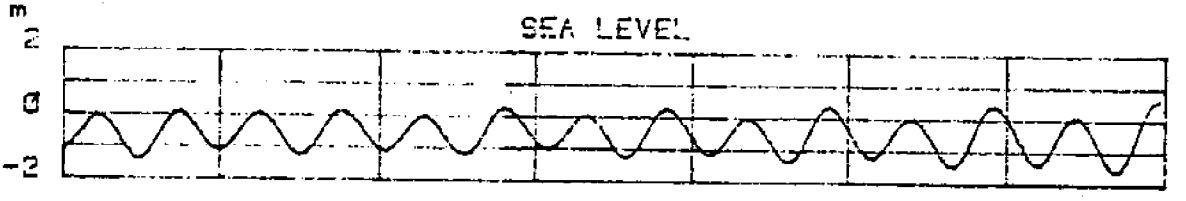
m
SEA LEVEL
2
0
-2

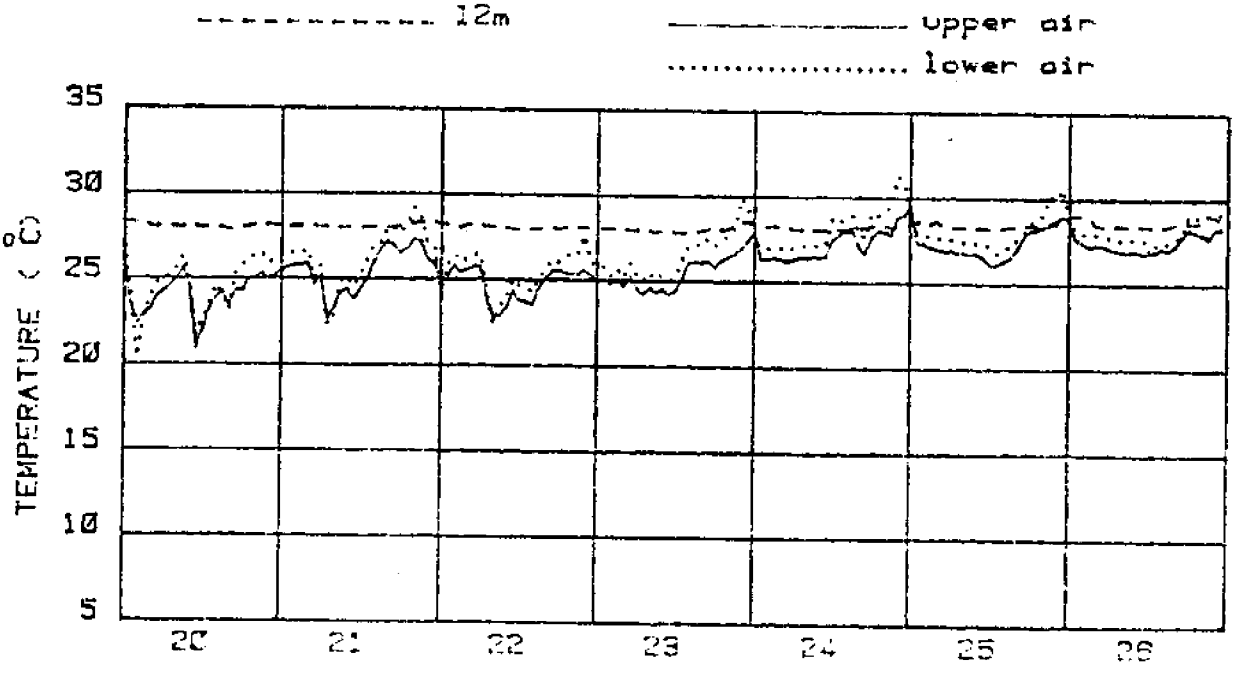
12m
upper air
lower air
TEMPERATURE (°C)
35
30
25
20
15
10
5
20
21
22
23
24
25
26

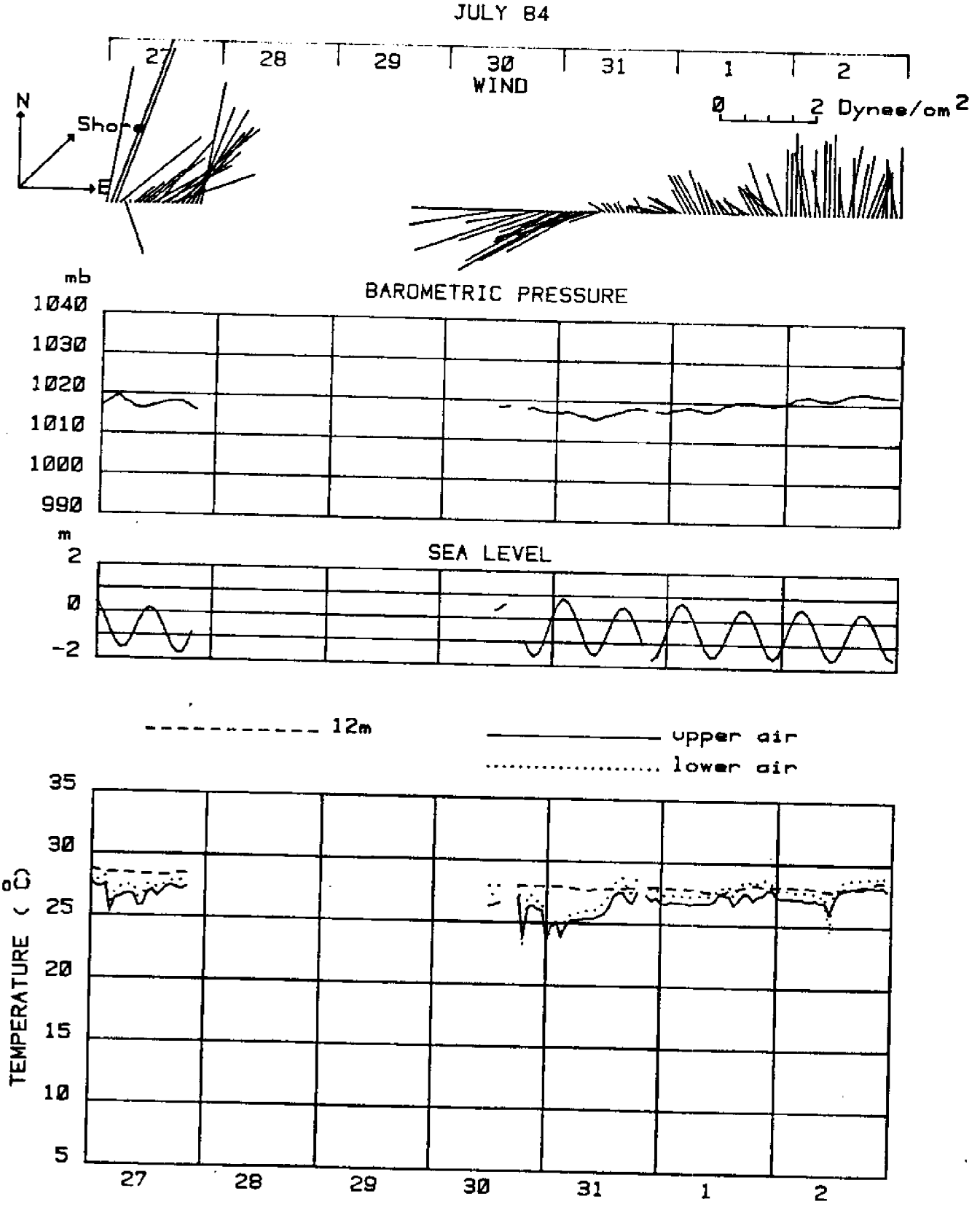
JULY 84
27
28
29
30
31
1
2
WIND
N
Shor
E
0
2 Dynee/cm 2
mb
1040
1030
1020
1010
1000
990
BAROMETRIC PRESSURE
m
2
0
-2
SEA LEVEL
12m
upper air
lower air
35
30
25
20
15
10
5
TEMPERATURE (°C)
27
28
29
30
31
1
2

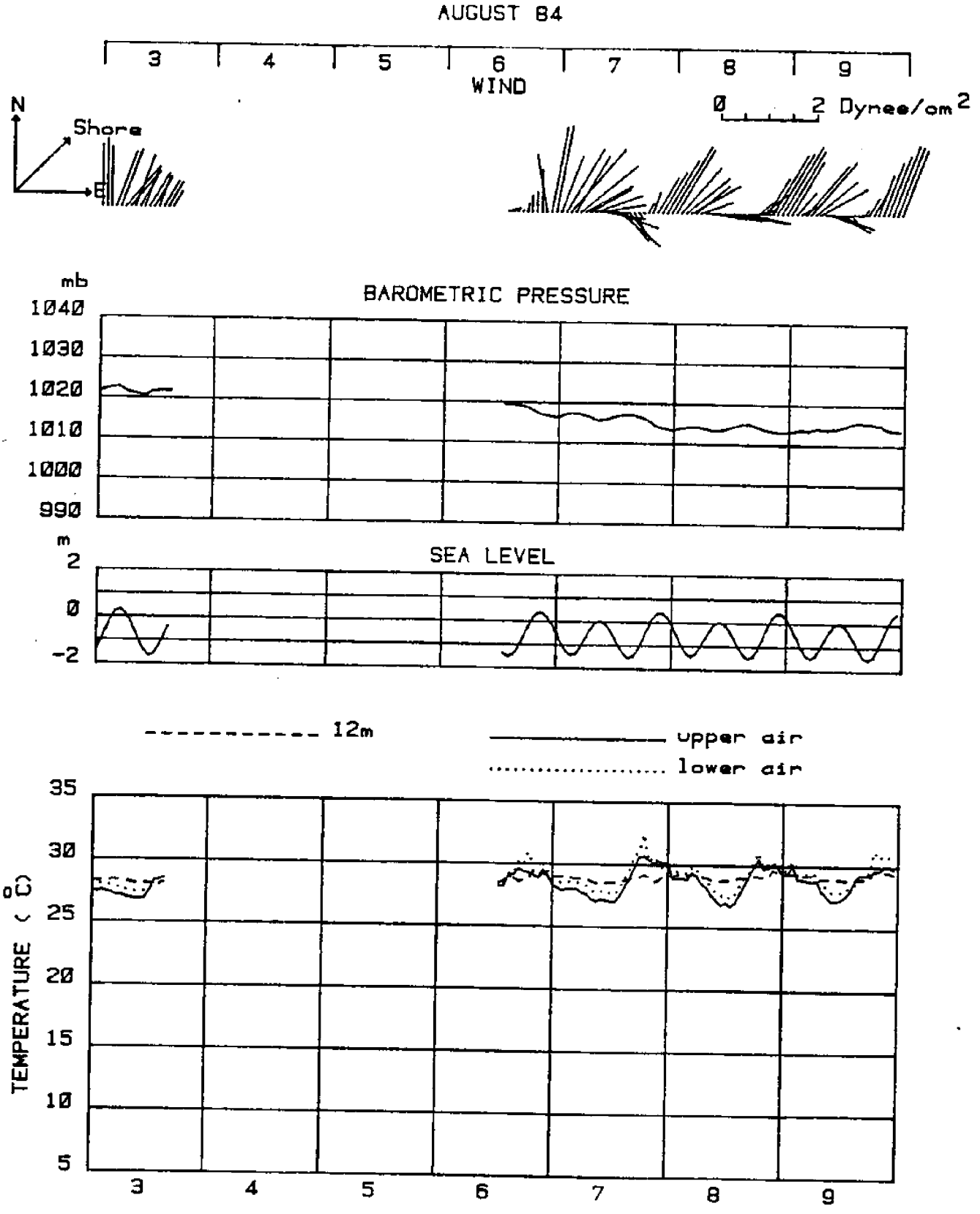
AUGUST 84
3
4
5
6
7
8
9
WIND
N
Shore
0
2 Dynes/cm 2
mb
BAROMETRIC PRESSURE
1040
1030
1020
1010
1000
990
m
SEA LEVEL
2
0
-2
12m
upper air
lower air
TEMPERATURE (°C)
35
30
25
20
15
10
5
3
4
5
6
7
8
9

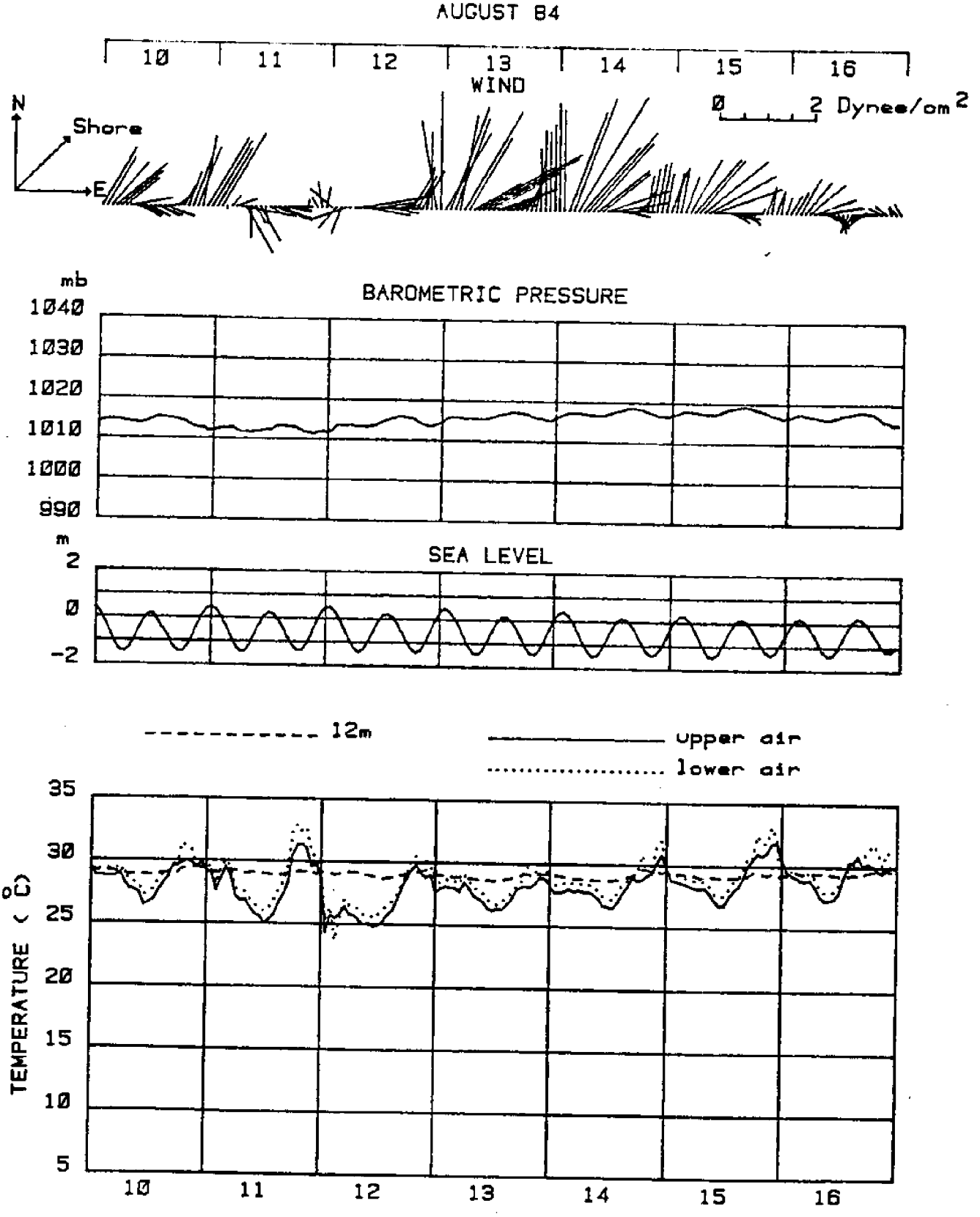
AUGUST 84
10
11
12
13
14
15
16
WIND
N
Shore
E
0
2 Dynes/cm2
mb
BAROMETRIC PRESSURE
1040
1030
1020
1010
1000
990
m
SEA LEVEL
2
0
-2
12m
upper air
lower air
TEMPERATURE (°C)
35
30
25
20
15
10
5
10
11
12
13
14
15
16

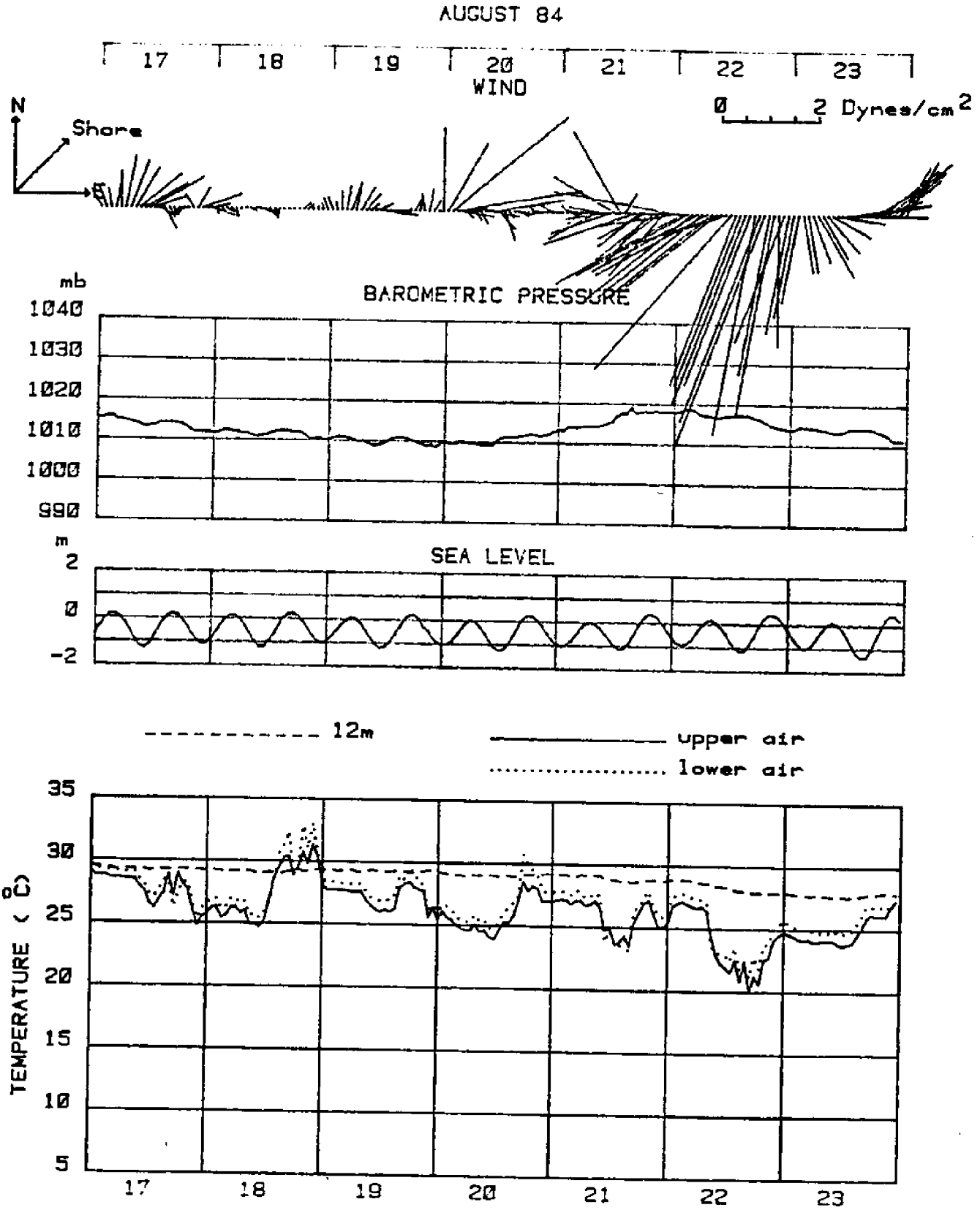
AUGUST 84
17
18
19
20
21
22
23
WIND
0
2 Dynes/cm 2
N
Shore
mb
BAROMETRIC PRESSURE
1040
1030
1020
1010
1000
990
m
SEA LEVEL
2
0
-2
12m
upper air
lower air
TEMPERATURE (°C)
35
30
25
20
15
10
5
17
18
19
20
21
22
23

AUGUST 84

24 99 99 99 99 99 99

WIND

0 2 Dynes/cm^2

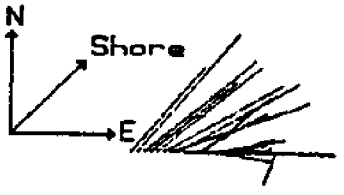

BAD DATA DISK

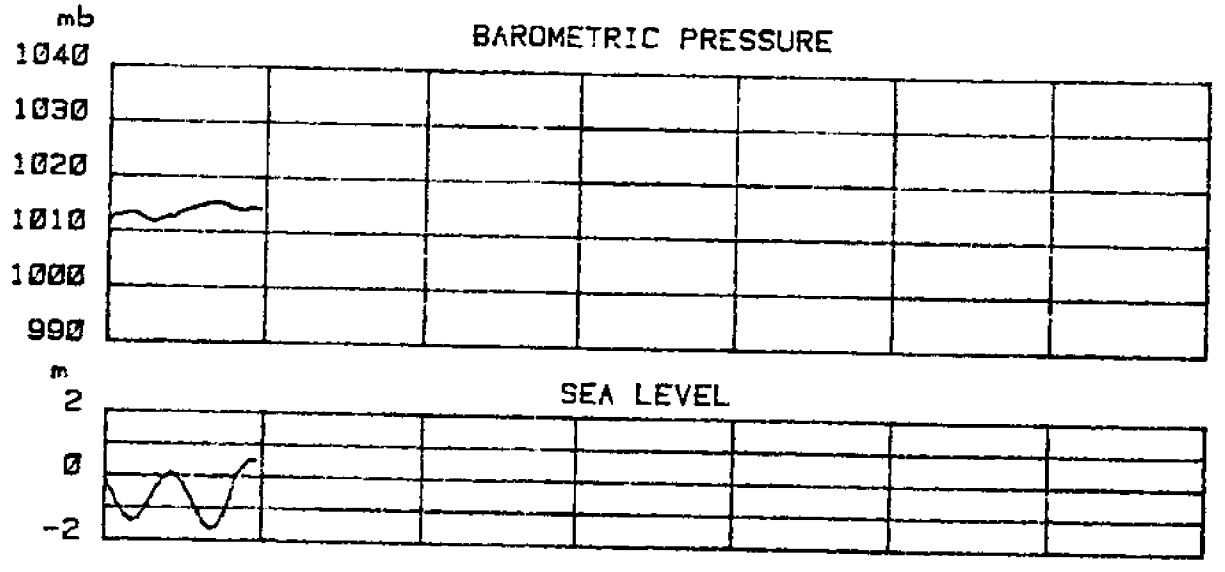

24 99 99 99 99 99 99

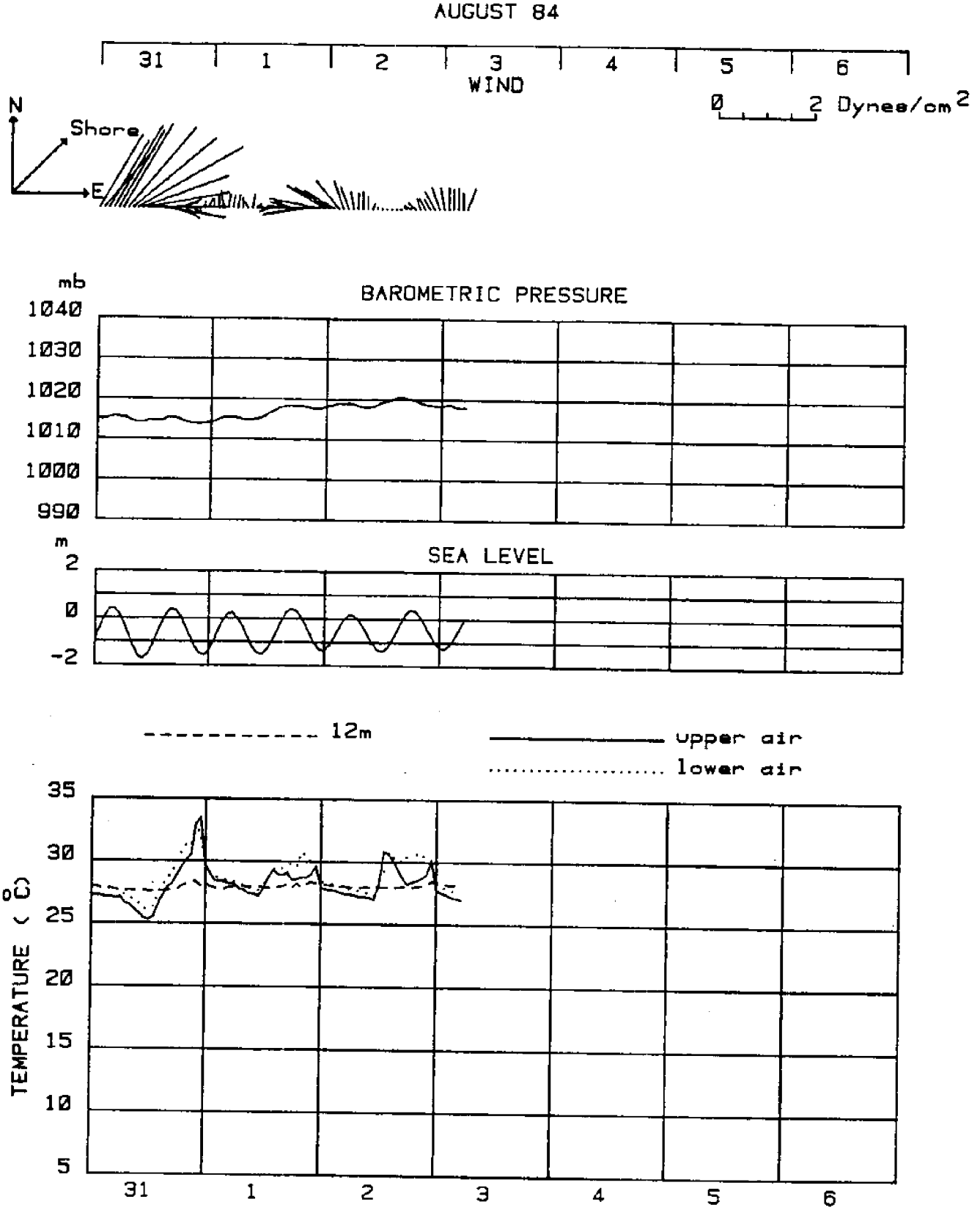
AUGUST 84
31
1
2
3
4
5
6
WIND
0
2 Dynes/cm2
N
Shore
E
mb
BAROMETRIC PRESSURE
1040
1030
1020
1010
1000
990
m
SEA LEVEL
2
0
-2
12m
upper air
lower air
TEMPERATURE (°C)
35
30
25
20
15
10
5
31
1
2
3
4
5
6

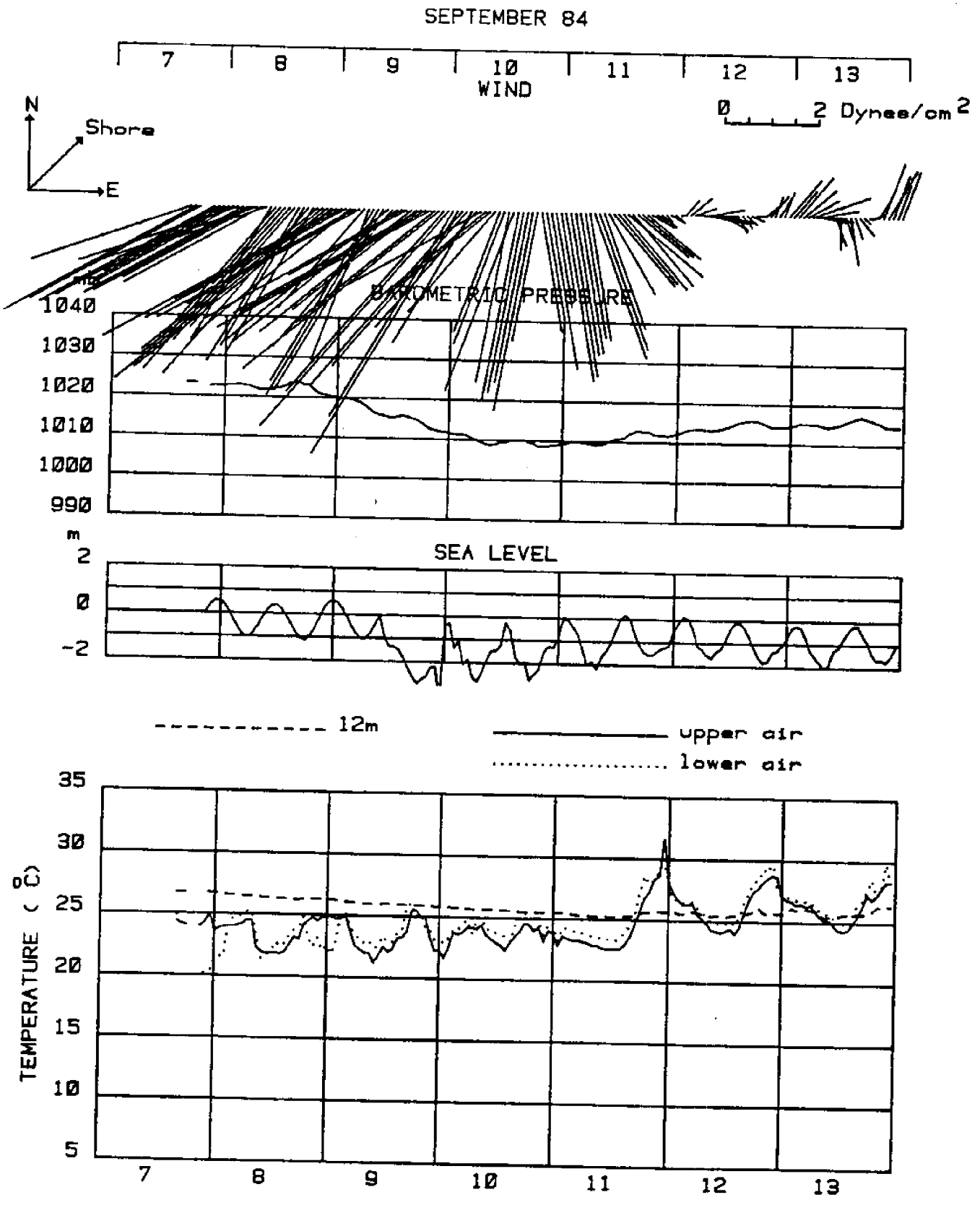
SEPTEMBER 84
7
8
9
10
11
12
13
WIND
0
2 Dynes/cm 2
N
Shore
E
mb
1040
1030
1020
1010
1000
990
BAROMETRIC PRESSURE
m
2
0
-2
SEA LEVEL
12m
upper air
lower air
35
30
25
20
15
10
5
TEMPERATURE (oC)
7
8
9
10
11
12
13

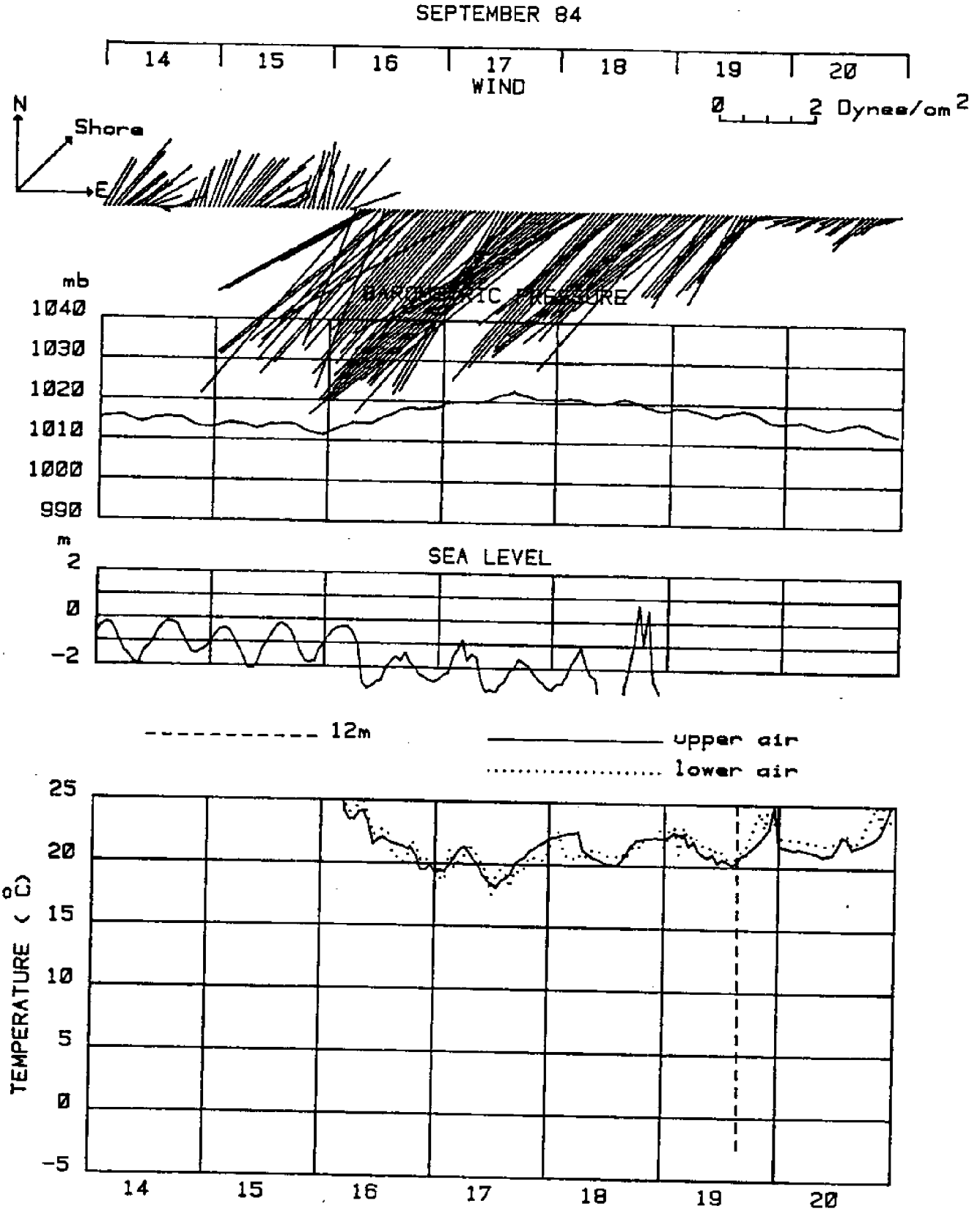
SEPTEMBER 84
14
15
16
17
18
19
20
WIND
0
2 Dynes/cm 2
N
Shore
E
mb
1040
1030
1020
1010
1000
990
BAROMETRIC PRESSURE
m
2
0
-2
SEA LEVEL
12m
upper air
lower air
25
20
15
10
5
0
-5
TEMPERATURE (°C)
14
15
16
17
18
19
20

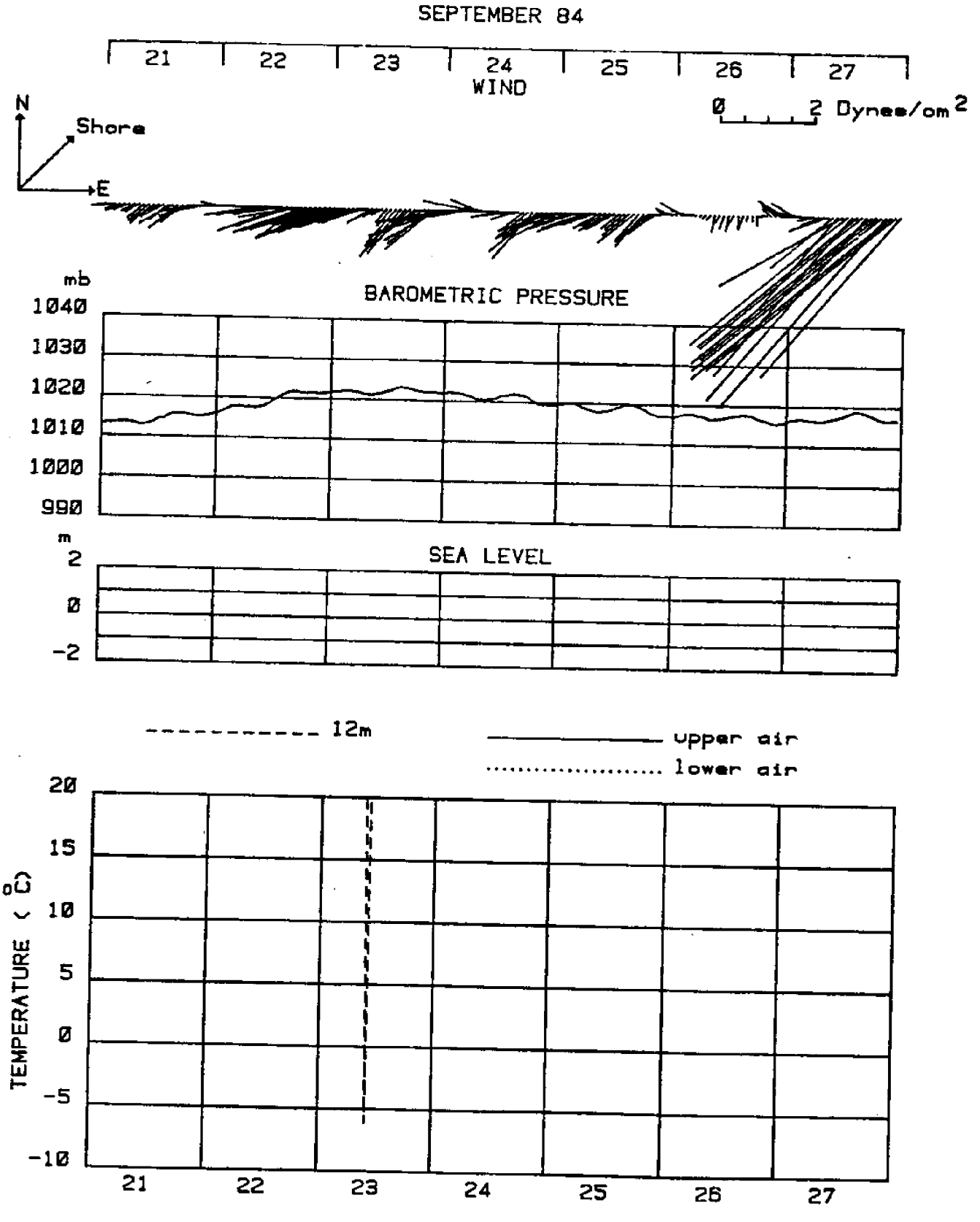
SEPTEMBER 84
21
22
23
24
25
26
27
WIND
0
2 Dynes/cm 2
N
Shore
E
mb
BAROMETRIC PRESSURE
1040
1030
1020
1010
1000
990
m
SEA LEVEL
2
0
-2
12m
upper air
lower air
TEMPERATURE (°C)
20
15
10
5
0
-5
-10
21
22
23
24
25
26
27

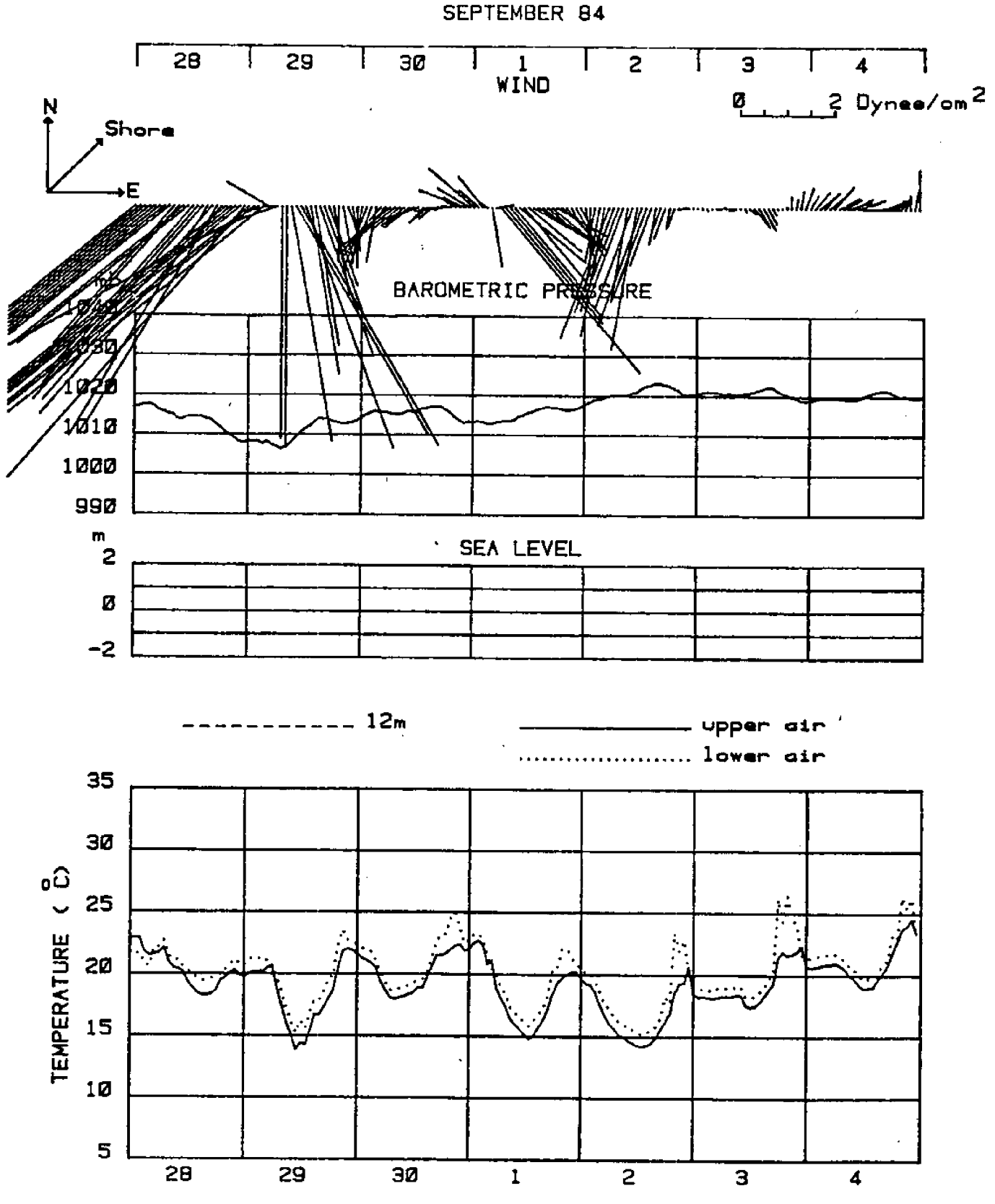
SEPTEMBER 84
28
29
30
1
2
3
4
WIND
0
2 Dynes/cm2
N
Shore
E
BAROMETRIC PRESSURE
1020
1010
1000
990
m
2
0
-2
SEA LEVEL
12m
upper air
lower air
35
30
25
20
15
10
5
TEMPERATURE (°C)
28
29
30
1
2
3
4

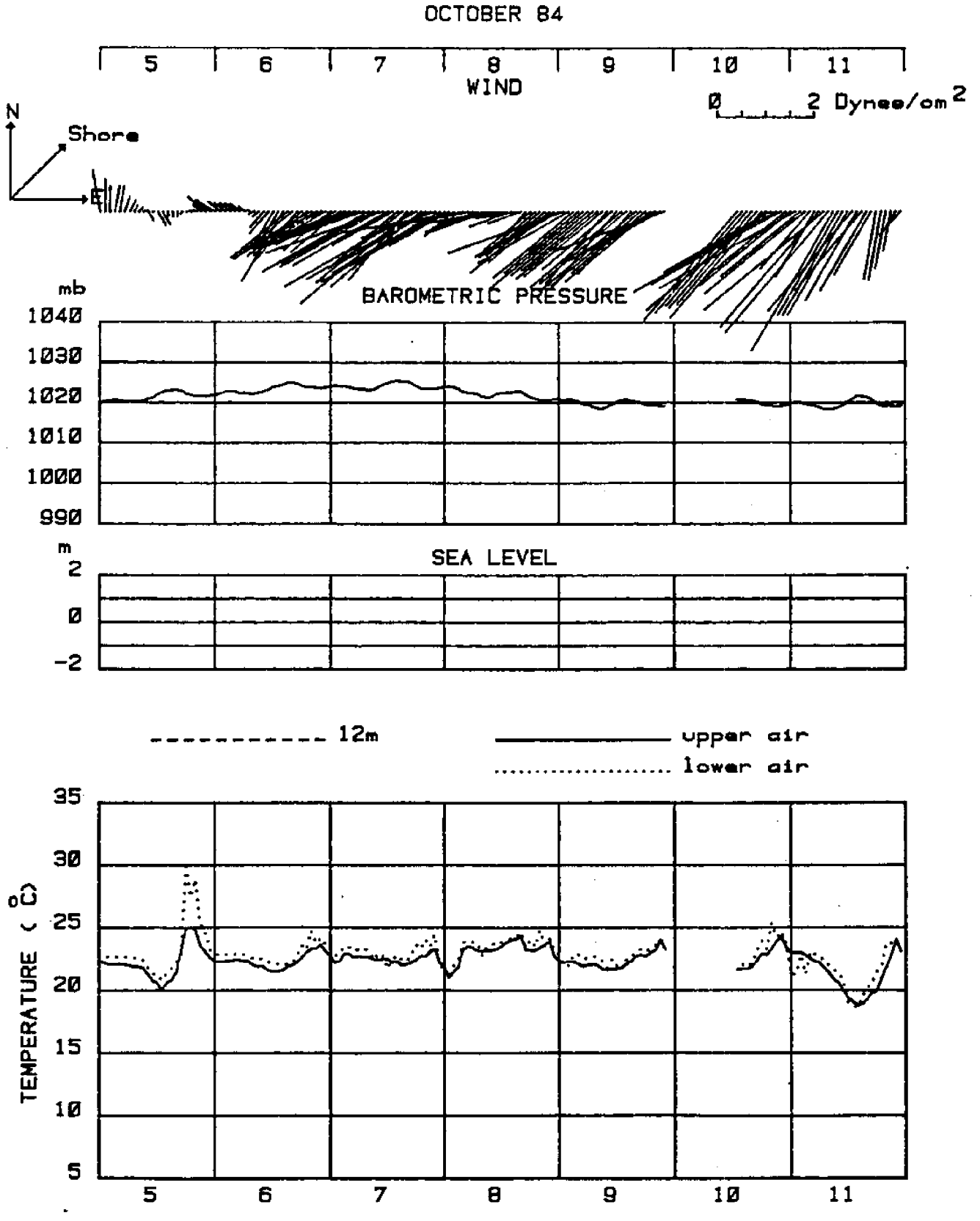
OCTOBER 84
5
6
7
8
9
10
11
WIND
0
2 Dynes/cm 2
N
Shore
E
mb
BAROMETRIC PRESSURE
1040
1030
1020
1010
1000
990
m
SEA LEVEL
2
0
-2
12m
upper air
lower air
TEMPERATURE (oC)
35
30
25
20
15
10
5

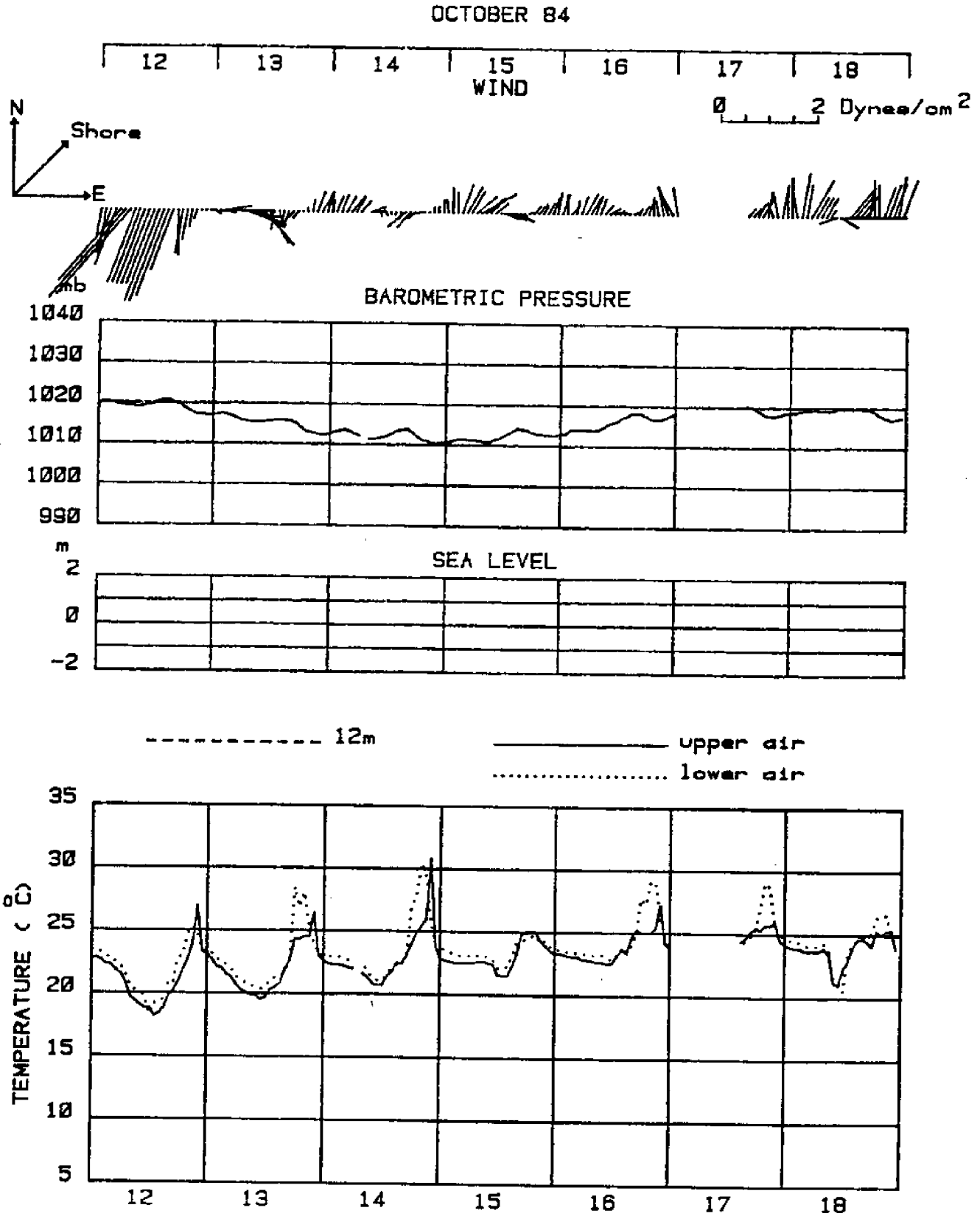
OCTOBER 84
12
13
14
15
16
17
18
WIND
0
2 Dynes/cm 2
N
Shore
E
mb
BAROMETRIC PRESSURE
1040
1030
1020
1010
1000
990
m
SEA LEVEL
2
0
-2
12m
upper air
lower air
TEMPERATURE (°C)
35
30
25
20
15
10
5
12
13
14
15
16
17
18

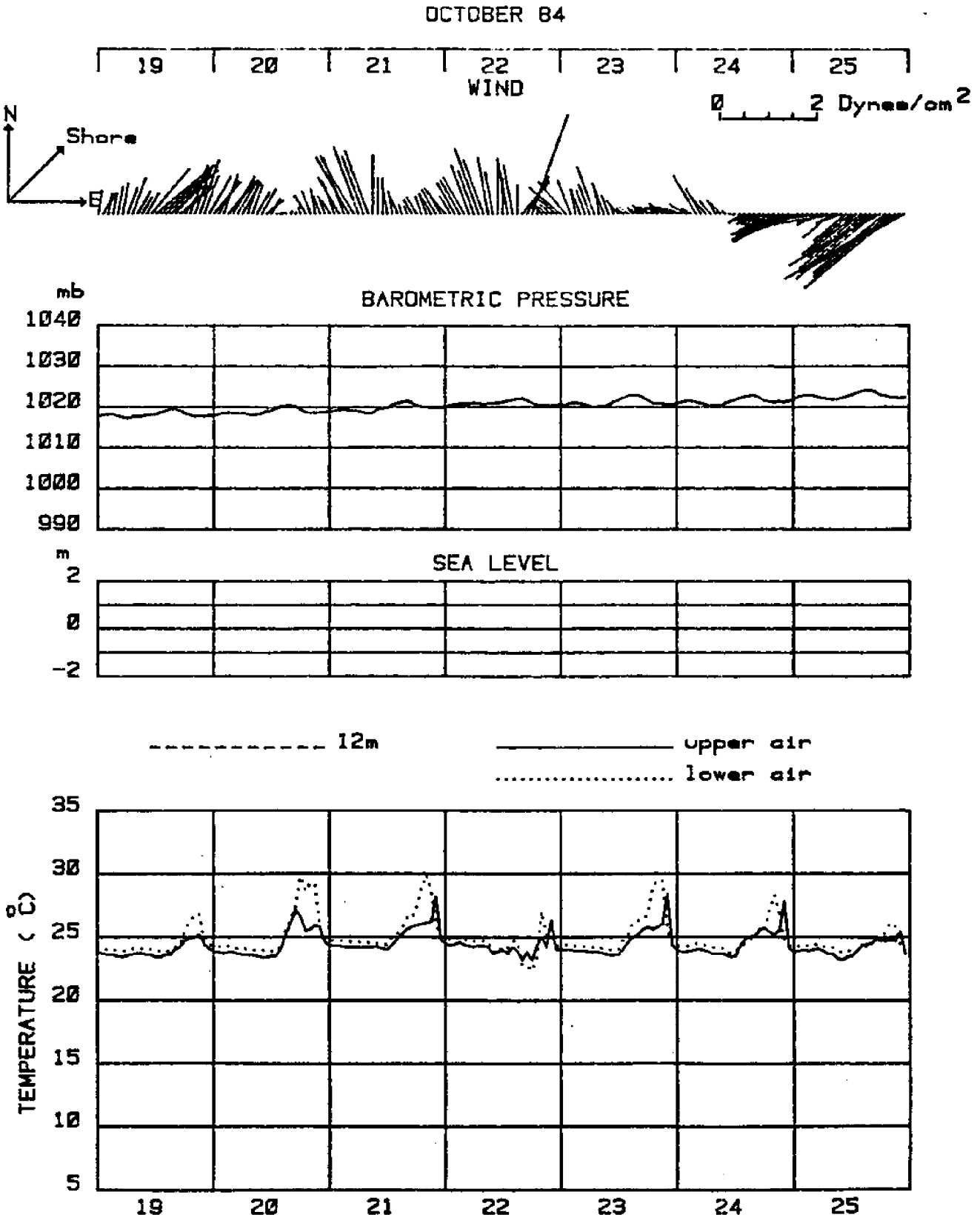
OCTOBER 84
19
20
21
22
23
24
25
WIND
0
2 Dynes/cm2
N
Shore
E
mb
BAROMETRIC PRESSURE
1040
1030
1020
1010
1000
990
m
SEA LEVEL
2
0
-2
12m
upper air
lower air
TEMPERATURE (°C)
35
30
25
20
15
10
5
19
20
21
22
23
24
25

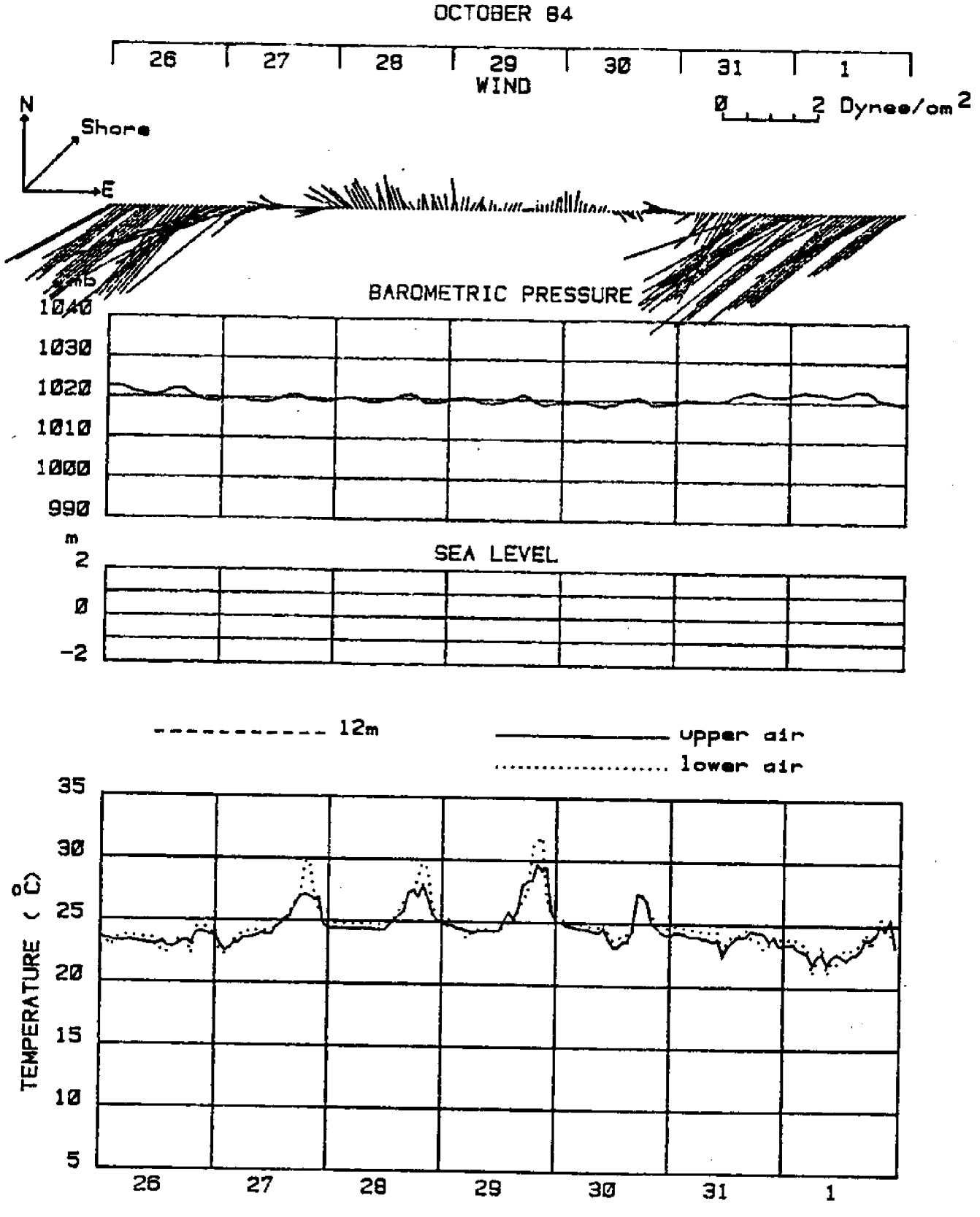
OCTOBER 84
26
27
28
29
30
31
1
WIND
0
2 Dynes/cm2
N
Shore
E
mb
BAROMETRIC PRESSURE
1040
1030
1020
1010
1000
990
m
SEA LEVEL
2
0
-2
12m
upper air
lower air
TEMPERATURE (°C)
35
30
25
20
15
10
5
26
27
28
29
30
31
1

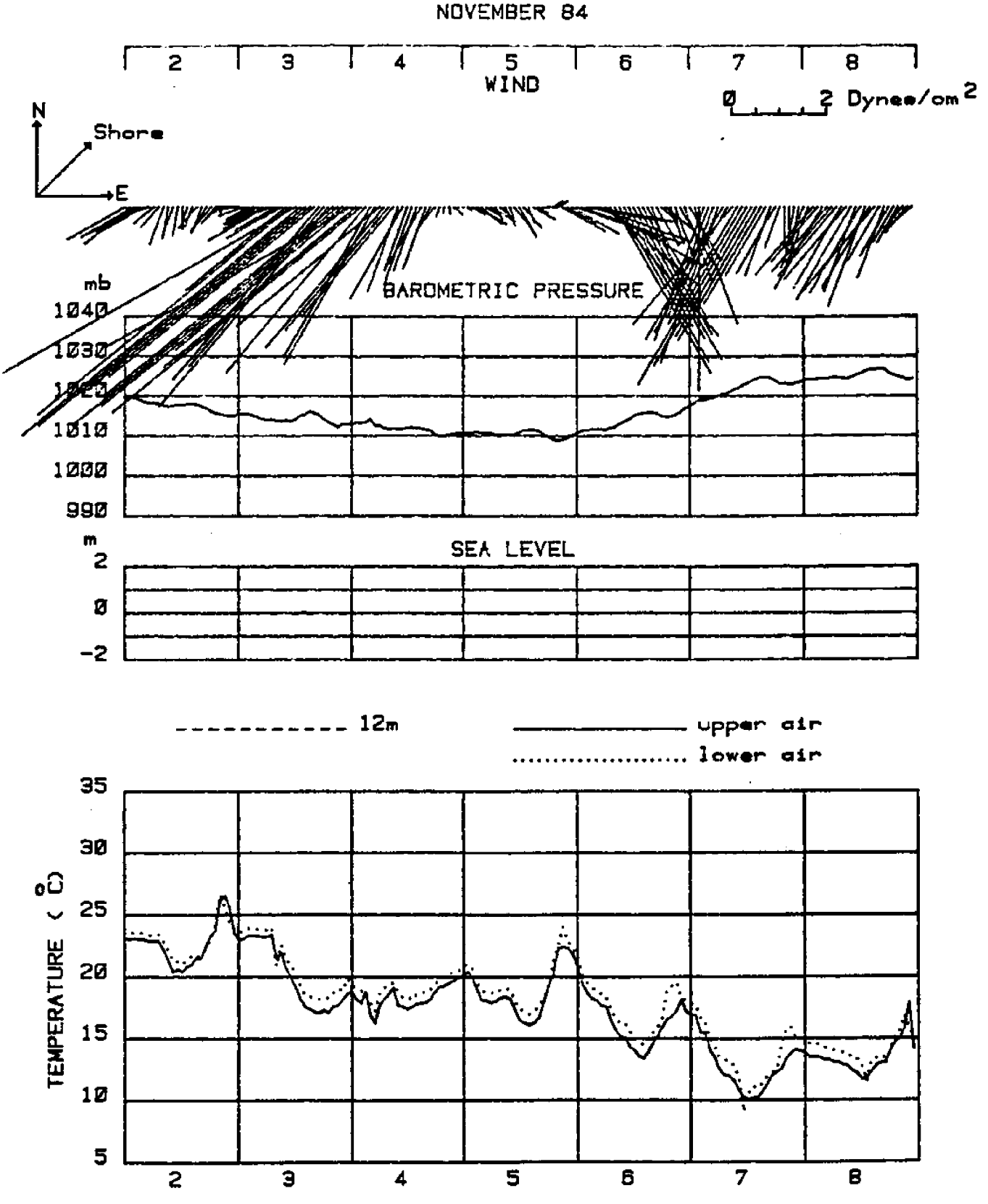
NOVEMBER 84
2
3
4
5
6
7
8
WIND
0
2 Dynes/cm 2
N
Shore
E
mb
1040
1030
1020
1010
1000
990
BAROMETRIC PRESSURE
m
2
0
-2
SEA LEVEL
12m
upper air
lower air
35
30
25
20
15
10
5
TEMPERATURE (°C)
2
3
4
5
6
7
8

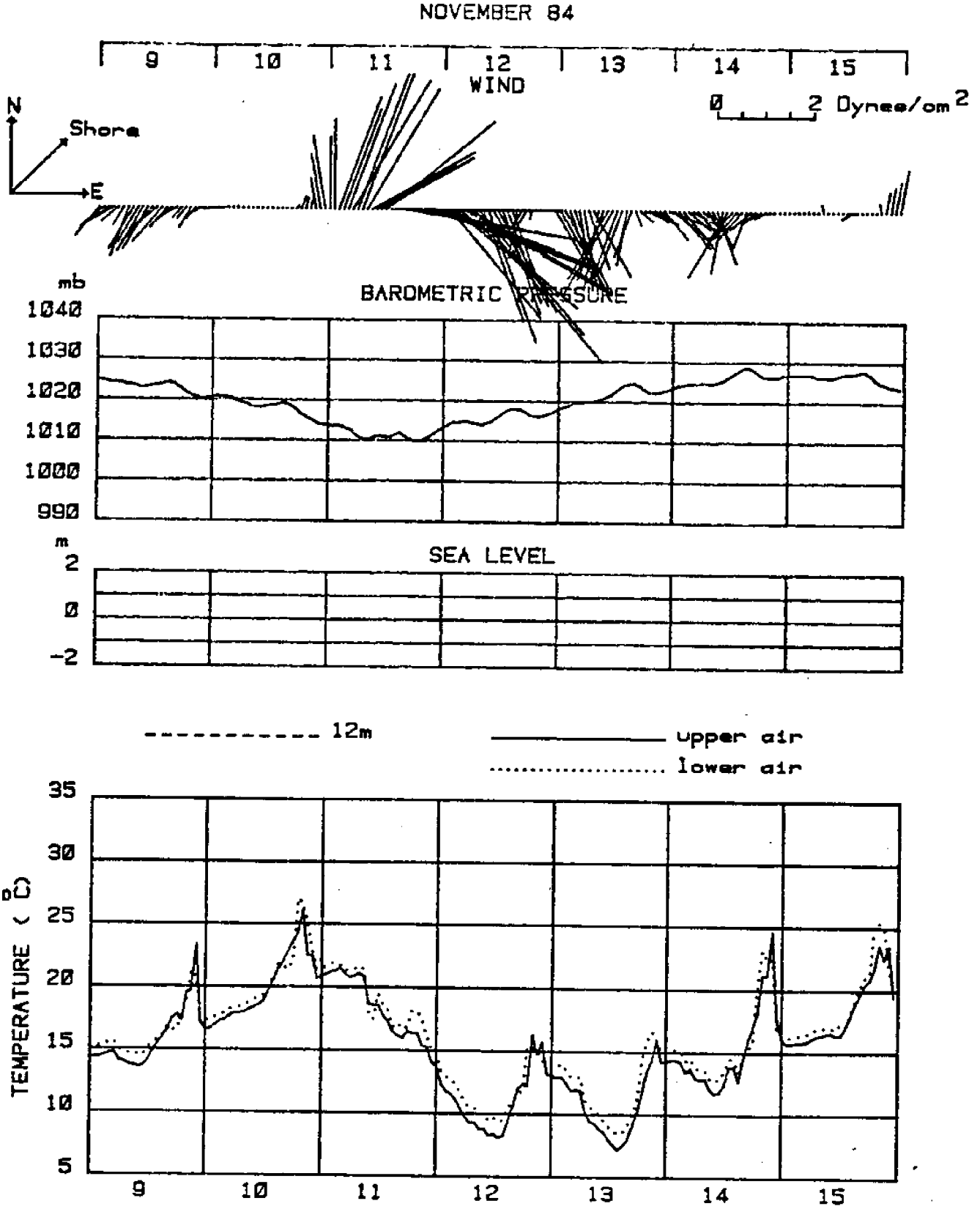
NOVEMBER 84
9
10
11
12
13
14
15
WIND
0 2 Dynes/cm 2
N
Shore
E
mb
1040
1030
1020
1010
1000
990
BAROMETRIC PRESSURE
m
2
0
-2
SEA LEVEL
12m
upper air
lower air
35
30
25
20
15
10
5
TEMPERATURE (°C)
9
10
11
12
13
14
15

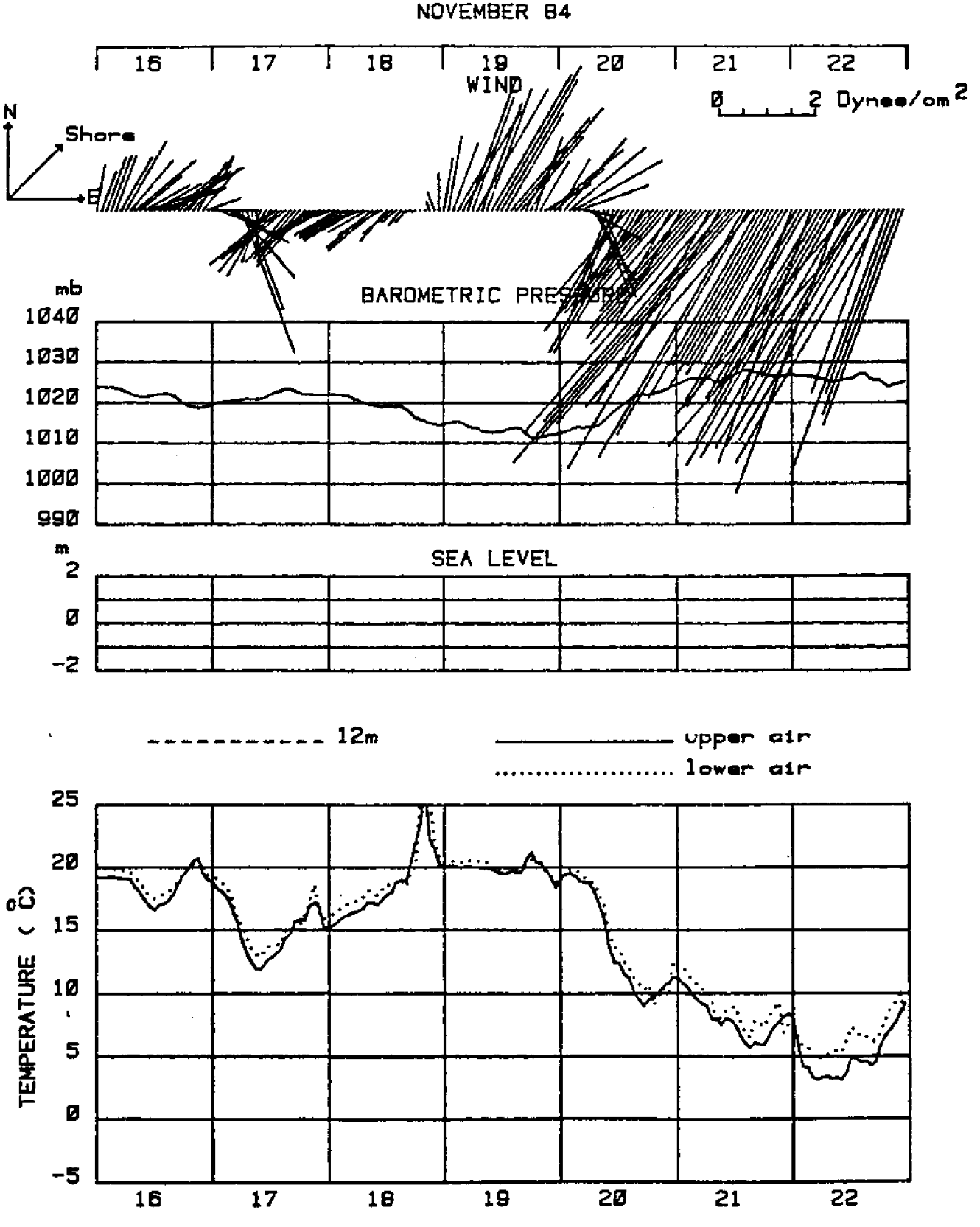
NOVEMBER 84
16
17
18
19
20
21
22
WIND
0 2 Dynes/cm2
N
Shore
E
mb
BAROMETRIC PRESSURE
1040
1030
1020
1010
1000
990
m
SEA LEVEL
2
0
-2
12m
upper air
lower air
TEMPERATURE (°C)
25
20
15
10
5
0
-5
16
17
18
19
20
21
22

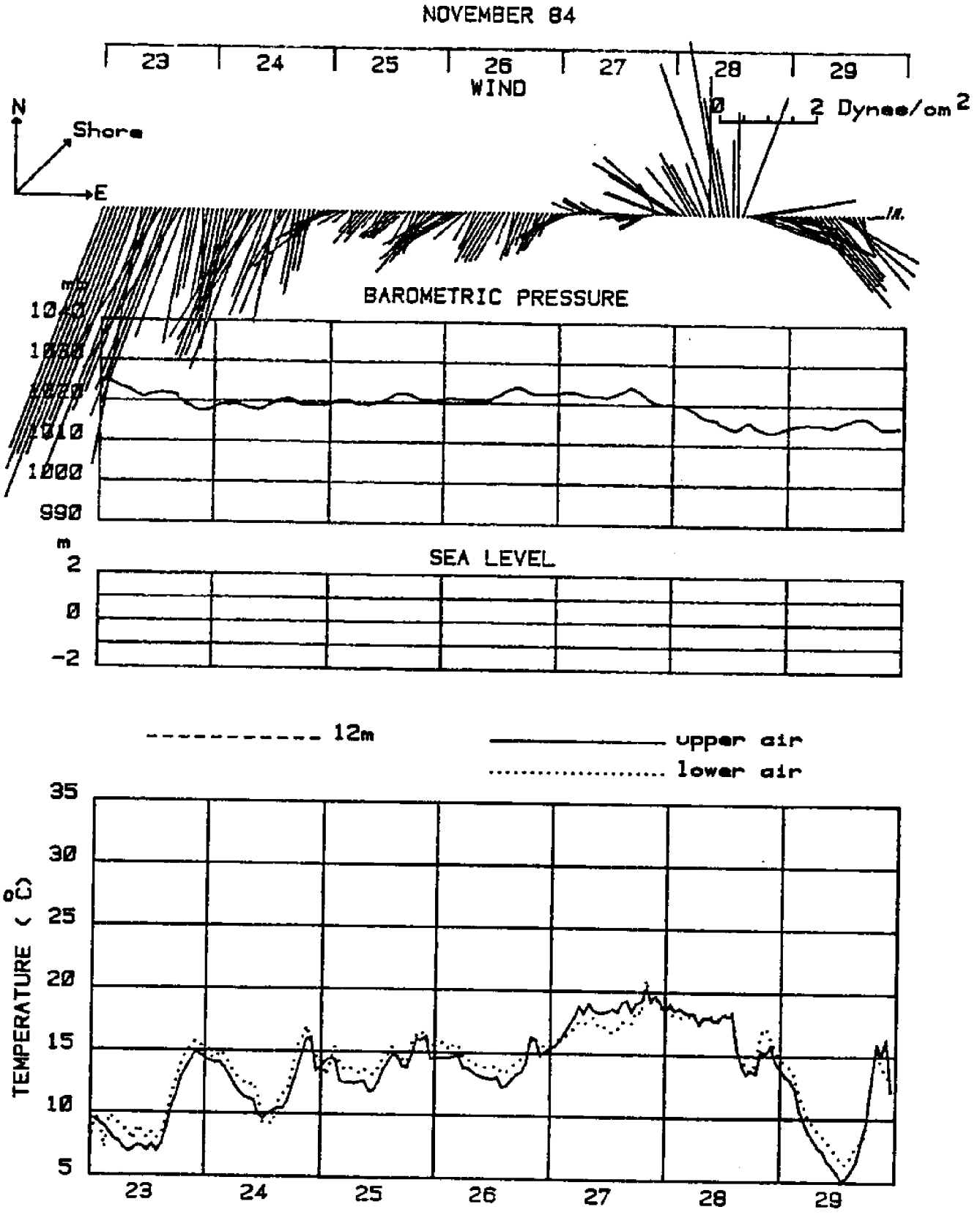
NOVEMBER 84
23
24
25
26
27
28
29
WIND
N
Shore
E
0
2 Dynes/cm 2
BAROMETRIC PRESSURE
mb
1010
1000
990
SEA LEVEL
m
2
0
-2
12m
upper air
lower air
TEMPERATURE (°C)
35
30
25
20
15
10
5
23
24
25
26
27
28
29

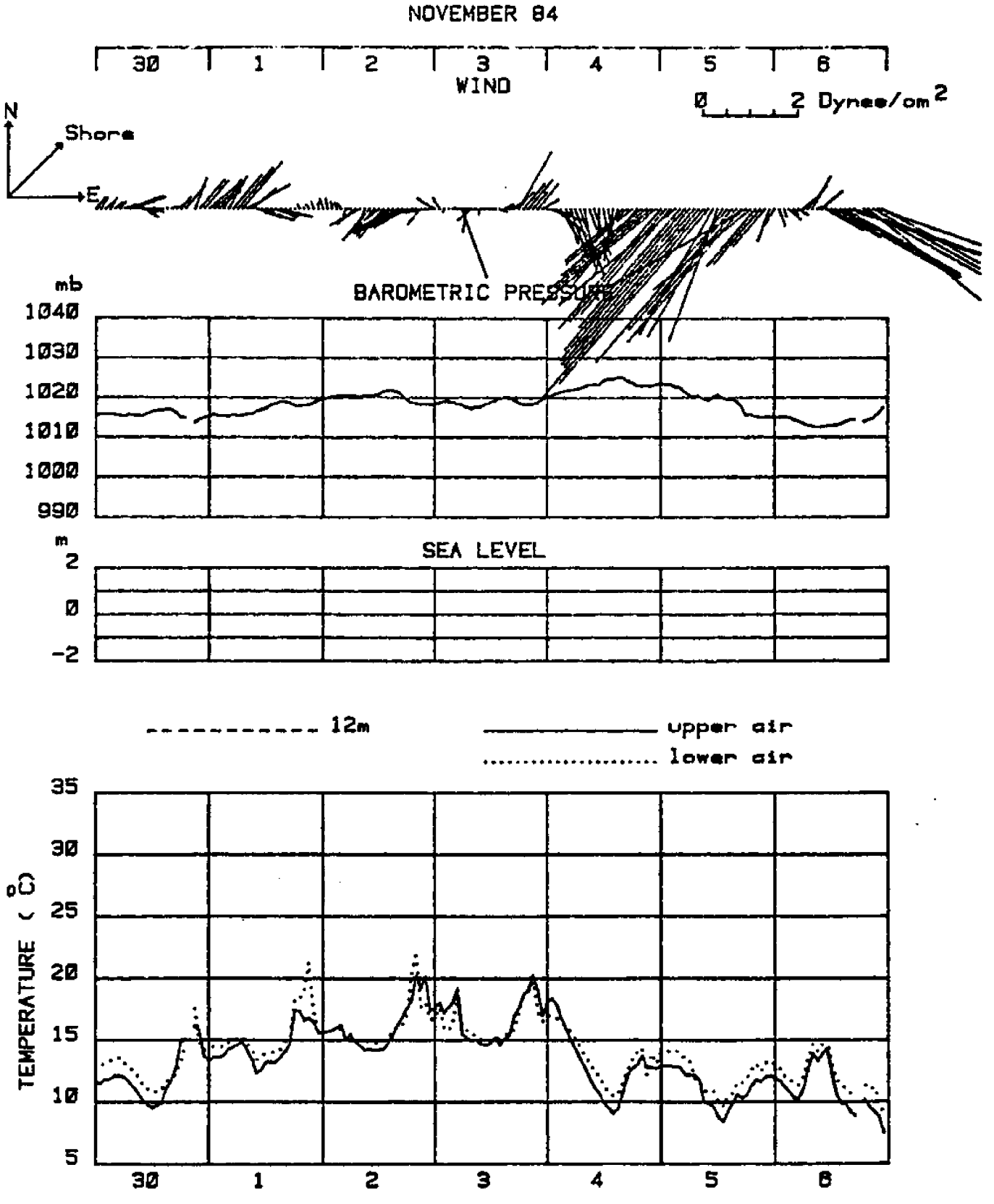
NOVEMBER 84
30
1
2
3
4
5
6
WIND
0 2 Dynes/cm 2
N
Shore
E
BAROMETRIC PRESSURE
mb
1040
1030
1020
1010
1000
990
m
SEA LEVEL
2
0
-2
12m
upper air
lower air
TEMPERATURE (oC)
35
30
25
20
15
10
5
30
1
2
3
4
5
6

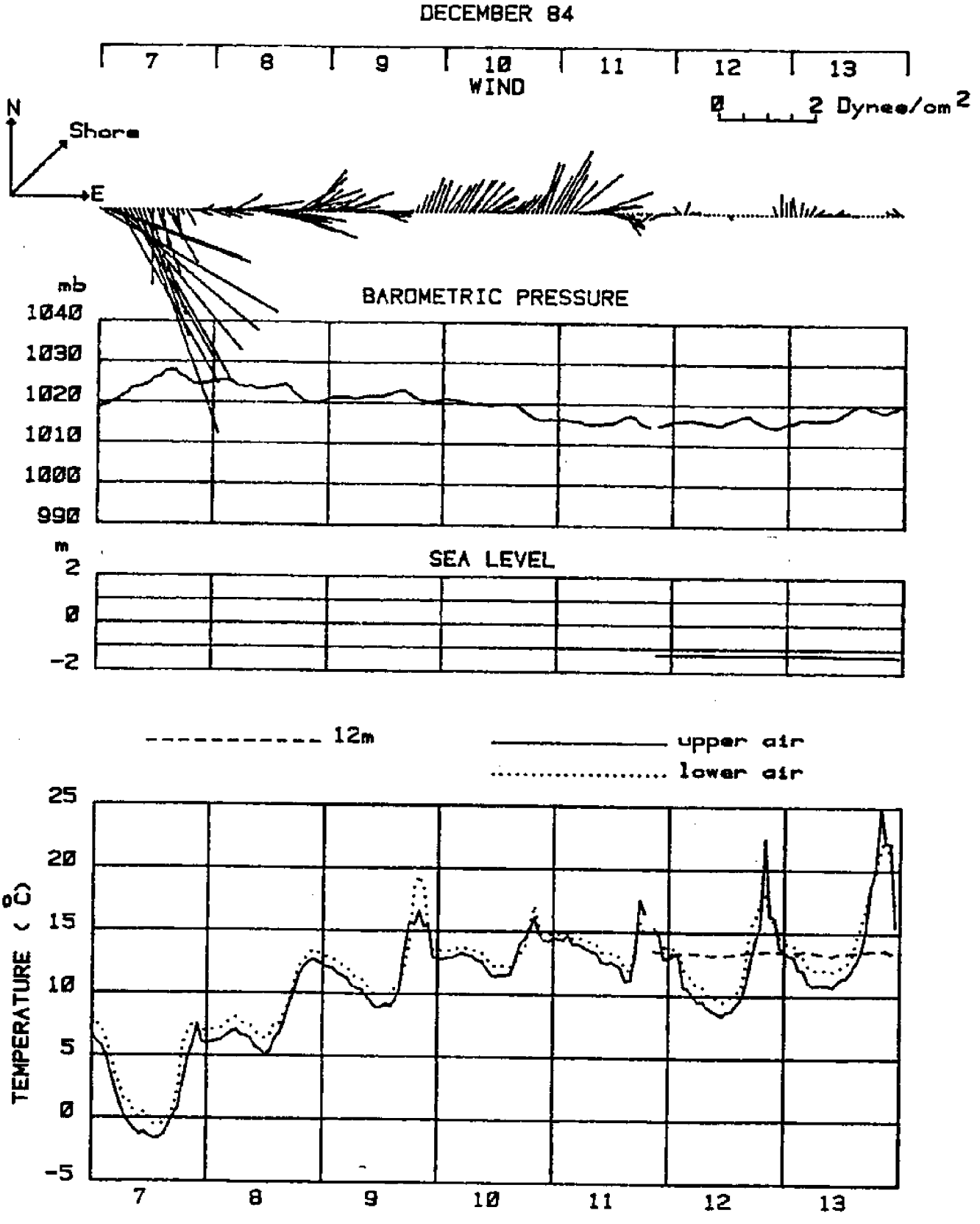
DECEMBER 84
7
8
9
10
11
12
13
WIND
0
2 Dynes/cm2
N
Shore
E
mb
BAROMETRIC PRESSURE
1040
1030
1020
1010
1000
990
m
SEA LEVEL
2
0
-2
12m
upper air
lower air
TEMPERATURE (°C)
25
20
15
10
5
0
-5
7
8
9
10
11
12
13

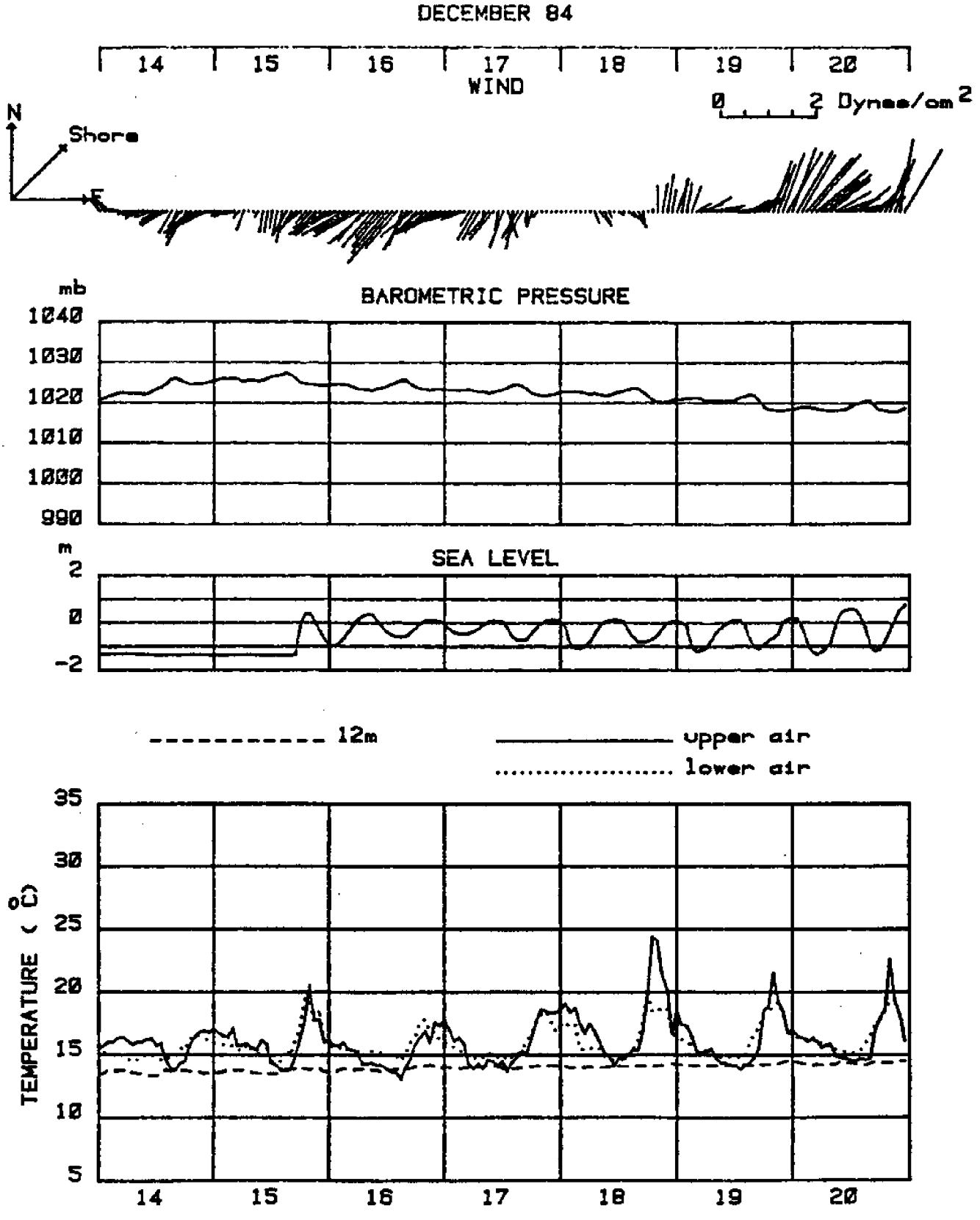
DECEMBER 84
14
15
16
17
18
19
20
WIND
0 2 Dynes/cm 2
N
Shore
E
mb
BAROMETRIC PRESSURE
1040
1030
1020
1010
1000
990
m
SEA LEVEL
2
0
-2
12m
upper air
lower air
TEMPERATURE (oC)
35
30
25
20
15
10
5
14
15
16
17
18
19
20

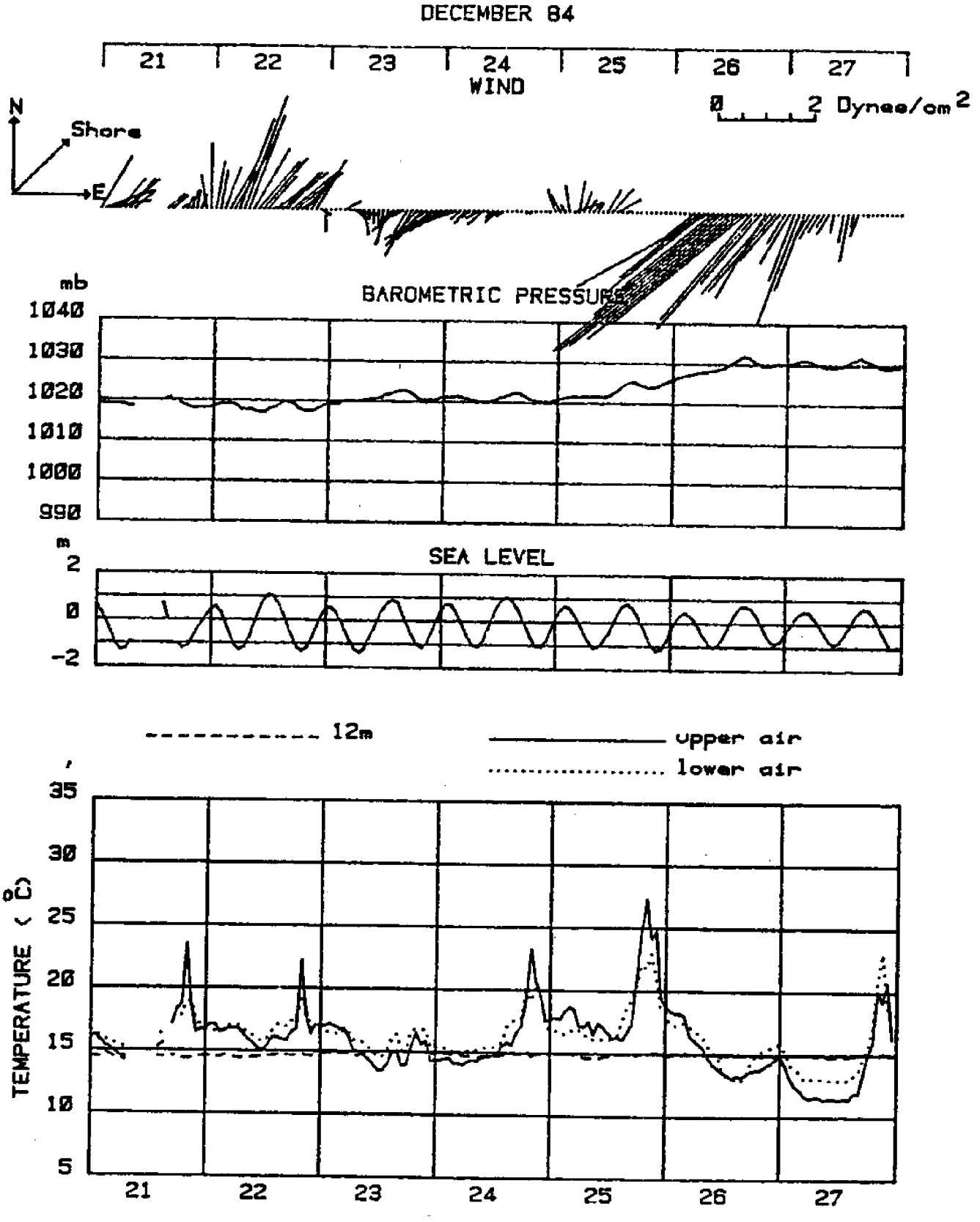
DECEMBER 84
21
22
23
24
25
26
27
WIND
0
2 Dynes/cm 2
N
Shore
E
mb
BAROMETRIC PRESSURE
1040
1030
1020
1010
1000
990
m
SEA LEVEL
2
0
-2
12m
upper air
lower air
TEMPERATURE (°C)
35
30
25
20
15
10
5
21
22
23
24
25
26
27

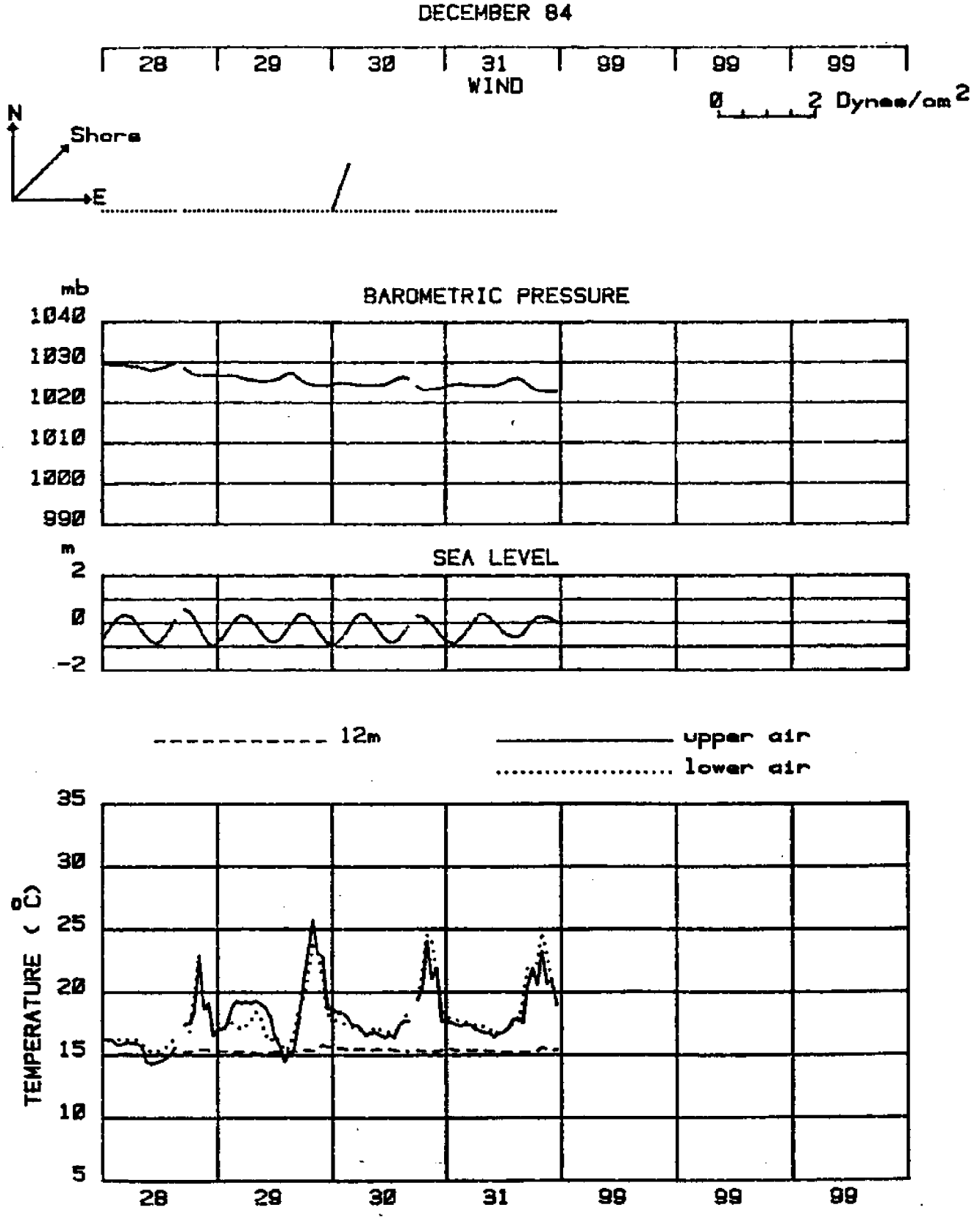
DECEMBER 84
28
29
30
31
99
99
99
WIND
0
2 Dynes/cm2
N
Shore
E
mb
BAROMETRIC PRESSURE
1040
1030
1020
1010
1000
990
m
SEA LEVEL
2
0
-2
12m
upper air
lower air
35
30
25
20
15
10
5
TEMPERATURE (oC)
28
29
30
31
99
99
99